ЖУРНАЛ
ЭКСПЕРИМЕНТАЛЬНОЙ И ТЕОРЕТИЧЕСКОЙ
ФИЗИКИ
АКАДЕМИЯ НАУК СССР

SOVIET PHYSICS

JETP

VOLUME 6 (33) NUMBER 5

A Translation

of the

Journal of Experimental and Theoretical Physics

of the

Academy of Sciences of the USSR

Volume 33

MAY, 1958

Published by the

AMERICAN INSTITUTE OF PHYSICS
INCORPORATED

SOVIET PHYSICS
JETP

A translation of the Journal of Experimental and Theoretical Physics of the USSR.

A publication of the

AMERICAN INSTITUTE OF PHYSICS

Governing Board

FREDERICK SEITZ, *Chairman*

Members:

WALTER S. BAIRD
JESSE W. BEAMS
RAYMOND T. BIRGE
R. H. BOLT
J. W. BUCHTA
J. H. DILLON
VERNET E. EATON
HERBERT A. ERF
IRVINE C. GARDNER
S. A. GOUDSMIT
C. KITTEL
WINSTON E. KOCK
R. BRUCE LINDSAY
WALTER C. MICHELS
G. E. PAKE
R. RONALD PALMER
JOSEPH B. PLATT
RALPH A. SAWYER
H. D. SMYTH
JOHN STRONG
GEORGE E. UHLENBECK

Administrative Staff

ELMER HUTCHISSON
Director

HENRY A. BARTON
Associate Director

WALLACE WATERFALL
Secretary and Treasurer

THEODORE VORBURGER
Advertising Manager

RUTH F. BRYANS
Publication Manager

ALICE MASTRO
Circulation Manager

KATHRYN SETZE
Assistant Treasurer

EUGENE H. KONE
Director of Public Relations

EDWARD P. TOBER
Manager, Production and Distribution

American Institute of Physics Advisory Board on Russian Translations

ROBERT T. BEYER, *Chairman*
FREEMAN J. DYSON, DWIGHT GRAY, DAVID HARKER,
MORTON HAMERMESH, VLADIMIR ROJANSKY

Editor of SOVIET PHYSICS—JETP

J. GEORGE ADASHKO, DEPARTMENT OF ELECTRICAL ENGINEERING,
THE CITY COLLEGE, CONVENT AVENUE AND 139TH STREET
NEW YORK 31, NEW YORK.

SOVIET PHYSICS is a monthly journal published by the American Institute of Physics for the purpose of making available in English reports of current Soviet research in physics as contained in the Journal of Experimental and Theoretical Physics of the Academy of Sciences of the USSR. The page size of SOVIET PHYSICS will be 8½" x 11", the same as other Institute journals.

Transliteration of the names of Russian authors follows the system employed by the Library of Congress.

This translating and publishing project was undertaken by the Institute in the conviction that dissemination of the results of researches everywhere in the world is invaluable to the advancement of science. The National Science Foundation of the United States encouraged the project initially and is supporting it in large part by a grant.

The American Institute of Physics and its translators propose to translate faithfully all the material in the Journal of EXPERIMENTAL AND THEORETICAL PHYSICS OF THE USSR appearing after January 1, 1955. The views expressed in the translated material, therefore, are intended to be those expressed by the original authors, and not those of the translators nor of the American Institute of Physics.

Two volumes are published annually, each of six issues. Each volume contains the translation of one volume of the Journal of EXPERIMENTAL AND THEORETICAL PHYSICS OF THE USSR.

Subscription Prices:

Per year (12 issues)

United States and Canada	$75.00
Elsewhere	79.00

Back Numbers

Single copies	$ 8.00

Subscriptions should be addressed to the American Institute of Physics, 335 East 45th Street, New York 17, New York.

Copyright by American Institute of Physics 1958

SOVIET PHYSICS

JETP

A translation of the Journal of Experimental and Theoretical Physics of the USSR.

SOVIET PHYSICS JETP VOL. 6 (33), NO. 5, pp. 835-1010 May, 1958

THE DEVELOPMENT OF PHYSICS IN THE USSR IN FORTY YEARS OF SOVIET POWER

TODAY our country is celebrating the fortieth anniversary of the great October socialist revolution. We are drawing up accounts, not only of the achievements of industry and agriculture, but also of the general growth of culture, and in particular of science. The progress of Soviet physics is of decisive importance in any review of the level of scientific culture in our country. Of all experimental sciences, it is physics which discovers the laws of material behavior which underlie the development of other natural sciences and of modern technology. The level which has been reached in the development of physics is thus an objective measure of the general growth of science and technology in the country. Of all experimental sciences, modern physics demands the most complicated and expensive equipment. Nowadays only a strong country, with widely diversified industry and a high level of technology, can achieve a successful development of experimental physics.

Even to the non-specialist it is clear that here in the USSR, after forty years of Soviet power, physics has risen to an exceptionally high level. The study of atomic nuclei is generally regarded as one of the most advanced parts of physics. Thanks to a succession of fundamental discoveries in recent decades, this branch of physics is being intensively developed. It has become an indispensable foundation for the technical utilization of atomic energy, both for peaceful purposes and for national defense. Soviet technology, with remarkable speed and success, found original solutions to the problems of designing thermonuclear weapons and of exploiting atomic energy for peaceful purposes. This would have been impossible, if there had not existed in the Soviet Union a massive and vigorous research effort in modern physics.

Soviet science recently achieved a new and outstanding success, the launching of the first artificial earth satellites. In this achievement also, the high level of our physics played an essential part.

A wide variety of scientific and physical research is carried out in the Soviet Union in a large number of institutes spread over the whole country. Our achievements in the fields of theoretical physics, nuclear physics, low-temperature physics, optics, semiconductors, solid state, theory of combustion, etc. are well-known to readers of this journal from the published reports of the members of these institutes. The continuous growth of Soviet physics is not only reflected in the increasing size of this journal, which has grown by a factor of 3 — 4 in the last five years. The USSR Academy of Sciences is also continually forced by the shortage of space in this journal to start new journals devoted to specialized parts of physics, for example crystallography, optics, metallurgy, technical physics, acoustics, electronics, etc.

If one tries to compare the volume of scientific work in physics before the revolution, 40 years ago, with the volume existing now, it is hard even to find a meaningful standard of comparison. One must remember that all physics in pre-revolutionary times was concentrated in the laboratories of a few institutions of higher education. In the cost of their equipment, all these physics laboratories taken together were equal only to a small fraction of a modern accelerator, such as the Synchrophasotron built at the Joint Institute of Nuclear Studies at Dubno on the Volga. This remarkable machine was put into operation this year, and it accelerated elementary particles to the record energy of 10 billion volts.

Of course, the large-scale growth of physical research in recent decades has occurred not only in our socialist country but also in the more advanced capitalist countries such as the United States and England. Both in capitalist and socialist countries, we observe the same nature encompassing us and we find the same laws governing the behavior of physical processes. But the organization of the same scientific work under socialist and capitalist governments is essentially different, and the difference becomes more and

more evident as the socialist economy develops. The difference arises from the fact that under a socialist government science is regarded as the foundation upon which the material and spiritual culture of a country is built. This attitude towards science has two consequences. First, the encouragement of scientific progress is one of the basic responsibilities of the government. Second, the various branches of science are not developed independently as in capitalist countries, but in accordance with the general growth of the material and spiritual culture of the country. Under a socialist government the development of science must be planned and financed out of government funds according to a unified plan. We must admit that it has not been easy in practice to find a form of organization in which science could develop not independently but according to a reasonable plan, and to find a rational method of governmental financing of scientific institutes which could preserve the creative approach of a scholar to his work. In spite of the excellent work of our physicists, we still have to continue striving for improved forms of organization for scientific work, so that our scientists can work as purposefully and as productively as possible.

When one compares the organization of scientific work under socialist and capitalist governments, the question always arises of the difficulty of reconciling the freedom necessary for effective creative work with a rigidly constituted plan. When the Academy of Sciences began to develop a planned organization of scientific work, there was an attempt to make the plan completely rigid and detailed, and this difficulty became a real one. But time and experience provided the remedy. The basic task of a plan is to point to those fields and programs of scientific development which are at a given moment most important to the country. Today the most effective method of ensuring the coherent development of science is to encourage those scientific endeavors which have a close relation to applied fields, to technology, to industry, to medicine, to agronomy and other studies concerned with the national economy, or to problems of basic importance for the whole of science. The more practical lines of research receive a greater share of attention, material support, and encouragement; the government gives official recognition to such work by the award of Stalin and Lenin prizes, etc. The state tries all the time to guide scientists into tackling either major problems of the national economy or problems of basic scientific importance. Scientists are confronted with broadly defined questions, for example, the production of extremely pure chemical elements or of high-quality heat-resistant steels, the understanding of physical processes in semiconductors, various problems of modern power technology connected with the transmission of energy over large distances, etc. These questions are usually complex, they can be divided into many independent parts belonging to various fields of science and technology, but it is still necessary to attack them in a unified way. Physicists often are allotted the most difficult questions of all. In order to answer such questions, a physicist must concentrate upon the study of some definite field of knowledge within which he himself must search for a concrete line of attack. He retains a wide freedom for personal and creative initiative. Several institutes often are attracted to the same question, each working along a direction of its own choice.

The USSR is still far from the end of the search for methods of organizing science as the foundation of a planned socialist economy. The form of organization, especially for the specialized branch institutes, is mainly determined by the administrative structure of industry. We have learned by experience that the structure of our economy changes continually. The change is certainly now in the direction of democratic centralism. A massive reorganization of the economy in this direction is now in progress. The basic idea of the reorganization is that the central authority should retain only general supervisory functions, such as the development and promotion of new techniques and the broad coordination of the economy of the whole country. The detailed management of industry is handed over to regional organizations. From this reorganization of the economy a reorganization of scientific work will inevitably follow. The detailed planning and organization of the actual work will be more and more concentrated in the working organs of the scientific institutes themselves, for example in committees of scientists. Broad scientific planning, dealing with the general problems of the growth of a socialist culture on a national scale, will be handled centrally by such organizations as the Academy of Sciences, Gosplan, and other departments of the central government. The planned organization of science which has been achieved in the Soviet Union is already producing greater efficiency and better utilization of scientific manpower and equipment.

When we consider the contact of science, and in particular of physics, with the practical problems of national life, we find that this contact is already far more effective in the Soviet Union today than in the most advanced capitalist countries. This explains the rapid pace at which Soviet scientists and engineers solved the most difficult problems of nuclear technology, jet-propulsion technology, aviation, radio, metallurgy, power technology, etc. Although the Soviet Union is still some way behind the United States in the production of some important items, the USSR has held and still holds the record for the speed at

which scientific and technical problems have been solved and the results put into practical operation. This can be explained only by the close and friendly contact between science and technology, which is possible under our government. It is possible mainly because in our socialist country there is only one all-powerful landlord, and that landlord is the people. Under capitalism, where industry is in private hands and companies are often competing against one another, scientific organizations are largely left to their own devices. The coordinated activity of all scientific and industrial resources, which is naturally and simply achieved in a socialist country, is under capitalism impossible.

The rate of growth of Soviet physics, and of all branches of science, is nevertheless influenced by our contacts with foreign science. We all believe that the basic task of science is the understanding of nature, and the basic purpose of this understanding is the conquest of nature for the benefit of mankind.

Scientific truth is one, and the more rapidly it is discovered and the more intensively science is developed the greater the benefit to all mankind. Nowhere in the history of human culture has international cooperation given such great benefits to humanity as in the field of science.

We are very happy that in all these years our journal has not only been widely read here in the Soviet Union but has also had a wide foreign circulation. We welcome the recent appearance of the "Journal of Experimental and Theoretical Physics" overseas in an English translation.

International professional contacts between scientists are valuable not only to progress in science. Understanding between scientists leads also to understanding and trust between countries. Peaceful coexistence, so necessary for happy and prosperous human life, is impossible without trust between peoples. Physicists more than anybody else should now be concerned for peace, since they have the responsibility before mankind for putting into our hands weapons of annihilation which if carelessly handled could lead to misery on an unprecedented scale.

Translated by F. J. Dyson
227

INVESTIGATION OF THE THERMAL PROPERTIES OF SUPERCONDUCTORS

1. TIN (DOWN TO 0.15°K)

N. V. ZAVARITSKII

Institute for Physical Problems, Academy of Sciences, U.S.S.R.

Submitted to JETP editor April 4, 1957

J. Exptl. Theoret. Phys. (U.S.S.R.) **33**, 1085-1098 (November, 1957)

Measurements have been made of the thermal and thermometric conductivities of several samples of tin in the range from 0.15 – 4°K. These make it possible to determine the specific heat of tin down to 0.15°K. It has been found that, below 0.45°K, the specific heat is due to the lattice and varies according to Debye's law, with $\Theta_D = 202 \pm 3$°K. Above 0.45°K, the specific heat of the electrons appears, which depends on temperature as $c_{es} = A(T) \times \exp(-\alpha T_c/T)$. The free energy of the superconducting electrons below 3°K, determined on the basis of these measurements, can be represented as $F_{es} = BT^n \exp(-\alpha T_c/T)$, where $B = 8.7 \times 10^{-4}$ joules/g-mole-deg, $n = 2.5 \pm 0.5$, $\alpha = 1.35 \pm 0.1$. The thermal conductivity of tin below 0.3°K for all specimens is due to the heat transfer by the phonons; one of the samples exhibited a reflection effect of the phonons from the mirror surface. For higher temperatures, the thermal conductivity of the electrons varied for all samples as $K_{es} = \text{const} \cdot \exp(-\beta T_c/T)$, $\beta = 1.45 \pm 0.05$. The results are discussed from the point of view of the presence of an energy gap in the excitation spectrum of superconductors.

As is well known, the analysis of data on the thermal properties allows us to obtain a number of indications concerning the energy excitation spectrum in solids. We can obtain the most definite conclusions in this case on the basis of the analysis of the specific heat of bodies over a wide range of temperatures.

extending to the lowest temperatures possible. This latter is connected with the fact that the strictest theoretical considerations of the phenomenon are usually successfully carried through only in the region close to absolute zero, where the number of excitations is small. At the present time, information on the specific heat of bodies in this temperature region is limited. This also applies to the phenomenon of superconductivity. Fundamental measurements of the specific heat of superconductors[1-4] have been made only in the temperature range down to $T_c/T \approx 3$, and do not allow us to draw any unique conclusions as to the character of the energy excitation spectrum. Furthermore, experiments[5-7] recently carried out in the temperature interval down to $T_c/T = 4$ have shown that the temperature dependence of the specific heat of superconductors discussed earlier does not correspond to reality.

The problem of the thermal conductivity is much clearer at present; at least, completely substantiated results have been obtained in a number of works[8-9] down to $T_c/T = 10$.

The aim of the present research was the investigation of the thermal properties of superconductors over the widest temperature range possible. Since the critical temperature for most superconductors amounts to a few degrees, measurements of the specific heat down to temperatures of a few tenths of a degree are necessary for the solution of the problem. At these temperatures, the specific heat of most substances is negligible, which poses difficulties in the application of the direct method of measurement of the specific heat. As a consequence of this fact, an indirect method has been chosen for the measurements, based on a calculation of the specific heat of a body from its thermal conductivity K and its thermometric conductivity $a^2 = K/c\rho$. The methods worked out at the present time permit us to measure the thermal conductivity of materials with relative ease at temperatures down to a few tenths of a degree, and the value of the thermometric conductivity can be determined by the method of temperature waves, already suggested by Angstrom.[10] The idea of this method is as follows. If the periodic variation of the temperature is $T(0, t) = A \cos \omega t$ at the point $x = 0$ of an infinite specimen, then a temperature wave

$$T(xt) = Ae^{-kx} \cos(\omega t - kx), \tag{1}$$

will be propagated, where

$$k = (1/a)\sqrt{\omega/2}.$$

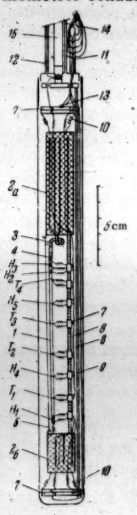

FIG. 1. Apparatus for the determination of thermal conductivity and temperature conductivity, (1) Sample under investigation; (2a, 2b) blocks of ferric ammonium alum; (3) copper heat conductors; (4) thermal resistance (bronze, of diameter 2 mm); (5) spring to draw lower end of sample with caprone thread; (6) coil of tinned constantan; (7) plexiglass blocks for fastening the leads; (8) copper rod for fastening the low-temperature components of the apparatus; (9) supporting frame (it consists of three bronze guide rods of 1.5 mm diameter and brass rings to which the salt is attached. All joints are sliding with stop screws); (10) spring for suspending the salt; (11) terminals of conductors from the apparatus by means of platinum sealed into the glass; (12) tube for the exit of conductors from thermometers T_2 and T_3; (13) carbon thermometer; (14) tube for evacuating and filling the apparatus with helium; (15) steel tube for fastening the apparatus; T = thermometers; H = heaters.

Thus, for the measurement of the thermometric conductivity, it suffices to determine either the propagation velocity of the temperature wave, or the law according to which its damping takes place. Until recently, the method of temperature waves has been applied only in the region of high temperatures;[11] very recently, it has been used in the region of liquid helium temperatures.[12] For low temperatures, this method takes on a number of specific peculiarities which are brought about by the sharp decrease in the specific heat, and correspondingly by an increase in the thermometric conductivity. As a consequence, while the length of the temperature wave for room temperatures amounts to centimeters at frequencies of hundreds of cycles, at helium temperatures these frequencies amount to thousands of cycles, which permits the use of standard radio methods in the measurements.

Tin was chosen as the object of investigation for the following reasons. In the first place, the new method of measurement of the specific heat is most successful on material whose specific heat has been

sufficiently well measured by generally accepted methods, if only in a narrow range of temperatures.[1,13,14] Second, the specific heat of the lattice and the superconducting electrons in the chosen material must be comparable in order to obtain even a preliminary indication as to the character of the change of both these quantities from analysis of the data.

METHOD OF MEASUREMENT

The apparatus used to determine the thermal and thermometric conductivities of samples at temperatures below 1.5°K is shown in Fig. 1. Cooling of the sample 1 was accomplished by two blocks of ferric ammonium alum 2a and 2b, the temperature of which was lowered by adiabatic demagnetization. To switch from isothermal magnetization to adiabatic demagnetization we used a method based on the absorption of residual gas by the salt.[15] The quantity of residual gas in the apparatus was controlled by heating the carbon thermometer 13, which is suspended on thin constantan conductors. The sample was cooled by means of the copper rod 3 of 2 mm diameter, the end of which, flattened out into a band of about 3 cm width, was pressed into the salt. A bronze rod 4 was sealed in between the sample and the copper heat conductor. The thermal resistance of this rod could be used to heat the sample up to one degree relative to the salt. For measurement, we used a coated carbon resistance thermometer. Thermometers T_2 and T_3 served to measure the thermometric conductivity of the sample, while thermometers T_1 and T_4 were used both to measure the thermal conductivity and to determine the temperature of the sample. These thermometers were calibrated in the course of each experimental run. Determination of the temperature was carried out by means of the susceptibility of the alum. To change from magnetic to absolute temperature, we used the data of Cook et al. of 1956.[16]

Several heaters were located on the sample. Heaters H_1, H_2 and H_3 were prepared from manganin wires, H_1 and H_2 being used in the measurement of the thermal conductivity of the sample and H_3 serving to increase the temperature of the sample above the temperature of the salt. The film heaters H_4 and H_5 were used in experiments on measurement of the thermometric conductivity of the sample. The electrical wiring inside the apparatus was accomplished by means of constantan wires coiled in springs. These wires were of diameter 50 μ, and were initially plated with a superconducting layer. To reduce electrical induction in measurements of temperature conductivity, the wires from the thermometers and the heaters were led separately through the salts 2a and 2b respectively.

The arrangement for the measurement of thermal conductivity did not differ from that used by us earlier[17] in the measurements at much higher temperatures. The mean error amounted to about 5% for a temperature gradient along the sample of several percent of the mean temperature. The accuracy of determination of the thermal conductivity was limited in this case not only by errors in the measurements of the temperature gradient along the sample or the power consumed in heating, but also by errors connected with the determination of the absolute temperature of the specimen. As a consequence of the fact that the thermal conductivity changes sharply with temperature, an error of 1% in the determination of the temperature is equivalent to three to eight times greater error in the thermal conductivity. On the other hand, it is hardly possible to determine an absolute temperature lower than 1°K by the generally accepted method of the susceptibility of a paramagnetic salt with an accuracy better than one percent.

Determination of the thermometric conductivity a^2 was carried out by means of the phase shift $\Delta\varphi$ of the temperature oscillations at two points of the specimen, the amplitude of which in all measurements did not exceed a few per cent of the mean temperature. As is easily seen from (1), $\Delta\varphi = k\Delta x$ for an infinite specimen, where Δx is the distance between the points at which the measurement is made, and

$$a^2 = \Delta x^2\omega/2\Delta\varphi^2. \qquad (2)$$

The method of temperature waves, which is simple in principle, requires a number of precautions. Above all, the temperature oscillations of the film thermometer, in spite of its minute dimensions, do not coincide with the temperature oscillations of the sample (the thickness of the coating of the carbon thermometer does not exceed 0.20 mm).

These phenomena are probably connected both with the small thermometric conductivity of the carbon and with the presence between the thermometer and the sample of a layer of BF dope of about 10 μ thickness, which serves as an electrical insulation of the thermometers from the sample. As a consequence, if φ is the phase shift of the temperature oscillation of the sample at the location of the thermometer relative to the signal from the generator, then the measured phase shift is $\xi = \varphi + \psi$, where ψ depends

on the construction peculiarities of the given thermometer. Correspondingly, the measured phase difference between the signals will be

$$\Delta\xi = \varphi_1 - \varphi_2 + \psi_1 - \psi_2.$$

Here, the quantity $\psi_1 - \psi_2$ can reach 30% of the quantity $\varphi_1 - \varphi_2$. However, since ψ does not depend on the direction of the temperature wave, $\psi_1 - \psi_2$ can be eliminated if we make use in the measurements of the temperature waves which are propagated in the two opposite directions. Actually,

$$\Delta\xi^+ - \Delta\xi^- = \varphi_1^+ - \varphi_2^+ + \varphi_2^- - \varphi_1^-,$$

where the plus and minus refer to the waves in different directions. We can obtain the actual value of the phase shift along the sample only if

$$\varphi_1^+ - \varphi_2^+ = \varphi_2^- - \varphi_1^-,$$

i.e., the law of phase change along the specimen is the same for waves of both directions. This holds either for an infinite specimen or when an identical reflection of the wave takes place from the ends of the sample. In the latter case, however, the connection of the phase shift and the thermometric conductivity is complicated, which makes the treatment of the results difficult. For example, as is easy to show, for thermal insulation of the end of the sample, $\varphi(x) = \arg\cosh k(1+i)x$, where x is the distance from the end of the sample, and correspondingly

$$\Delta\varphi = \arg\cosh k(1+i)x_1 - \arg\cosh k(1+i)x_2. \qquad (3)$$

Therefore, it is always desirable to have conditions in which the effect of the reflected wave is negligibly small.

In the work the measurement of the phase shift was carried out between thermometers placed in the central part of the sample, so that the distance to each of the ends of the sample exceeded by two the distance between them.

TABLE I. Phase shift $\Delta\varphi$ of the temperature wave along finite and infinite specimens.

Ratio of the distance between thermometers to the wavelength	$\Delta\varphi_\infty$ in radians	$\Delta\varphi_{fin}$ for $2x_1 = 3x_2\Delta\varphi$, in radians
0.1	0.314	0.408
0.12	0.376	0.500
0.15	0.472	0.600
0.20	0.628	0.690
0.225	0.706	0.785
0.25	0.795	0.792
0.30	0.940	0.930
0.375	1.178	1.168
0.500	1.571	1.571

If we compare $\Delta\varphi_\infty$ for the infinite specimen and $\Delta\varphi_{fin}$ computed according to (3) for the chosen geometry, for various ratios of the distance between the thermometers $\Delta x = x_2 - x_1$ to the length of the temperature wave $\lambda = 2\pi/k$, then it turns out (see Table I) that for $\Delta x/\lambda \geq 0.25$, the difference between the phase shifts $\Delta\varphi_\infty$ and $\Delta\varphi_{fin}$ does not exceed 1%. In actuality, this is the upper limit of possible deviation, since only one end of the sample is thermally insulated. At the point of connection of the sample with the bronze, only partial reflection of the wave takes place. We can estimate the magnitude of the amplitude of the reflected wave in terms of data on the thermal conductivity and specific heat of the bronze and the tin. For equal diameters of the sample and the bronze rod, it amounts to about 90% of the amplitude of the indident wave for 1°K, and to about 30% for 0.3°K.

Reflection of the temperature wave also takes place from inhomogeneties in the cross section of the specimen, especially from the thermometers and heaters located on the sample. This effect could play an especially important role for temperatures of a few tenths of a degree, where, because of the different temperature dependence of the specific heat of the tin and the copper wires leading to the thermometer, the specific heats of the thermometer and of the cross section of the sample which it occupies are equal. It is also easy to compute the reflection of the wave from the thermometer, under the assumption that it takes part as a whole in the temperature oscillations of the sample. If the dimensions of the thermometer are much smaller than the wavelength of the temperature wave, then the ratio of the reflected wave to the incident is

$$\gamma \approx \frac{c_t}{c_s}\frac{\pi\Delta}{\lambda},$$

where c_s and c_t are respectively the specific heat of the sample and the thermometer; λ is the length of the temperature wave, Δ is the width of the thermometer. Assuming that the specific heat of the thermometer is equal to the specific heat of the cross section of the sample, it is easy to obtain that for $\Delta = 0.2$ mm, at wavelengths greater than 4 cm, $\gamma \approx 10^{-2}$. In reality, the amplitude of the reflected wave

from the thermometers and the heaters is still smaller, since the temperature oscillations of the thermometer, especially at high frequencies, are much less than the temperature oscillations of the specimen. In particular, this appears as a sharp decrease in the signal from the thermometer for increase of the frequency of the temperature oscillations (in a frequency change from 40 to 800 cps, the signal decreases by a factor of 20). All that has been pointed out above shows that the effect of reflection of the temperature wave from the thermometer cannot have a material effect on the measurements. This is further confirmed by the absence of the effect of the mutual location of the thermometers and heaters on the results of the measurement of the thermometric conductivity (see below).

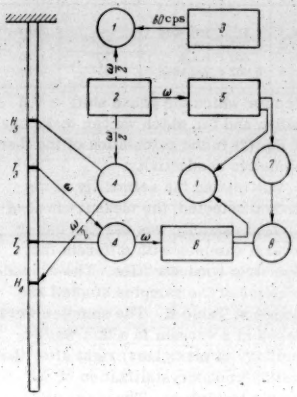

FIG. 2. Circuit for measurement of thermometric conductivity. 1—oscillograph, 2—generator, 3—quartz generator, 4—switch, 5—tuned filter, 6—tuned amplifier, 7—phase shifter, 8—phase detector.

A block diagram of the apparatus used for the measurement of the phase shift is shown in Fig. 2. The signal from an oscillator of frequency $\omega/2$ is applied to the heaters H_4 or H_3. Since the heat liberated in the heater is proportional to I^2R, a temperature wave of frequency ω is propagated along the sample. The signal from thermometer T_2 or T_3 is fed to a tuned amplifier of center frequency ω and with a bandwidth of 10% of the center frequency. From the output of the amplifier, the signal is fed to an oscilloscope which serves as a control of the amplitude of the signal from the amplifier and to a cathode follower which is connected to a phase lag detector.[18] A signal is also applied to the phase detector through a calibrated phase-shifter from a separate generator of frequency ω. In order to increase the stability of the circuit against possible changes in the frequency, this signal was passed through a filter exactly the same as that used in the amplifier. The measurements were carried out by a null method. Successive measurements were made of the phase angle between the signals from thermometers T_2 and T_3 and from the generator, which made it possible to determine the phase shift between the signals from the thermometers. In this case, by this method of measurement, one of the signals on the phase lag detector was of a strict definite frequency ω, and the whole circuit was little sensitive to a stray electric pickup. The error in the determination of the angle between the signals from the thermometers did not exceed 0.01 radian ordinarily, and was governed with the accuracy of calibration of the phase shifter. The measurements were carried out at several frequencies, multiples of 60 cps — the frequency of the quartz generator which served for testing the frequency of the fundamental generator. Before the measurements the oscillator was usually turned on and the dc current through the thermometers left turned off to check whether the thermometers picked up any extraneous signals.

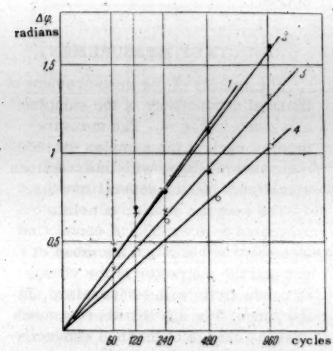

FIG. 3. Dependence of the phase shift on the frequency f of the oscillator. Sample Sn 2; distance between thermometers 23.2 mm, length of sample 100 mm. 1—T = 4.35; 2—T = 0.558; 3—T = 0.730; 4—T = 1.12°K. Abscissa is plotted in terms of $f^{1/2}$.

The typical dependence of the phase shift of the temperature wave along the sample $\Delta\varphi = (\Delta\xi^+ - \Delta\xi^-)/2$ on the frequency of the oscillator $f = \omega/2\pi$ is plotted in Fig. 3. For sufficiently high frequencies, even in an infinite sample, $\Delta\varphi$ is proportional to $f^{1/2}$; in the region of much lower frequencies, there are observed significant departures from the proportionality of $\Delta\varphi$ and $f^{1/2}$, which is in qualitative agreement with the calculation of the effect of the reflected temperature wave from the end of the sample, carried out above. Therefore, the fundamental measurements were carried out only at frequen-

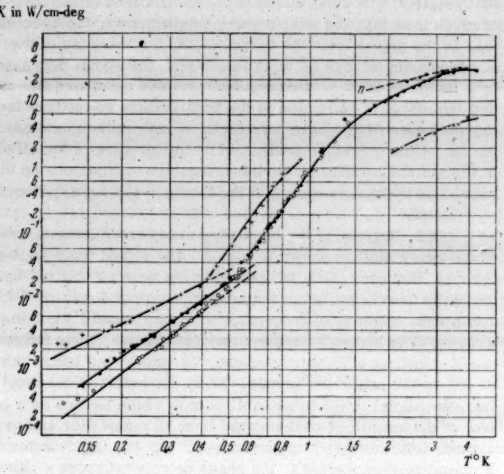

FIG. 4. Thermal conductivity of investigated samples of tin. n — thermal conductivity of tin in normal state. × — sample 1, ● — sample 2, ○ — sample 3, and + — sample 4.

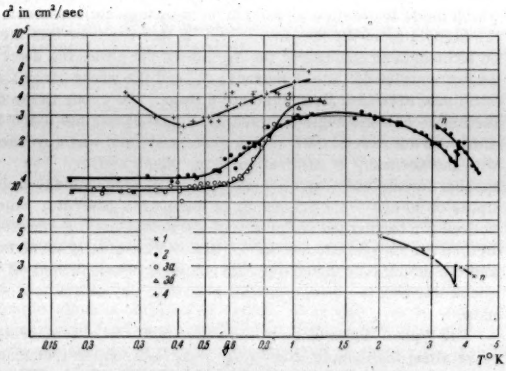

FIG. 5. Thermometric conductivity of investigated samples. 1, 2, 3, 4 — number of samples, n — tin in the normal state; 3a and 3b — measurements for different reciprocal positions of thermometers and heaters; a — distance between thermometers 15.6 mm, from thermometer to nearest heater 15 mm; b — distance between thermometers 20 mm, to heater 5 mm.

TABLE II. Characteristics of samples

Number of sample	Percentage impurity	State of surface	Angle between axis of sample and (001) direction	Diameter mm
Sn 1	0.1	polished	—	1.89
Sn 2	0.002	rough	30°	1.72
Sn 3	0.002	rough	70°	1.40
Sn 4	0.002	polished	45°	1.81

cies for which the phase shift ≥ 0.8 radian and for which we can make use of Eq. (2) in the calculation of the thermometric conductivity.

For testing the reliability of the method selected, the measurement of the heat capacity was carried out on several samples with different thermometric conductivities. The characteristics of the samples studied are plotted in Table II. The samples were placed in a vacuum in a thin walled capillary of plexiglass; right after the casting, monocrystallization of the sample took place. The glass was usually removed by etching with hydrofluoric acid. For preparation of the specimen Sn 4, such a thin wall capillary was chosen that after casting of the tin, the glass cracked and fell off the specimen without external action.

RESULTS OF MEASUREMENT

The results of the measurement of thermal conductivity of the samples are given in Fig. 4. The measurement of each of the samples extended over several days, with interruptions sometimes lasting several months.

The average scatter of points amounted to about 5%. A connection was observed between the mean error and the character of the change of conductivity with temperature. In the range $T > 0.5°K$, where a much sharper change of thermal conductivity takes place with change in temperature, it does not exceed 4%. All this is in agreement with the analysis of errors worked out above.

In Fig. 5, results are given for the measurement of the thermometric conductivity of all samples studied.

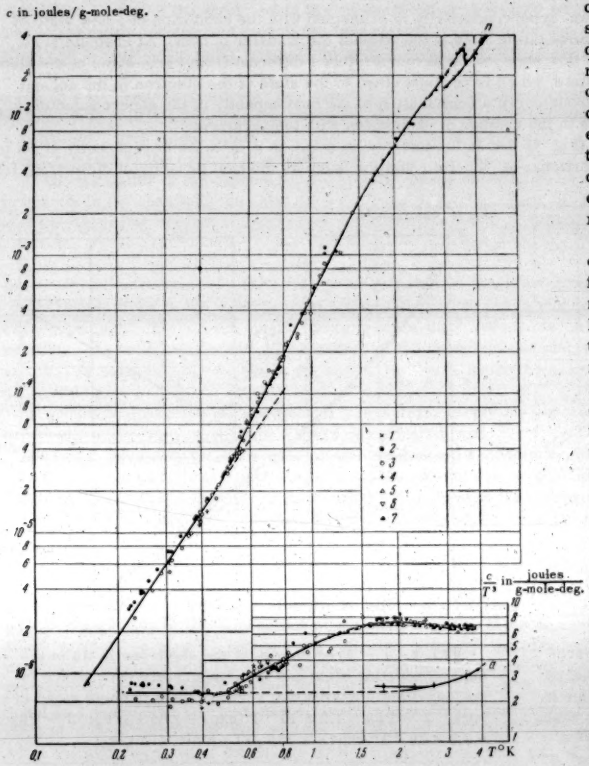

FIG. 6. Heat capacity of tin. 1, 2, 3, 4 — our measurements, n — normal state, 5, 6, 7 — calorimetric measurements; 5 — from the data of Ref. 1, 6 — from the data of Ref. 13, 7 — from the data of Ref. 14; a — heat capacity of the lattice from Ref. 14. The ordinate is plotted in terms of $(c/T^3) \times 10^4$.

As in measurements of thermal conductivity, measurement of each sample was extended over several days, between which the arrangements of thermometers and heater on one of the samples (Sn 3) was completely changed. The mean error in the determination of the thermal conductivity does not exceed 2.5%, which agrees with the characteristics which apply to a radio circuit.*

The results of the calculation of the heat capacity of the samples from their thermal and thermometric conductivities are given in Fig. 6. In this case, at temperatures above 1.7°K, where the thermometric conductivity is more strongly changed than the thermal conductivity, the mean value of the thermal conductivity and the exact thermometric conductivity were used; for temperatures lower than 1.7°K — conversely — we used the mean value of the thermometric conductivity and the exact thermal conductivity. The mean scatter of the values of the heat capacity for temperatures below 1°K amounted to about 7% and at temperatures higher than 1.5°K to about 2%, which is in agreement with the accuracy of measurement of the thermal and thermometric conductivity. We note that the value of the heat capacity obtained can differ systematically from the true value by 3 — 5% because of possible errors in the determination of the geometric dimensions of the samples and the distance between thermometers.

If we compare Figs. 4, 5, and 6, it is easy to note that while the thermal and thermometric conductivities of the samples studied differ in absolute value (up to 8 times), the temperature dependence of the heat capacity is the same for all samples. This is an additional confirmation of the reliability of the method of measurement employed. We note that in the region of helium temperatures the values of the heat capacity we obtained are, within the limits of accuracy, in agreement with the results of their determination by calorimetric methods.[1,13,14]

*The results of measurement of the thermal conductivity of sample Sn 4 at $T > 0.8$°K are not very reliable, since even for the highest frequency $\omega = 1.22 \times 10^4$, the phase shift along the sample for several measurements did not exceed 0.8 radian. These data were not used in the determination of the heat capacity.

DISCUSSION OF RESULTS

Heat capacity. As is well known, superconductivity is connected with the excitation of a new state of the electrons, in which they can move through the metal without the transfer of heat. At absolute zero, evidently, all the electrons are in this state, while at temperatures different from zero, some of the electrons pass over into the excited state, which is perhaps close to the state of the electron in the normal metal. It is natural that the electrons carry a contribution to the heat capacity of the superconductor c_{es}, connected perhaps with the change in the number of excitations with temperature.

Results of measurement show (Fig. 6) that in the interval from 0.2 to 0.45°K the heat capacity of tin in the superconducting state is proportional to T^3, i.e., just the same as the heat capacity of dielectrics for

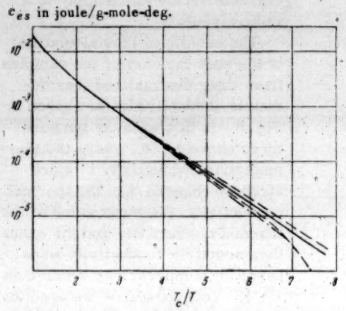

FIG. 7. Electronic heat capacity in tin in the superconducting state. The dashed lines represent the mean error, the dot-dash is $c_{es} = A \exp(-1.5\, T_c/T)$.

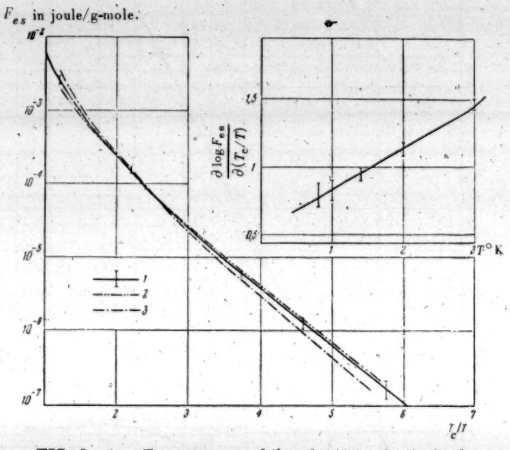

FIG. 8. 1 — Free energy of the electrons in tin in the superconducting state and the temperature dependence of its logarithmic derivative; vertical lines indicate mean errors; 2 — $F_{es} = 1.2 \times 10^{-3} T^2 \exp(-1.45\, T_c/T)$; 3 — $F_{es} = 5.3 \times 10^{-4} T^3 \exp(-1.25\, T_c/T)$ joule/g-mole.

sufficiently low temperatures. Therefore, it is natural to assume that below 0.45°K the heat capacity of tin is due in general only to the lattice. In this case, although the absolute value of $c/T^3 = 2.36 \pm 0.10 \times 10^{-4}$ joule/g-mole-deg^4 (this corresponds to $\Theta_D = 202 \pm 3$°K) is 10% smaller than the limiting value of c_p/T^3 (c_p = heat capacity of the lattice), obtained from the analysis of the heat capacity of tin in the normal state,[14] it is not excluded that in actuality this difference is due to an insufficiently accurate determination of c_p above 1°K, and the heat capacity of the lattice in the normal and the superconducting states agree with one another, changing with temperature in accord with the curve denoted by the dashed line in Fig. 6. The entire difference between c and c_p from this point of view is due to the heat capacity of the electrons.

The dependence of the heat capacity on T_c/T is plotted semi-logarithmically in Fig. 7. It can be represented in the form of the expression $c_{es} = A(T) \exp(-\alpha T_c/T)$. It should be emphasized that if in the heat capacity which is not connected with the lattice, a term in present which is proportional to T^3, as follows from a series of theoretical researches,[19,21] then its value at the critical temperature does not amount to 5% of the total electronic heat capacity. It should be noted that recently a series of experimental researches[6,14] reached conclusions on the change in the heat capacity of superconductors according to the much simpler law $c_{es} = \text{const} \exp(-1.5\, T_c/T)$. These results show that the erroneous results were probably connected with an insufficiently wide interval of measurement of the heat capacity (the measurements were carried out only down to $T_c/T = 4$).

From the analysis of the dependence $c_{es} = \Phi(T_c/T)$, it could be established only that the factor of the exponent is some polynomial function of T. However, it could be expected that on the basis of ther-

modynamic functions it will have a simpler form. We therefore determined by double integration the part of the free energy of the electrons in the superconductor depending on the temperature [F_{es} (Fig. 8)]. The temperature independent part of the free energy F_{es0} can be obtained from the equality of the free energy of the electrons in the normal and superconducting states at the critical temperature. Under the assumption of the equation for the free energy of the electrons in the normal state $F_{en} = \frac{1}{2}\gamma T^2$, where $\gamma = 1.75 \times 10^{-3}$ joule/g-mole-deg is a constant in the linear law of variation of the heat capacity, $F_{es0} = (5.8 \pm 0.4) \times 10^{-3}$ joules/g-mole, which corresponds to the critical magnetic field for 0°K, $H_{c0} = 301 \pm 6$ oersted. This value, within the limits of accuracy of determination, agrees with the results of direct measurements of the critical magnetic field.

If the multiplier of the exponential in the free energy depends on temperature, then this manifests itself primarily in the change in the value of $\partial \log F_{es}/\partial(T_c/T)$. Thus, if $F_{es} = B T^n \exp(-\alpha T_c/T)$, then

$$\frac{\partial \log F_{es}}{\partial (T_c/T)} = \frac{1}{2.3}\left(\alpha + n\frac{T}{T_c}\right),$$

which lets us determine both the quantity α and also n. Analysis of the dependence of $\partial \log F_{es}/\partial(T_c/T)$ on the temperature in the interval from 0.8 to 3°K (Fig. 8) shows that $\alpha = 1.35 \pm 0.1$; $n = 2.5 \pm 0.5$ and correspondingly, $B = 0.7 \pm 3.4 \times 10^{-4}$ joule/g-mole-deg^n (of course, all these quantities are in functional relation). As an illustration of the character of the change in the quantity F_{es} in its dependence on n and α, we have also drawn $F_{es} = \psi(T_c/T)$ in Fig. 8, under the assumption of the most extreme values of n and α.

It should be noted that the exponent n characterizes only the general change of the factor before the exponent, which can actually have a more complicated form.

Thermal conductivity. As is well known, the thermal conductivity of a metal can be represented as the sum of electron and lattice conductivities. In the case of a superconductor, we can thus consider separately the thermal conductivity of the electrons K_{es} and of the lattice K_{ps}. As studies have shown, in the region of sufficiently low temperatures, the lattice plays an essential role in the transfer of heat. Let us consider our results from this point of view.

The thermal conductivity and heat capacity of the lattice are related: $K_p = \frac{1}{3} l u c_\rho$, where l is the mean free path of the phonon, u is the mean velocity of sound, c_ρ is the heat capacity. As is known, in perfect dielectric crystals at temperatures below $\Theta_D/30$ (Θ_D is the Debye temperature) the mean free path is determined by the dimensions of the sample and by the condition of its surface. In samples with a rough surface, from which phonons are reflected diffusely, the path length does not depend upon the temperature, coinciding with the diameter of the sample. At temperatures below 0.45°K, this is observed in the samples Sn 2 and Sn 3 investigated by us. Thus, the free path length in these samples is shown to be equal to 1.45 mm and 1.18 mm, respectively, which, taking into account the approximate character of the method of determination of this quantity, we can consider reasonably satisfactory agreement. However, while the path length does not change with temperature in Sn 3 ($K_p \sim T^3$), in Sn 2, a certain increase in the free path length takes place upon decrease in temperature in Sn 2 ($K_p \sim T^{2.9}$). Evidently this is connected with the presence of reflection of the phonons from the surface of the sample. This effect is especially sharp in the sample Sn 4, which possesses a polished surface, the thermal conductivity of which below 0.4°K changes proportionally to T^2, appreciably exceeding the thermal conductivity of samples with a rough surface. Actually, as is easily shown,[22] the specular reflection of n phonons from the surface of the specimen leads to an increase in the mean free path by $(1 + n)/(1 - n)$. The value of n increases upon lowering of the temperature as a consequence of the increase of the wavelength of the phonon, up to a value comparable with the inhomogeneities of the surface of the specimen. Experiments with etching of the surface of sample Sn 4 (which led to a decrease in its thermal conductivity for $T < 0.4$°K to the value of the thermal conductivity of samples Sn 2 and Sn 3) confirm this point of view.

A similar reflection was observed in the study of the thermal conductivity of a series of dielectrics.[22,23*] Thus, from the point of view of the essential representation of the thermal conductivity of dielectrics it proves possible to explain both the absolute value of the thermal conductivity of tin below 0.4°K, and also its temperature change. This result agrees entirely with the conclusions of previous investigations of the thermal conductivity of superconductors at temperatures below 1°K.[8,9]

*According to a private communication from D. Shoenberg, reflection of phonons from a surface of tin has also been observed by Graham at Cambridge.

Everything that has been said above permits us to connect the sharp change in the temperature dependence of the thermal conductivity of Sn 2, Sn 3 and Sn 4 at 0.57, 0.5 and 0.42°K, respectively, with the appearance of the electronic thermal conductivity K_{es}, which can itself be determined under the assumption of the constancy of the laws of change of the lattice thermal conductivity even for temperatures above 0.5°K. A similar assumption, as the measurements of Laredo show, is valid up to 0.8 — 1°K. Above these temperatures, the thermal conductivity of the lattice begins to fall off sharply, because of the scattering of the phonons by electronic excitations. The value of this conductivity reaches a negligible value for helium temperatures, which allows us to determine K_{es} in this region of temperatures also. The dependence of K_{es} on T_c/T, obtained by the method described above, is shown in Fig. 9. As is easy to see, the change in the thermal conductivity with temperature is determined for all the samples studied by one and the same exponential term

$$K_{es} = \text{const} \cdot \exp(-\beta T_c/T),$$

where $\beta = 1.45 \pm 0.05$. All the results known to us of the determination of the electron thermal conductivity of tin below 1°K[8,24] do not contradict this dependence.

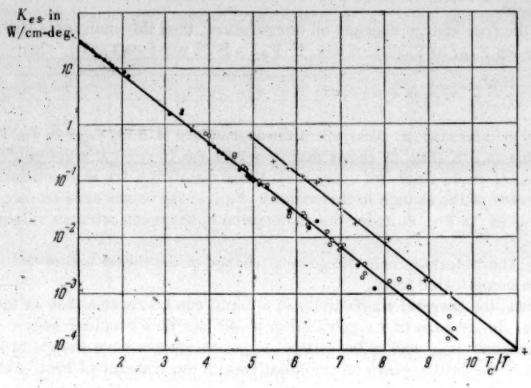

FIG. 9. Electronic thermal conductivity in tin in the superconducting state ● — Sn 2; ○ — Sn 3; + Sn 4.

The dependence on the temperature of the electronic thermal conductivity of the superconductor in the region of temperatures where the number of excitations is small, is determined primarily by the change of the number of excitations with temperature. The length of the free path of the excitations at these temperatures is evidently the same as in the normal metal, depending only on the chemical and physical purity of the sample, and does not change with the temperature. From this viewpoint, the character of the temperature dependence of K_{es} points out the exponential change with temperature of the number of excitations in the superconductor.

This position could be verified also by the temperature dependence of the normal conductivity in the superconductor, the depth of penetration of the magnetic field in the superconductor, the absorption of ultrasound in the superconductor, but the measurement of all these quantities at sufficiently low temperatures has not been carried out.

The results of the measurement both of the thermal conductivity and the heat capacity show the fundamental temperature change of these quantities is determined by the exponential factor. This testifies to the fact that the excited state of the electrons in the superconductor is distinct from the basic energy gap. Actually, similar representations (see Ref. 25) lead at once both to the presence of the exponent in the free energy of the electrons and to an exponential change of the number of excitations with temperature. From this viewpoint, most attention attaches to the measurement of the value of the energy gap by different methods. The fact is that the exponent in αT_c is, generally speaking, only proportional to the width of the energy gap Δ. The coefficient of proportionality is connected with the character of the appearance and annihilation of the excitations or, more precisely, with the location of the Fermi surface at the middle of the gap as, for example, in semi-conductors, $\alpha T_c = \Delta/2$. However, at the present time, direct measurements which would permit the determination of Δ with sufficient accuracy are lacking, although qualitative observations of the transparency of films of tin[26] in the region of high frequencies show that possibly αT_c is actually close to $\Delta/2$.

The author expresses his deep gratitude to A. A. Abrikosov, P. L. Kapitza, L. D. Landau, and A. I. Shal'nikov for valuable discussions in the course of completion of the work.

[1] W. H. Keesom and P. H. Van Laer, Physica **5**, 193 (1938).
[2] B. N. Samoilov, Dokl. Akad. Nauk SSSR **86**, 385 (1952).
[3] Horowitz, Silvidi, Malaker, and Daunt, Phys. Rev. **88**, 1182 (1952).
[4] J. R. Clement and E. H. Quimell, Phys. Rev. **92**, 258 (1953).
[5] Worley, Zemansky, and Boorse, Phys. Rev. **92**, 52 (1953); **99**, 447 (1955).
[6] Corak, Goodman, Satterthwaite, and Wexler, Phys. Rev. **102**, 656 (1956).
[7] B. B. Goodman, Conference de Physique des Basses Temperatures, Paris, 1955, p. 506.
[8] S. G. Laredo, Proc. Roy. Soc. (London) **229 A**, 473 (1955).
[9] K. Mendelssohn and C. A. Renton, Proc. Roy. Soc. (London) **230 A**, 157 (1955).
[10] A. J. Angstrom, Ann. Physik **114**, 513 (1861).
[11] E. G. Shvidkovskii, J. Tech. Phys. (U.S.S.R.) **8**, 934 (1938).
[12] Howling, Mendoza, and Zimmerman, Proc. Roy. Soc. (London) **229 A**, 86 (1955).
[13] K. G. Ramanathan and T. M. Srinevasan, Phil. Mag. **46**, 338 (1955).
[14] W. S. Corak and C. B. Satterthwaite, Phys. Rev. **102**, 662 (1956).
[15] N. Kurti and F. Simon, Physica **1**, 1107 (1934).
[16] Cooke, Meyer, and Wolf, Proc. Roy. Soc. (London) **233 A**, 536 (1956).
[17] N. V. Zavaritskii and A. G. Zel'dovich, J. Tech. Phys. (U.S.S.R.) **26**, 2033 (1956); Soviet Phys. JTP **1**, 1970 (1956).
[18] C. Schafer, Electronics **27**, No. 6—A, R—16 (1954).
[19] C. J. Gorter and H. B. G. Casimir, Phys. Z. **35**, 963 (1934).
[20] V. L. Ginzburg, Usp. Fiz. Nauk **48**, 25 (1952).
[21] Iu. L. Klimontovich, J. Exptl. Theoret. Phys. (U.S.S.R.) **28**, 754 (1955), Soviet Phys. JETP **1**, 602 (1955).
[22] Berman, Simon, and Ziman, Proc. Roy. Soc. (London) **220 A**, 171 (1953).
[23] Berman, Foster, and Ziman, Proc. Roy. Soc. (London) **231 A**, 130 (1955).
[24] B. B. Goodman, Proc. Phys. Soc. (London) **66 A**, 217 (1953).
[25] V. L. Ginzburg, J. Exptl. Theoret. Phys. (U.S.S.R.) **14**, 133 (1946).
[26] R. E. Glover and M. Tinkham, Phys. Rev. **104**, 844 (1956).

Translated by R. T. Beyer
228

THE INTERACTION BETWEEN LIGHT ATOMIC NUCLEI AND PARTICLES WITH ENERGIES OF 10^{12} TO 10^{13} EV

N. L. GRIGOROV, V. Ia. SHESTOPEROV, V. A. SONINIAKOV, and A. V. PODGURSKAIA

Moscow State University

Submitted to JETP editor April 29, 1957

J. Exptl. Theoret. Phys. (U.S.S.R.) **33**, 1099-1109 (1957)

At an altitude of 3200 meters above sea level, a study has been made of the spectrum of large pulses of ionization from 44 ionization chambers shielded by 10 and 12 cm of lead. The probability of an ionization event coinciding with an air shower affords some indication as to the range in air of particles with an energy of the order of 10^{12} ev. Some cases have been observed in which two or three pulses of commensurate magnitude have occurred simultaneously in ionization chambers at some distance from each other (ionization events with spatial structure).

1. APPARATUS

A study of the interaction between high-energy nuclear-active particles and the nuclei of air atoms has been carried out with the aid of an assembly (Fig. 1) consisting of two layers of ionization chambers, I and II. The chambers were cylindrical with a length of 90 cm, a diameter of 40 mm, and walls 1 mm thick, made of brass and filled with pure argon at a pressure of 5 atm. The collector electrodes were 0.4 mm in diameter. A potential of 800 volts was applied to the chambers. According to published data[1] this should be sufficient to reduce the electron collection time below 10 microseconds.

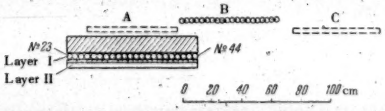

FIG. 1. Diagram of the assembly. I — upper layer of ionization chambers, numbers 23 to 44. II — lower layer of ionization chambers, numbers 1 to 22. The letters A, B, and C show the location of the counter tray in the different series of measurements.

There were 22 chambers in each layer, giving an overall active area of some 0.6 square meters. The chambers in each layer were oriented at right angles to those in the other layer. A 2 cm lead filter was placed between the two layers, and a 10 cm lead shield covered the upper layer.

Each ionization chamber was connected to its own individual amplifier, capable of recording the size of an ionization pulse in the range 100 to 500 relativistic particles. (In this paper the ionization pulse sizes will be expressed in terms of the number of relativistic particles which would give the same ionization if they passed through the chamber along a diameter perpendicular to its axis.) The pulses from each chamber were amplified and greatly prolonged by a special circuit, and applied to a segment of a mechanical commutator, whose wiper connected them in sequence to an oscilloscope with a long-persistence screen. In addition, the pulses from all amplifiers (before being stretched) were added together in a mixer. If the total pulse was equivalent to the ionization from 600 relativistic particles (this value, corresponding to 5 — 6 Po α-particles, was taken as the 100% probability level on the oscilloscope scale) it triggered the recording mechanism and photographed the amplitudes of all ionization chamber pulses.

Figure 2 shows the appearance of the photographs taken during the ionization events. With the system described above, the dead time for recording an event was about 0.25 seconds. Since the events were recorded at a rate of about two per hour, we can reasonably neglect the possibility of finding two separate events recorded on the same photograph. At periodic intervals, several times a day, calibrating signals were applied to the amplifiers to provide a continual check on the amplification factor of each amplifier.

In addition to the ionization chambers, there was a tray of ten Geiger counters, each connected to a hodoscope. A gating pulse to operate the hodoscope was generated every time the control system was

triggered, i.e., whenever the total signal exceeded 600 particles. The resolving time of each hodoscope cell was about 15 microseconds. The area of each counter was 420 cm^2 (when used in positions A and B in Fig. 1) and 330 cm^2 in the third series of experiments (with the counters located at C). The number of chance coincidences was determined experimentally for each group of counters, and amounted to 0.9 ± 0.3% of the number of triggering pulses. During each event, the discharge of any counter was indicated on the same photograph which recorded the amplitudes of the ionization chamber pulses (cf. Fig. 2).

The measurements were carried out on Mount Aragats at a height of 3200 meters above sea level. The basic measurements were made with the center of the counter tray 70 cm away from the center of the ionization chamber assembly (position B). Some of the measurements were made with the counters lying on top of the chambers (position A); in this case the counters covered about 70% of the total area of the assembly. A third series of measurements was made with the counters separated by a distance of 2 meters from the center of the chamber assembly (position C).

2. RESULTS OF THE MEASUREMENTS

1. Spectrum and Nature of the Events

We have analyzed separately the events registered in a single layer of chambers (either top or bottom), and the events registered simultaneously in both layers. In the latter case we could consider the pulse amplitude distribution in either layer to be independent of the pulse amplitudes in the other layer only if a pulse of at least 100 particles was recorded in the other layer.

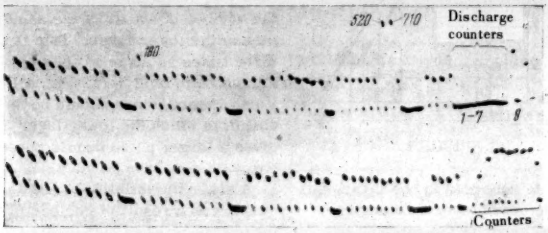

FIG. 2. Typical record of pulses from the chambers, and the hodoscopic chart of the discharged counters, from one of the recorded events. The figures beside the individual pulses denote the amount of ionization (as a number of relativistic particles) produced in each chamber. On the right-hand side of the figure, the numbers indicate which of the counters were operated by the event.

There is some physical significance in treating the two cases separately. If we had selected only those events which produced pulses in both layers, we would have had a greater probability of selecting showers with larger numbers of relativistic particles. On the other hand, a significant fraction of the pulses in a single layer could be the result of strongly ionizing particles coming from radioactive nuclear disintegrations in the lead, brass, or argon of the chambers.

The results of these separate analyses are shown in Figs. 3 and 4. In both figures, the sizes of the recorded events are plotted along the X axis in terms of the equivalent number of relativistic particles N. The number of events per second per cm^2, which are greater than or equal to N, is plotted along the ordinate axis. Figure 3 shows the events which were recorded in a single layer only, and Figure 4 shows the events which were registered in both layers simultaneously. It is evident from Figs. 3 and 4 that the spectrum of events registered in a single layer has the same form as the spectrum of events involving both layers. They can be approximated by a power-law function of the type $AN^{-\gamma}$ with the exponent γ equal to 1.6 ± 0.2.

We shall now consider in more detail the recordings of both types of event where the magnitude of N is 1000 or more. As already mentioned, the two-layer events appear to be due to showers of relativistic particles. A large number of the particles in the shower (1000 or more) might arise merely from electron-photon showers developed in the lead. In principle, there are two possible reasons for the appearance of such showers under 10 — 12 cm of lead. In the first place, electrons (or photons) of high energy may strike the lead from the air above it. In this case, however, the maximum intensity of the shower would lie at a depth of about 5 cm, and all the pulses in the upper layer would be, on the average, twice as large as the pulses in the lower layer.

Before continuing the discussion of the experimental data, we must mention that the two layers of

chambers in our assembly were not in identical surroundings. Located underneath the upper layer was a layer of lead, which would scatter the slow electrons that occur in large numbers in the showers. There was no lead underneath the lower layer of chambers, which was supported on a wooden platform. Thus, a "reverse current" of particles was practically non-existent in the lower layer. From the literature[2] we may estimate that, in the events observed in our apparatus, the reverse current of particles amounted to about 30% of the forward current. Hence, if the event in the upper layer of chambers is equivalent to N particles, then the same shower in the lower layer of chambers would give a pulse equivalent to 0.7 N particles.

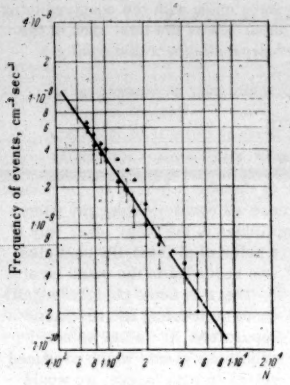

FIG. 3

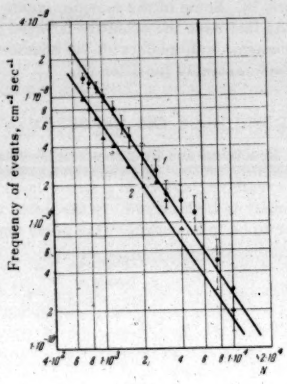

FIG. 4

FIG. 3. Integral distribution of events recorded in one layer of chambers only. Circles — events in the upper layer. Triangles — events in the lower layer (the statistical error is the same as in the case of events in the upper layer of chambers).

FIG. 4. Integral distribution of events recorded simultaneously in both layers of chambers. Curve 1 — distribution of events in the upper layer of chambers. Curve 2 — distribution of events in the lower layer of chambers (the statistical errors are the same as for the points of Curve 1).

In Figure 4, curve 1 is the distribution of pulses in the upper layer, and curve 2 is the distribution of the lower-layer pulses, for events recorded simultaneously in both layers. Had the recorded events been due to high-energy electrons (or photons) knocking the assembly out of the air, then the number of events exceeding N in the upper layer should have been $(2 \times 1.4)^{1.8} = 5$ times larger than the number of events of the same size in the lower layer. This is three times as large as the observed ratio of 1.7 (cf. Fig. 4). Furthermore, there should be no events in which the lower layer gives a larger pulse than the upper one.

A second possibility is that the events are a result of nuclear interactions between high-energy particles and lead nuclei. The π^0 mesons generated by this interaction could cause the electron-photon showers. This mechanism would allow cases in which the pulse from the lower layer of chambers is greater than the pulse from the upper layer. The experimental results show that, out of a total of 142 events with $N \geq 1000$, the upper layer gave a bigger pulse than the lower layer in 85 cases, while in 57 cases the reverse was true. Thus, the upper-layer pulse was the larger of the two 1.49 ± 0.25 more times than the lower-layer pulse. Theoretical calculation (cf. Sec. 3) gives a value of 1.56 for this ratio.

These experimental results make it possible to conclude that events recorded in both layers simultaneously are fundamentally caused by the interaction of high-energy nuclear-active particles with lead nuclei.

2. Atmospheric Effects Accompanying the Events

An analysis of the Geiger counter operation can give some information about the atmospheric phenomena accompanying events of different types and sizes. The experimental results show that events which are recorded in only a single layer of chambers (the upper one only) are practically never accompanied by the discharge of a counter. The average probability that a counter will fire (in positions A and B) when only the upper layer of chambers is activated, amounts to $10 \pm 7\%$. The small probability that an atmospheric event accompanies such an ionization event is apparently due to the fact that a pulse from a single layer is generally caused by a nuclear disintegration.

The situation is quite different for events which are recorded in both layers. Such events are accompanied as a rule by atmospheric events; there is a high probability that a large number of the counters will be discharged.

Table I shows the number of cases in which n of the counters ($0 \leq n \leq 10$) are discharged during the recording of an event of size N from one of the layers, while the other layer registers a pulse equal to or less than N. From Table I it can be seen that the probability of an atmospheric event increases with the number of particles in the ionization event (i.e., with increased energy of the nuclear-active particles which trigger the recording). The closer the counter tray is to the chamber assembly, the greater is the observed frequency of the accompanying atmospheric events, and the greater their density. When the counters are lying on top of the chamber assembly (position A), it is only once in 11 times that a single counter is discharged; the rest of the time two or more counters fire. Hence the discharging of the counters in this case cannot be due entirely to the passage of the primary nuclear-active particle, which causes the event, through the counter tray.

TABLE I

Number of counters discharged	Counters in position A			Counters in position B			Counters in position C	
	$1000 > N$	$1000 \leq N < 5000$	$N \geq 5000$	$1000 > N$	$1000 \leq N < 5000$	$N \geq 5000$	$1000 \leq N < 5000$	$N \geq 5000$
10	0	3	2	6	9	4	2	0
9	0	1	0	5	2	2	0	0
8	1	1	0	2	0	1	1	0
7	1	2	0	6	2	0	0	0
6	3	0	0	1	5	2	1	0
5	2	0	0	6	2	0	0	0
4	5	0	0	10	1	0	2	0
3	2	2	0	6	1	0	1	1
2	2	1	0	8	4	0	2	0
1	8	1*	0	13	2	0	1	0
0	12	0	0	83	12	0	11	0
Total	36	11	2	146	40	9	21	1
Percentage of cases in which any counters operated	66±10	90±10	100	43±7	70±9	100	48±19	
Average number of counters discharged in one event	2.2±0.5	6.3±2.0	10	2.0±0.2	4.5±0.8	8.7±1.0	2.4±0.6	

* This case does not contradict the assumption that the counter was operated by the passage of the nuclear-active particle which produced the event. We therefore consider that in this case there were no atmospheric effects.

Another reason for the high probability of discharging a counter might be the reverse current of particles coming up out of the lead. However, the following considerations contradict this assumption. When the counters are located off to one side of the assembly (position B), 30% of the recorded events (for N between 1000 and 5000) were not accompanied by any discharge of the counters. There could be two reasons for this. Either 30% of the events were actually not accompanied by atmospheric showers, or else the showers exist but are of such small area that they are not recorded by the counter tray located 70 cm away from the center of the assembly. In order to decide which of these two hypotheses was correct, we carried out the following test.

Chambers 23 to 44 of the upper layer were arranged parallel to the counters (the counter tray being in position B). From a total of 40 events we selected those in which there was no accompanying discharge of a counter (12 events) and those in which only a small number (four or less) of the counters fired. But if the particle producing the ionization pulses produces no accompanying atmospheric shower, then the selection of events with $n = 0$ does not imply any discrimination on the part of the different ionization chambers, i.e., it would be expected that the pulses would occur with equal frequency in the left-hand chambers (Nos. 23 to 33) and in the right-hand chambers (Nos. 34 to 44), see Fig. 1. However, if the particles which caused the ionization also produced narrow atmospheric showers, then to select the cases where $n = 0$ would effectively mean to "repel" the generating particle and its accompanying shower to the side away from the counter tray. In this case ionization chambers 23 to 33 should operate more often than chambers 34 to 44.

Table II shows the experimental frequency distribution of the two halves of the chamber assembly (chambers 23 to 33, and chambers 34 to 44) for the cases $n = 0$; $1 \leq n \leq 4$; and $n > 4$, for events with $1000 \leq N \leq 5000$ and $N < 1000$.

The large difference in the frequency with which events were recorded in the two halves of the assembly indicates that, even when $n = 0$, the events are in fact accompanied by atmospheric showers, albeit of small area. The last line in Table II shows that the observed dependence of the different chambers' operating frequencies upon the number of counters discharged, for events with $1000 \leq N \leq 5000$ particles, is not due to a difference in the sensitivities of the individual chambers or amplifier channels. If we assume that for $n = 0$, the two cases of events in chambers 34 to 44 correspond to the absence of atmospheric effects, then we must expect the same number of analogous cases to occur when the event takes place in chambers 23 to 33. Then the remaining $10 - 2 = 8$ events were accompanied by narrow showers. That is, out of 40 events, only 4 ± 2 were unaccompanied by atmospheric effects. Consequently, the probability of atmospheric effects is equal to $90 \pm 5\%$, which is the same figure resulting from direct measurement, with the counter tray lying on top of the chambers (position A).

TABLE II

Number of counters discharged	Number of cases where chambers operated		Remarks
	No. 23 to 33	No. 34 to 44	
$n = 0$	10	2	Events with $1000 \leqslant N \leqslant 5000$ particles
$1 \leqslant n \leqslant 4$	6	2	
$n > 4$	6	9	
$n = 0$	42	41	Events with $N < 1000$ particles

3. Ionization Events with Spatial Structure

The use of ionization chambers 4 cm in diameter, covering a relatively large area, made it possible to observe cases in which two or more widely separated chambers gave ionization pulses, although there was no ionization in the intermediate chambers. Events with this type of spatial structure will hereafter be referred to as "structured" events. An example of one such event is shown in Fig. 5. If we consider only the pulses with $N \geq 300$ relativistic particles to be contributing to the structure of an event, then the frequency of structured events is given in Table III as a function of the type and size of the recorded event.

TABLE III

	Events in one layer only		Events in both layers of chambers		
	$500 \leqslant N \leqslant 1000$	$1000 \leqslant N \leqslant 5000$	$500 \leqslant N \leqslant 1000$	$1000 < N \leqslant 5000$	$N > 5000$
Total number of events	163	69	129	102	14
Number of events with structure	1	2	1	17	5
Average distance between chambers giving structured pulses	—	—	—	35 cm	15 cm

Events which occur in only one layer of chambers are, in general, caused by nuclear disintegrations. Hence the small percentage of structured events occurring in a single layer shows that the structure cannot be attributed to nuclear disintegrations (if we limit ourselves to amplitudes ≥ 300 particles). It can be seen from Table III that structure appears in a considerable fraction of the events involving both layers of chambers. The proportion of structured events increases with increasing total amplitude of the event. It is particularly noteworthy that the larger the event, the smaller is the average distance between ionized chambers when structure is present.

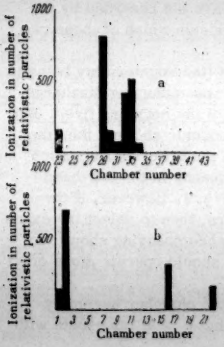

FIG. 5. Example of an event with spatial structure. In the upper layer (a) chambers 23, 29, 30, 31, 32, 33, and 34 operated, with pulses of 160, 810, 160, 80, 420, 510, and 80 relativistic particles respectively. In the lower layer (b) chambers 1, 2, 16, and 22 operated, with pulses of 150, 700, 320 and 160 particles, respectively.

As a measure of the amplitude differences in the ionization pulses making up the structure of an event, we used the mean ratio between the amplitudes of the smallest and largest pulses, $\overline{V_{min}/V_{max}}$. For 17 structureed events with $1000 \leq N \leq 5000$ particles, $\overline{V_{min}/V_{max}}$ was 0.55 ± 0.23. For the five structured events with $N > 5000$ particles, $\overline{V_{min}/V_{max}}$ was 0.5. From these mean values of V_{min}/V_{max} it follows that the ionization pulses produced during structured events are all of the same order of magnitude, and that in a large majority of cases they differ by less than a factor of 2.

In six of the 22 cases of structured events with $N \geq 1000$ particles, the structure appeared only in the lower layer of chambers, while the total ionization in the upper layer was considerably less than the total ionization in the lower layer of chambers. This circumstance rules out the formation of structured events by electrons (or photons) of high energy striking the assemply from the atmosphere.

From a study of the experimental data it can be concluded that the structured events are due to several nuclear-active particles of high energy, striking the assembly simultaneously. Events which have spatial structure are accompanied by more extensive atmospheric showers. Thus, the average number of discharged counters (when the tray is in position B) amounts to 3.9 ± 0.7 for events without structure, and 6.5 ± 0.7 for structured events with $1000 \leq N \leq 5000$ particles.

3. DISCUSSION OF RESULTS

1. Estimates of the Recording Efficiency and of the Energy of the Particles Causing the Events

Events of a given size (N particles) could be caused by particles of various energies, depending on the distance between the nuclear interaction and the ionization chamber. In order to estimate the efficiency of recording the particles which cause an event of a given size, we have made the following assumptions:

(1) Particles with energy E lose 50% of their energy during interaction with a lead nucleus; the π^0 mesons carry away one third of the energy lost.

(2) The π^0 mesons produce an electron-photon cascade in the shield, described by a cascade curve for a photon with half the total energy acquired by the π^0 mesons during the nuclear interaction.

(3) We have taken the range of the particles for interaction with lead to be 160 g/cm^2.

The calculated recording efficiency for particles which cause events from 1000 to 5000 particles in size, and which are registered in both layers of chambers, is equal to 24%. In this case E_{min}, the smallest energy which will enable a particle to cause such an event, is 6×10^{11} ev, and the average energy (taking into account the variation in recording efficiency with particle energy, and the upper limit of 5000 particles for the recorded events) is 2.6 E_{min}, namely 1.6×10^{12} ev. The recording efficiency for particles which cause events with $N \geq 5000$ particles is 30%.

Using the same cascade curve which we used in estimating the recording efficiency, we calculated the ratio of the number of events with $1000 \leq N \leq 5000$ in which the pulse from the upper layer of chambers was greater than the pulse from the lower layer, to the number of events in which the lower layer gave the larger pulse. The calculated ratio was equal to 1.56. The experimental value of this same quantity, derived above, was 1.49 ± 0.25. Hence the agreement between calculation and experiment is still another argument in favor of the view that the events which involve both layers are caused, in the overwhelming majority of cases, by nuclear-active particles interacting with the lead in the shield.

2. Interaction Range of Particles with $E \sim 10^{12}$ ev

We denote by $n(x; \geq E)$ the number of all particles with energy E at a depth of x g/cm^2 in the atmosphere; and by $n_1(x; \geq E)$ the number of particles with the same energy, at the same depth, which are unaccompanied by any atmospheric events. If L_a is the range of particles with energy E for absorption, and L_i is their range for interaction in the atmosphere, then

$$n(x; \geqslant E) = n(0; \geqslant E) \exp\{-x/L_a\}. \tag{1}$$

The number of particles which arrive from the top of the atmosphere without any interaction is denoted by $n_0(x; \geq E)$, and is equal to

$$n_0(x; \geqslant E) = n(0; \geqslant E) \exp\{-x/L_i\}. \tag{2}$$

It is obvious that $n_1(x; \geq E) > n_0(x; \geq E)$ if $x \sim 700$ g/cm^2. Therefore

$$n_1(x; \geqslant E) > n(0; \geqslant E) \exp\{-x/L_i\}. \tag{3}$$

Dividing (3) by (1), we obtain

$$\frac{n_1(x; \geqslant E)}{n(x; \geqslant E)} > \exp\left\{-x\left(\frac{1}{L_i} - \frac{1}{L_a}\right)\right\}$$

and hence

$$\frac{L_a}{L_i} > 1 + \frac{L_a}{x} \ln \frac{n(x; \geqslant E)}{n_i(x; \geqslant E)}. \qquad (4)$$

From our experimental results (section II), $n_i/n = 0.1 \pm 0.05$. From the literature[3] $L_a = 112 \pm 11$ g/cm^2 for particles with energy $E \sim 10^{12}$ ev. Hence, according to the inequality (4),

$$L_a / L_i > 1.36^{+0.11}_{-0.04},$$

and, taking $L_a = 112$ g/cm^2, we obtain

$$L_i < 84^{+4}_{-6} \text{ g/cm}^2.$$

Our results show that as the size of the recorded event increases, the probability of atmospheric side-effects does not decrease. Thus, for events with $N > 5000$ particles, corresponding to a mean energy of the order of 10^{13} ev for the original particle, the probability of an accompanying air shower is almost 100%. This means that for particles with $E \sim 10^{13}$ ev, the range for interaction in air is no greater than 80 g/cm^2.

3. The Relation of High Energy Particles to Extensive Atmospheric Showers

The tray of counters connected to the hodoscope enable us to estimate the number of particles in the air showers accompanying the ionization events. To estimate the number of particles, we started from two assumptions:

(1) The current density of the counted particles $\rho(r)$ is a single-valued function of r, the distance of the counter from the shower axis. For small r, the function is of the form $\rho(r) = AN_s/r$, where N_s is the total number of particles in a shower.

(2) The axis of the shower coincides approximately with the trajectory of the nuclear-active particle causing the ionization event (within 30 – 50 cm).

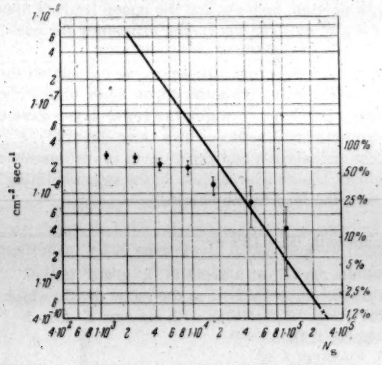

FIG. 6. Atmospheric effects of particles with energy 6×10^{11} to 3×10^{12} ev.

The results we obtained for the density of atmospheric showers accompanying ionization events are shown in Figure 6. N_s, the number of particles in the atmospheric showers accompanying ionization events of 1000 to 5000 particles, is plotted along the abscissa. The ordinate axis represents the number of ionizing particles which are accompanied by showers of N_s or more particles. (The right-hand scale shows the relative fraction of such particles, taking as 100% the nuclear-active particle flux equivalent to the total of all the observed events, regardless of whether or not they were accompanied by showers.) The solid line in the figure gives the absolute number of large atmospheric showers with N_s or more particles which fall on 1 cm^2 every second at an altitude of 3200 meters above sea level.* Comparing this curve with our experimental data shown in Fig. 6, we may conclude that in showers of more than 10^5 particles there are on the average one or two particles with energies $\bar{E}$ of the order of 10^{12} ev. In showers where $N_s \geq 10^4$ there is on the average only one particle with $\bar{E} \sim 10^{12}$ ev in every three showers, i.e., not every shower contains even one particle lying in the energy range from 6×10^{11} to 3×10^{12} ev.

If we assume, as several authors have done,[4] that the formation of large atmospheric showers is due to individual high-energy particles, then in order that each shower with 10^4 or more particles at mountain-

*The curve was constructed by using the size distribution of showers taken from the data placed at our disposal by A. P. Abrosimov, N. N. Goriuniv, A. V. Dmitriev, V. I. Solov'ev, B. A. Krenov, and G. B. Christiansen from their paper which is being prepared for publication.

top altitudes can be ascribed to a single energetic particle with energy E_1, it follows that this energy must be about $3^{1/\kappa}$ times smaller than 6×10^{11} ev. For large atmospheric showers, $\kappa \simeq 1.5$. Hence $E_1 = 3 \times 10^{11}$ ev. But if the shower contains N_s particles, then in order to avoid contradicting our data we must assign to the primary high-energy particle an energy of

$$E_{primary} = 3 \times 10^{11} N_s \times 10^{-4} \text{ ev} = 3 \times 10^7 N_s \text{ ev}.$$

It is easy to show that such a particle could only lengthen the mean range of showers between the mountain tops and sea level by about 15 g/cm^2 in all, i.e., if each large shower at mountain-top level also has its energetic primary particle, then on the average its energy is not sufficient to account for the subsequent absorption of showers in the lower atmosphere.

We come to exactly the same conclusion by comparing the absolute flux of nuclear-active particles in the atmosphere at a depth of $x = 700$ g/cm^2, which can be obtained from the literature[5] by extrapolation into the high-energy region, to the number of showers with the given number of particles.

4. Events with Spatial Structure, and the Nature of the Interaction Between Light Nuclei and Particles with Energies of 10^{12} to 10^{13} ev

About 20% of the events possessed structure. If we take into account the recording efficiency for the events and the fact that in the majority of cases the structured events are characterized by pulses in both groups of chambers, we may estimate the relative number of cases in which the showers falling on our assembly contained particles with an energy $\sim 10^{12}$ ev. It is estimated that, in about 40 — 50% of the cases where events with more than 1000 particles were registered, groups of 2 or 3 nuclear-active particles with energies of about 10^{12} ev fell on the 0.6 square meter area of the assembly.

The relatively frequent occurrence of showers composed of several nuclear-active particles with energies of 10^{12} ev or more in the atmosphere, accompanied as a rule by a greater density of air showers than in the case of individual nuclear-active particles of the same energy, suggests that the interactions of particles with energies of $10^{12} - 10^{13}$ ev with light nuclei can be divided schematically into two classes of interaction. One class is a relatively weak interaction, as a result of which the nuclear-active particle loses a small part of its energy, and the remainder is carried away by a single particle, possibly of the same type as the "primary" particle. The second class is a strong interaction, in which the "primary" particle loses all its energy. As a result of the second type of interaction, there is formed a shower of a few high-energy nuclear-active particles, which give ionization events with spatial structure, accompanied by wider atmospheric showers.

The assumption that there are two classes of interaction may be reconciled with the observed height dependence of the number of 10^{12} ev particles, if we assume that in the "weak" interactions the average energy loss amounts to 20 — 30%, and in the "strong" interactions the energy loss is practically 100%. It is curious to note that if such a mechanism of interaction is extrapolated to the region of super-high nucleon energies, corresponding to the formation of extensive atmospheric showers, then it is possible to explain almost quantitatively such shower characteristics as (1) the variation of showers with height, (2) the spectrum of showers with a given number of particles, and (3) the small variation in shower diameter S as the altitude varies from 0 to 4000 meters above sea level.

In conclusion, the authors express their thanks to A. I. Alikhanian, who made it possible for us to carry out the experiments on Mount Aragats; to N. M. Kocharian and his co-workers for the substantial kindness they showed us during the course of the experiments on Mount Aragats; to A. A. Sanin for his assistance in developing the electronic apparatus, and to A. E. Chudakov for valuable comments during the discussion of the results.

[1] B. Rossi and G. Staub, "Ionization Chambers and Counters" New York, 1949.

[2] O. N. Vavilov, Dissertation. Trudy, Phys. Inst. Acad. Sci., (U.S.S.R.) 4, Acad. of Sci. Press, Moscow 1949.

[3] K. P. Ryzhkova and L. I. Sarycheva, J. Exptl. Theoret. Phys. (U.S.S.R.) 28, 618 (1955), Soviet Phys. JETP 1, 572 (1955).

[4] Nikol'skii, Vavilov, and Batov, Dokl. Akad. Nauk SSSR 111, 71 (1956), Soviet Phys. "Dokalady" 1, 625 (1956).

[5] Kocharian, Saakian, Aivazian, Kirakosian, and Aleksanian, Izv. Akad. Nauk SSSR, Ser. fiz. 19, 515 (1955). Translated by D. C. West

ANGULAR DISTRITUTION OF AXES OF EXTENSIVE AIR SHOWERS AT SEA LEVEL

A. T. ABROSIMOV, V. I. GOMAN'KOV, I. A. IVANOVSKAIA, and L. I. SARYCHEVA

Moscow State University and the P. N. Lebedev Physics Institute, Academy of Sciences, U.S.S.R.

Submitted to JETP editor May 8, 1957

J. Exptl. Theoret. Phys. (U.S.S.R.) 33, 1110-1115 (November, 1957)

A cloud-chamber study was made of the angular distribution of the axes of extensive air showers at sea level. The angular distribution was approximated by a $\cos^n\theta$ law of exponent $n = 8.3 \pm 1.4$.

FOR the purpose of studying the characteristics of extensive air showers in 1954 we constructed apparatus which consisted of a large cloud chamber and 288 hodoscope counters. This apparatus was used in Moscow to obtain the angular distribution of the axes of extensive air showers, the energy spectra of the electron-photon and nuclear-interacting components, the lateral distribution of the nuclear-interacting particles and a number of other characteristics of the showers. In the present paper we present only the results for the angular distribution of the axes. The other data will be published later.

The arrangement of the cloud chamber and four hodoscopic points is shown in Figs. 1a and 1b. The cloud chamber,[1] which measured $60 \times 60 \times 30$ cm (with an effective area of 0.15 m^2), contained 7 lead plates. The thickness of the uppermost plate was 0.5 cm; that of the others was 1.5, 2, 2, 2.5, 2 and 2.5 cm. The cloud chamber served for the determination of the directions of the particles, for detection of the interactions between nuclear-interacting particles and lead nuclei, and for determination of the energies of electrons and photons from their cascade multiplication in the lead plates.

The hodoscopic sets, each of which consisted of 72 counters (24 counters with each of the areas 330, 100 and 24 cm^2) enabled us to determine the flux of particles at four points of the shower cross section, thus making it possible to find the position of the axis and the total number of particles in individual showers.

In the first series of measurements the hodoscope and cloud chamber were controlled by a pulse M_1 which resulted from coincident discharges in four groups of counters, each of 660 cm^2 area, located at the center of the apparatus and denoted by numbers 1, 2, 3, and 4 in Fig. 1b. In the second series the hodoscope and cloud chamber were actuated by either of two master pulses. One of these pulses, M_2, resulted from the coincidence of discharges in counters 1, 2, 3, and 4 and the absence of discharges in counters of the same area in groups I and V (Fig. 1a); the other pulse, M_3, resulted from the coincidence of pulses in any four counters of the 10 (each of 180 cm^2 area) placed under 10 cm of lead alongside of the cloud chamber (Fig. 1b), with pulses in two unshielded counters (5 and 6 in Fig. 1b) of 330 cm^2 area placed at about 2 meters from the lead block. In the second series hodoscopic point I was shifted to position Ia.

The position of the axis r and the number of particles N in an extensive shower were determined in the usual manner[2] from the particle flux ρm^{-2} registered by three groups (II, III, and IV in Fig. 1a) of hodoscope counters. It was assumed that the lateral distribution of the flux was known,[3] and that in the range of r from 2 to 10 meters it was represented by * $\rho(r) = 2.7 \times 10^{-3}\, Nr^{-1}$. The flux in group I and in the cloud chamber had to correspond to the observed distance from the shower axis.

The number of hodoscope counters which we used enabled us to determine the particle flux in each of the groups I, II, III, and IV with an error which fluctuated between 20 and 35%. The resulting errors in the determination of distances from the axis were of the order of 40% for $r \leq 3$ m, 50 – 60% in the range 3 – 6 m and approximately 80% in the range 6 – 10 m. Because of this relatively low accuracy in determining the axis position we grouped all detected showers according to the three given ranges of distances

*The numerical value of the coefficient, 2.7×10^{-3}, was taken from the preliminary results in Ref. 3, whose authors have now corrected the value. However, since we were interested only in relative data concerning showers with different numbers of particles, we did not readjust the values of N in the detected showers.

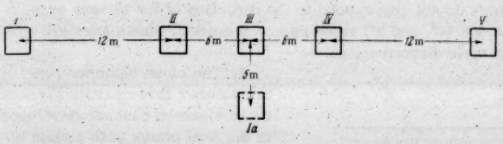

FIG. 1a. Arrangement of the groups of hodoscope counters.

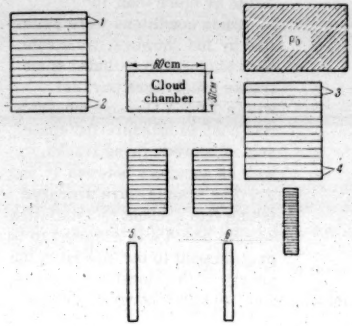

FIG. 1b. Arrangement of the hodoscope counters and cloud chamber in group III.

and put into a separate group those showers whose axes were more than 10 m distant from the cloud chamber. In addition to distributing showers according to intervals of distance we combined into different groups the showers which contained different numbers of particles. Table I contains the distribution of all of the detected showers according to intervals of r and N.

TABLE I

N	$r\leq 3$	$3<r\leq 6$	$6<r\leq 10$	$r>10$	$\sum_r$
10^3—$5\cdot10^3$	33	4	—	—	37
$5\cdot10^3$—10^4	96	8	—	—	104
10^4—$5\cdot10^4$	407	349	54	26	836
$5\cdot10^4$—10^5	97	221	139	81	538
10^5—$5\cdot10^5$	50	192	131	190	563
$5\cdot10^5$—10^6	8	14	15	26	63
10^6—$5\cdot10^6$	—	6	5	23	34
$\sum_N$	691	794	344	346	2175

Figs. 2a and 2b show the distribution with respect to r and N of showers registered by the different systems of control. As can be seen from Fig. 2a, the M_2 and M_3 systems effectively selected showers whose axes were less than 10 m distant from the cloud chamber, while the M_1 system registered the large number of showers whose axes were more than 10 m distant from the cloud chamber.

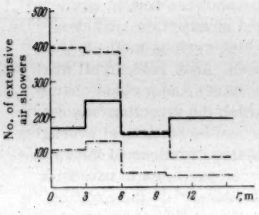

FIG. 2a. Distribution of showers over intervals of distance for different systems of control. Solid line — M_1; dashed line — M_2; dots and dashes — M_3.

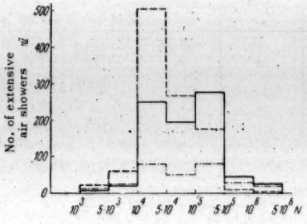

FIG. 2b. Histogram of shower distribution over intervals of N for different systems of control. Solid line — M_1; dashed line — M_2; dots and dashes — M_3.

From the error in determining distances to the shower axis we estimated the probability that a group of showers at a given distance from the cloud chamber would include showers from other distance intervals. These estimates are given in Table II, from which we see that each group of showers within a definite interval of distances between the axis and the cloud chamber contains some admixture of showers from other distance intervals. This fact was taken into account in studying the dependence of various shower characteristics on the distance of the axis.

For determination of the angular distribution of the axes we selected showers which satisfied the following requirements:

1. The shower axis passes the cloud chamber at a distance $r \leq 3$m in the horizontal plane. This requirement is associated with the fact that the direction of the shower axis is determined by the directions of the electrons, and that at large distances from the axis the electrons have low energies, are

strongly scattered, and move in directions which do not correspond to the direction of the shower axis.

2. The number of shower particles is $N \geq 3 \times 10^4$, and all showers are recorded, whose axes are ≤ 3 m from the cloud chamber, regardless of their directions.

TABLE II

Interval of distances r, m	Total number of showers in the distance intervals.*	Probable fraction of the showers assigned to adjacent distance intervals**	Probable addition from adjacent distance intervals**	
			Interval, m	Addition, %
$r \leq 3$	554	10.5%	3–6 m	23
			6–10 m	2.5
			Total	25.5
3–6	762	28%	$r \leq 3$	8
			6–10	9
			Total	17
6–10	324	57%	3–6	–27
$r > 10$	297			

*Table II includes only showers in which the number of particles is between 10^4 and 5×10^5.

**Relative to the total number of showers in the given distance interval.

3. The cloud chamber contains either three parallel tracks or an electron cascade developed in the lead plates with a clearly defined core and a parallel track. Tracks were regarded as parallel if their directions did not differ by more than 10°.

These conditions were satisfied by 154 showers. As a rule, each photograph included some tracks which were parallel within 10°. A stereocomparator was used to measure the space angles between these tracks, with an accuracy between 1° and 3°. The results were averaged taking into account the statistical weight, which was assumed to be proportional to the square of the energy of the electron producing a given track.* Thus the direction of the shower axis was determined mainly by high-energy electrons which pass close to the shower axis and maintain its direction.

Table III contains the distribution of extensive showers over the intervals of angles which their axes formed with the vertical. If this angular distribution is approximated by a $\cos^n\theta$ law, we see from Fig. 3 that the exponent is $n = 8.3 \pm 1.4$.

TABLE III

Angular interval	0°–10°	10–20°	20–30°	30–40°	40–50°
$\bar{\theta}$*	0°	15°50′	25°	35°40′	43°40′
Number of extensive air showers	22	49	51	22	10
Number of extensive air showers per unit solid angle** $J(\bar{\theta})$	232±54	178±25	121±17	42.7±9	18.4±6

*$(\bar{\theta})$ is defined as the arithmetic mean of the angles which were registered in the respective intervals.

**The variation of the effective area in the registering of extensive showers forming the angle θ with the vertical was taken into account by introducing the factor $1/\cos\theta$.

The literature contains numerous investigations of the angular distribution of extensive air showers both at sea level[4–7] and at mountain altitudes,[8–12] in which various methods were used. As a rule, in all work with counters and a cloud chamber, in which the direction was determined by statistical averaging of the directions of the registered particles in extensive showers,[6,7,12] the exponent n in the $\cos^n\theta$ approximation of the angular distribution was found to be smaller than in those investigations where the directions of the showers were measured according to the flux of high-energy particles[4,8,9–11] or by means of scintillation counters.[5] It must be noted that when the directions of individual particles are averaged statistically a distortion is introduced by the scattering of these particles, whereas the high-energy particles in the cores of extensive air showers are scattered less and preserve the direction of the shower axis. The most reliable measurements of the angular distribution are those in which the directions of high-energy particles are determined. Our results are in agreement with these measurements.[4]

*We know that the statistical weight w is by definition inversely proportional to the square of the error: $w \sim 1/(\Delta\theta)^2$. Since the error in the angle, due to scattering, is inversely proportional to the particle energy, $\Delta\theta \sim 1/E$, and we have $w \sim E^2$.

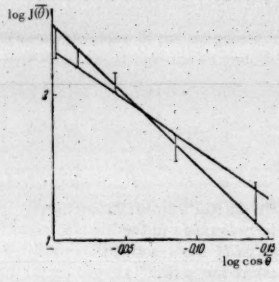

FIG. 3. Angular distribution of the axes of extensive air showers.

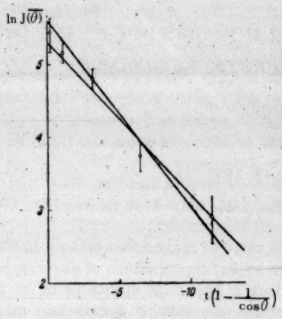

FIG. 4

From the angular distribution of the axes we can determine μ, the shower absorption coefficient in air. If it is assumed that the primary particles enter the atmosphere isotropically and that showers are absorbed exponentially, depending only on the amount of matter traversed and not on the length of path (thus neglecting decay processes), we easily obtain the following relation between the shower intensity $J(\theta)$ at angle θ and the vertical shower intensity $J_\perp$:[13]

$$J(\theta) = J_\perp \exp\left\{\mu t\left(1 - \frac{1}{\cos\theta}\right)\right\}.$$

Figure 4 shows the experimentally determined relation between $\ln J(\theta)$ and $t(1 - 1/\cos\theta)$ for $t = 30$ radiation units. The slope of the line is determined by the value of the shower absorption coefficient, which is 0.237 ± 0.025 or 145 ± 15 g/cm^2, in agreement with the value obtained from a study of the barometric effect.[14]

In conclusion the authors wish to thank G. T. Zatsepin for discussions of the results and for a number of valuable suggestions. We also wish to thank I. V. Rakobol'skaia, D. F. Rakitin, and P. S. Chikin, who assisted with the measurements.

[1] I. A. Ivanovskaia and A. G. Novikov, J. Tech. Phys. (U.S.S.R.) 26, 209 (1956), Soviet Phys. JETP 1, 206 (1956).
[2] G. B. Khristiansen, Dissertation, 1953.
[3] Abrosimov, Zatsepin, Solov'eva, Kristiansen, and Chikin, Izv. Akad. Nauk SSSR, Ser. Fiz. 19, 677 (1955).
[4] M. Deutschmann, Z. Naturforschung A2, 61 (1947).
[5] G. Clark, Report at Conference in Mexico, 1955.
[6] Bassi, Bianchi, Cadorin, and Manduchi, Nuovo cimento 9, 1037 (1952).
[7] H. L. Kraybill, Phys. Rev. 93, 1362 (1954).
[8] R. W. Williams, Phys. Rev. 74, 1689 (1948).
[9] W. W. Brown and A. S. McKay, Phys. Rev. 76, 1034 (1945).
[10] J. Daudin, J. phys. et radium 6, 302 (1945).
[11] Miura, Matano, Toyoda and Murayama, J. Phys. Soc. Japan 10, 595 (1955).
[12] Cresti, Loria and Zago, Nuovo cimento 10, 779 (1953).
[13] G. T. Zatsepin, Dissertation, 1950.
[14] A. Daudin and J. Daudin, J. phys. et radium 14, 169 (1953).

Translated by I. Emin
230

DETERMINATION OF NUCLEAR MOMENTS OF Gd^{155} AND Gd^{157} FROM THE HYPERFINE STRUCTURE OF PARAMAGNETIC RESONANCE

A. A. MANENKOV and A. M. PROKHOROV

P. N. Lebedev Physics Institute, Academy of Sciences, U.S.S.R.

Submitted to JETP editor May 11, 1957

J. Exptl. Theoret. Phys. (U.S.S.R.) 33, 1116-1118 (November, 1957)

The nuclear spins (3/2) and the ratio of magnetic moments $|\mu(Gd^{155})| : |\mu(Gd^{157})| = 0.73 \pm 0.03$ are determined from the hyperfine structure of paramagnetic resonance in the phosphor SrS — Gd. A comparison of hyperfine splittings in the spectra of Eu^{2+} and Gd^{3+} in the phosphor SrS and assignment of a value of 3.6 nuclear magnetons for $\mu(Eu^{151})$ yields $|\mu(Gd^{155})| = 0.25$ and $|\mu(Gd^{157})| = 0.34$ nuclear magnetons.

THE hyperfine structure in the optical spectrum of gadolinium has been investigated in several papers,[1-4] but the nuclear spins of Gd^{155} and Gd^{157} were not reliably determined for a long time, and only Speck[4] showed them to be equal to 3/2 for both odd isotopes. The values of the nuclear magnetic moments for the same gadolinium isotopes given in the various references quoted above differ widely among themselves. The table contains a summary of the data on the spins and the magnetic moments (in nuclear magnetons) of the isotopes Gd^{155} and Gd^{157} obtained in Refs.[1-4]

Nuclear spins and magnetic moments of Gd^{155} and Gd^{157} determined from the optical hyperfine structure.

Isotope	References quoted			
	1	2*	3	4
Gd^{155}	$I \geqslant 3/2$ $\lvert\mu\rvert = 0.25 \pm 0.15$	$I \geqslant 5/2$ $\mu = -0.19 \pm 0.05$	$I = 3/2$ $\mu = -0.31$	$I = 3/2$ $\mu = -0.30$
Gd^{157}	$I \geqslant 3/2$ $\lvert\mu\rvert = 0.3 \pm 0.2$	$I \geqslant 5/2$ $\lvert\mu\rvert = -0.33 \pm 0.06$	$I = 3/2$ $\mu = -0.38$	$I = 3/2$ $\mu = -0.37 \pm 0.04$

*The value of the magnetic moment is calculated on the assumption[2] that $I(Gd^{155}) = I(Gd^{157}) = 3/2$.

In Ref. 5 we have pointed out the possibility of determining the nuclear moments of Gd^{155} and Gd^{157} from the hyperfine structure of paramagnetic resonance in the phosphor SrS — Gd. In that reference it was possible to determine the values of the nuclear magnetic moments of Gd^{155} and Gd^{157} only approximately since the investigation was carried out on a natural mixture of gadolinium isotopes and the hyperfine structure was not completely resolved as a result of the overlapping of lines from different isotopes.

In the present work we have investigated the paramagnetic resonance in the phosphor SrS — Gd making use of separated isotopes Gd^{155} and Gd^{157}. The content of each of these isotopes in the corresponding enriched mixture was about 93%. The concentration of gadolinium in the phosphor was about 10^{-4} and at room temperature we observed a well resolved hyperfine structure for both odd gadolinium isotopes. The spectra were investigated at a frequency of 9383 Mcs with the aid of a superheterodyne radiospectroscope. The magnetic field was measured by means of proton resonance.

Oscillograms of the observed spectra are shown in the figure. The hyperfine structure consisting of four components for both the odd gadolinium isotopes shows that the nuclear spins of Gd^{155} and Gd^{157} are equal to 3/2. The total splittings (between the outermost hyperfine structure components) in the spectra of SrS — Gd^{155} and SrS — Gd^{157} are respectively equal to:

$$\Delta H(Gd^{155}) = 11.04 \pm 0.18\,G, \quad \Delta H(Gd^{157}) = 15{,}0 \pm 0.15\,G.$$

From a comparison of the total splittings in the spectra of Gd^{155} and Gd^{157} we have obtained the ratio of the nuclear magnetic moments of Gd^{155} and Gd^{157}:

$$|\mu(Gd^{155})/\mu(Gd^{157})| = 0.73 \pm 0.03. \quad (1)$$

The magnitudes of the magnetic moments of Gd^{155} and Gd^{157} may be determined by means of comparing the hyperfine splittings due to gadolinium nuclei with the splittings due to europium nuclei. The hyperfine structure of the paramagnetic resonance spectrum of Eu^{2+} in the phosphor SrS — Eu was investigated in Refs.[6-8] The Gd^{3+} ion is isoelectric with the Eu^{2+} ion and both have the electronic ground state $4f^7\ {}^8S_{7/2}$. Therefore direct comparison of the hyperfine splittings observed in SrS — Eu and SrS — Gd gives for the ratio of the magnetic moments of Eu^{151} and Gd^{157} the value:*

a b

Hyperfine structure for the electronic transition $M = \frac{1}{2} \longleftrightarrow -\frac{1}{2}$: a — SrS — Gd^{155}, b — SrS — Gd^{157}.

$$|\mu(Eu^{151})/\mu(Gd^{157})| = 10.60 \pm 0.03. \quad (2)$$

Using the value $\mu(Eu^{151}) = 3.6$ nuclear magnetons[9] we obtain from the ratios (1) and (2):

$$|\mu(Gd^{155})| = 0.25,\ |\mu(Gd^{157})| = 0.34 \text{ nuclear magnetons} \quad (3)$$

These values agree with the data obtained recently by Low[10] from the hyperfine structure of the paramagnetic resonance spectrum of gadolinium in single crystals of $LaCl_3 \cdot 7D_2O$ and $Bi_2Mg_3(NO_3)_{12} \cdot 24H_2O$. However, in Low's work[10] the hyperfine structure of Gd^{155} was not completely resolved and the conclusion with respect to the spin of Gd^{155} was made only on the basis of the shape of the observed line. Probably also due to the incomplete resolution of the hyperfine structure the ratio of the magnetic moments of Gd^{155} and Gd^{157} was found by Low[10] to be equal to 0.75 ± 0.07, i.e., its accuracy is lower than that of our ratio (1).

The ratio of the magnetic moments of Eu^{151} and Gd^{157} was found by Low to be equal to $\mu(Eu^{151})/\mu(Gd^{157}) = 11.3$ by comparing the hyperfine structure of europium and gadolinium in various compounds (and consequently in different crystalline surroundings). Since the hyperfine structure depends on the crystalline environment† the ratio of $\mu(Eu^{151})/\mu(Gd^{157})$ found by us is probably more accurate than that given by Low[10] since we compared the hyperfine splittings in the spectra of Eu and Gd in the same compound SrS.

In conclusion we would like to note the influence of the mechanical deformations of the crystal on the observed spectrum. In the sample of the phosphor SrS — Gd compressed into a tablet at a pressure of 150 atmos the resolution of the hyperfine structure of the spectrum is considerably worse than the resolution in the spectrum observed for a non-compressed sample. This is probably explained by the fact that at such a pressure a noticeable deformation of the crystalline lattice occurs which leads to a decrease in the symmetry of the crystalline electric field acting on the Gd^{3+} ion. Such changes in the electric field of the crystal lead to a larger anisotropic broadening of the paramagnetic resonance lines. It is also possible that in the case of such deformations of the crystalline lattice a change in the magnitude of the hyperfine splittings occurs, which can also lead to poorer resolution of the spectrum if non-uniform deformations take place over the whole sample. A similar effect of the influence of mechanical deformations of the crystal on the paramagnetic resonance spectrum was found by Van Wieringen[11] in the case of ZnS — Mn.

The authors sincerely thank G. Ia. Shchepkin, and also B. A. Alekseev, B. V. Panin, A. F. Soldatov, and E. S. Chernorotov who prepared the separated gadolinium isotopes

[1] S. Suwa, Phys. Rev. 86, 247 (1952).
[2] K. Murakawa, Phys. Rev. 96, 1543 (1954).

*We assume here that the degree of configuration interaction on which the magnitude of the hyperfine structure depends[6] is the same for both ions.

†Although for ions in an S-state one should expect a weak dependence of the hyperfine splitting on the crystalline environment, nevertheless, for example, in SrS — Eu and in CaF_2 — Eu, a considerable difference was found[7] (about 15%) in the values of the hyperfine structure constants for Eu.

[3] F. A. Jenkins and D. R. Speck, Phys. Rev. 100, 973 (1955).
[4] D. R. Speck, Phys. Rev. 101, 1725 (1956).
[5] Manenkov, Prokhorov, Trapeznikova, and Fock, Оптика и спектроскопия (Optics and Spectroscopy) 2, 470 (1957). (The results pertaining to this reference were reported at the Conference on the Physics of Magnetic Phenomena (Moscow, May 1956) and at the Fifth Conference on Luminescence (Tartu, June 1956)).
[6] B. Bleaney and W. Low, Proc. Phys. Soc. A68, 55 (1955).
[7] A. A. Manenkov and A. M. Prokhorov, Dokl. Akad. Nauk SSSR 107, 402 (1956); Soviet Phys. "Doklady" 1, 196 (1956).
[8] Manenkov, Prokhorov, Trukhliaev, and Iakovlev, Dokl. Akad. Nauk SSSR 112, 623 (1957); Soviet Phys. "Doklady" 2, 64 (1957).
[9] P. F. A. Klinkenberg, Revs. Mod. Phys. 25, 63 (1952).
[10] W. Low, Phys. Rev. 103, 1309 (1956).
[11] J. S. Van Wieringen, Physica 19, 397 (1953).

Translated by G. Volkoff
231

SOVIET PHYSICS JETP VOLUME 6 (33), NUMBER 5. MAY, 1958

AN ANOMALOUS MAGNETIC TRANSITION IN ANHYDROUS COPPER SULFATE

A. S. BOROVICK-ROMANOV and N. M. KREINES

Institute for Physical Problems, Academy of Sciences, U.S.S.R., and Institute for Technical Physics and Radio Measurements

Submitted to JETP editor May 15, 1957

J. Exptl. Theoret. Phys. (U.S.S.R.) 33, 1119-1122 (November, 1957)

We have investigated the magnetic properties of small crystals of anhydrous $CuSO_4$ from 1.5 to 300°K. Below $T_c = 34.4$°K this substance shows antiferromagnetic properties. The transition to the antiferromagnetic state is accompanied by an anomalous, twofold increase of the susceptibility in a temperature interval of about 1.5°.

In a previous paper[1] we investigated the temperature dependence of the magnetic susceptibility of anhydrous copper sulfate in the temperature range from 14 to 300°K. At T = 35°K the susceptibility showed a sharp increase, corresponding to a change of 30% over a temperature interval of about 2°K. A further lowering of the temperature was accompanied by a smoother increase of the susceptibility. The specimen of anhydrous copper sulfate we used in that experiment was obtained by heating copper sulfate to 300° C for two hours with constant stirring (see Ref. 2). All operations were performed in a current of dry nitrogen. The specimen was obtained in the form of a light blue, very hygroscopic powder.

Our investigations at helium temperatures have shown that the increase of the susceptibility which is observed below 35°K is apparently caused by the presence of paramagnetic impurities. The most likely impurity to be present can be assumed to be some singly hydrated copper sulfate. An approximate estimate showed that in the specimen used by us there could be found 20% singly hydrated copper sulfate.

The specimens of anhydrous copper sulfate used by us in the present experiment were obtained in two ways. The first specimen was obtained from a solution of copper sulfate in molten ammonium sulfate.[3] Above 360°C $(NH_4)_2SO_4$ decomposes and anhydrous copper sulfate remains in the form of a precipitation. In this case the specimen was obtained in the form of small transparent crystals of $1 \times 0.2 \times 0.2$ mm,

with a faint blue color. These crystals were far less hygroscopic than the powder used by us in the first experiment.*

In Fig. 1 we have shown the two most successful of the crystals obtained in this way. We hope, after improving our methods slightly, to investigate the anisotropy of magnetic properties with these crystals.

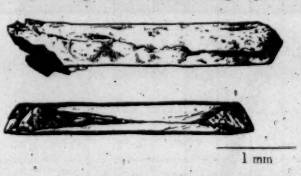

FIG. 1. Crystals of anhydrous $CuSO_4$.

The second specimen was obtained by annealing copper sulfate at 270°C until its weight was constant. The vessel with the specimen was evacuated both before and after the heating, since the material lost 5 molecules of water. If we pump continuously during the annealing the specimen decomposes before the complete dehydratation has taken place.

We measured the magnetic susceptibility of anhydrous copper sulfate, obtained by the first method, in the range of temperatures between 1.5 and 300°K. The measurements were performed in an apparatus similar to the one described in Ref. 4.

From Fig. 2, which gives the temperature dependence of the reciprocal of the molar susceptibility, we see that in the temperature range from 300 to 120°K a Curie-Weiss law with $\Theta = -77.5°$ and $C = 0.517$ is followed. Below 120°K we observe a deviation from the straight line corresponding to the Curie-Weiss law. In the same figure we have drawn the results of the measurements by de Haas and Gorter[5] on anhydrous copper sulfate, which agree reasonably well with ours.

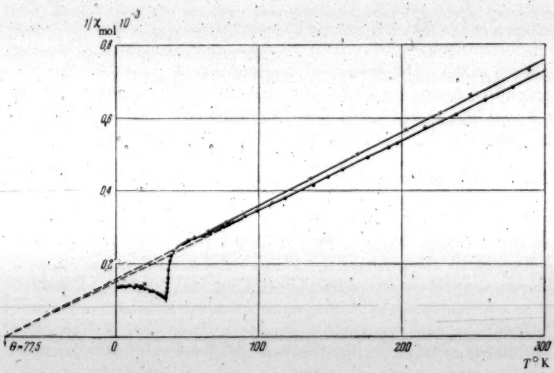

FIG. 2. Temperature dependence of the reciprocal of the molar magnetic susceptibility $1/\chi_{mol}$ of anhydrous copper sulfate. × — results from Ref. 5; ● — our results.

In Fig. 3 we have given the temperature dependence of the molar magnetic susceptibility of $CuSO_4$. At about 35°K the susceptibility rises sharply, changing almost by a factor of two in a temperature interval of about 1.5 degrees. At 34.4°K the susceptibility attains a maximum and then falls to a value which is $^3/_4$ of its maximum value. Starting at about 12°K down to 1.5°K the susceptibility stays constant. In the region where the susceptibility rises steeply it depends on the value of the magnetic field. One can see in Fig. 4 that an increase in the magnetic field produces a fall in the susceptibility while its maximum is displaced towards lower temperatures. The maximum change in the susceptibility observed by us was about 10% when the field was changed from 3,400 to 13,000 oersted. The results obtained with the second specimen were similar to the ones just described except in the temperature range from 4 to 1.5° K where the susceptibility slightly increased. Such a behavior of the susceptibility is apparently produced through an insufficient dehydration of the specimen.

The results which we have obtained for the temperature dependence of the magnetic susceptibility of anhydrous copper sulfate show that at 34.4°K this material undergoes a transition below which it apparently becomes antiferromagnetic. The transition itself is unusual and differs from the normal ones by an anomalously steep rise of the susceptibility in the neighborhood of the transition. The question as to the character of the transition remains for the time being an open one.

*The authors are very grateful to N. N. Mikhailov for his assistance in preparing the specimens.

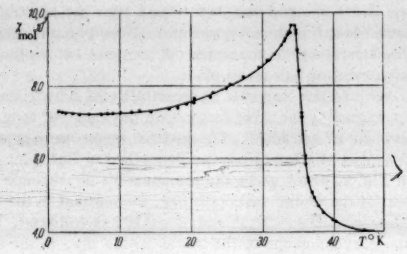

FIG. 3

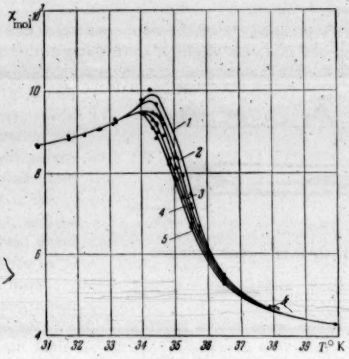

FIG. 4

FIG. 3. Temperature dependence of the molar magnetic susceptibility χ_{mol} of anhydrous copper sulfate.

FIG. 4. Temperature dependence of the molar magnetic susceptibility χ_{mol} of anhydrous copper sulfate in the transition region for different intensities of the magnetic field: 1 — 3,370; 2 — 6,660; 3 — 9,700; 4 — 11,780; 5 — 12,900 oersted.

The authors express their sincere thanks to P. L. Kapitza for his constant interest in their work. The authors also thank P. G. Streikov for some valuable advice.

[1] Borovik-Romanov, Karasik, and Kreines; J. Exptl. Theoret. Phys. (U.S.S.R.) **31**, 18 (1957), Soviet Phys. JETP **4**, 109 (1957).

[2] Iu. V. Kariakin and I. I. Angelov, Чистые химические реактивы (Pure Chemical Reagents) Goskhimizdat, Moscow, 1955.

[3] M. P. Klobb, Compt. rend. **114**, 836 (1892).

[4] A. S. Borovik-Romanov and N. M. Kreines, J. Exptl. Theoret. Phys. (U.S.S.R.) **29**, 790 (1955), Soviet Phys. JETP **2**, 657 (1956).

[5] W. J. de Haas and C. J. Gorter, Leiden Commun., 215a, 1931; Proc. Roy. Acad. Sc., Amsterdam **34**, 317 (1931).

Translated by D. ter Haar
232

SOVIET PHYSICS JETP VOLUME 6 (33), NUMBER 5 MAY, 1958

YIELD AND ANGULAR DISTRIBUTION OF FAST PHOTONEUTRONS FROM DEUTERIUM AND CARBON

P. S. BARANOV, V. I. GOL'DANSKII, and V. S. ROGANOV

P. N. Lebedev Physics Institute, Academy of Sciences, U.S.S.R.

Submitted to JETP editor May 20, 1957

J. Exptl. Theoret. Phys. (U.S.S.R.) 33, 1123-1130 (November, 1957)

The yield and angular distribution of fast photoneutrons (of energy > 20.6 Mev) from carbon and deuterium were investigated on the 265 Mev synchrotron of the Physics Institute, Academy of Sciences. Results of the experiments are interpreted from the point of view of the two-nucleon model for photon energies both below and above the threshold for meson production.

1. INTRODUCTION

PHOTODISINTEGRATION of the deuteron is the simplest example of the interaction of γ-rays with nuclei. At one time the study of this reaction near threshold gave various information about the interaction of protons with neutrons and quantiatively established two types of dipole absorption of γ-rays, photoelectric and photomagnetic absorption.

In recent years the photodisintegration of the deuteron has been studied in especial detail for photons of high energy — near to and above the threshold for meson production — in so far as it was of interest to establish whether an essential change in the mechanism of γ-ray absorption occurred in this energy region. However, up to the present there has not been a theory which completely explains the experimental data on photodisintegration of the deuteron for photons of energy exceeding 50 Mev. Besides this, the investigation of photodisintegration of the deuteron by high-energy photons is necessary for an analysis of the interaction of γ-rays with complex nuclei which depends, according to the two-nucleon model[1,2] on the absorption of γ-rays by pairs of nucleons in the nuclei, in particular, proton-neutron pairs (quasi deuterons).

At present, a considerable number of experiments on photodisintegration of the deuteron have been carried out from threshold for the reaction $\gamma + d \rightarrow n + p$ up to energies of approximately to 450 Mev. In all experiments on the photodisintegration of the deuteron with high-energy photons, the emitted protons were counted. Data on the emission of photo neutrons could serve as a check on these experiments. In addition, in order to verify the two-nucleon model, it is of interest to compare the yield and angular distribution of fast neutrons from deuterium for photon energies below and above the threshold for meson production with analogous data obtained by the same method for complex nuclei.

2. EXPERIMENTAL ARRANGEMENT

In the present work, carried out on the 265 Mev synchrotron of the Physics Institute of the Academy of Sciences, the photodisintegration of the deuteron by photons of energies greater than 50 Mev was studied by counting the neutrons. For this we employed a high-threshold scintillation neutron detector[3] based on producing the reaction $C^{12}(n, 2n)C^{11}$ with threshold of 20.6 Mev in a liquid scintillator. The C^{11} activity was detected by fluorescence of the scintillator coming from decay positrons, using FEU-19 M photomultipliers connected in coincidence ($\tau \approx 3 \times 10^{-8}$ sec).

In order to increase the efficiency of counting positrons from the decay of C^{11}, the dependence of this efficiency on the form and volume of the container of the scintillation counter and on the voltage of the photo-multiplier was studied in special experiments. As a result of this investigation, a solution of terphenyl in xylene of volume 50 cm^3 in a spherical glass container was used as a scintillator. The voltage on the photomultiplier was about 2100 v. Under these conditions the effective number of atoms of carbon in the scintillator comprised $N \approx 7.2 \times 10^{24}$, which allowed detection of a neutron beam of 20 neutrons/cm^2 sec (for neutrons of high energy this beam corresponds to the tolerance dose) with an accuracy of ~ 6% for activation by neutrons for 30 min and a counting time of the scintillator of 40 min.

Using such a detector, the yield and angular distribution of photoneutrons from deuterium was studied by the difference of D_2O and H_2O yields under bremsstrahlung radiation of maximum energy 255 Mev. The experimental arrangement is given in Fig. 1. The neutron sources D_2O and H_2O, in cubical containers with walls of 15 μ copper foil, were placed in the center of the γ-ray beam. The mass of the irradiated liquid was ~ 200 g; here the thickness of material did not exceed ~ 0.2 radiation units and ~ 0.1 mean free paths of 30 Mev neutrons relative to inelastic scattering. Such dimensions of the target did not lead to a noticeable distortion in the angular distribution of the neutrons or in the form of the excitation function.

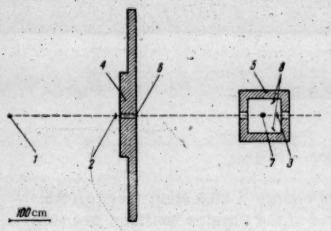

FIG. 1. Experimental arrangement. 1 — target of the synchrotron, 2 and 3 — carbon monitors of the photon beam, 4 and 5 — lead shielding, 6 — collimator of diameter 40 mm, 7 — target of D_2O or H_2O, 8 — neutron detector.

The liquid organic scintillator which served as a neutron detector was placed during the irradiation at a definite angle relative to the direction of the photon beam in five containers ($2 \times 5 \times 10$ cm^3). The use of several containers made it possible to improve the statistics without worsening the angular resolution, which constituted $\pm 6°$ in our experiments. The beam of γ-rays proceeded through a lead collimator of diameter 4 cm. The thickness of the lead shields for the neutron detectors on the side of the synchrotron target was 40 cm. In addition, the entire apparatus was shielded on all sides by lead walls of thickness 20 cm.

In order to separate off accessory activation of the detectors on account of the reactions $C^{12}(p, pn)C^{11}$ and $C^{12}(\gamma, n)C^{11}$, by particles emitted from the targets (D_2O and H_2O), we also screened the neutron detectors on all sides with sheets of lead of thickness 1 cm. A check showed that with raising the thickness of the shields to several millimeters, the activation of the detectors decreased rapidly and was practically independent of the further increase in thickness of the target above several millimeters, i.e., it was determined at the thickness of shielding noted.

An absolute value for the photon beam was determined by activation of graphite plates ($0.2 \times 3 \times 6$ cm^3) using the reaction $C^{12}(\gamma, n)C^{11}$. The accuracy of absolute measurement of the photoneutron beam was ~ 15% and was basically determined by the accuracy with which the cross section for the reaction $C^{12}(n, 2n)C^{11}$ is known (see, for example, Ref. 3) in the range of neutron energies from 30 to 60 Mev.

3. EXPERIMENTAL RESULTS

We obtained the angular distribution of photoneutrons from deuterium for maximum bremsstrahlung energies $E_{\gamma m}$ = 170 Mev and $E_{\gamma m}$ = 255 Mev and the dependence of the yields on the maximum photon energy at 75° in the laboratory system (l.s.), corresponding in this energy interval to approximately 90° in the center-of-mass system (c.m.s.). This dependence is shown on Fig. 2, on which there is also given the analogous dependence obtained by way of evaluating the neutron yields from the results of recent results on photodisintegration of the deuteron.[4-10] The evaluation was carried out in the following way. The differential cross section for emission of photoprotons in the disintegration of the deuteron in the c.m.s. was transposed by replacing the angle θ by $\pi - \theta$ (transition from protons to neutrons). Going to the l.s., we integrated over the spectrum of bremsstrahlung, and took into account the energy dependence of the reaction $C^{12}(n, 2n)C^{11}$. From Fig. 2 it can be seen that our data for photons with energies up to ~ 200 Mev agree well with the other experiments.

For photon energies greater than 200 Mev the yield of neutrons increased sharply. This growth was connected with meson production in the photodisintegration. Consideration of photoproduction of mesons in deuterium in the impulse approximation shows that only two reactions can lead to production of neutrons with energies > 20 Mev in our energy interval: photoproduction of π^0 mesons on the neutron and of π^+ mesons on the proton. Photoproduction of a π^0 meson on the proton in deuterium does not lead in the impulse approximation to the production of fast neutrons.

In production of a meson on a nucleon at rest by photons of energy up to 255 Mev it is impossible to have a nucleon of energy $\geq$ 20 Mev emitted at an angle $\geq 40°$. However, already at the energies of motion of the nucleons in deuterium ($E \geq 12$ Mev) the emission of neutrons of energy 20 Mev is possible up to

90° (l.s.) for $E_{\gamma m}$ = 255 Mev and at angles up to 70° for $E_{\gamma m}$ = 200 Mev.

The angular distribution of neutrons in the l.s. obtained by us for $E_{\gamma m}$ = 170 Mev is given on Fig. 3. Curve 1 corresponds to the data of Refs. 4 — 10 (transposed for neutrons), which can be approximated in the c.m.s. by a curve of the form

$$\sigma(\theta) = (A + B\sin^2\theta)(1 - C\cos\theta),$$

where θ is the angle of emission of neutrons in the c.m.s. and $A = 4.5 \times 10^{-30}$ cm²/sterad·Q, $B = 3.8 \times 10^{-30}$ cm²/sterad·Q, $C = 0.35$. As follows from Fig. 3, our data for $E_{\gamma m}$ = 170 Mev agree with the results of these other experiments within the accuracy of the experiments.

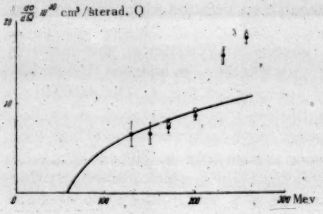

FIG. 2. Yield of fast photo neutrons from deuterium at 75° in the l.s. vs. maximum energy of the photon bremsstrahlung spectrum. The solid curve gives the results of the experiments, Refs. 4 — 10, transposed for neutrons; ● — yield of fast neutrons from deuterium, ○ — yield of fast neutrons from carbon.

For $E_{\gamma m}$ = 255 Mev, as can be seen from Fig. 3, the angular distribution obtained by us differs markedly from the results of transposing data for the photodisintegration of deuterium without the production of mesons (curve 2). It is clear that the contribution of photoproduction of mesons leads to a noticeable increase in the general yield of fast photoneutrons from deuterium and to a marked change in the form of their angular distribution — to the appearance of an additional group of neutrons, sharply peaked forward.

It should be noted that although we employed a difference method which gives, instead of the yield of fast neutrons from deuterium, the difference in yields from deuterium and hydrogen, the yield from hydrogen is different from zero only for angles ≤ 40°, so that its contribution at 30° constitutes 25% of the yield from deuterium at 30° and, after integration over angles, 5% of the total yield.

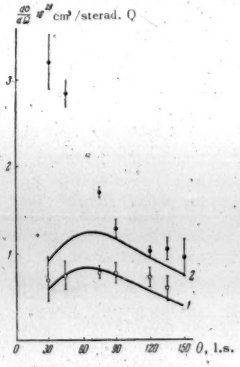

FIG. 3. Angular distributions of photoneutrons of energy > 20 Mev from deuterium; ○ — $E_{\gamma m}$ = 170 Mev, ● — $E_{\gamma m}$ = 255 Mev. The solid curve gives the results of the experiments, Refs. 4 — 10, transposed for neutrons: 1 — for $E_{\gamma m}$ = 170 Mev, 2 — for $E_{\gamma m}$ = 255 Mev.

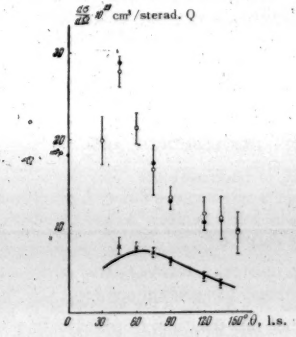

FIG. 4. Angular distributions of neutrons of energy > 20 Mev from carbon and deuterium. ○ — yield of neutrons from carbon for $E_{\gamma m}$ = 225 Mev;[15] × — the same for $E_{\gamma m}$ = 170 Mev; ● — yield of neutrons from deuterium for $E_{\gamma m}$ = 255 Mev. The solid curve gives the angular distribution of neutrons from deuterium for $E_{\gamma m}$ = 170 Mev, obtained from the results, Refs. 4 — 10, transposed for neutrons.

The integral yield of neutrons of energy > 20 Mev from deuterium in processes of production of π^+ mesons and π^0 mesons can be determined as the difference between the total yield of neutrons from deuterium measured by us and the yield, taken from the literature, of neutrons from deuterium in processes without production of photomesons. The magnitude of this difference constitutes 8×10^{-29} cm²/sterad·Q and, within the limits of experimental error, agrees with the estimate of the yield of neutrons in reactions with the production of π^+ and π^0 mesons from deuterium obtained by superposition of data in the literature[11] on the photoproduction of mesons on nucleons.

From the point of view of the quasi-deuteron model[1] it is of particular interest to compare our data on the yield and angular distribution of fast neutrons from deuterium with analogous data obtained earlier by the same method for complex nuclei. The two-nucleon model was verified qualitatively in direct experiments on n−p coincidences[12-14] of photonucleons from complex nuclei. These experiments showed that a considerable number of protons from the nucleus have that angular correlation with photoneutrons determined by photodisintegration of the deuteron.

In Fig. 4 we show the angular distribution of fast neutrons from carbon for a maximum photon energy $E_{\gamma m}$ = 255 Mev, obtained earlier,[15]* and our data for carbon for $E_{\gamma m}$ = 170 Mev. In addition, the yields of neutrons from deuterium for the same maximum photon energies are given on Fig. 4. The data for carbon and deuterium were normalized using the total cross section.

From Fig. 4 it can be seen that the angular distributions of neutrons from carbon and deuterium are similar both for $E_{\gamma m}$ = 170 Mev and $E_{\gamma m}$ = 255 Mev. Some difference occurs only for 30° and $E_{\gamma m}$ = 255 Mev. It is possible that the difference is connected with the Pauli principle, which allows only those processes of photodisintegration of quasi deuterons and production of mesons on them in which the energy of both nucleons exceeds the Fermi energy (20 Mev). Several differences between the nucleon yield at small angles from complex nuclei and deuterium were noticed also in the experiments of Odian et al.,[13] in which the correlations in the emission of neutrons and protons from lithium, nitrogen and deuterium were studied.

TABLE I. Yield of photoneutrons of energy $\gtrsim$ 20 Mev from deuterium and carbon

$E_{\gamma m}$ (Mev)	Yield from deuterium (without meson production) according to Ilefs. 4-10 10^{28} cm^2/Q	Total yield from deuterium $\sigma_D \times 10^{28}$ cm^2/Q	Total cross section from carbon $\sigma_C \times 10^{28}$ cm^2/Q	σ_C/σ_D
170	0.82	0.84±0.07	7.2±0.25	8.58±0.66
255	1.27	2.06±0.06	18.9±1.35	9.18±1.44

In Table I we give the total yields of fast neutrons from carbon and deuterium for $E_{\gamma m}$ = 170 and 255 Mev and the data in the literature on photodisintegration of deuterium without meson production.

From Table I it can be see that the ratio of yields of fast neutrons from carbon and deuterium is the same for $E_{\gamma m}$ = 170 Mev, where such neutrons are emitted exclusively in the process of photodisintegration of deuterium without meson production, as for $E_{\gamma m}$ = 255 Mev where the process of meson production is essential.

4. DISCUSSION OF RESULTS

The connection between the emission of photonucleons from complex nuclei and deuterium is usually described in the framework of Levinger's two-nucleon theory,[1] according to which the cross section σ_A for photodisintegration of a nucleus with mass number A and the cross section for photodisintegration of deuterium σ_D are connected by the relation

$$\sigma_A = 6.4\,(NZ/A)\,\sigma_D, \tag{1}$$

where Z is the number of protons and N = A − Z is the number of neutrons in the nucleus. In the work of Odian et al.[13] in which it was assumed that the quasi deuteron is in a $^3S_1$ state and the nuclear radius is taken equal to R = 1.2 $A^{1/3} \times 10^{-13}$ cm (instead of R = 1.4 $A^{1/3} \times 10^{-13}$ cm) and the Hulthén wave function for deuteron was used, it was found that

$$\sigma_A = 3.8\,(NZ/A)\,\sigma_D. \tag{2}$$

The two-nucleon model has been verified in a series of experiments in which the yield of high-energy photoprotons from the nucleus and the angular correlation of photoprotons and photoneutrons were observed. However, in all of these, the experimental conditions were such that only processes of two-nucleon disintegration without meson production were counted. Correspondingly, the verification of the validity of the predictions of the two-nucleon model was carried out by comparison of results for complex nuclei with data on the photodisintegration of deuterium into protons and neutrons without meson production. In the present work it was possible to compare total cross sections and angular distributions of neutrons in photodisintegration of deuterium both without and with meson production. From Table I it can

*The data of Ref. 15 should be decreased by 10% because of a more accurate measurement of the intensity of the photon beam and its absorption in the target.

be seen that for photon energies below the threshold of meson production, as well as for higher energies, the relation satisfied for carbon is

$$\sigma_c \approx 3(NZ/A)\sigma_D,$$

in good agreement with the calculations and experimental data of reference 13, obtained for only the non-mesonic processes.

In order to interpret the results, it is useful to turn to the concept of Wilson[16,17] about the disintegration of deuterium by photons of energy 40 – 500 Mev, extending it to the disintegration of quasi deuterons. According to Wilson, photodisintegration of deuterium proceeds, together with disintegration not connected with mesonic processes, with reabsorption of virtual and real mesons. In the interaction in deuterium of γ-rays with one of the two nucleons, a virtual or real π-meson is produced. If the second nucleon is then close to the first one ($r \lesssim \hbar/\mu c$), the meson will be reabsorbed with a probability close to unity and there will be photodisintegration of deuterium without meson production (the probability of repeated emission of mesons in the disintegration is very small). The larger the distance between the nucleons, the smaller is the probability of reabsorption of a meson produced on one of them by the other one, and the larger is the probability of photoproduction of a meson (if, of course, it is allowed by conservation laws).

We will assume, for simplicity, that if the nucleons are found closer to each other than $r \leq \kappa\hbar/\mu c$, then reabsorption occurs with unit probability; if $r \geq \kappa\hbar/\mu c$, then there is no absorption. Then the probability of reabsorption ω can be determined as the probability of finding the nucleons in the deuteron or quasi deuteron at distances $r \leq \kappa\hbar/\mu c$.

The cross section for photodisintegration of the deuteron or quasi deuteron without production of real mesons can be written in the form

$$\sigma_{np} = \sigma_1\omega + \sigma_2, \tag{3}$$

where σ_1 is the cross section for absorption of a γ-ray with production of a π^+, π^- or π^0 meson on the neutron or proton of the deuteron or quasi deuteron; σ_2 is the cross section for photodisintegration of the deuteron or quasi deuteron not connected with meson processes. Then the cross section for photodisintegration with production of real mesons can be written in the form

$$\sigma_\pi = \sigma_1(1-\omega), \tag{4}$$

and the total cross section is equal to

$$\sigma_t = \sigma_{np} + \sigma_\pi. \tag{5}$$

From Eqs. (3), (4), and (5) it follows that $\omega \leq \sigma_{np}/\sigma_t$ and $1-\omega \geq \sigma_\pi/\sigma_t$. In the case of a complex nucleus these inequalities are strengthened because the σ_π observed can be below the true one on account of reabsorption of mesons by other nucleons of the nucleus.

From our and other experimental data it is possible to evaluate the upper limits of the probability of reabsorption of mesons in deuterium $\omega = \omega_D$ and in the quasi deuterons $\omega = \omega_C$ in the carbon nucleus. These are given in Table II.

The values of the quantities in Table II were obtained by using the results of the work, Refs. 4 – 10, for the cross section of photodisintegration of deuterium without production of real mesons, cross sections for photoproduction of mesons on nucleons from Ref. 11, the data from Ref. 18 $\sigma\pi^{\pm} = 7.3\sigma_{\gamma p \to \pi^+ n}$ for $E_{\gamma m} = 310$ Mev and $^{23}\sigma_{\pi^0} = 12\sigma_{\gamma p \to \pi^0 p}$ for $E_{\gamma m} = 256$ Mev for a rough estimate of the cross section of production of mesons on carbon and, finally, our data on the ratios of the total cross sections of carbon and deuterium: $\sigma_C \approx 9\sigma_D$. From the table it can be seen that the quantity ω_D is, in the range of photon energies ~ 250 Mev, near to that calculated by Austern[20] using the isobar model ($\omega_D = 0.11$), which corresponds to a value $r = 0.7\,\hbar/\mu c$ (for the wave function of Hulthén).

TABLE II. Probability of reabsorption of mesons in deuterium and in quasi deuterons in carbon.

E_γ (Mev)	160	180	200	220	240	260	280	300	320	360	400	450
$\omega_D \leq$	0.39	0.24	0.17	0.13	0.11	0.09	0.07	0.053	0.041	0.039	0.039	0.038
$\omega_C \leq$	0.74	0.68	0.64	0.61	0.58	0.55	0.52	0.49	0.47	0.47	0.49	0.50

The quantity ω_C for the quasi deuterons in the carbon nucleus is substantially less than unity. This indicates that in the production of mesons in the carbon nucleus the probability of their reabsorption in the same quasi deuteron in which they were formed is sufficiently small.

A qualitative indication that the value of ω_C should be even less than the upper limits given in Table II comes from the similar angular distributions of photoneutrons from deuterium and carbon noted in our experiments. The angular distribution of photoneutrons for $E_{\gamma m} = 255$ Mev is the sum of two completely different distributions arising from the photodisintegration of deuterium without photoproduction of mesons and photodisintegration with meson production (see Figs. 3 and 4). Under the conditions $\omega_D \ll 1$ and $\omega_C \gg \omega_D$ (because of the much greater compactness of the carbon nucleus compared with deuterium) similar angular distributions would result only if $\omega_C \ll 1$.

In connection with the results obtained we note that the increase in yield of fast photoneutrons as $\sim A^{4/3}$ from carbon to lead noted in Ref. 15 for $E_{\gamma m} = 255$ Mev, and also the somewhat larger fraction of neutrons emitted from heavy nuclei (for example, from lead) at large angles, is apparently caused by secondary processes (interaction of the nucleons and absorption of mesons in the nucleus) leading to the production of stars with emission of fast neutrons.

CONCLUSIONS

1. The yield and angular distribution of fast photoneutrons emitted by deuterium and carbon interacting with bremsstrahlung γ-rays with maximum energies 170 and 255 Mev were studied. An effective scintillation counter for fast neutrons, based on the reaction $C^{12}(n, 2n)C^{11}$ (threshold 20.6 Mev) in a volume of liquid scintillator, was used.

2. For γ-rays of maximum energy 170 Mev, the results obtained for deuterium agree with the results of experiments in which the photodisintegration of deuterium was studied by registering protons. For a maximum γ-ray energy of 255 Mev the angular distribution of fast photoneutrons from deuterium changed markedly on account of the appearance of a substantial yield of photoneutrons produced in the process of photoproduction of mesons and emitted in the forward direction.

3. Both for a maximum γ-ray energy of 170 Mev, where the detector did not count neutrons connected with meson production, and for 255 Mev, where these processes were essential, the ratio of total yields was

$$\sigma_C/\sigma_D \approx 3(NZ/A) = 9$$

Thus, this consequence of the two-nucleon model was verified not only for the disintegration of deuterium and carbon without mesons, but also for the photomeson processes in these nuclei. For both maximum energies the same angular distributions of fast neutrons result for deuterium and carbon, in spite of the marked change in their form in the transition from one maximum energy to the other.

4. Comparison of the results obtained with data on the photoproduction of mesons from deuterium and carbon makes it possible to evaluate the upper limit of the probability of reabsorption of the meson produced on one nucleon of the deuteron or quasi deuteron in carbon by the second nucleon. In the energy range $\sim$ 250 Mev and above this probability is < 0.1 for deuterium and, apparantly, less than 0.5 for carbon.

In conclusion, we express our gratitude to A. M. Baldin and V. A. Petrun'kin for taking part in the discussion of our results.

[1] J. S. Levinger, Phys. Rev. 84, 43 (1951).

[2] Iu. K. Khokhlov, J. Exptl. Theoret. Phys. (U.S.S.R.) 23, 241 (1952).

[3] P. S. Baranov and V. I. Gol'danskii, J. Exptl. Theoret. Phys. (U.S.S.R.) 28, 627 (1956), Soviet Phys. JETP 1, 576 (1955).

[4] E. Whalin, Phys. Rev. 95, 1362 (1954).

[5] J. Keck and R. M. Littauer, Phys. Rev. 93, 827 (1954).

[6] L. Allen and A. Hanson, Phys. Rev. 95, 629 (1954).

[7] L. Allen, Phys. Rev. 98, 705 (1955).

[8] Tollestrup, Keck, and Smythe, Phys. Rev. 96, 850 (A) (1954). J. C. Keck and A. V. Tollestrup, Phys. Rev. 101, 360 (1956).

[9] Whalin, Schriever, and Hanson, Phys. Rev. 101, 377 (1956).

[10] Aleksandrov, Delone, Slovokhotov, Sokol, and Shtarkov, J. Exptl. Theoret. Phys. (U.S.S.R.) (in press)

[Possibly: 33, 614 (1957); Soviet Phys. JETP 6, 472 (1958)].

[11] H. A. Bethe and F. de Hoffmann, Mesons and Fields, 1955.

[12] M. Barton and J. Smith, Phys. Rev. 95, 573 (1954). H. Myers and A. Odian, Phys. Rev. 95, 576 (1954).

[13] Odian, Stein, and Feld, Phys. Rev. 102, 837 (1956).

[14] Odian, Stein, and Feld, Phys. Rev. 104, 1710 (1956).

[15] P. S. Baranov and V. I. Gol'danskii, J. Exptl. Theoret. Phys. (U.S.S.R.) 28, 746 (1955), Soviet Phys. JETP 1, 613 (1955).

[16] R. R. Wilson, Phys. Rev. 86, 125 (1952).

[17] R. R. Wilson, Phys. Rev. 104, 218 (1956).

[18] R. M. Littauer and D. Walker, Phys. Rev. 86, 838 (1952).

[19] Govorkov, Gol'danskii, Karpukhin, Kutsenko, and Pavlovskaia, Dokl. Akad. Nauk SSSR 112, 37 (1957), Soviet Phys. "Doklady" 2, 4 (1957).

[20] N. Austern, Phys. Rev. 100, 1522 (1955).

Translated by G. E. Brown
233

SOVIET PHYSICS JETP VOLUME 6 (33), NUMBER 5 MAY, 1958

α-PARTICLES EMITTED BY HEAVY EMULSION NUCLEI IN EMULSIONS BOMBARDED BY HIGH-ENERGY PROTONS

P. A. VAGANOV and V. I. OSTROUMOV

Leningrad Polytechnic Institute

Submitted to JETP editor May 25, 1957

J. Exptl. Theoret. Phys. (U.S.S.R.) 33, 1131-1139 (November, 1957)

An investigation has been made of the energy spectra of α-particles emitted by heavy nuclei in emulsions bombarded by protons with energies of 360, 560, and 660 Mev, assuming different excitation energies for these nuclei. The calculated evaporation spectrum is found to be in satisfactory agreement with experiment in the α-particle range up to 14 Mev without requiring any reduction of the Coulomb barrier as proposed by Le Couteur. By subtracting the calculated evaporation spectrum from the experimental spectrum the energy distribution for the cascade α-particles and the relative number of such particles which appear in one disintegration event at the three experimental energies cited above have been obtained.

INTRODUCTION

THE α-particles emitted in the disintegration of nuclei in emulsions bombarded by high-energy nucleons have been studied by many investigators.[1-14] However, most of these studies have been carried out with non-monoenergetic fast-particle sources (cosmic rays); thus there is a high degree of uncertainty in the interpretation of the results. In addition, the methods used for distinguishing between stars due to heavy nuclei and light nuclei are not always effective. Finally, in most cases the investigators did not have at their disposal a sufficient number of events to ensure good statistics for studying the α-particle energy spectra at different excitation energies.

In a number of papers[1,3-5,12-14] it has been noted that among the α-particles emitted from silver and bromine nuclei there is an anomolously large (from the point of view of nuclear evaporation theory) number of slow α-particles. Le Couter[15] and Fujimoto and Yamaguchi,[16] on the basis of an idea suggested by

Begge concerning the thermal vibrations of the nuclear fluid, have assumed that the appearance of these so-called "sub-barrier" particles is due to the significant reduction of the potential barrier in strongly excited nuclei. Certain other investigators, however, have found this interpretation to be inadequate. Thus Perkins[3] has advanced the hypothesis that at high excitation energies nuclei emit fragments which are unstable and decay into α-particles in flight. Süssmann,[17] developing this hypothesis further, has proposed that the assumed excitation in these nuclei can lead either to particle evaporation or to fission and subsequent evaporation, both modes being equally probable. Thus, according to Süssmann the appearance of α-particles with energies significantly below the Coulomb barrier of the original nucleus can be explained, firstly, by the lower barrier in the daughter nuclei and, secondly, by the Doppler effect (evaporation of particles from a moving fragment).

In the work discussed above it has also been noted that in the energy distributions of both α-particles and protons emitted from the emulsion nuclei, there is a long "tail" in the high energy region. This "tail" cannot be accounted for by evaporation theory because the particle angular distribution in the high-energy region is anisotropic — the motion of these particles is peaked in the direction of the bombarding-nucleon beam. In Ref. 18, in which stars exhibiting a recoil-nucleus track were studied, 40 — 50 percent of all the α-particles emitted by silver and bromine nuclei in stars induced by 460 and 660 Mev protons were assigned to the cascade stage of the disintegration process in the nucleus. This conclusion was reached on the basis of a comparison of the observed number of α-particles in these stars with the number of particles expected from evaporation theory.

In the present work, which is essentially an extension of the work carried out in Ref. 18, a detailed study has been made of the energy distribution of α-particles from stars produced in heavy emulsions by high energy protons. Several α-energy spectra have been considered; each of these corresponds to a definite range for the nuclear excitation energy. An attempt has been made to interpret the "sub-barrier" α-particles from the point of view of ordinary evaporation theory and to obtain information on the number of cascade α-particles and their energy distribution.

EXPERIMENT AND EXPERIMENTAL DATA

The work was carried out with fine-grained P-9 nuclear emulsions having a sensitivity of 30 Mev for protons.[18] The plates were irradiated by placing them in the proton beam of the synchrocyclotron of the Joint Institute for Nuclear Research. The beam direction was parallel to the plane of the emulsion. The bombarding-proton energies were 360, 560 and 660 Mev. The protons with energies below 660 Mev were obtained by degrading the beam in graphite blocks.

In the measurements we chose stars exhibiting recoil tracks; these are produced, for the most part, by heavy nuclei in the emulsion. On the basis of the available data,[19,20] the number of stars exhibiting a recoil track, associated with light nuclei in the emulsion, is less than 10 percent of the total number of stars exhibiting recoil tracks. Obvious cases of "light" disintegration were rejected even when accompanied by a dense track of length less than 10μ so that the actual admixture of "light" stars was less than 1 percent in the cases chosen for measurement.

The tracks formed by α-particles were distinguished from tracks due to other charged particles by visual means; the scanners received preliminary training. The reliability of this method of identification was checked by control observations of individual tracks as in Ref. 21.

The α-particle energy was determined from the length of those tracks which remained in the emulsion layer, using the range-energy relation given in Ref. 22. The emulsion shrinkage factor was taken as 2.5. The correction for α-particles with energies below 12 Mev which escaped from the emulsion was computed assuming an isotropic particle distribution. To correct for high-energy α-particles, a measurement of the angular distribution with respect to the beam was carried out in the plane of the field of view. Expressing this distribution in the form $a + b\cos^2\theta$ it is possible to compute the corrections for the isotropic and anisotropic parts of the distribution separately for the forward and backward hemispheres. The corrections for the $\cos^2\theta$ distribution were determined from the expression:

$$\frac{N_0}{N} = \frac{2d\sqrt{d^2+R^2}}{2d^2+R^2-R\sqrt{R^2+d^2}},$$

where N_0 is the total number of tracks with range greater than R, N is the observed number of tracks, and d is the thickness of the emulsion.

Using the true geometric correction we obtain the "mean star" value of the isotropic and anisotropic correction coefficient. Although the actual angular distribution differs from the projected distribution obtained in the present work this fact is not of importance because corrections to the track yields are small for short-range particles and the high-energy distribution is approximately the same as the spatial distribution.

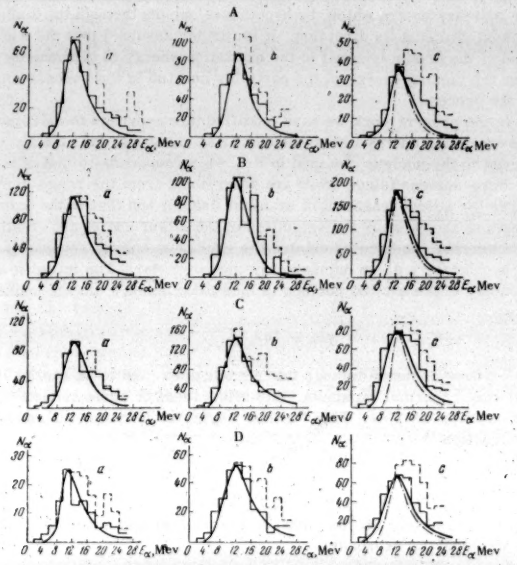

FIG. 1. α-particle energy spectra in Ag and Br stars corresponding to the following initial excitation energies of the nucleus U: A — 0 — 50 Mev; B — 50 — 100 Mev; C — 100 — 150 Mev; D — 150 — 200 Mev. The bombarding-proton energies are as follows: a — 360 Mev; b — 560 Mev; c — 660 Mev; the solid line indicates the "back" spectrum; the dashed line the "front" spectrum and the dot-dash line is the calculated spectrum.

All the recorded α-particles were assigned to groups corresponding to a given excitation energy range for the nucleus. Using the relations given in Ref. 18, which establish the connection between the number of prongs in a star and the mean excitation energy of the nucleus, these groups were taken as shown in Table I.

In Fig. 1 are shown the energy spectra for α-particles emitted by silver and bromine nuclei in the forward ("front" spectrum) and rear ("back" spectrum) hemispheres corresponding to various proton energies. The difference in the "front" and "back" spectra is small at α-particle energies below 12 Mev and is explained by the imparted motion of the evaporating nucleus. When the appropriate corrections are introduced (cf. Ref. 18) the "front" and "back" spectra become almost identical in the energy region up to 12 — 14 Mev and overlap in the figure; however, the difference in the high-energy spectra remains.

In order to compare the present data with the results obtained by Deutsch[10] a plot has been made of the energy distribution of α-particles emitted by silver and bromine nuclei at small angles (below 30°) to the 360-Mev proton beam (Fig. 2). The small difference in the energy spectra is apparently due to the fact that stars due to silver nuclei were considered in Deutsch's work whereas in the present work a considerable fraction of the events occur in the lighter bromine nucleus.

TABLE I

Proton energy, Mev	360		560		660	
Excitation energy of nucleus, Mev	Number of prongs	Number of α-particles	Number of prongs	Number of α-particles	Number of prongs	Number of α-particles
0—50	1—2	366**	1—2	272	1—2	379
50—100	3—4	753	3—4	683	3—5	1551
100—150	5—6	570	5—7	980	6—7	867
150—200*	7 or more	314	8 or more	403	8 or more	777

* For stars due to 660-Mev protons the upper limit for the excitation energy is approximately 250 Mev.
** The statistics in each group have been taken arbitrarily.

EVAPORATION SPECTRUM AND CASCADE PARTICLES

As a rule, in work on stars in heavy-emulsion nuclei the excitation energy has been determined for an average nucleus of mass 94 and

charge 41. Our calculations of the evaporation spectra were carried out separately for the Ag_{47}^{108} and Br_{35}^{80} nuclei.

In Ref. 18 the excitation energy was determined for the mean imparted velocity of a target nucleus with A = 94, obtained as the difference of the velocity components of the recoil nucleus in the direction of the beam and perpendicular to it. This imparted velocity implies a certain loss of energy and momentum for the primary proton which, by hypothesis, moves through the nucleus without changing its direction. It is further assumed that the energy loss of the proton is equal to the excitation energy of the nucleus plus the binding energy of the particles emitted in the cascade stage of the process.

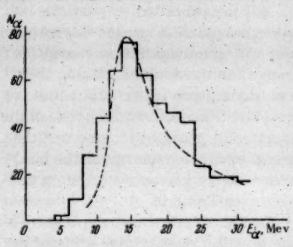

FIG. 2. Energy spectrum of α-particles emitted by heavy-emulsion nuclei at angles smaller than 30° with respect to a beam of 360-Mev protons. The dashed curve refers to results reported by Deutsch.[10]

TABLE II

Proton energy, Mev	360	660
α-particle energy, Mev	Percentage of the α-particles emitted in the forward direction	
12–15	53±6*	54±7
15–25	61±6	59±5
>25	90±21	74±12

*The statistical errors in the experiment are shown.

In the present work we have modified this approach to calculating the excitation energy of the nucleus. Assuming that the velocity imparted to the nucleus obtained in Ref. 18 corresponds to that of a bromine nucleus (since these are determined from the range-energy curve for a light fragment of uranium fission) and that in the same length of recoil track the velocities of the silver nuclei are smaller by 5 percent, we have calculated the excitation energy separately for Ag and Br for a given number of prongs in a star. The initial temperature of the excited nucleus is then determined from the expression:

$$T = \sqrt{(12.5/A)\,U}.$$

We have assumed further that a nucleus excited to an energy U undergoes thermal expansion; this effect leads to some reduction of the potential barrier. This thermal expansion is characterized by the function:[23]

$$R = R_0(1 + 0.008\,T^2),$$

where $R_0 = [1.4(A-4)^{1/3} + 1.2] \times 10^{-13}$ cm.

The α-particle Coulomb barriers for silver and bromine are determined by the expression

$$V = 2(Z-2)\,e^2/R,$$

where the symbols A and Z in the formulas written above are to be understood as the mass and charge of the original nucleus, taking into account the emission of several nucleons as a result of the cascade process.[18] As particle evaporation proceeds the nuclear temperature is reduced; at the same time the charge and mass are reduced and these quantities affect the value of V. Calculation shows that with a given initial excitation energy the height of the barrier remains constant throughout the entire evaporation process.

The energy spectrum of the evaporated α-particles is given by the expression

$$N(E)\,dE = \Phi(E/T^2)\exp(-E/T)\,dE,$$

where $\Phi = \exp[-2g\gamma(E/V)]$ is the quantum-mechanical penetrability of the Coulomb barrier for α-particles given by Bethe,[25] $\gamma(E/V)$ is a tabulated function,[24] $g = (2MZze^2R)^{1/2}/\hbar$ and z is the charge of the α-particle.

Since the emission of each particle results in a noticeable "cooling" of the nucleus, the process in which the excitation energy is dissipated must be divided into a number of stages, each of which is characterized by its own value of T. The energy spectrum which characterized the α-particle evaporation process for a given nucleus is actually the sum of the energy distributions calculated for each cooling stage. A step-by-step calculation of the evaporation process was carried out as by Shamov[26] but with these differences: firstly, in Ref. 26 a stronger, functional dependence V(T) was assumed; secondly, in our case the values of the relative probability of emission of various particles from Ref. 27 were used whereas Shamov based his work on the analysis given by Le Couter.[15] The summation of the individual-stage spectra is carried out taking account of the number of emitted α-particles in each stage. The partial

α-spectra obtained in this manner for Ag and Br nuclei are then added, after being normalized. The probability of α-particle emission by a nucleus characterized by temperature T can be given in the form

$$\psi = \sigma w \gamma.$$

Here σ is the cross section for an inelastic interaction between the proton and nucleus, w(T) is the probability that a nucleus is excited to a temperature T in such an interaction, γ(Z, T) is the probability of α-particle emission by a nucleus of mass A and charge Z at tem-

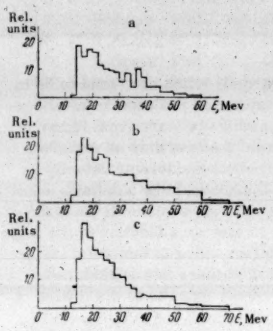

FIG. 3. Energy spectra for cascade α-particles emitted from Ag and Br nuclei at the following proton energies: a — 360 Mev; b — 560 Mev; c — 660 Mev.

TABLE III

Proton energy, Mev	360			560			660			460*	660*
Excitation energy of the nucleus, Mev	Forward	Backward	Total	Forward	Backward	Total	Forward	Backward	Total	Total	Total
0—50**	56***	19	39	47	21	37	80	42	66	67	80
50—100	45	17	33	42	18	31	52	22	39	50	52
100—150	43	16	30	43	10	29	49	29	40	33	38
150—200	60	13	40	40	9	27	47	16	35	29	40
Mean	52	18	36	45	18	34	66	33	53	39	50

* Taken from the data of Ref. 18.

** Here and in all other cases the values of the excitation energy are for an "average" nucleus.

*** The relative errors shown in Table III are approximately 15-20 percent.

perature T. Assuming that Ag and Br contents are the same in the emulsion, the intensity ratio of the α-spectra for these nuclei is given by:

$$\frac{N_1}{N_2} = \left(\frac{A_1}{A_2}\right)^{1/3} \cdot \frac{w_1}{w_2} \cdot \frac{\gamma_1}{\gamma_2}$$

(the subscripts 1 and 2 refer to Ag and Br respectively).

It would seem that no great error is introduced by assuming $w_1 = w_2$. From Ref. 27 [Eq. (24)].

$$\frac{\gamma_1}{\gamma_2} = \frac{\sigma_1}{\sigma_2} \exp\left\{-\frac{1}{T}\left[(V_1 - V_2) + (p_1' - p_2') + (Q_1 - Q_2)\right]\right\}, \quad (p' = p - V).$$

The quantities p' and Q do not differ greatly for Ag and Br. It may be assumed that they are equal. In general an exact calculation of these quantities is not possible since the masses and binding energies of the nuclei formed in the cascade process are not known. Thus,

$$N_1/N_2 = (A_1/A_2)^{1/3} \exp\left[(V_1 - V_2)/T\right].$$

The dependence of α-particle emission probability on the barrier V is taken into account by the factor Φ. Hence the total α-spectrum for stars in heavy nuclei may be obtained approximately if we add the partial spectra for Ag and Br, multiplying the first by 1.5. In Fig. 1 are shown the α-spectra (solid smooth curves) which result from these calculations. The experimental and theoretical distributions are normalized at the maximum. The discrepancy in the position of the maxima in these two distributions is less than 1 Mev.

If it is assumed that the calculated curves yield the proper energy spectra for α-particles which result from evaporation and that the excess of "evaporated" particles with energies above 14 Mev is due to the cascade process, we can obtain the spectrum of the cascade α-particles as the difference between the experimental and theoretical distributions (Fig. 3). The shape of the ejected α-particle spectra is the same in the "forward" and "backward" directions with the one difference that the "forward" spectrum contains a considerably larger number of particles with energies greater than 30 Mev. In Table III is shown the relative number of cascade α-particles for stars characterized by various excitation energies.

It is further assumed that the "back" spectrum is completely due to the evaporation component, it

turns out that about 20 percent of the total number of α-particles are a result of the cascade process (cf. Table II, in which the relative number of α-particles with energies greater than 12 Mev emitted in the "forward" direction is shown).

DISCUSSION OF THE RESULTS

As is to be expected, the spectra for α-particles emitted in the backward direction are found to be in good agreement with evaporation theory. The discrepancy between the evaporated and experimental distribution in the region of low α-particle energy is due partially to the admixture of stars from light nuclei. This slow-particle excess (approximately 5 — 6 percent for all groups of stars) may be explained by the fact that emission takes place in a moving nucleus which has acquired a considerable velocity as a result of prior evaporation of particles. If this assumption is correct, there should be a definite angular correlation between the recoil nucleus and the low-energy α-particle. In Fig. 4 is shown the distribution of α-particles with energies below 10 Mev as a function of the angle formed by motion of these particles and the direction of motion of the recoil nucleus (in projection). It is apparent that there is a considerable concentration of these particles in the direction opposite to the motion of the residual nucleus.

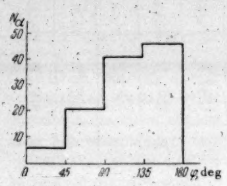

FIG. 4. Angular distribution (in projection) of α-particles with energies less than 10 Mev with respect to the recoil track.

Thus "sub-barrier" α-particles can be considered in terms of ordinary evaporation theory without assuming that fission occurs or that there is a considerable reduction in the Coulomb barrier in excited nuclei. It should be noted that even if one assumes a Coulomb barrier reduction, following Le Couter, taking $V = V_0/(1 + U/200)$ (V_0 is the normal height of the nuclear barrier and U is the excitation energy in Mev), it is impossible to obtain reasonable agreement between the theoretical spectrum and the observed spectrum if the usual calculation for an "average" nucleus at "average" temperature is used. In Fig. 1c are shown evaporation spectra (dot-dash lines) computed as by Le Couter for a nucleus with A = 94, but with cooling taken into account (calculations based on an "average" temperature would lead to a still greater deviation between the curves and experimental data). The fission model is also unable to furnish any additional interpretations of the experimental facts, for example, the sharp anisotropy in the recoil tracks (approximately 50 percent of these are at angles smaller than 30° with respect to the beam), the low number "sub-barrier" α-particles in the small-angle region with respect to the recoil track and so on.

In the last two columns of Table III are shown data on the number of cascade α-particles obtained in Ref. 18 obtained by comparing the observed number of α-particles with the number to be expected from evaporation theory. When account is taken of the experimental uncertainties and the approximations used in the theory one would expect the results of these two papers to be in agreement.

It would be of interest to verify the suggestion that elastic interactions between the incoming proton and the α-aggregates are responsible for the high-energy α-particles. Sörenson,[9] who has analyzed the fast α-particles in cosmic stars, concludes that the correlation between the energy and emission angle of these particles cannot be explained by elastic collisions. The analysis of α-particles with energies higher than 25 Mev carried out by us corroborates this result. However, account should be taken of the fact that the proton does not collide with a free α-particle; it is necessary to introduce appropriate corrections for effects which are due to the existence of a potential well. Under these conditions the absence of a direct relationship between the emission angle of fast α-particles and energy may still not be a sufficient basis for rejecting the notion of an elastic interaction between the primary proton and a nucleon complex inside the nucleus.

In conclusion the authors wish to express their gratitude to Professor H. A. Perfilov and his laboratory co-workers for their constant interest and assistance in this work. The authors are also indebted to the following at the Laboratory for Nuclear Problems of the Joint Institute for Nuclear Research who have been of great help in carrying out this experiment: Professor V. P. Dzhelepov, E. L. Grigor'ev, B. S. Neganov, and G. A. Leksin.

[1] Harding, Lattimore and Perkins, Proc. Roy. Soc. (London), **A 196**, 325 (1949).

[2] D. H. Perkins, Phil. Mag., **40**, 601 (1949).
[3] D. H. Perkins, Phil. Mag. **41**, 138 (1950).
[4] G. Cortini, Nuovo cimento **6**, 470 (1950).
[5] P. E. Hodgson, Phil. Mag. **42**, 83 (1951).
[6] P. E. Hodgson, Phil. Mag. **43**, 934 (1952).
[7] P. E. Hodgson, Phil. Mag. **44**, 1113 (1953).
[8] P. E. Hodgson, Phil. Mag. **45**, 190 (1954).
[9] S. O. C. Sörensen, Phil. Mag **42**, 188 (1951).
[10] R. W. Deutsch, Phys. Rev. **97**, 1110 (1955).
[11] Morrison, Muirhead, and Rosser, Phil. Mag **44**, 1326 (1953).
[12] C. Zangger and J. Rossel, Helv. Phys. Acta **28**, 349 (1955).
[13] C. Zangger and J. Rossel, Helv. Phys. Acta **29**, 507 (1956).
[14] E. L. Grigor'ev and L. P. Solov'eva, J. Exptl. Theoret. Phys. (U.S.S.R.) **31**, 932 (1956), Soviet Phys. JETP **4**, 801 (1957).
[15] K. J. Le Couteur, Proc. Phys. Soc. (London), **A 63**, 259 (1950).
[16] Y. Fujimoto and Y. Yamaguchi, Progr. Theor. Phys. **5**, 76 (1950).
[17] G. Sussmann, Z. Naturforsch. **8a**, 404 (1953).
[18] Blau, Oliver, and Smith, Phys. Rev. **91**, 949 (1953).
[19] V. I. Ostroumov, J. Exptl. Theoret. Phys. (U.S.S.R.) **32**, 3 (1957); Soviet Phys. JETP **5**, 12 (1957).
[20] Iu. I. Serebrennikov, Scientific-Technical Information Bulletin, Leningrad Polytechnic Institute 1 (1957). (In press.)
[21] Iu. I. Serebrennikov, Scientific-Technical Information Bulletin, Leningrad Polytechnic Institute II (1957). (In press.)
[22] Experimental Nuclear Physics (E. Segre) Vol. I, p. 60, Russian translation.
[23] Experimental Nuclear Physics (E. Segre) Vol. II, p. 154, Russian translation.
[24] Experimental Nuclear Physics (E. Segre) Vol. II, p. 162, Russian translation.
[25] H. Bethe, Nuclear Physics, Vol. II, p. 188, Russian translation.
[26] V. P. Shamov, Атомная энергия (Atomic Energy) Appendix No. 1 (1957).
[27] R. Hagedorn and W. Macke, Kosmische Strahlung, p. 201, Berlin (1953).

Translated by H. Lashinsky
234

THE $Bi^{212} \rightarrow Po^{212}$ DECAY SCHEME

A. G. SERGEEV, E. M. KRISUIK, G. D. LATYSHEV, Iu. N. TROFIMOV, and A. S. REMMENNYI

Leningrad Institute of Railroad Engineers

Submitted to JETP editor May 29, 1957

J. Exptl. Theoret. Phys. (U.S.S.R.) **33**, 1140-1143 (November, 1957)

Data obtained in the investigation of the conversion spectrum of an active precipitate of radiothorium are used in an attempt to refine the $Bi^{212} \rightarrow Po^{212}$ decay scheme. It is shown that in addition to the known 727.2, 1620.5, 1679.9 and 1800.4 kev levels, the Bi^{212} decay scheme contains a 1512.16-kev level. The 830, 2180, 2200 and 2230 kev levels suggested in the literature are confirmed experimentally. The possibility of the existence of vibrational levels in Po^{212} is discussed.

In spite of repeated studies of the α, β, and γ conversion spectra of active precipitates of radiothorium, the data available do not make it possible to construct a sufficiently complete scheme of levels of Po^{212} (ThC′). This is explained by the weak excitation of the Po^{212} levels, whereby the β decay Bi^{212} (ThC) $\rightarrow$ Po^{212} (ThC′) goes principally into the ground state Po^{212} (approximately 80%).

The most reliable data are those on the long-range particles.[1-3] Investigations devoted to a study of the conversion spectrum of an active precipitated RaTh[4-6] contained very little information on the Po^{212} spectrum. As regards the γ spectrum of Po^{212}, Refs. 7 – 11, devoted to its investigation, contain many contradictory data. The following γ lines, which belong to Po^{212}, were found in these investigations: 727 kev,[8,9,11] 1030 kev,[8,11] 1340 kev,[7,8,11] 1500 kev,[7,11] 1620 kev,[7,8,11] 1800 kev,[7,8,11] and 2200 kev,[7,8,11] Level schemes of Po^{212}, given in some of these works, differ noticeably from each other.

E_γ, Kev	Shell	J_e percent per decay
	K	0.106
727.2	L	0.024
	M	0.0045
	K	0.051
785.4	L	0.007
	K	0.014
893.4	L	0.004
952.7	K	0.010
1073.7	K	0.006
1078.5	K	0.014
1512.6	K	0.008
1620.4	K	0.013
1800.2	K	0.007

In the present work we attempt a refinement of the level scheme of Po^{212} on the basis of data[12,13] obtained by us in a study of a spectrum of internal-conversion electrons of an active precipitate of RaTh, made with a "ketron" type magnetic spectrometer. The relatively high sensitivity of the procedure had made it possible to detect lines of very low intensity. The line energies were determined with an accuracy of ~ 0.5 kev. The table lists the results of our investigations,[12,13] pertaining to the conversion spectrum of Po^{212}.

Data on long-range α-particles[3] indicate that there exists in Po^{212} three excited levels: 726, 1674, and 1979 kev (see diagram). These levels appear also in the conversion spectrum. The first excited level gives rise to the well-known 727.2 kev γ transition. The existence of a 1088.4 kev level is confirmed not only by the direct γ transition into the ground state, but also by the transition with $E_\gamma = 1073.7$ kev to the first excited level, which we found.

These three excited levels of Po^{212} are not enough to interpret the remaining five γ lines listed in the table. In Refs. 7, 8, 10, and 14 the decay scheme of Bi^{212} includes a 1620 kev level. Our data confirm the existence of this level. It gives rise to the 1620.4 and 893.4 kev γ lines. The sum of the energies of the 727.2 and 893.4 kev cascade γ quanta coincided, within experimental accuracy, with the energy of the direct 620.4 kev transition.

Along with the above levels, we propose that there exists an excited state with energy 1512.6 kev. This level explains the origin of the 1512.6 and 785.4 kev γ lines. The 1500 kev line was found in the γ spectra,[7,12] and the 785.4 kev γ line, which was observed in the conversion spectra,[4,6] was not identified previously. The existence of a 1512.6 kev level in Po^{212} is confirmed by the good agreement between the sum of the energies of the 727.2 and 785.4 kev γ lines with the γ-transition energy of 1512.6 kev.

The proposed $Bi^{212} \rightarrow Po^{212}$ decay scheme does not include the 1078.5 kev γ transition. This indicates that Po^{212} contains at least one more excited state. There are not enough data at the present time

to prove this statement. The decay achemes proposed in Refs. 7 and 8 contain 830 and 2200 kev levels, and Ref. 14 contains in addition the 2180 and 2230 kev levels. The 830 kev level introduced into the scheme appears to be in error. Its assumed presence was based, on one hand, on the existence of the corresponding group of long-range upper particles,[15] and on the other hand on the 860 kev γ line observed in the conversion spectrum.[4,6] However, in later works,[1,2] the existence of a group of α-particles that differ from the fundamental group by a decay energy of 830 kev has not been confirmed. In addition, it was shown that the 860 kev γ line belongs not to Po^{212} but to Pb^{208} (Refs. 16 and 17).

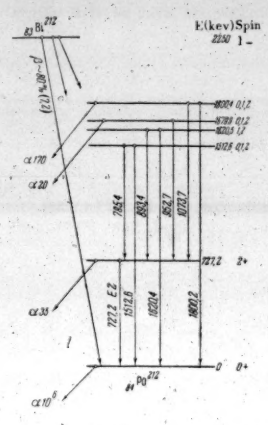

$Bi^{212} \rightarrow Po^{212}$ decay scheme

The 2180 and 2230 kev levels, proposed by Demichelis,[14] are also absent from Po^{212}. It was shown in that reference on the basis of experiments on $\gamma-\gamma$ coincidences that Po^{212} contains the $1.50-0.73$ Mev and $1.35-0.83$ Mev $\gamma-\gamma$ cascades. This gave rise to the assumption of the existence of 2230 and 2180 kev levels. However, the Demichelis conclusions may be in error, since in processing his experimental data he assumed that the 830 kev (more accurately 860 kev) γ transition belongs to Po^{212}. It was indicated above that the transition belongs to Pb^{208}. The Pb^{208} level scheme[16-18] discloses the existence of an intense $860-2620$ kev cascade, which has probably also played an important role in the Demichelis experiments.

The existence of a 2200 kev level cannot be assumed at the present time to be sufficiently well proven. This level was proposed in Ref. 7 on the basis of a 2200 kev γ line found in the spectrum of the recoil electrons. However, no such γ line was observed in Ref. 10, and the upper limit proposed for this line is 10 times greater than the intensity given in Ref. 7. No lines in this energy region were observed when we plotted the conversion spectrum of an active precipitate of RaTh. The upper limit for the intensities of the possible conversion lines that are possible here amounts to approximately 10^{-5} electrons per Po^{212} decay act. Nor did we find the γ lines that could be explained by the transition from the 2200 kev to the first excited level.

As to the spins of the excited states, one can speak with certainty only concerning the spin of the 727.2 kev level. It follows from Ref. 9 that the spin of this level is 2^+, according to the general rules for even-even nuclei. This is confirmed also by our data; it follows from the K/R ratio for the 727.2 kev γ transition that this transition is of type E2. To determine the multipolarity of the γ transitions from higher levels one could use our data on the intensity of conversion lines and on the data of Refs. 7, 8, and 10 on the intensities of the γ rays. However, the data of these references are quite contradictory, and if one shows no preference to any one of these data, the following possibilities appear permissible for the level spins: for the 1620.5 kev level — 1 or 2, for the 1512.5, 1800.4 kev and apparently also for the 1670.9 kev levels — 0, 1, and 2. To determine the spins of these levels it is necessary to have more accurate and more reliable data on the intensities of the γ rays. It is impossible to determine the multipolarity of the 785.4 and 893.4 kev γ transitions from the K/L ratio, since the corresponding L-lines have intensities that are close to the sensitivity limit of our apparatus.

From theoretical considerations,[10] nuclei having four particles or more above the filled shells should exhibit a vibrational level structure. However, at the present time it is impossible to state with certainty that such a level structure takes place in Po^{212}. The following facts favor the existence of a vibrational structure in Po^{212}: (1) the equidistant nature of the first two excited levels 727.2 and 1512.6 kev; the ratio of their energies is 2.08; (2) according to the generalized nuclear model, one expects the transition from the second vibrational level to the first (single-phonon transition) to be easier than the transition into the ground state (two-phonon transition). This takes place in Po^{212}, if one assumes that the 1512.6 and 785.4 kev transitions are of type E2. In this case it follows from our data on the intensities of the conversion lines that the 785.4 kev transition is approximately twice as intense than the 1512.6 kev transition. Were these transitions to be single-particle ones, the 1512.6 kev γ transition would be approximately 40 times more intense than the 785.4 kev transition.

For further refinement of the level scheme of Po^{212} it is desirable to obtain sufficiently reliable data on the spectrum of Po^{212}.

Note added in proof (October 16, 1956). The 1679.9 kev level does not appear in the γ spectra.[7-11] Nor did we observe in the conversion spectrum the direct transition from this level into the ground state, although we did find a line with energy 952.7 kev, corresponding to the transition from this level into the first excited state.

[1] W. B. Lewis and B. V. Bowden, Proc. Roy. Soc. (London) **A 145**, 235 (1934).
[2] A. Rytz. Compt. rend. **233**, 790 (1951).
[3] G. H. Briggs, Revs. Mod. Phys. **26**, 1 (1954).
[4] C. D. Ellis, Proc. Roy. Soc. (London) **A 138**, 318 (1932).
[5] C. D. Ellis, Proc. Roy. Soc. (London), **A 143**, 350 (1934).
[6] J. Sugrue, Ann. phys. **8**, 484 (1937).
[7] G. D. Latishev, Revs. Mod. Phys. **19**, 132 (1947).
[8] A. Johansson, Arkiv f. Mat. Astr. Fysik, **A 34**, 9 (1947).
[9] D. G. E. Martin and H. O. W. Richardson, Proc. Phys. Soc. **A 63**, 223 (1950).
[10] D. G. E. Martin and G. Parry, Proc. Phys. Soc. **A 68**, 1177,(1955).
[11] B. Chinaglin and F. Demichelis, Nuovo cimento **4**, 1160 (1956).
[12] Krisiuk, Vitman, Vorob'ev, Latyshev, and Sergeev, Izv. Akad. Nauk SSSR, ser. fiz. **20**, 877 (1956).
[13] Vorob'ev, Il'in, Kol'chinskaia, Latyshev, Sergeev, Trofimov, and Fadeev, Izv. Akad. Nauk SSSR, ser. fiz. (in press), 1957.
[14] F. Demichelis, Nuovo cimenta **12**, 407 (1954).
[15] S. Rosenblumand M. Valadares, Compt. rend. **194**, 467 (1932).
[16] H. O. W. Richardson, Nature **161**, 516 (1948).
[17] Elliott, Graham, Walker, and Wolfson, Phys. Rev. **93**, 356 (1954).
[18] Krisiuk, Sergeev, Latyshev, Il'in, and Fadeev, this issue, p 880.
[19] L. K. Peker, Dissertation, Leningrad Physico-technical Institute, Academy of Sciences, U.S.S.R. (1956).

Translated by J. G. Adashko
235

SOVIET PHYSICS JETP VOLUME 6 (33), NUMBER 5 MAY, 1958

THE DECAY SCHEME OF Pl^{208}

E. M. KRISIUK, A. G. SERGEEV, G. D. LATYSHEV, K. I. IL'IN and V. I. FADEEV

Leningrad Institute of Railroad Engineers

Submitted to JETP editor May 29, 1957

J. Exptl. Theoret. Phys. (U.S.S.R.) **33**, 1144-1146 (November, 1957)

The data obtained in an investigation of the conversion electron spectrum are used in an attempt to refine the decay scheme of Tl^{208}. It is shown that the spin of the ground state of Tl^{208} is 5^+, while the spin of the 3.961-Mev level of Pb^{208} is 6^-. It is assumed that there exists a 3.750 Mev level with spin 7^-. All the excited levels of Pb^{208} are explained by the excitation of one proton.

To study the decay schemes of nuclei belonging to the active precipitate of radiothorium, we investigaged the conversion spectrum of these nuclei.[1-3] The present work is an attempt to refine the decay scheme $Tl^{208} \rightarrow Pb^{208}$ on the basis of experimental data obtained.

The position of the Pb^{208} levels appearing in the decay of Tl^{208} was established in the works by Martin and Richardson.[4,5] An analysis of the intensities and the energies of the β and γ transitions was used

by them to show the existence in lead of excited levels with energies 2.62, 3.20, 3.48, and 3.71 Mev. Elliot et al. have established the spins and parities of these levels. From the measurement of the coefficients of internal conversion, from the study of the $\gamma-\gamma$ angular correlations they established the following sequence of spins of the Pb^{208} levels: 0 Mev — 0^+, 2.615 Mev — 3^-, 3.198 Mev — 5^{-1}, 3.475 Mev — 4^{-1}, and 3.709 Mev — 5^{-1}.

It was noted in Ref. 7 that the 0.252 and 0.763 Mev γ rays coincide with the 2.6-5-Mev γ rays. It follows therefore that the 0.252 and 0.763-Mev γ rays belong to the $Tl^{208} \rightarrow Pb^{208}$ decay. To explain the origin of these rays, the authors have proposed the existence of a 3.961-Mev level.

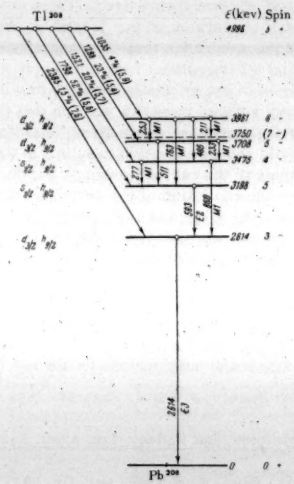

E_γ, Kev	Shell	I_e, %	Multi-polarity	I_{trans}, %
211.4	K L	0.15 0.02	M1	0.32
233.4	K L	0.13 0.03	M1	0.34
252.54	K L	0.37 0.085	M1	1.1
277.35	K L M N	2.4 0.44 0.10 0.03	M1	8.4
485.9	K	0.01		0.5
510.84	K L M N	1.7 0.073 0.03		22.6
583.2	K $L_I + L_{II}$ L_{III} M N	0.77 0.09 0.097 0.03	E2	83.2
763.2	K L	0.058 0.01	M1	2
860.5	K L M	0.27 0.048 0.01	M1	12.3
2614.3	K L M	0.17 0.031 0.0093	E3	100

Our own measurements of the spectrum of the internal-conversion electrons confirm such a level scheme for Pb^{208} (see figure). Furthermore:

(1) All the known γ transitions fit energywise into this decay scheme with an accuracy of ~ 0.1 kev, which is within the experimental error of our measurements.

(2) The multipolarities of all the lines agree with the ascribed spins and parity (see table). The multipolarities of the lines were determined from the conversion ratios on the K and L shells, and for the 2.614-Mev lines also from the absolute value of the conversion coefficient on the K shell.[8]

(3) The existence of a 3.961-Mev level was confirmed not only by the 0.253 and 0.763-Mev transitions, which were identified by Elliot,[7] but also by the 0.486-Mev transition; the conversion line corresponding to this transition was not identified previously. There are no data in the literature concerning the spin and parity of the 3.961 Mev level. According to our measurements, the 0.253 Mev transition is magnetic dipole. Therefore the 3.961 Mev level can have three spin values, 4^-, 5^-, and 6^-. However, the first two values are of little likelihood, since the 0.486-Mev transition for these values should also be of the magnetic-dipole type and should show an intensity considerably greater than experimentally observed. We therefore assigned a spin 6^- to the 3.961 Mev level.

As to the spin of the ground state of the Tl^{208}, the data available in the literature are contradictory. On the basis of the changes in the $\alpha-\gamma$ angular correlation in the $Bi^{212} \rightarrow Tl^{208}$ decay, Horton[9] assigns

a spin 5^+ to the ground state of Tl^{208}, although he cannot exclude completely a spin value 4^+. Demichelis[10] assigns a spin 4^+ to the ground state of Tl^{208}, on the basis of measurement of the $\beta-\gamma$ angular correlation in the $Tl^{208} \rightarrow Pb^{208}$ decay. To resolve this question we estimated $\log(\tau f)$ for β transitions at all excited levels of Pb^{208}. The calculations were made from the measured absolute intensities of the conversion lines and from the theoretical conversion coefficients.[11] The intensity of the β transition at the 2.614-Mev level was taken according to Demichelis;[12] its value was obtained by direct measurement. Our value in this case is not exact, since it is obtained as the difference of two nearly equal numbers. The values of $\log(\tau f)$ obtained by us can be explained only if the spin of Tl^{208} is taken to be 5^+.

It should be noted that all β transitions in this decay scheme are first-order forbidden and the dispersion in the values of $\log(\tau f)$ for the transitions with $\Delta J = 0$ is very small; the same applies to transitions with $\Delta J = 1$. The values of $\log(\tau f)$ themselves are in very good agreement with their classification for nuclei near the twice-filled shells of Pb^{208} (see, for example, Ref. 13), which confirms the correctness of the decay scheme for Tl^{208}.

We undertook an attempt to include the 0.211 Mev γ line in the decay scheme of Tl^{208}. Its presence in this scheme is due to the energy difference of the K and L conversion lines. This transition is of the magnetic-dipole type with respect to the probabilities of conversion on the K and L shells. The diagram shows the possible position of this transition. If the spin of the thus-obtained 3.750-Mev level is 7^-, it should be weakly excited in the β decay of Tl^{208}, and all transitions from this level should be too weak to be detected by their conversion electrons. Attempts to assign another spin to this level or to place the 0.211-Mev transition somewhere else in the decay scheme in such a manner that the initial or final level is a known level lead to the necessity of observing strong γ transitions. Careful searches of the conversion lines corresponding to such transitions did not give positive results. In the work by Tauber[14] an attempt is made to assign definite configurations to the excited levels of Pb^{208}. The 2.614, 3.708, and 3.961 Mev levels are attributed by the author to the excitation of the proton from the $d_{3/2}$ state to the $h_{9/2}$ state, i.e., to the $d_{3/2}h_{9/2}$ proton configuration. The 3.198 and 3.475-Mev levels are assigned either a proton configuration $s_{1/2}h_{9/2}$ or a neutron configuration $p_{1/2}g_{9/2}$. If the scheme for Pb^{208} has any proton and neutron levels, the transitions between them should be noticeably forbidden compared with the single-particle transitions.

We calculated the probability ratios for the competing transitions, using the Moszkowski formula for the single-particle γ transitions.[15] These ratios were compared with the intensity ratios of the γ transitions, given in the table. The comparison shows that the transitions between the levels with various configurations are not strongly forbidden. It follows therefore that both configurations should be of the proton type.

[1] Zhernovoi, Krisiuk, Latyshev, Remennyi, Sergeev, and Fadeev, J. Exptl. Theoret. Phys. (U.S.S.R.) **32**, 682 (1957), Soviet Phys. JETP **5**, 563 (1957).

[2] Vorob'ev, Il'in, Kol'chinskaia, Latyshev, Sergeev, Trofimov, and Fadeev, Izv. Akad. Nauk SSSR, ser. fiz. (in press), 1957.

[3] Krisiuk, Vitman, Vorob'ev, Latyshev, and Serveev, Izv. Akad. Nauk SSSR, ser. fiz. **20**, 877 (1956).

[4] H. O. W. Richardson, Nature **161**, 516 (1948).

[5] D. G. E. Martin and H. O. W. Richardson, Proc. Phys. Soc. **60**, 466 (1948).

[6] Elliot, Graham, Walker, and Wolfson, Phys. Rev. **93**, 356 (1954). G. T. Wood and P. S. Jastram, Phys. Rev. **100**, 1237 (1955).

[7] Elliot, Graham, Walker, and Wolfson, Proc. Phys. Soc. Canada **48**, 12 (1954).

[8] Krisiuk, Vitman, Vorob'ev, Vorob'ev, Il'in, Latyshev, Listengarten, and Sergeev, Izv. Akad Nauk SSSR, ser. fiz. **20**, 883 (1956).

[9] J. W. Horton, Phys. Rev. **101**, 717 (1956).

[10] F. Demichelis, and R. A. Ricci, Nuovo cimento **4**, 96 (1956).

[11] L. A. Sliv and I. M. Band Таблицы коэффициентов внутренней конверсии. (Tables of Coefficients of Internal Conversion of Gamma Radiation), Acad. Sci. Press, 1956.

[12] Demichelis, Ricci, and Trivera, Nuovo cimento **3**, 377 (1956).

[13] Krisiuk, Sergeev, Latyshev, and Vorob'ev, Nucl. Phys. (in press), 1957.

[14] G. E. Tauber, Phys. Rev. **99**, 176 (1955).

[15] S. A. Moszkovski, in K. Siegbahn's Beta and Gamma Ray Spectroscopy, Amsterdam, 1955, p 373.

Translated by J. G. Adashko
236

ON THE ELASTIC BACKWARD SCATTERING OF 660 MEV PROTONS AGAINST CARBON NUCLEI

G. A. LEKSIN and Iu. P. KUMEKIN

Joint Institute for Nuclear Research

Submitted to JETP editor June 1, 1957

J. Exptl. Theoret. Phys. (U.S.S.R.) 33, 1147-1149 (November, 1957)

It is shown that the elastic backward scattering of 660-Mev protons by carbon nuclei does not exceed 3×10^{-33} cm^2/sterad. The mechanism for ejection of rapid fragments for nuclei interacting with high-energy nucleons is discussed in connection with this result.

SEVERAL experiments[1-3] on the elastic scattering of protons by deuterons have been recently carried out in the energy range of 340 — 660 Mev; the energy and momentum transfer to the latter particles exceeds in this case by hundreds of times the binding energy of the nucleons in the deuteron. Such elastic scattering is the result of a three-nucleon collision when the two nucleons of the deuteron are tightly bound to each other. On the other hand, it is well known that when nuclei are bombarded with high-energy nucleons, deuterons, and α-particles, nuclei of Li, Be, C, B and other elements are ejected with an energy considerably in excess of the repulsive Coulomb energy between the ejected fragments and the residual nucleus. The characteristic sequence of this process and, above all, the angular and energy distributions of the ejected fragments attest without a doubt to their direct participation in the reaction as distinguished from evaporation from an excited nucleus. It is natural to try to relate these two groups of observations, and assume that the ejection of energetic fragments from nuclei can similarly be explained by a collective interaction of the incident nucleons with the whole nucleus or with a tight aggregate of nucleons within the nucleus. One may further regard such an interaction, by analogy with quasi-elastic nucleon-nucleon scattering, as a quasi-elastic collision of the nucleon with the moving fragments within the nucleus. In that particular case, one must first of all observe a correlation between the direction of emergence of the fragments and the nucleon recoil (specifically, the emergence of the energetic fragments in the forward direction must be accompanied by the emission of an energetic nucleon to the rear); in the second place, the cross section for quasi-elastic scattering by the fragments in the nucleus must be of the same order of magnitude as the cross section for elastic scattering by the corresponding free nuclei. The hypothesis of quasi-elastic scattering of nucleons by fragments inside the nucleus has been discussed in a series of articles,[4-7] together with a more definitive analysis of the available experimental data. It appears that the existing facts can be made to agree qualitatively with this hypothesis if one takes into account the fact that the nucleon, and especially the fragment, undergoes a series of changes in the process of development of an intranuclear cascade. This last circumstance must be underlined as most of the available data was observed from heavy nuclei in photoemulsions.

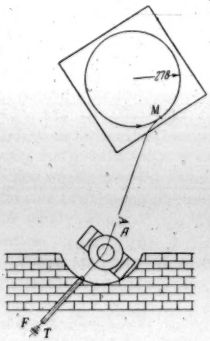

Experimental arrangement: M — carbon target; A — analyzing magnet; T — telescope; F — filter.

In order to verify the hypothesis of quasi-elastic scattering of incident nucleons by heavy fragments within the nucleus, we have attempted to detect the presence of high-energy protons generated as a result of the backward scattering of 660-Mev protons by carbon nuclei (at angles 180 ± 15°), and to select a group of protons elastically scattered by the carbon nuclei.

Investigations of angular and energetic distributions of high-energy protons scattered into the backward hemisphere present the best experimental possibility for analyzing collisions of high-energy nucleons against nuclei for the purpose of verifying collective interaction. Protons pass more easily through nuclear matter than the heavier fragments, and when the reaction is detected by electronic means, they

turn out to be practically the only source of information about an interaction between an incident proton and an aggregate of nucleons.

The experimental arrangement is shown on the figure. The carbon target M is irradiated by the internal proton beam of the synchrocyclotron of the Laboratory for Nuclear Problems, Joint Institute for Nuclear Research. The protons scattering at angle of approximately 180° are deflected by the magnetic field of the accelerator into an analyzing magnet. The particles then travel through a 4 m collimating slit and strike a registering telescope. In order to separate protons from other particles of the same momentum, a filter F is placed between the second and third counter of the telescope. The experimental arrangement permits the use of an intense proton beam while still avoiding excessive noise in the telescope since the main beam from the target goes in the opposite direction to the collimator. At the same time this experimental arrangement does not allow an exact determination of the solid exit angle of the detected protons; it is possible, although this is still not too accurate, to evaluate (as is usually done with internal beams) the intensity of protons incident on the target and the effective number of nuclei which they irradiate.* This experimental arrangement proved very convenient, however, to verify the hypothesis and evaluate cross sections.

The trajectory of the proton beam was traced by means of a thin current-carrying filament.[8] It was shown that particles of comparatively wide momentum range fall in the solid angle subtended by the telescope. The telescope received protons emerging backward with a momentum ranging from its maximum possible value in the indicated angular range for the p–C reaction, to a minimum value corresponding to a proton energy of 350 Mev.

No effect was observed in the experiment. The noise count of the telescope remained unaltered when an absorber was mounted in the path of the proton beam in front of the analyzing magnet, when the target in the synchrocyclotron chamber was rotated by an azimuthal angle of 40°, and again when the carbon target was replaced by a beryllium target. Calculations show the lower limit for elastic backward p–C scattering cross section cannot exceed 3×10^{-33} cm^2/sterad. Such is also the probability of absence of protons ranging in energy from maximum to 350 Mev, corresponding to elastic collisions between protons and aggregates of 8 – 9 nucleons.

These results permit the following conclusions within the indicated degree of accuracy: (a) the mechanism for ejection of fragments consisting of 8 – 12 nucleons differs (at least for most of the fragments) from a quasi-elastic scattering by corresponding fragments inside the nucleus; (b) the interaction between a 660-Mev proton and a carbon nucleus is not accompanied by the backward ejection of a proton of more than 350 Mev.

In view of the obtained results, it is necessary to suggest some other mechanism of collective interaction satisfying particularly the established experimental facts.

The authors wish to thank Professors D. I. Blokhintsev and M. G. Meshcheriakov for discussions of the subjects mentioned, and V. M. Sidorov for a discussion of the experimental arrangement.

[1] Meshcheriakov, Bogatchev, Leksin, Neganov, and Piskarev, Symposium CERN, 2, 101 (1956).
[2] G. A. Leksin, J. Exptl. Theoret. Phys. (U.S.S.R.) 32, 440 (1956), Soviet Phys. JETP 5, 371 (1957).
[3] O. Chamberlain and D. Clark, Phys. Rev. 102, 473 (1956).
[4] S. O. C. Sorensen, Phil. Mag. 42, 188 (1951).
[5] J. Combe, J. Phys. Rad. 16, 445 (1955).
[6] O. V. Lojkin and N. A. Perfilov, J. Exptl. Theoret. Phys. (U.S.S.R.) 31, 913 (1956), Soviet Phys. JETP 4, 790 (1957).
[7] G. A. Leksin, Dissertation (1956).
[8] M. S. Kozodaev and A. A. Tiapkin, Приборы и техника эксперимента (Instr. and Meas. Eng.) 1, 21 (1956).

Translated by M. A. Melkanoff
237

*This estimate was based on the data of Iu. D. Prokoshkin and A. A. Tiapkin.

ON THE FORM OF THE BETA-DECAY INTERACTION

G. R. KHUTSISHVILI and S. G. MATINIAN

Institute of Physics, Academy of Sciences, Georgian S.S.R.

Submitted to JETP editor April 10, 1957

J. Exptl. Theoret. Phys. (U.S.S.R.) 33, 1150-1153 (November, 1957)

A study is made of the effect of parity nonconservation on the interpretation of the experimental data relating to the Fierz interference and the $\beta-\nu$ angular correlation. Formulas are obtained for the β-decay of polarized nuclei.

UNTIL recently it has been supposed that the β-decay interaction was a combination of the scalar and tensor types. This conclusion was based on the following facts:

(a) The experimental absence in allowed β-ray spectra of the Fierz interference between the scalar (S) and vector (V) types on one hand, and between the tensor (T) and axial-vector (A) types on the other; this leads to the following relations for the coefficients in the combination of the types: $C_S C_V = C_T C_A = 0$.

(b) The positive sign of the $\beta-\nu$ angular correlation coefficient a in the β-decay of He^6 indicates[1] that $C_T \neq 0$. Then it follows from point (a) that $C_A = 0$.

(c) The negative sign of a in the β-decay of Ne^{19} (Refs. 2 and 3) shows that $C_S \neq 0$, and this leads to $C_V = 0$.

(d) The absence of the Fierz interference between V and T in non-unique first forbidden β-ray spectra, together with point (b), also gives $C_V = 0$. The most essential point in this derivation is the absence of the SV and TA interferences, which makes possible the unique solution of the problem of the form of the β-decay interaction on the basis of the sign of a alone.

The discovery of parity nonconservation in β-decay[4,5] has changed the situation somewhat. In fact, the absence of the Fierz interferences, points (a) and (d), now gives only (for real C_i, C_i')

$$C_S C_V + C_S' C_V' = C_T C_A + C_T' C_A' = C_V C_T + C_V' C_T' = 0. \quad (1)$$

Unlike the former situation, one cannot get from Eq. (1) and points (b) to (d) the conclusion that $C_V = C_A = C_V' = C_A' = 0$.* It is obvious that a knowledge of just the sign of a is insufficient for the solution of the problem of the form of the β-decay interaction. For this it is necessary to obtain values of a with greater precision (at present the errors in the determination of a are at least 35 to 45 percent), since for small values of C_V/C_S, C_V'/C_S' and C_A/C_T, C_A'/C_T' the value of a is very insensitive to these ratios.

From what is said above it can be seen that the polarization effects in β-decay must be calculated for a superposition of all the types of interaction. In the present paper the calculation of the polarization effects is carried out for the allowed β-transitions, $\Delta I = 0, \pm 1$ (no). We have carried out the calculations in the Born approximation. For this reason the results can be applied quantitatively only for the lightest nuclei. But the set of experiments presented below as required for the determination of all the constants C_i, C_i' will also be correct in the general case. For generality we regard the coefficients C_i, C_i' as complex, since their reality is connected with the still open question of the invariance of weak-interaction processes with respect to time reversal. All notations are the standard ones.[4]

To calculate the probability $W(\mathbf{p}, \mathbf{q}, \boldsymbol{\eta}, \boldsymbol{\zeta})$ (per unit time, unit energy range of the β-particle, and unit solid angles) of emission of a β-particle with momentum $\mathbf{p}$ and spin along the unit vector $\boldsymbol{\zeta}$ and a neutrino with momentum $\mathbf{q}$, in the β-decay of oriented nuclei with the axis of quantization along the unit vector $\boldsymbol{\eta}$, we use the method of Tolhoek and de Groot.[7]

After averaging over the nuclear spins the formula for W contains the following sorts of expressions:

$$g = 1,\ -I/(I+1),\ 1/(I+1)$$

*We note that this relation will again hold in the two-component theory of the neutrino.[6]

respectively for $I \to I-1$, $I \to I+1$, and $I \to I$ (I is the spin of the β-radioactive nucleus);

$$h = 1, \quad I(2I-1)/(I+1)(2I+3), \quad -(2I-1)/(I+1)$$

respectively for $I \to I-1$, $I \to I+1$, and $I \to I$; f_1 and f_2 are quantities characterizing the orientation of the nuclei,

$$f_1 = \overline{m}/I, \; f_2 = (3/I(2I-1))[\overline{m^2} - I(I+1)/3],$$

(m is the projection of I along the axis of quantization z, and the averaging is taken over the nuclei of the given type contained in the specimen); and the matrix

$$N_{ik} = \begin{pmatrix} -1/2 & 0 & 0 \\ 0 & -1/2 & 0 \\ 0 & 0 & 1 \end{pmatrix}.$$

Finally, the phase α is defined by the formula

$$e^{2i\alpha} = \left(\int 1\right)^{+} \left(\int \sigma_z\right) \Big/ \left(\int 1\right)\left(\int \sigma_z\right)^{+};$$

it is equal to zero for β-decay transitions in which the state of the nucleon remains unchanged.

The expression for $W(\mathbf{p}, \mathbf{q}, \boldsymbol{\eta}, \boldsymbol{\zeta})$ is cumbersome, and we shall not give it here. Other probabilities are obtained by averaging $W(\mathbf{p}, \mathbf{q}, \boldsymbol{\eta}, \boldsymbol{\zeta})$ with respect to different variables (the upper sign refers to β^- and the lower to β^+ transitions; $\hbar = c = m_e = 1$ throughout);

$$W(\mathbf{p}, \boldsymbol{\eta}, \boldsymbol{\zeta}) = (2\pi)^{-4} pEq^2 \Big\{ |\int 1|^2 \Big[|C_S|^2 + |C_S'|^2 + |C_V|^2 + |C_V'|^2 \pm \frac{2}{E} \operatorname{Re}(C_S C_V^{+} + C_S' C_V'^{+}) \pm 2\operatorname{Re}(C_S C_S'^{+} - C_V C_V'^{+}) \frac{\mathbf{p}\boldsymbol{\zeta}}{E} \Big]$$

$$+ |\int \sigma|^2 \Big[(|C_T|^2 + |C_T'|^2 + |C_A|^2 + |C_A'|^2) \Big(1 + gf_1 \Big(\frac{\boldsymbol{\eta}\boldsymbol{\zeta}}{E} + \frac{(\mathbf{p}\boldsymbol{\eta})(\mathbf{p}\boldsymbol{\zeta})}{E(E+1)}\Big)\Big) \pm 2\operatorname{Re}(C_T C_T'^{+} - C_A C_A'^{+}) \frac{\mathbf{p}\boldsymbol{\zeta} + gf_1 \mathbf{p}\boldsymbol{\eta}}{E}$$

$$\pm 2\operatorname{Re}(C_T C_A^{+} + C_T' C_A'^{+}) \Big(\frac{1}{E} + gf_1 \Big(\boldsymbol{\eta}\boldsymbol{\zeta} - \frac{(\mathbf{p}\boldsymbol{\eta})(\mathbf{p}\boldsymbol{\zeta})}{E(E+1)}\Big)\Big) \pm 2gf_1 \operatorname{Im}(C_T C_A'^{+} + C_T' C_A^{+}) \frac{\mathbf{p}[\boldsymbol{\eta}\boldsymbol{\zeta}]}{E} + 2f_1 \sqrt{\frac{I}{I+1}} \Big| \int 1 \Big| \int \sigma \Big|$$

$$\times \Big[\operatorname{Re}\Big(e^{\mp i\alpha} \Big[(C_S C_A^{+} + C_S' C_A'^{+} + C_V C_T^{+} + C_V' C_T'^{+}) \Big(\boldsymbol{\eta}\boldsymbol{\zeta} - \frac{(\mathbf{p}\boldsymbol{\eta})(\mathbf{p}\boldsymbol{\zeta})}{E(E+1)}\Big) \pm (C_S C_T^{+} + C_S' C_T'^{+} + C_V C_A^{+} + C_V' C_A'^{+}) \Big(\frac{\boldsymbol{\eta}\boldsymbol{\zeta}}{E} + \frac{(\mathbf{p}\boldsymbol{\eta})(\mathbf{p}\boldsymbol{\zeta})}{E(E+1)}\Big)$$

$$+ (C_S C_T'^{+} + C_S' C_T^{+} - C_V C_A'^{+} - C_V' C_A^{+}) \frac{\mathbf{p}\boldsymbol{\eta}}{E} \Big] \Big) + \operatorname{Im}(e^{\mp i\alpha} (C_S C_A'^{+} + C_S' C_A^{+} - C_V C_T'^{+} - C_V' C_T^{+})) \frac{\mathbf{p}[\boldsymbol{\eta}\boldsymbol{\zeta}]}{E} \Big] \Big\};$$

$$W(\mathbf{p}, \mathbf{q}, \boldsymbol{\zeta}) = \frac{1}{2}(2\pi)^{-5} pEq^2 \Big\{ \Big| \int 1 \Big|^2 \Big[(|C_S|^2 + |C_S'|^2) \Big(1 - \frac{\mathbf{p}\mathbf{q}}{qE}\Big) + (|C_V|^2 + |C_V'|^2) \Big(1 + \frac{\mathbf{p}\mathbf{q}}{qE}\Big)$$

$$\pm \frac{2}{E} \operatorname{Re}(C_S C_V^{+} + C_S' C_V'^{+}) - 2\operatorname{Im}(C_S C_V^{+} + C_S' C_V'^{+}) \frac{\mathbf{s}[\mathbf{pq}]}{qE} \pm 2\operatorname{Re}(C_S C_S'^{+} - C_V C_V'^{+}) \frac{\mathbf{p}\boldsymbol{\zeta}}{E}$$

$$- 2\operatorname{Re}(C_S C_V'^{+} + C_S' C_V^{+}) \Big(\frac{\mathbf{q}\boldsymbol{\zeta}}{q} - \frac{(\mathbf{p}\boldsymbol{\zeta})(\mathbf{pq})}{qE(E+1)}\Big) \mp 2\operatorname{Re}(C_S C_S'^{+} + C_V C_V'^{+}) \Big(\frac{\mathbf{q}\boldsymbol{\zeta}}{qE} + \frac{(\mathbf{p}\boldsymbol{\zeta})(\mathbf{pq})}{qE(E+1)}\Big) \Big]$$

$$+ \Big| \int \sigma \Big|^2 \Big[(|C_T|^2 + |C_T'|^2) \Big(1 + \frac{\mathbf{pq}}{3qE}\Big) + (|C_A|^2 + |C_A'|^2) \Big(1 - \frac{\mathbf{pq}}{3qE}\Big) \pm \frac{2}{E} \operatorname{Re}(C_T C_A^{+} + C_T' C_A'^{+}) + \frac{2}{3} \operatorname{Im}(C_T C_A^{+} + C_T' C_A'^{+}) \frac{\boldsymbol{\zeta}[\mathbf{pq}]}{qE}$$

$$\pm 2\operatorname{Re}(C_T C_T'^{+} - C_A C_A'^{+}) \frac{\mathbf{p}\boldsymbol{\zeta}}{E} \pm \frac{2}{3} \operatorname{Re}(C_T C_T'^{+} + C_A C_A'^{+}) \Big(\frac{\mathbf{q}\boldsymbol{\zeta}}{qE} + \frac{(\mathbf{p}\boldsymbol{\zeta})(\mathbf{pq})}{qE(E+1)}\Big) + \frac{2}{3} \operatorname{Re}(C_T C_A'^{+} + C_T' C_A^{+}) \Big(\frac{\mathbf{q}\boldsymbol{\zeta}}{q} - \frac{(\mathbf{p}\boldsymbol{\zeta})(\mathbf{pq})}{qE(E+1)}\Big) \Big] \Big\};$$

$$W(\mathbf{p}, \mathbf{q}, \boldsymbol{\eta}) = (2\pi)^{-5} pEq^2 \Big\{ \Big| \int 1 \Big|^2 \Big[(|C_S|^2 + |C_S'|^2) \Big(1 - \frac{\mathbf{pq}}{qE}\Big) + (|C_V|^2 + |C_V'|^2) \Big(1 + \frac{\mathbf{pq}}{qE}\Big) \pm \frac{2}{E} \operatorname{Re}(C_S C_V^{+} + C_S' C_V'^{+}) \Big]$$

$$+ \Big| \int \sigma \Big|^2 \Big[(|C_T|^2 + |C_T'|^2) \Big(1 + \frac{\mathbf{pq}}{3qE}\Big) + (|C_A|^2 + |C_A'|^2) \Big(1 - \frac{\mathbf{pq}}{3qE}\Big) \pm \frac{2}{E} \operatorname{Re}(C_T C_A^{+} + C_T' C_A'^{+})$$

$$+ 2gf_1 \Big(\pm \frac{1}{E} \operatorname{Re}(C_T C_T'^{+} - C_A C_A'^{+}) \mathbf{p}\boldsymbol{\eta} \pm \frac{1}{q} \operatorname{Re}(C_T C_T'^{+} + C_A C_A'^{+}) \mathbf{q}\boldsymbol{\eta} + \frac{1}{qE} \operatorname{Re}(C_T C_A^{+} + C_T' C_A'^{+}) \mathbf{q}\boldsymbol{\eta} \Big) + 2hf_2 (|C_T|^2 + |C_T'|^2$$

$$- |C_A|^2 - |C_A'|^2) \frac{N_{ik} q_i p_k}{qE} \Big] + 2f_1 \sqrt{\frac{I}{I+1}} \Big| \int 1 \Big| \Big[\operatorname{Re}\Big(e^{\mp i\alpha} \Big((C_S C_T'^{+} + C_S' C_T^{+} - C_V C_A'^{+} - C_V' C_A^{+}) \frac{\mathbf{p}\boldsymbol{\eta}}{E} - (C_S C_T'^{+} + C_S' C_T^{+}$$

$$+ C_V C_A'^{+} + C_V' C_A^{+}) \frac{\mathbf{q}\boldsymbol{\eta}}{q} \mp (C_S C_A'^{+} + C_S' C_A^{+} + C_V C_T'^{+} + C_V' C_T^{+}) \frac{\mathbf{q}\boldsymbol{\eta}}{qE} \Big) \Big) + \operatorname{Im}(e^{\mp i\alpha} (C_S C_T'^{+} + C_S' C_T^{+} - C_V C_A'^{+} - C_V' C_A^{+})) \frac{\boldsymbol{\eta}[\mathbf{pq}]}{qE} \Big] \Big\}.$$

A special feature is the appearance in $W(\mathbf{p}, \eta, \zeta)$ of a term in $\mathbf{p}[\eta\zeta]$; this quantity is not invariant with respect to time reversal, but nevertheless it is present in the formulas for $\alpha \neq 0$, becuase, as can be seen without difficulty, α changes sign on reversal of the time.

The first comparison of theory with experiment is conveniently carried out for the β-decay transition $\Delta I = \pm 1$ (no). Measurements of the β-ray spectrum and the $\beta-\nu$ correlation fix the values of

$$|C_T|^2 + |C'_T|^2, \quad |C_A|^2 + |C'_A|^2, \quad \mathrm{Re}(C_T C_A^+ + C'_T C'^+_A).$$

Furthermore, measurement of $W(\mathbf{p}, \zeta)$ [or of $W(\mathbf{p}, \eta)$] makes it possible to determine $\mathrm{Re}(C_T C'^+_T - C_A C'^+_A)$, and measurement of $W(\mathbf{p}, \mathbf{q}, \zeta)$ gives

$$\mathrm{Re}(C_T C'^+_T + C_A C'^+_A), \quad \mathrm{Re}(C_T C'^+_A + C'_T C^+_A), \quad \mathrm{Im}(C_T C^+_A + C'_T C'^+_A).$$

By carrying out measurements of the β-ray spectrum and the $\beta-\nu$ correlation in the case of the transition $\Delta I = 0$ (no) one can find the quantities

$$|C_S|^2 + |C'_S|^2, \quad |C_V|^2 + |C'_V|^2, \quad \mathrm{Re}(C_S C^+_V + C'_S C'^+_V).$$

Measurement of $W(\mathbf{p}, \zeta)$ and $W(\mathbf{p}, \mathbf{q}, \zeta)$ gives

$$\mathrm{Re}(C_S C'^+_S - C_V C'^+_V), \quad \mathrm{Re}(C_S C'^+_S + C_V C'^+_V), \quad \mathrm{Re}(C_S C'^+_V + C'_S C^+_V) \text{ and } \mathrm{Im}(C_S C^+_V + C'_S C'^+_V).$$

Thus we get 14 relations for the determination of 15 quantities (8 absolute values and 7 phase differences). The additional relation necessary for the determination of the relative phase of the Fermi and Gamow-Teller interactions can be found by measuring $W(\mathbf{p}, \eta)$ for the β-decay transitions $\Delta I = 0$ (no).

Note added in proof (September 19, 1957). After this paper had been submitted for publication, there appeared a paper [J. D. Jackson, S. B. Treiman, and H. W. Wyld, Jr., Phys. Rev. 106, 517 (1957)] devoted to the same problem. But these authors differ from us in that they take the phase α to be zero.

[1] J. S. Allen and W. K. Jentschke, Phys. Rev. 89, 902 (1953).
[2] Maxson, Allen, and Jentschke, Phys. Rev. 97, 109 (1955).
[3] W. P. Alford and D. R. Hamilton, Phys. Rev. 95, 1351 (1954).
[4] T. D. Lee and C. N. Yang, Phys. Rev. 104, 254 (1956).
[5] C. S. Wu et al., Phys. Rev. 105, 1413 (1957).
[6] L. Landau, Nuclear Physics 3, 127 (1957).
[7] H. A. Tolhoek and S. R. de Groot, Physica 17, 81 (1951).

Translated by W. H. Furry
238

CONCERNING A MODEL FOR A NON-IDEAL FERMI GAS

A. A. ABRIKOSOV and I. M. KHALATNIKOV

Institute of Physical Problems, Academy of Sciences, U.S.S.R.

Submitted to JETP editor April 24, 1957

J. Exptl. Theoret. Phys. (U.S.S.R.) 33, 1154-1159 (November, 1957)

The energy of the ground state and the effective mass of the excitations are found for a non-ideal Fermi gas with short-range forces, the radii of action of which are small in comparison with the average wavelength.

YANG and Huang[1] and Yang and Lee[2*] have recently investigated the properties of non-ideal Bose and Fermi gases consisting of particles whose dimensions are small in comparison with their average wavelength. The study of such a model is of considerable interest. The method developed by Yang, et al., however, is extremely cumbersome.

In the present work another method will be described which allows the thermodynamic quantities in the model of Yang, et al., to be found reasonably simply for the case of Fermi statistics. The idea for this method is due to Landau.

The model, called a hard-sphere model in the work of Yang et al., has in reality a more general character. It describes a system of particles with arbitrary short-range forces whose radii of action are short compared to the average wavelength.

We first find an expression for the energy of the system correct to terms of order $(a/\lambda)^2$ (where a is the radius and λ the wavelength). It would be possible in principle to determine the terms of order $(a/\lambda)^3$ in an analogous manner; terms of higher order, however, are in principle impossible to find by means of the method presented below, since beginning with terms of the fourth order it is necessary to take into account the contribution of multiple collisions (cf. Ref. 1).

We make use of perturbation theory as applied to the interaction energy of the particles, which we write (taking the volume of the gas as unity, for simplicity)

$$V=2U \sum_{\substack{n_1 n_2 m_1 m_2 \\ n_1<n_2}} a^+_{m_1} a^+_{m_2} a_{n_2} a_{n_1}, \tag{1}$$

where a_i^+ and a_i are the creation and annihilation operators for the particle. The summation is performed with conservation of the total momentum taken into account, with the projection of the spin of the state m_1 equal to the projection of the spin of the state n_1, and similarly for m_2 and n_2. The placing of U ahead of the summation sign reflects the fact that the interaction is identical for all pairs of particles, while the scattering amplitude is independent of the angle. The magnitude of U is in the first approximation related to this amplitude by the expression

$$U = 4\pi a k^2/m \tag{2}$$

(a being the s-scattering amplitude).

The first-order contribution to the energy is equal to the diagonal matrix element of V:

$$E_n^{(1)} = 2U \sum_{n_1<n_2} N_{n_1} N_{n_2} Q_{n_1 n_2}, \tag{3}$$

where the N_i are the occupation numbers.

The factor Q_{ik} in Eq. (3) takes into account the circumstance that Fermi particles, having an angle-independent scattering amplitude, do not interact in the case of parallel spins. Thus we shall assume that

*We take this opportunity to express our gratitude to Professors Yang, Huang, and Lee for sending us their manuscripts prior to publication.

$$Q_{ik} = {}^1/_4 - \sigma_i\sigma_k \tag{4}$$

(σ_i being the spin operator for the i-th particle).

Substituting Eqs. (2) and (4) into (3), we obtain

$$E^{(1)} = (2\pi a\hbar^2/m)N^2/2. \tag{5}$$

To find the second-order correction we use the perturbation-theory expression

$$E_n^{(2)} = \sum_{m\neq n} |V_{nm}|^2/(E_n - E_m). \tag{6}$$

Substituting Eq. (1) into this formula, we obtain the following sum:

$$4U^2 \sum_{\substack{n_1n_2m_1m_2\\ n_1<n_2}} \frac{N_{n_1}N_{n_2}(1-N_{m_1})(1-N_{m_2})Q_{n_1n_2}}{E_{n_1}+E_{n_2}-E_{m_1}-E_{m_2}}, \tag{7'}$$

where the N_i are the equilibrium occupation numbers and the E_i are the particle energies.

Since our objective is an expansion of the energy in powers of a, we must recall that the relation (2) between U and the scattering amplitude is not exact, but correct only to terms of the first order. Taking second-order terms into account we obtain in place of relation (2) the following:

$$2U + 4U^2 \sum_{m_1m_2} Q_{n_1n_2}/(E_{n_1}+E_{n_2}-E_{m_1}-E_{m_2}) = 8\pi a\hbar^2/m. \tag{2'}$$

If from this we express U in terms of a and substitute the result into Eq. (3), then the expression for $E^{(1)}$ will contain terms proportional to a^2, which are naturally to be referred to the second-order correction. Taking this into account, we obtain the following value for the second approximation to the energy:

$$E^{(2)} = 2U^2 \sum_{n_1n_2m_1m_2} \{N_{n_1}N_{n_2}(1-N_{m_1})(1-N_{m_2})Q_{n_1n_2}/(E_{n_1}+E_{n_2}-E_{m_1}-E_{m_2}) - N_{n_1}N_{n_2}Q_{n_1n_2}/(E_{n_1}+E_{n_2}-E_{m_1}-E_{m_2})\}. \tag{7}$$

In view of the fact that the expression in brackets is symmetrical in n_1 and n_2, we replace the limit $n_1 > n_2$ by the factor $\frac{1}{2}$.

The reason for the operation we have just performed is that the expansion in powers of U does not actually take place. The presence of the constant U would simply have led to an infinite value for the energy, as can be seen directly from Eq. (7'). In the present case the essential circumstance is that the scattering amplitude a has a finite, and moreover a small, value, which makes possible the expansion in terms of this quantity.

In the first part of Eq. (7) the term containing the product of four N_i's is equal to zero, since the denominator is antisymmetric relative to the interchange $n_1n_2 \rightarrow m_1m_2$, while the numerator is symmetrical and the total range of summation is the same. The remaining two terms containing the products of three N_i's are identical. Thus we obtain, finally

$$E^{(2)} = -4U^2 \sum_{n_1n_2m_1m_2} N_{n_1}N_{n_2}N_{m_1}Q_{n_1n_2}/(E_{n_1}+E_{n_2}-E_{m_1}-E_{m_2}). \tag{8}$$

This is the fundamental expression for the energy, which is correct so long as the assumption $(a/\lambda \ll 1)$ is fulfilled.

Our goal is to obtain the characteristics of a degenerate Fermi gas. From Eq. (8) we find for the energy of the ground state

$$E^{(2)} = -\frac{4U^2}{(2\pi\hbar)^9} \int_{|p_1|<p_0} dp_1 \int_{|p_2|<p_0} dp_2 \int_{|p_3|<p_0} dp_3 \int_{|p_4|<p_0} dp_4 \frac{\delta(p_1+p_2-p_3-p_4)}{(p_1^2+p_2^2-p_3^2-p_4^2)/2m}, \tag{9}$$

where p_0 is the limiting momentum, equal to $\hbar(3\pi^2N)^{1/3}$.

In accordance with the work of Landau on the theory of a Fermi liquid,[3] the excitation energy is determined by the relation

$$\varepsilon_i = \delta E/\delta N_i. \tag{10}$$

Taking the variation of Eqs. (3) and (8) with respect to N_i gives

$$\varepsilon(\mathbf{p}) = \frac{p^2}{2m} + \frac{UN}{2} + \frac{2U^2}{(2\pi\hbar)^6}\int_{|p_1|<p_0} d\mathbf{p}_1 \int_{|p_2|<p_0} d\mathbf{p}_2 \int d\mathbf{p}_3 \left[\frac{\delta(p_1+p_2-p-p_3)}{(p^2+p_3^2-p_1^2-p_2^2)/2m} - 2\frac{\delta(p_1+p-p_2-p_3)}{(p^2+p_1^2-p_2^2-p_3^2)/2m}\right]. \quad (11)$$

Thus the problem of calculating the energy of the ground state and the effective mass of the excitations reduces to that of computing the integrals in (9) and (11). The integration is quite involved, due to the high multiplicity of the integrals and the inconvenience of the regions of integration (the computation of the integral in (9) will be carried out in the Appendix). It is possible, instead, to use a simpler method based on the relations obtained by Landau. If we introduce the function

$$f_{ik} = \delta^2 E/\delta N_i \delta N_k, \quad (12)$$

which depends upon the momenta and spins of the i-th and k-th particles, then, in accordance with Ref. 3,

$$\frac{1}{m} = \frac{1}{m^*} + \frac{p_0}{2(2\pi\hbar)^3}\mathrm{Sp}_{\sigma,\sigma'}\int f(\mathbf{p}, \sigma; \mathbf{p}'\sigma')\cos\theta d\Omega; \quad (13)$$

$$c^2 = \frac{p_0^2}{3m^2} + \frac{1}{6m}\left(\frac{p_0^2}{2\pi\hbar}\right)^2 \mathrm{Sp}_{\sigma,\sigma'}\int f(\mathbf{p}, \sigma; \mathbf{p}', \sigma')(1-\cos\theta)\, d\Omega, \quad (14)$$

where c is the velocity of sound, m^* is the effective mass, the two vectors p and p' in f are taken equal in absolute magnitude to p_0, and θ is the angle between these vectors. From Eq. (13) we find at once the effective mass, and from Eq. (14), after appropriate integration, the energy of the ground state.

The problem thus reduces to that of determining the quantity f. Taking the variation of Eqs. (3) and (8) with respect to N_i and then to N_k, we find

$$f = 2UQ_{\sigma,\sigma'} - \frac{8U^2}{(2\pi\hbar)^3}\int d\mathbf{p}_1 \int_{|p_1|\leqslant p_0} d\mathbf{p}_2 \left[Q_{\sigma,\sigma'}\frac{\delta(p+p'-p_1-p_2)}{(p^2+p'^2-p_1^2-p_2^2)/2m} + \frac{1}{4}\frac{\delta(p+p_1-p'-p_2)}{(p^2+p_1^2-p'^2-p_2^2)/2m} + \frac{1}{4}\frac{\delta(p'+p_1-p-p_2)}{(p'^2+p_1^2-p^2-p_2^2)/2m}\right]. \quad (15)$$

In this calculation we shall at once set $|\mathbf{p}| = |\mathbf{p}'| = p_0$. Integration over the second term in f is considerably simpler than the integrations in (9) and (11). We find as a result

$$f = \frac{2\pi a\hbar^2}{m}\left[1 + 2\left(\frac{3}{\pi}\right)^{1/3} aN^{1/3}\left(2 + \frac{\cos\theta}{2\sin(\theta/2)}\ln\frac{1+\sin(\theta/2)}{1-\sin(\theta/2)}\right)\right]$$

$$-\frac{8\pi a\hbar^2}{m}(\sigma_1\sigma_2)\left[1 + 2\left(\frac{3}{\pi}\right)^{1/3} aN^{1/3}\left(1 - \frac{\sin(\theta/2)}{2}\ln\frac{1+\sin(\theta/2)}{1-\sin(\theta/2)}\right)\right]. \quad (16)$$

A peculiarity of this expression deserves some attention. For angles θ near π the function f has a logarithmic singularity

$$f(\theta) \sim \left(\frac{1}{4} - \sigma_1\sigma_2\right)\ln\frac{1}{\pi-\theta}. \quad (17)$$

It is clear that the approximation we have used is not applicable, strictly speaking, in this case. Analysis of the subsequent approximations shows that f does not go to infinity at the point $\theta = \pi$, but remains finite; i.e., this singularity does not actually occur.†

†Correction added in proof (September 15, 1957). The singularity in the function $f(\theta)$ at $\theta = \pi$ reflects the singularity in the scattering amplitude for excitations colliding at the angle π. The corresponding expression, obtained by summing the principal terms in the perturbation theory, is proportional to

$$\left[1 + 2\left(\frac{3}{\pi}\right)^{1/3} aN^{1/3}\ln\frac{p_0^2}{\varepsilon}\right]^{-1},$$

where $\epsilon = p^2 + p'^2 - p_0^2$.

For the case in which a is positive, this expression goes to 0 at $p^2 = p'^2 = p_0^2$.

If, however, $a < 0$ (this is possible for a Fermi system), the scattering amplitude has a pole near the Fermi boundary. This corresponds to the possibility of formation of associated pairs from excitations having opposite momenta, which has recently been noted by Cooper,[5] and is evidently the principal reason for the occurrence of superconductivity in metals.[6]

Thus the expression found for f is invalid at angles near to π. In view, however, of the fact that the singularity is a logarithmic one, it is manifested only in the immediate vicinity of the singular point; and, since into the equations in which we are interested there enter only integrals of f with regular functions, the logarithmic singularity in the function f is not important.

Substituting Eq. (16) into (13), we find for the value of the effective mass

$$m/m^* = 1 - (8/15)(3/\pi)^{1/3}(7\ln 2 - 1)\,a^2N^{1/3}. \qquad (18)$$

We note that if the value $m^* = 1.43$ m, corresponding to liquid He^3 (cf. Ref. 4), is substituted here, the resulting value for a is found to 1.6×10^{-8} cm, i.e., it is of the same order as the gas-kinetic diameter of the helium atom. Such a comparison has, of course, no strict significance. The model under consideration cannot describe liquid He^3. This is already evident from the fact that the quantity $(m^* - m)/m^*$, which should be a second-order quantity with respect to a in accordance with theory, is equal to $1/3$ for the case of He^3.

Setting the formula for f into the expression for the velocity of sound, we obtain

$$c^2 = \frac{\pi^{1/3}}{3^{1/3}}N^{1/3}\frac{\hbar^2}{m^2} + 2\frac{\pi a\hbar^2}{m^2}N\left[1 + \frac{4}{15}\left(\frac{3}{\pi}\right)^{1/3}aN^{1/3}(11 - 2\ln 2)\right]. \qquad (19)$$

From the value found for c^2 it is not difficult to obtain the energy of the ground state for a Fermi liquid. For this we use the relation[3]

$$c^2 = (N/m)(\partial\mu/\partial N). \qquad (20)$$

From this we obtain

$$E = \int \mu dN = E^{(0)} + \frac{\pi a\hbar^2}{m}N^2\left[1 + \frac{6}{35}\left(\frac{3}{\pi}\right)^{1/3}aN^{1/3}(11 - 2\ln 2)\right]. \qquad (21)$$

Equation (21) agrees with the result of Lee and Yang.[2] The same result may be obtained by direct integration in Eq. (9); this is done in the Appendix.

In conclusion, the authors express their deep gratitude to Academician L. D. Landau for his valued advice and criticism of the results of this work, to V. Galitskii for his helpful discussions, and, finally, to L. Pogodina for her aid in the preparation of the manuscript for publication.

APPENDIX

For the computation of the integral in Eq. (9) it is convenient to introduce the new variables

$$\mathbf{p} = \mathbf{p}_1 - \mathbf{p}_2,\ \mathbf{q} = \mathbf{p}_3 - \mathbf{p}_4,\ \mathbf{s} = \mathbf{p}_1 + \mathbf{p}_2 = \mathbf{p}_3 + \mathbf{p}_4.$$

In terms of these variables, $E^{(2)}$ takes on the form

$$E^{(2)} = -\frac{mU^2}{4(2\pi\hbar)^9}\int d\mathbf{s}\int d\mathbf{p}\int d\mathbf{q}\,\frac{1}{p^2 - q^2},$$

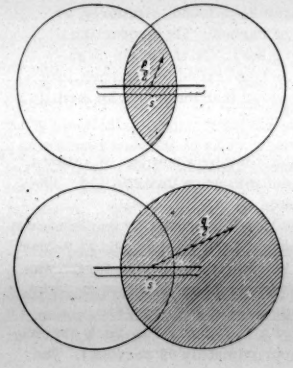

where the region of integration for the vector s is $0 < |\mathbf{s}| < 2p_0$ and the range of values for p and q is shown in the figure. If we introduce the variables $x_q = \cos(\mathbf{q}, \mathbf{s})$ and $x_p = \cos(\mathbf{p}, \mathbf{s})$, $E^{(2)}$ becomes

$$E^{(2)} = -\frac{8mU^2\pi^3}{(2\pi\hbar)^9}\int_0^{2p_0} s^2\,ds\int_0^1 dx_p\int_0^{z(x_p)} p^2\,dp\int_{-1}^1 dx_q\int_0^{z(x_q)} q^2\,dq\,\frac{1}{p^2 - q^2},$$

where z(x) satisfies the relation

$$z^2 + 2zsx + s^2 = 4p_0^2.$$

From this, by means of a series of transformations and partial integrations over dx_p and dx_q we find

$$E^{(2)}=\frac{2m U^2 p_0^7}{\pi^6\hbar^9}\int_0^1 s^2\,ds\left[\int_0^{1+s} p^2\,dp\int_0^{1-s} q^2\,dq+\frac{1}{4s^2}\int_{\sqrt{1-s^2}}^{1+s} p\,dp\,(1-p^2-s^2)\int_{\sqrt{1-s^2}}^{1-s} q\,dq\,(1-q^2-s^2)\right]\frac{1}{p^2-q^2}.$$

Integrating further by parts over s and then carrying out the remaining integration, we obtain

$$E^{(2)}=(^6/_{35})\,(3/\pi)^{1/3}(11-2\ln 2)\,aN^{1/3}E^{(1)}.$$

Here we have expressed U in accordance with Eq. (2) and set $p_0=\hbar(3\pi^2N)^{1/3}$. The result thus obtained is identical with the second-order term in Eq. (21).

[1] K. Huang and C. N. Yang, Phys. Rev. 105, 767 (1957).
[2] T. D. Lee and C. N. Yang, Phys. Rev. 105, 1119 (1957).
[3] L. D. Landau, J. Exptl. Theoret. Phys. (U.S.S.R.) 30, 1058 (1956), Soviet Phys. JETP 3, 920 (1957).
[4] I. M. Khalatnikov and A. A. Abrikosov, J. Exptl. Theoret. Phys. (U.S.S.R.) 32, 915 (1957), Soviet Phys. JETP 5, 745 (1957).
[5] L. N. Cooper, Phys. Rev. 104, 1189 (1956).
[6] Bardeen, Cooper, and Schrieffer, Phys. Rev. 106, 162 (1957); N. N. Bogoliubov, J. Exptl. Theoret. Phys. (U.S.S.R.) 34, 58 (1958), Soviet Phys. JETP 7 (in press).

Translated by S. D. Elliott
239

SOVIET PHYSICS JETP VOLUME 6 (33), NUMBER 5 MAY, 1958

NUCLEAR REACTIONS IN Li^7 AND C^{12} INDUCED BY N^{14} IONS

D. G. ALKHAZOV, Iu. P. GANGRSKII, and I. Kh. LEMBERG

Leningrad Physico-Technical Institute, Academy of Sciences, U.S.S.R.

Submitted to JETP editor June 3, 1957

J. Exptl. Theoret. Phys. (U.S.S.R.) 33, 1160-1162 (November, 1957)

In an investigation of the reaction products induced by the bombardment of Li^7 by 15.6-Mev nitrogen ions, activities associated with F^{18}, Ne^{19}, N^{16}, and O^{15} have been found; similarly, an activity associated with Al^{25} has been found in the bombardment of carbon. The production cross sections for the above-mentioned products have been determined. On the basis of an examination of the F^{18}-production cross sections in light elements bombarded by nitrogen ions and the α-particle binding energy in these same nuclei, it is proposed that the F^{18} is formed by capture of an α-particle from the nucleus by the incoming N^{14} nucleus.

NUCLEAR reactions induced in light elements by N^{14} ions have been studied by a number of authors.[1-6] However, in all this work only nuclides with half-lives T greater than 1 min were investigated. The products resulting from the bombardment of Li^7 by N^{14} have not been studied at all.

In the present work we have measured yields for nuclides with $T > 1$ sec produced by bombardment of Li^7 and C^{12} by N^{14} ions. The experiments were carried out with a beam of triply-charged, 15.6-Mev N^{14} ions from a cyclotron; the beam was focussed by two magnetic-quadrupole lenses. The target was placed at the end of a Faraday cylinder. The electric charge deposited by the beam was measured by electronic integration. In these experiments the ion-beam intensity was $4-7\times10^{10}$ ions/sec.

The lithium bombardment was carried out with a target consisting of a LiCl layer 70μ thick precipitated from an aquaeous solution enriched in Li^7 (the Li^7 content was approximately 99 percent). The

TABLE I

Target nucleus	Reaction product	T	B for nitrogen ions	$\sigma \times cm^2$*
Li^7	F^{18}	112 min	$1.4 \cdot 10^{-7}$	$1.8 \cdot 10^{-26}$
Li^7	Ne^{19}	18.5 sec	$3.1 \cdot 10^{-8}$	$4.0 \cdot 10^{-27}$
Li^7	N^{16}	7.4 sec	$1.1 \cdot 10^{-7}$	$1.5 \cdot 10^{-26}$
Li^7	O^{15}	1.97 min	$1.0 \cdot 10^{-6}$	$1.3 \cdot 10^{-25}$
C^{12}	Al^{25}	7.6 sec	$3.2 \cdot 10^{-9}$	$2.0 \cdot 10^{-28}$

*The cross sections are computed for ions with $E_{lab} = 15.6$ Mev

carbon bombardment was carried out with a graphite target 70μ thick. In both cases the target substrate was a copper slab 70μ thick. The copper end of the Faraday cylinder was 100μ thick. The radiation associated with the induced activity was detected by a MST — 17 end-window β-counter which was placed directly against the end of the cylinder (in this work the solid angle ranged from $0.46 \times 4\pi$ to $0.22 \times 4\pi$). The counter pulses were fed to an amplifier and then to the input of a 10-channel time analyzer in which the pulses were recorded in various channels depending on their relative time delay. By varying the time width of a channel it was possible to measure to 10^{-3} sec and better. In the present work only $T > 1$ sec has been investigated. The analyzer was synchronized with the cyclotron beam and automatically switched on a short time after the beam was switched off.

An analysis of the activity in graphite resulting from the bombardment of Li^7 indicated the presence of nuclides with half-lives of 6.8 sec, 17.5 sec, 2 min, and 130 min. When Li^7 is bombarded by N^{14} formation of the following nuclides with values of T ranging from 5 to 20 sec is possible: F^{20} (T = 7.35 sec, $E_{\beta\,max} = 10.4$ Mev); N^{16} (T = 10.7 sec, $E_{\beta\,max} = 7$ Mev); Ne^{19} (T = 18.5 sec, $E_{\beta\,max} = 2.2$ Mev). For control purposes a decay curve was taken with an aluminum absorber between the counter and the target. The thickness of the absorber (3 mm) was sufficient to stop β radiation from Ne^{19}. In this case the 6.8-sec activity was observed. This result serves as a basis for assuming that when Li^7 is bombarded by nitrogen N^{16} is formed and the F^{20} yield (if it exists at all) is less than 0.1 of the N^{16} yield. The 17.5-sec activity has been assigned to Ne^{19}; the 2-min and 130-min activities have been assigned to O^{15} (T = 1.97 sec) and F^{18} (T = 112 sec).

The bombardment of C^{12} by N^{14} has been studied in Ref. 2; a 112-min activity (F^{18}), a 15-hour activity (Na^{24}) and 2.6-year activity (Na^{22}) were found. In the present work the short-lived activities were studied. A 7.4-sec activity, apparently due to the $C^{12}(N^{14}, n)Al^{25}$ reaction was observed.

Extrapolating the decay curves to the origin, introducing corrections for β-ray absorption in the target, substrate, and end of the Faraday cylinder, and introducing solid-angle corrections we have determined the yields for the various nuclides formed in N^{14} reactions. In Table I are shown the yield values B for thick targets, referred to a single nitrogen ion. In this same table are shown the cross sections σ for the various reactions which result in the formation of the nuclides shown in the table. To compute the values of σ, starting from the values of B determined in the experiments, one must know the excitation function $\sigma(E)$ and the stopping power of the target material for nitrogen ions. We have compared the experimentally determined excitation functions[2-4] for the reactions

$$Be^9(N^{14}, He^5)F^{18}, \quad (1)$$

$$B^{10}(N^{14}, Li^6)F^{18}, \quad (2)$$

$$C^{12}(N^{14}, Be^8)F^{18}, \quad (3)$$

$$O^{16}(N^{14}, C^{12})F^{18} \quad (4)$$

and are convinced that these functions are very much the same for energies E less than the height of the Coulomb barrier E_b; for nitrogen-ion interactions with Be^9 and B^{10} the excitation functions are essentially identical. Hence, in computing σ for reactions occurring in the bombardment of lithium by nitrogen ions we have used the $\sigma(E)$ curve for the reactions in (1) and (2) published in Refs. 3 and 4; in the carbon case the $\sigma(E)$ curve for reaction (3) given in Ref. 2 has been used. The stopping power for nitrogen ions was computed by converting the range-energy curves for α-particles using the method proposed by Lonchamp.[7] We have obtained the following results: nitrogen ions with $E \leq 15.6$ Mev in LiCl, $dE/dpx = 6.1$ Mev-mg^{-1}-cm^2; in graphite $dE/dpx = 7.6$ Mev-mg^{-1}-cm^2.

The high value of the F^{18}-production cross section in Table I is noteworthy. An anomalously high F^{18} yield is also noted in bombardment of certain other elements by nitrogen ions. It is possible that F^{18} formation takes place as the result of the capture of an α particle from the target nucleus by the incoming N^{14} nucleus as in "inverse stripping" reactions in which the incoming nucleon can cause the ejection of another nucleon from the nucleus and continue on in the form of a deuteron. It is apparent that with a re-

TABLE II

Target nucleus	E_{bind}, Mev	E_B, Mev	σ, cm^2	Reference
Li^7	2.5	5.0	$1.8 \cdot 10^{-26}$	Present work
Be^9	2.2	6.4	$1.0 \cdot 10^{-25}$	[3]
B^{10}	4.4	7.9	$6.5 \cdot 10^{-27}$	[4]
C^{12}	7.4	9.2	$1.0 \cdot 10^{-27}$	[5]
N^{14}	11.6	10.5	*	
O^{16}	7.2	11.7	$1.5 \cdot 10^{-27}$	[4]
Al^{27}	10.0	17.4	**	

* Activity due to F^{18} production is not observed.[5]
** Activity due to F^{18} production is observed but the value of σ is not given.[6]

action mechanism of this kind a larger value of the F^{18}-production cross section will be observed when the nitrogen ions bombard nuclei with smaller α particle binding energies (E_{bind}). In Table II we compare nitrogen-ion induced F^{18}-production cross sections and values of α particle binding energy in light nuclei. In order to compare the results, the values of σ are taken for collision energies equal to the height of the Coulomb barrier.

It was obvious from Table II that σ decreases as E_{bind} increases.

[1] L. D. Wyly and A. Zucker, Phys. Rev. 89, 524 (1953).
[2] H. L. Reynolds and A. Zucker, Phys. Rev. 96, 1615 (1954).
[3] H. L. Reynolds and A. Zucker, Phys. Rev. 100, 226 (1955).
[4] Reynolds, Scott, and Zucker, Phys. Rev. 102, 237 (1956).
[5] H. L. Reynolds and A. Zucker, Phys. Rev. 101, 166 (1956).
[6] Webb, Reynolds, and Zucker, Phys. Rev. 102, 749 (1956).
[7] J. P. Lonchamp, J. phys. et radium 14, 89 (1953).

Translated by H. Lashinsky
240

SOVIET PHYSICS JETP VOLUME 6 (33), NUMBER 5 MAY, 1958

A STUDY OF SLOW μ MESONS IN THE STRATOSPHERE BY THE METHOD OF DELAYED COINCIDENCES

V. F. TULINOV

P. N. Lebedev Physics Institute, Academy of Sciences, U.S.S.R.

Submitted to JETP editor June 3, 1957

J. Exptl. Theoret. Phys. (U.S.S.R.) 33, 1163-1165 (November, 1957)

A study has been made of the altitude dependence of μ mesons of ~ 100 Mev up to altitudes of about 25 km at 51° and 31° N latitude. The μ-meson production spectrum in the atmosphere has been measured at these latitudes.

EXPERIMENTS on the altitude dependence of slow μ mesons by the method of delayed coincidences were carried out by Sands[1] and Conversi[2] in airplanes at altitudes up to ~ 10 — 11 km. In the present experiment the altitude dependence of slow μ mesons has been studied using that method in balloon flights up to the altitude of ~ 25 km at 51° and 31° N geomagnetic latitude.

The counter arrangement used is shown in Fig. 1. The counter trays T_1 and T_2, separated by a Pb absorber 5 cm thick, formed a telescope. The two groups of counters marked "del" detected delayed particles. The counters of the groups A and B were connected in parallel and the anti-coincidences (A-B) were recorded. The mesons stopped in the graphite block C 7 cm in thickness.

The array detected μ mesons with kinetic energies of 100 — 115 Mev. The "del" counters were oper-

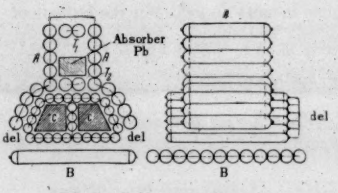

FIG. 1. Schematic diagram of the apparatus

ated in the following way: the high voltage was set at 40 – 50 v below the counting threshold, and the appearance of the master pulse (coincidence T_1T_2) caused a voltage pulse of ~ 180 – 200 v to be applied to the counters for ~ 3 μsec.

The pulsed operation of the delay counters increased the efficiency of the decay-electron detection. In the ordinary method of delayed coincidences it is necessary that the pulse width of the counters detecting decay electrons be less than the chosen delay. A considerable narrowing of the counter pulse necessitates, however, a much more elaborate electronic circuitry, increases the dissipated power and the total weight of the apparatus, etc. It is therefore necessary to increase considerably the delays in experiments sent into the stratosphere, which reduces the detection efficiency of decay electrons. The background cosmic radiation is a further reason for reduced efficiency of the decay electron detection in the conventional counter connection. The total time of counter insensitivity due to dead time becomes appreciable at high altitudes, thus reducing the efficiency. The pulsed operation of counters eliminates all those deficiences of the delayed coincidence method.

The measurement of chance coincidences recorded during the flight was carried out as follows: after each operation of the delay counters due to the master pulse trigger, the counters were operated again about 100 μsec later, when chance coincidences only could be detected. All data obtained during flight were relayed by a radio transmitter, displayed on an oscilloscope, and recorded photographically.

The experiments on the altitude dependence of slow μ mesons were carried out during 1953 – 1955. Two flights were made at each latitude, 51° and 31° N. The results of corresponding flights were consistent. The number of chance coincidences was subtracted from the measured number of delayed coincidences. At high altitudes chance coincidences amounted to ~ 40 – 50% of all recorded events. The detection efficiency η of stopping μ mesons was then accounted for. The efficiency was determined in the course of an auxiliary experiment at sea-level by comparison of the measured number of delayed coincidences with the absolute intensity of μ mesons at sea-level;[3] it was found that $\eta = 0.23 \pm 0.02$.

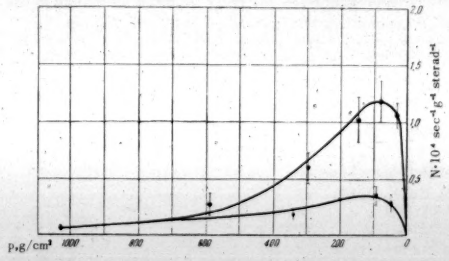

FIG. 2. Altitude dependence of slow mesons for 51° N latitude (upper curve) and 31° N latitude (lower curve)

The altitude dependence of slow μ mesons at the latitudes of 51° and 31° N is shown in Fig. 2. The x axis represents the pressure in g/cm², and the y axis – the number of mesons in $g^{-1}sec^{-1}sterad^{-1}$.

The measurements of the slow μ-meson intensity at high altitudes make it possible to correct the low-energy end of the production spectrum in the atmosphere averaged over the total flux of nuclear-active particles. The expressions for the μ-meson production spectrum in the atmosphere given in Refs. 1 – 4 are not accurate for low energies. This is due to the fact that the experiments[1,2] upon which the calculations are based were carried out at relatively low altitudes (up to 10 – 11 km) where the intensity of slow μ mesons is insensitive to the shape of the meson production spectrum in the low-energy region.

The data on the absolute intensity of slow μ mesons in the stratosphere at the altitude of ~ 30 – 50 g/cm² obtained in the present experiment were used for the determination of the μ-meson production spectrum in the low-energy region. The differential equation[5] expressing the balance of the number of mesons with total energy ϵ at any atmospheric depth was used. The chosen spectrum had, on one hand, to satisfy the measured intensity according to the equation of Ref. 5 and, on the other, to coincide with the known μ-meson production spectrum for energies $\geq 7\mu c^2$.[6] The obtained μ-meson production spectrum in the atmosphere at 51° N latitude can be written as follows:

$$\Pi_{51^\circ N}(\varepsilon) = \frac{360}{(B+\varepsilon)^{2.7}}(\mu c^2)^{-1} \quad \text{min}^{-1}\,\text{sterad}^{-1},$$

where $B = (2 \pm 0.3)\mu c^2$ and ϵ is the total energy of the μ mesons in units of μc^2. For the latitude of 31° N the expression for the spectrum is:

$$\Pi'_{31°N}(\varepsilon) = \frac{2700}{(12+\varepsilon)^{2.7}}(\mu c^2)^{-1} \text{ min}^{-1} \text{ sterad}^{-1} \text{ for } 2\mu c^2 < \varepsilon < 7\mu c^2;$$

$$\Pi''_{31°N}(\varepsilon) = \frac{360}{(2+\varepsilon)^{2.7}}(\mu c^2)^{-1} \text{ min}^{-1} \text{ sterad}^{-1} \text{ for } \varepsilon \geqslant 7\ \mu c^2,$$

under the condition

$$\Pi'_{31°N}(7\mu c^2) = \Pi''_{31°N}(7\mu c^2).$$

It can be easily seen that the observed spectrum exhibits a large latitude effect for slow mesons and that such an effect is absent (cf. Ref. 6) for mesons with energy $\geq 7\mu c^2$ between the latitudes of 51° and 31° N. It should be noted that the μ-meson production spectrum at 51° N latitude, obtained as the result of the present work, yields a slightly larger value for the number of mesons with energy between 2 and $7\mu c^2$ compared with Ref. 1.

In the present experiment, therefore,

(1) new apparatus has been developed for the study of slow μ mesons in the stratosphere by the delayed coincidence method;

(2) the altitude dependence of slow μ mesons has been measured at 51° and 31° north latitude;

(3) the meson production spectrum in the atmosphere at the latitudes of 51° and 31° N has been determined in the low-energy region ($E \gtrsim 100$ Mev).

In conclusion I wish to express my deep gratitude to G. B. Zhdanov and A. N. Charakhch'ian for directing the work, to S. N. Vernov, Iu. A. Smorodin, and T. N. Charakhch'ian for their valuable remarks in the discussion of results and to A. F. Krasotkin for help in assembling the apparatus and carrying out the flights.

[1] M. Sands, Phys. Rev. 77, 180 (1950).
[2] M. Conversi, Phys. Rev. 79, 750 (1950).
[3] A. Fafarman and M. H. Shamos, Phys. Rev. 96, 1096 (1954).
[4] G. M. Garibian and I. I. Gol'dman, J. Exptl. Theoret. Phys. (U.S.S.R.) 26, 257 (1954).
[5] Hamilton, Heitler, and Peng, Phys. Rev. 64, 78 (1943).
[6] T. N. Charakhch'ian, Dissertation, Moscow State Univ., 1954.

Translated by H. Kasha
241

ELECTRON SPECTRUM AT 3200 m ABOVE SEA LEVEL

M. I. DAION

P. N. Lebedev Physics Institute, Academy of Sciences, U.S.S.R.

Submitted to JETP editor June 7, 1957

J. Exptl. Theoret. Phys. (U.S.S.R.) 33, 1166-1174 (November, 1957)

Using a magnetic spectrometer in conjunction with a multiplate cloud chamber, a momentum spectrum was obtained for cosmic-radiation electrons in the range from 4×10^8 to 4×10^9 ev/c. The penetrating power of fast electrons ($E \geq 4 \times 10^8$ ev) is discussed.

1. INTRODUCTION

THE energy spectrum of cosmic-radiation electrons at sea level and at various altitudes in the atmosphere has been studied in Refs. 1 – 10 and elsewhere. The principal methods of investigation were: (1) a comparison of the absorption of cosmic rays in heavy and light substances such as Pb and Al,[1,2] (2) a cloud chamber with lead plates,[3,6,7] (3) large flat scintillation counters separated by lead absorbers,[8,9] (4) a cloud chamber with lead plates in a magnetic field,[4] and (5) an old form of the magnetic mass spectrometer of Alikhanian and Alikhanov.[5]*

In the present work the electron spectrum was studied by means of an Alikhanian-Alikhanov mass spectrometer in conjunction with a multiplate cloud chamber.[11] The principal advantages of this method are that, unlike methods 1, 2, and 3, it enables us to determine the energy of an electron directly by measuring the radius of curvature of its trajectory in the magnetic field and to determine the sign of the charge in each instance. The transmission is much greater than for method 4. The advantage over method 5 is the possibility of identifying electrons reliably by their multiplication in the lead plates of the cloud chamber.

2. ELECTRON SPECTRUM

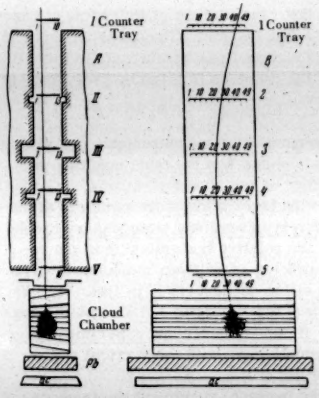

FIG. 1. Experimental arrangement

Our measurements were obtained at 3200 m above sea level and pertained to electron energies E in the range from 4×10^8 to 4×10^9 ev. For the same altitude and for the same energy region the electron spectrum was previously obtained by Muskhelishvili,[5] and the electron and photon spectrum was obtained by Hazen[3] and Lovati, Mura et al.[6] using a multiplate cloud chamber.

In Ref. 3 the energy of the primary particles was determined on the basis of the calculations of Rossi and Greisen[12] from the observed number of particles in the shower maximum. In Ref. 6 the electron and photon energies were determined from the total number of shower particles, using the cascade curves of Wilson[13] for ($E < 3 \times 10^8$ ev) and of Arley[14] ($E > 3 \times 10^8$ ev). Both methods are indirect, because the energies of the primary electrons and photons are determined from theoretical cascade curves by using the number of secondary particles observed in the cloud chamber. However, as we know, the cascade curves have recently been considerably improved (as in Ref. 15) and lead, in particular, to different values of the average number of particles at given depths. It

*In Ref. 10 a magnetic spectrometer was used in conjunction with a proportional counter.

TABLE I

Counter Tray	Number of counters in tray	Counter diameter, mm	Distance between centers of adjacent counters, mm	Counter length, mm	Material and wall thickness, mm
I and *5*	49	4.6	5.3	120	0.1 Cu
2, 3, 4	49	4.6	5.3	120	0.1 Al
I and *V*	11	10	10.3	290	0.1 Cu
II, III, IV	13	8	8.5	290	0.1 Al
Anticoincidences, *ac*	27	20		900	0.15 Cu

must also be noted that aside from the errors in determining the primary electron energy, (errors associated with fluctuations in the number of secondary particles), the secondary particles in multiplate cloud chambers can often be determined only approximately because of the background of extraneous particles and the relatively large number of slow electrons, as was pointed out by Wilson in Ref. 16.

With respect to Ref. 5 it can be stated that although electron energies were here determined directly by measuring the radius of curvature of trajectories in a magnetic field, the electrons were identified by an insufficiently reliable method. In approximating the differential spectra by the law $N(p)\,dp = N_0 p^{-\gamma_d}\,dp$ in Refs. 3, 5, and 6 the values $\gamma_d = 3.0$, 1.5, and 2.5 were used, respectively. It was important to determine the electron spectrum by a direct method which would be free of the shortcomings mentioned above.

Figure 1 shows the experimental arrangement.* In the $100 \times 30 \times 12$ cm gap of the electromagnet, which provided a field of 4500 oersteds, we placed a hodoscopic system of Geiger counters which enabled us to "trace" the trajectory in two mutually perpendicular planes A and B, using 5 points in each plane. Details concerning the counters are given in Table I. Between the poles of the magnet we placed a rectangular cloud chamber ($620 \times 280 \times 180$ mm) containing 7 lead plates each 7 mm thick. An 8 cm thick lead block was below the cloud chamber and counter tray ac was below this block. Practically all of the electrons which entered the apparatus could be registered because the total thickness of the matter above ac was ~ 28 shower units. At the same time there was a considerable reduction of the dead time resulting from the elimination of the "hard" component, which is of no interest here.

TABLE II

No. of interval	Momentum $p \times 10^{-9}$ ev/c	Integral number of registered electrons and positrons	Integral number of electrons and positrons (corrected for the "transmission" of the apparatus)	
			Assuming isotropic scattering	Assuming a $\cos^2\vartheta$ distribution
1	4.0	307	311	319
2	4.5	264	266	270
3	5.0	233	234	236
4	6.0	172	172	172
5	7.0	138	138	138
6	8.0	117	117	117
7	9.0	96	96	96
8	10.0	88	88	88
9	11.0	71	71	71
10	13.0	65	65	65
11	16.0	37	37	37
12	20.0	22	22	22
13	30.0	10	10	10

Electrons were identified by their cascade multiplication in the lead plates of the cloud chamber, because for electrons with $E > 4 \times 10^8$ ev there is practically no possibility of passage through two or three lead plates without multiplication. The momentum p of a primary electron was determined from the measurement of its radius of curvature in the magnetic field. The probable error in momentum determinations because of the finite dimensions of the counters is given by (see Ref. 11)

$$(\Delta p/p)_{\text{prob}} = 0.66 \cdot 10^{-10}\, p.$$

The electron momentum measurements are given in Table II.† Column 3 of the table contains the integral number of registered electrons. In order to determine the true ratios of the numbers of particles in different intervals it is necessary to take into account the relative transmission in the recording of particles of a given momentum. The method used in calculating the transmission of the mass spectrometer is described in Ref. 11. We note that the relative transmission depends not only on the geometry of the apparatus but also on the angular distribution of the primary particles that enter the apparatus. However, under our experimental conditions the trajectories of particles with $p \geq 4 \times 10^8$ ev/c form a small angle with the vertical and the

*A detailed description of the apparatus is given in Ref. 11. In the present experiment the thickness of the layer of light material over the apparatus was about 2 g/cm^2. The roof of the chamber was 8 mm of Al.

†We shall give henceforth the total number of electrons and positrons.

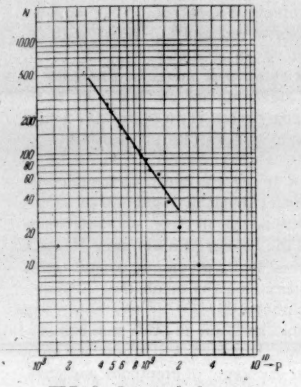

FIG. 2. Integral electron spectrum

transmission is relatively insensitive to the angular distribution of the particles. Column 4 gives the numbers of electrons corrected for the transmission upon the assumption of isotropic scattering of incident particles. Column 5 gives the corresponding numbers for a $\cos^3\theta$ distribution.

Figure 2 is a logarithmic representation of the integral electron spectrum. Electron momentum (or energy) is denoted on the horizontal axis, while the vertical axis denotes the numbers of electrons which possess energy above each given amount. In the energy range $4 \times 10^8 - 2 \times 10^9$ ev the points fall on a straight line and the corresponding integral spectrum can be approximated by $N(p) = N_0/p^{\gamma_{int}}$ with $\gamma_{int} = 1.45 \pm 0.20$. It should be noted that the passage of an electron through the telescopic system is accompanied by the triggering of counters which do not lie on the trajectory of the particle. This may be caused by extraneous particles, random coincidences, etc. Yet even in such instances it is easy to establish the true trajectory, because the counters which determine the latter lie on a straight line in plane A and on a circle in plane B. In addition to the total spectrum in Fig. 2 we have plotted the spectrum of single electrons, which is described by the exponent $\gamma_{int} = 1.55 \pm 0.20$ and does not differ from Fig. 2 within the limits of statistical error.

3. ELECTRON FLUX

For the purpose of determining the absolute electron flux we used data on the proton component which we obtained at the same time. Taking the transmission into account, approximately 135 protons, which were stopped in plates 3 — 6 were registered during the measurements. Taking into account the increase of the range due to the inclination of the trajectories with respect to the planes of the plates as well as due to scattering in the plates, the proton momentum interval corresponding to these residual ranges is approximately $4.8 \times 10^8 - 6.15 \times 10^8$ ev/c. From the data of Ref. 17, obtained at the same altitude, the absolute proton flux in this momentum interval is 0.18×10^{-3} cm^{-2} sterad^{-1} sec^{-1} and comprises $(0.18 \times 10^{-3})/(13.8 \times 10^{-3}) = 1.3\%$ of the muon flux with momenta $p > 370$ Mev/c. Since the 311 electrons which we counted exceed by 2.3 times the number of protons in the same solid angle, it can be concluded that the electron flux for momenta $p > 4 \times 10^8$ ev/c is $\sim 3\%$ of the muon flux for momenta $p > 370$ Mev/c.

The absolute flux of electrons with momenta $p \geq 4 \times 10^8$ ev/c is 0.41×10^{-3} cm^{-2} sterad^{-1} sec^{-1}. This value is probably somewhat too low because it is not always possible to take into account all of the electrons in dense showers. References 3, 5, and 6 give the intensity of the electron-photon component as a percentage of the flux of "hard" particles, which are muons with momenta $p \gtrsim 1.6 - 2.0 \times 10^8$ ev/c and protons with momenta $p \gtrsim 5 - 8 \times 10^8$ ev/c. If for convenience of comparison with these references we relate our electron count to the flux of "hard" particles, we obtain $\sim 2.5\%$ for the electron flux with momenta $p \geq 4 \times 10^8$ ev/c.

We shall now compare our results with those of Refs. 3, 5, and 6. According to Muskhelishvili[5] the electron flux for $2 \times 10^8 \leq p \leq 10^9$ ev/c is $\sim 3\%$, while for $4 \times 10^8 \leq p \leq 10^9$ ev/c it is 1.5%. According to our data the number of electrons in the interval $4 \times 10^8 \leq p \leq 10^9$ ev/c is $\sim 1.8\%$ of the number of "hard" particles. Hazen[3] gives the total intensity of the electron-photon component as 7% and the ratio 2.5 : 1 for the numbers of electrons and photons with $p > 2 \times 10^8$ ev/c. Thus, according to Hazen, the electron flux for $p > 2 \times 10^8$ ev/c is $\sim 5\%$. Lovati, Mura, et al.[6] give the total intensity of the electron-photon component in the same momentum range ($p > 2 \times 10^8$ ev/c) as 12.2%, which is almost 1.7 times greater than the result obtained by Hazen. Using Hazen's ratio between the numbers of electrons and photons, from the data of Lovati et al. we obtain 8.6% for the electron flux. For comparison

TABLE III

Author	Momentum range, ev/c	Electron flux as a fraction of the flux of "hard" particles, %	Electron flux from the previous experiment, %
Hazen[3]	$\geq 4 \cdot 10^8$	1.6—1.8	~2.5
Lovati et al.[6]	$4 \cdot 10^8$—10^9	3.0—3.6	
Muskhelishvili[5]		1.5	1.8

with our own results we take $\gamma_{int} = 1.5$ as the exponent of the integral electron spectrum in the momentum range $2 - 4 \times 10^8$ ev/c (for $p < 2 \times 10^8$ ev/c this exponent is apparently reduced[18]). Then for the electron flux with $p > 4 \times 10^8$ ev/c we obtain 1.8[3] and 3%[6] instead of our result, ~ 2.5%.

According to Refs. 3 and 6 it is possible to estimate the electron flux by another method. From the histograms given in these references it follows that the total number of electrons and photons with $p \geq 4 \times 10^8$ ev/c is 2.2% (Ref. 3) and 5.1% (Ref. 6). Assuming the electron-photon ratio to be 2.5 : 1 in this momentum range, we find that the electron flux with $p \geq 4 \times 10^8$ ev/c is 1.6% (Ref. 3) and 3.6% (Ref. 6).

It is clear that these values for the electron component (with $p \geq 4 \times 10^8$ ev/c), based on the data of Refs. 3 and 6 for the total electron-photon component with $p > 2 \times 10^8$ ev/c, must be regarded as very approximate. We also note that even the value given for the total intensity of the electron-photon component in Ref. 3 is in need of correction. For example, Hazen determined the energy of a primary electron (or photon) on the basis of Rossi and Greisen's calculations[12] and assumed that a given number of particles in the shower maximum corresponds to identical energy for a primary electron or photon. Specifically, it was assumed that when the energy of the primary electron (or photon) is 2×10^8 ev, the average number of particles in the maximum is 5. According to more recent data (see Ref. 15) this number of particles corresponds to higher energy for the primary electron or photon, that is, 2.4×10^8 ev for electrons and 3.3×10^8 ev for photons. Therefore Hazen's form for the total spectrum of electrons and photons can hardly be regarded as correct and his value for the intensity of the electron-photon component is too low.

In conclusion we summarize the data for the electron component in Table III. Keeping in mind the low accuracy for all of the results presented, we find our data in agreement with those of Refs. 3, 5, and 6.

4. REMARK ON THE PENETRATING POWER OF FAST ELECTRONS

TABLE IV

Energy of the primary electron, ev	Average number of particles at depths: 22 t-units		28 t-units	
	According to Rossi[19]	According to Ivanenko[15]	According to Rossi[19]	According to Ivanenko[15]
$7 \cdot 10^8$	0.0026	0.19	0	0.03
10^9	0.0045	0.48	0	0.07
$5 \cdot 10^9$	0.049	3.93	0.002	0.62
10^{10}	0.3	11.6	0.013	2.10

We know that calculations of cascade curves for lead, which take into account the energy dependence of the photon absorption cross section as well as electron scattering (see Ref. 15), lead to essentially new results concerning the penetrating power of fast electrons.* As an illustration, Table IV shows the average number of particles at depths of 22 and 28 t-units (shower units) for a few fixed values of the primary electron energy, based on both older work[19] and the most recent work of Ivanenko.[15]

We see from the table that: (a) according to Rossi the average number of particles at depths of 22 and 28 t-units is negligibly small even for showers produced by electrons with the high energy $E \sim 5 \times 10^9$ ev; (b) Ivanenko's work yields much larger values for the average number of particles at the same depths and thus greater penetrating power of the showers.

To check these conclusions experimentally, we measured the electron spectrum again with a somewhat different experimental arrangement (Series II) in which the total absorber thickness above counter tray ac was 22 shower units instead of the 28 units of Series I. It is clear that according to Rossi's theory[19] this reduction in the thickness of absorbing material should have practically no effect on the form of the spectrum. A quite different result follows from Ivanenko's work:[15] Since in a considerable number of instances electrons are able to pass through 22 t-units of absorbing material and enter counters ac, thus being eliminated from consideration, the resultant spectrum must be steeper. In Fig. 3 the electron spectrum of Series II is represented by crosses. The spectrum of Series I is given for comparison after adjustment for the total number of electrons. Despite the small statistical accuracy, we can affirm qualitative agreement with Ivanenko.[15]

We shall now attempt, on the basis of Ref. 15, to introduce a correction into spectra I and II by taking into account the electrons which escaped registration in our experiments because their multiplication products entered counters ac. It is obvious that after this correction spectra I and II must be approximated by curves with the same exponent γ, which is the true exponent for the spectrum of the electron

*References to earlier work are given in Ref. 15.

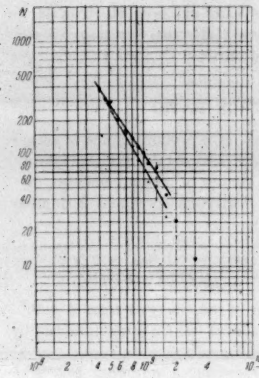

FIG. 3. Electron spectrum. ×—for Series II (22 t-units); •—for Series I (28 t-units)

TABLE V

$E \cdot 10^{-9}$ ev	22 t-units			28 t-units		
	$\bar{n}$	$\bar{n}/2$	σ, %	$\bar{n}$	$\bar{n}/2$	σ, %
4.0	0.014	0.007	99.3	0.01	0.005	99.5
6.0	0.12	0.06	94.0	0.025	0.012	99.0
8.0	0.27	0.135	87.4	0.045	0.022	98.0
10.0	0.48	0.24	78.7	0.072	0.036	96.5
12.0	0.59	0.295	74.4	0.088	0.044	95.7
15.0	0.77	0.385	68.0	0.13	0.065	93.7
20.0	1.09	0.545	58.0	0.18	0.09	91.0
30.0	1.89	0.945	38.8	0.297	0.148	86.0
50.0	3.93	1.965	14.0	0.62	0.31	73.0
100.0	11.6	5.8	0.3	2.1	1.05	35.0

flux entering the apparatus, and that the straight lines which approximate these spectra must be parallel if Ivanenko's cascade curves, upon which the calculation is based, are correct. Since the exclusion of high-energy electrons occurs because their multiplication products enter counters ac, it is necessary to calculate the probability σ that, for a primary electron of given energy, the number of secondary electrons at a given depth (above ac) becomes zero when the average number of secondary electrons is $\bar{n}$. σ is thus the probability that our apparatus will register an electron of a given energy.

At the present time this problem cannot be solved exactly, because the distribution function of the number of particles is unknown. However, there are some grounds for assuming that the Poisson distribution can be used to approximate σ. For example, Wilson's data[16] on the fluctuations of the number of particles, which were obtained by the Monte Carlo method, show that the numerical value of σ is approximately that calculated from Poisson's formula.* In determining σ we have not used the average number of particles at our depths $\bar{n}$ as given by the theory but rather $\bar{n}/2$, because the theory takes into account the reflux of electrons back-scattered in lower-lying layers of lead, which constitutes about half of the total number of electrons. Figure 1 shows that this reflux is absent in our experimental arrangement.

Table V contains the values of σ which were calculated from the Poisson distribution for lead filters 22 and 28 t-units thick. The energy of the primary electron is given in column 1. Columns 2 and 5 give the average number of electrons at depths of 22 and 28 t-units, respectively, which we calculated from the formulas in Ref. 15. The table shows that with an absorber thickness of 28 t-units the efficiency of electron registration is large even at the high energy $E \sim 2-3\times10^9$ ev. With 22 t-units of absorber thickness the picture is quite different: At $E \sim 8\times10^8$ ev $\sigma \approx 87\%$ and at $2-3\times10^9$ ev σ is below 50%.

The values of σ which are given here were used to correct our experimental electron spectra. Numerical values for intermediate energies were determined by interpolation. For each energy interval we related the number of registered electrons to σ, after which we plotted the integral spectra I′ and II′ shown in Fig. 4. It can be seen that in the energy range which is of interest spectrum I′ duplicates spectrum I (Fig. 2) and the exponent $\gamma_{int} = 1.4-1.45$ remains practically unchanged. The total number of particles in the spectrum increased by only ~ 4%.

Spectrum II′, which was obtained by correcting spectrum II (Fig. 3), differs considerably from the latter in its slope and in the integral number of particles, which have increased by ~ 23%. The figure shows that the straight lines which approximate II′ and I′ are now practically parallel.

It is interesting that the ratio of the total numbers of electrons in spectra II and I is $N_2/N_1 = 370/319 = 1.16$, whereas the ratio of the durations of the measurements is $t_2/t_1 = 1.4$. For the corrected spectra II′ and I′ we have the ratio $N_2'/N_1' = 1.4$; this also shows that the total number of unregistered electrons has been taken into account correctly. Our results show† that Ref. 15 gives the correct average number

*We note that according to the same data the probability that one or two particles will appear at a given depth, given the average number $\bar{n}$, differs greatly from that calculated using the Poisson distribution.

†If the comments made in connection with the calculation of σ are valid.

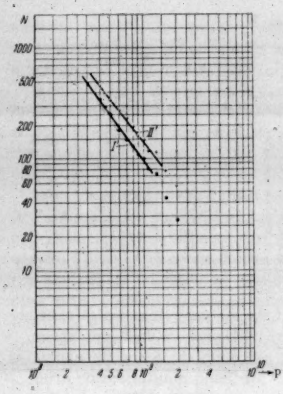

FIG. 4

TABLE VI

Momentum Interval $p \times 10^{-8}$ ev/c	Number of Electrons	Number of Positrons
4—6	178	153
6—10	99	92
10—15	48	53
15—20	15	14
>20	19	18
Totals	359±19	330±18

of secondary electrons at various depths for primary electron energies $E \geq 4 \times 10^8$ ev. Of course, the low statistical accuracy of our experimental data must also be kept in mind.

5. ELECTRON-POSITRON RATIO

There is apparently no reason to expect a predominance of either electrons or positrons, but it is of interest to obtain pertinent data. Table VI gives the results for the two series of measurements. In all energy intervals the electrons and positrons are equal in number within the limits of statistical accuracy.

6. GENERAL RESULTS OF THE INVESTIGATION

(a) The integral electron spectrum in the energy range $4 \times 10^8 \leq E < 2 \times 10^9$ ev at 3200 m above sea level can be approximated by $N(p) = N_0/p^{\gamma_{int}}$, where $\gamma_{int} = 1.5 \pm 0.2$.

(b) The vertical flux of electrons possessing momenta $p \geq 4 \times 10^8$ ev/c is 0.41×10^{-3} cm^{-2} sterad^{-1} sec^{-1}, which comprises $\sim 3.0\%$ of the flux of muons with momenta $p > 370$ Mev/c.

(c) The number of electrons is equal to the number of positrons in all momentum intervals with $p \geq 4 \times 10^8$ ev/c.

(d) Our experimental data concerning penetration by fast electrons ($p \geq 4 \times 10^8$ ev/c) are in approximate agreement with calculations based on Ivanenko's cascade curves.[15]

The author is profoundly grateful to Professor A. I. Alikhanian for making it possible to do this research and for valuable suggestions, to B. A. Doleoshein, who took an active part in the measurements, and to A. A. Abagian for assistance with the measurements and analysis of the data.

[1] J. Clay, Physica **14**, 499 (1948).
[2] J. Clay and E. Van Alphen, Physica **17**, 711 (1951).
[3] W. E. Hazen, Phys. Rev. **65**, 67 (1944).
[4] Bastin, Becker, Chanson, Naglotte, and Treille, J. phys. et radium **2**, 273 (1950).
[5] G. N. Muskhelishvili, Dissertation, Tbilisi, 1952.
[6] Lovati, Mura, Succi, and Tagliaferri, Nuovo cimento **12**, 526 (1954).
[7] Critchfield, Ney, and Oleksa, Phys. Rev. **85**, 461 (1952).
[8] C. N. Chou, Phys. Rev. **90**, 473 (1953).
[9] C. N. Chou and M. Shein, Phys. Rev. **97**, 206 (1955).
[10] V. Kanavets, Thesis, (Moscow Physico-Engineering Institute), 1955.
[11] Daion, Fedorov, Merzon, and Shostakovich, Приборы и техника эксперимента (Instr. and Meas. Eng.) **1**, 3 (1957).
[12] B. Rossi and K. Greisen, Revs. Mod. Phys. **13**, 240 (1941).
[13] R. R. Wilson, Phys. Rev. **79**, 204 (1950).
[14] N. Arley, On the Theory of Stochastic Processes and their Application to the Theory of Cosmic Radiation (G.E.C. Gad, Copenhagen, 1943).
[15] I. P. Ivanenko, Dokl. Akad. Nauk SSSR **107**, 819 (1956), Soviet Phys. "Doklady" **1**, 231 (1956).
[16] R. R. Wilson, Phys. Rev. **86**, 261 (1952).
[17] N. M. Kocharian, Dissertation, Yerevan, 1954.
[18] P. R. Barker, Phys. Rev. **100**, 860 (1955).
[19] B. Rossi, High-Energy Particles (Prentice-Hall, New York, 1952).

Translated by I. Emin
242

SOVIET PHYSICS JETP VOLUME 6 (33), NUMBER 5 MAY, 1958

EXPERIMENTAL DATA ON CASCADE MULTIPLICATION OF ELECTRONS IN LEAD

M. I. DAION

P. N. Lebedev Physics Institute, Academy of Sciences, U.S.S.R.

Submitted to JETP editor June 7, 1957

J. Exptl. Theoret. Phys. (U.S.S.R.) 33, 1175-1178 (November, 1957)

Experimental data have been obtained on the number of secondary electrons at the depth of 1.4, 2.8, and 4.2 radiation units in lead for primary electron energies of 200 — 500 Mev. A comparison is made with theoretical calculations carried out by the Monte Carlo method.

1. INTRODUCTION

A large number[1,2*] of theoretical studies has been devoted to the passage of electrons through matter and particularly to the calculation of the so-called cascade curves. In recent years, an advancement in the methods of computation was accompanied by a further improvement of the cascade curves due to a more accurate account of the ionization losses of electrons and of their scattering, and of the energy dependence of the photon absorption coefficient. Many other important aspects, however, remain obscure or are known only to a crude degree of approximation. These comprise fluctuations of the number of particles, angular and lateral distributions, etc.

It should be noted that, apart from its intrinsic interest, the problem is of great value for various applications. The study of the cascade multiplication of secondary photons, for instance, makes it possible to determine the energy of π^0 mesons produced in nuclear interactions. Another example is supplied by the application of the cascade theory to energy measurements of γ-rays emitted in the decay of unstable particles (e.g. K mesons). We do not have to stress the widely recognized importance of the cascade theory for the general picture of cosmic radiation.

In the present work we deal with the electron cascade multiplication in a dense material, namely lead. It is our aim to compare experimental data on cascade multiplication of electrons in lead with the cascade theory.

2. EXPERIMENTAL PART

The study of electron cascade multiplication was carried out by means of a multiplate cloud chamber combined with the magnetic spectrometer of Alikhanian and Alikhanov.[3,4] The momentum of primary electrons was determined from the curvature of the trajectory in the magnetic field by means of a counter hodoscope placed in the field. Data concerning the accuracy of momentum measurement of a single particle are given in the table.

Electron momentum $p \cdot 10^{-9}$ ev/c	$(\Delta p/p)_{prob}$, %
2.0	1.3
3.0	2.0
4.0	2.6
5.0	3.3

Electron multiplication was observed in a large rectangular cloud chamber (650 × 280 × 180 mm) placed below the hodoscope array. The chamber contained seven lead plates, 7 mm thick. The top of the chamber consisted of 8 mm Al and 2 mm Cu. The tracks were photographed with a stereoscopic camera.

The conditions of the experiment made it possible to identify electrons without any difficulty. The momentum of primary electrons was determined in every case and secondary electrons under the first, second, and third lead plates were counted in the cloud chamber pictures. The most appropriate procedure, evidently, was to compare the results with the cascade curves obtained by Wilson[5] by means of the Monte Carlo method. The reason for this, as correctly observed by Wilson,[5] is that a marked background due to stray slow electrons is usually present in cloud chamber pictures. These electrons could be erroneously identified as slow electrons of the shower, which, in general, propagate at

*For additional bibliography cf. Refs. 1 and 2.

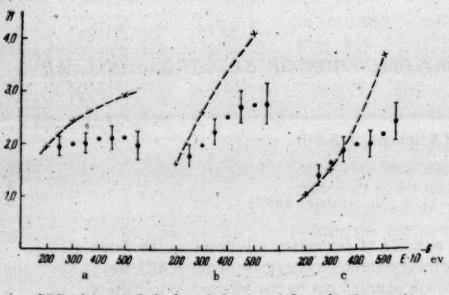

FIG. 1. a — 1.4; b — 2.8; c — 4.2 radiation units

large angles to the shower axis. For this reason Wilson introduces apart from the ordinary cascade curves [denoted in the following by (I)], another set of cascade curves (II) for comparison with cloud-chamber results. The cascade curves (II) give the mean number of electrons $\bar{n}$ at a given depth going in a relatively narrow cone of angle ± 30° to the axis. A marked background of slow electrons was observed in the present experiment, and the electrons going at an angle of ± 30 — 40° to the shower axis were therefore counted and the results compared with the curves (II).

The results are shown in Fig. 1. The x-axis represents the primary electron energy, and the y-axis — the mean number of secondary electrons at a given depth. The graphs 2a, 2b, and 2c correspond to depths of 1.4, 2.8, and 4.2 radiation units respectively.* The points in the graphs represent the experimental values of the mean number of secondary electrons at the given depths for mean primary electron energies equal to 250, 300, 350, 400, 450, 500, and 550 Mev. The width of the energy interval at each point is 100 Mev, and the intervals overlap. For example, the mean energy of 350 Mev, corresponds to the 300 — 400 Mev interval, and the mean energy of 400 Mev — to the 350 — 450 Mev interval of primary electron energy. Values obtained from Wilson's theoretical curves for the energies of 200, 300, and 500 Mev are denoted by crosses. The dashed line gives the interpolated intermediate energies.

3. DEDUCTIONS

Comparison of the experimental data with the theory shows that for the primary electron energy of ~ 200 Mev the observed number of secondary electrons at depths of 1.4, 2.8, and 4.2 radiation units approximates the values predicted according to Wilson. For large energies, the theoretical values are systematically greater than the experimental results; the difference in the mean number of particles amounts to ~ 25 — 30%. This discrepancy cannot, however, be regarded as quantitatively accurate since the experimental bias has been different from conditions represented by the curves. In particular, the theoretical curve gives the average number of particles within a solid angle while experimental data are expressed in plane angles measured in the photographs and are therefore rather low. Inclinded incidence of primary electrons, a factor increasing the effective thickness of plates, has not been taken into account. The inclination is small for electrons of $E \geq 300$ Mev and the effect is negligible.

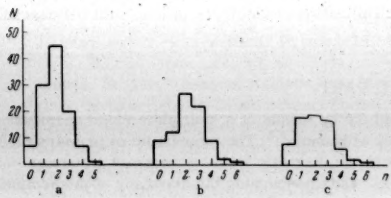

FIG. 2. a — 1.4 radiation units, E = 250 Mev; $N_{tot} = 110$; $\bar{n} = 1.97$; $(n - \bar{n})^2/\bar{n} = 0.5$; b — 2.8 radiation units, E = 350 Mev; $N_{tot} = 82$; $\bar{n} = 2.24$; $(n - \bar{n})^2/\bar{n} = 0.76$; c — 4.2 radiation units, E = 450 Mev; $N_{tot} = 71$; $\bar{n} = 2.07$; $(n - \bar{n})^2/\bar{n} = 0.85$

The following explanation of the observed discrepancy seems very plausible: the cascade curves (I) have been obtained by Wilson from the general cascade curves by exclusion of all secondary electrons with energy $E < 8$ Mev. It has been assumed that essentially electrons with $E > 8$ Mev are present in the narrow cone close to shower axis. It is clear that such a criterion is approximate and that no great accuracy can be claimed for cascade curves (II). The cascade curves would fall lower than those shown in the graph were the limiting energy greater. It should be noted that Wilson's general cascade curves are in a good agreement with accurate calculations of Ivanenko[2] based on computation of the moments of cascade curves.

*It has been assumed, as in Ref. 5, that one radiation unit in lead equals 0.5 cm.

Two experiments on the multiplication of electrons in lead plates of a cloud chamber can be mentioned. Wilson[5] reports that the experimental results of Shapiro[6] are in a good agreement with the theory for electrons of 200 Mev. The results of a detailed study of d'Adlau[7] refer to primary electrons with mean energies of 63, 104, 170, 280, 460, and 770 Mev and do not contradict our results in the region that permits comparison with the curves of Wilson. We have not considered the experiments of Hinotani et al.[8] since an indirect method of primary electron energy determination had been used, nor that of Hazen[9] dealing mainly with electron cascades in copper.

In conclusion we shall discuss several histograms (Fig. 2) representing the fluctuations in the number of particles observed at a given depth, for a given energy of the primary particle. In Fig. 2 the x-axis represents the number of particles within the angle of ± 30° with the shower axis, and the y-axis – the corresponding number of cases. It should be noted that in some cases similar histograms for high-energy primary electrons have a wider distribution, although the statistical accuracy of the results is then considerably lower. It has been found that almost in all cases the expression $\overline{(n-\bar{n})^2}/n$ is smaller than unity, while it should equal 1 for the Poisson distribution.

The author wishes to express his deep gratitude to A. I. Alikhanian for making it possible to carry out the experiment and for his valuable advice, and to B. A. Dolgoshein for taking part in the measurements.

The experimental part of the work was carried out at the High Altitude Laboratory on Mt. Aragats and the author takes advantage of the opportunity to express his appreciation to the staff.

[1] B. Rossi, High-Energy Particles, Prentice-Hall, New York, 1952.

[2] I. L. Ivanenko, Dokl. Akad. Nauk SSSR **107**, 819 (1956), Soviet Phys. "Doklady" **1**, 231 (1956).

[3] Daion, Fedorov, Merzon, and Shostakovich, Приборы и техника эксперимента (Instr. and Meas. Eng.) **1**, 3 (1957).

[4] M. I. Daion, J. Exptl. Theoret. Phys. (U.S.S.R.) **33**, 1166 (1957), Soviet Phys. JETP **6**, 897 (1958).

[5] R. R. Wilson, Phys. Rev. **86**, 261 (1952).

[6] A. M. Shapiro, Phys. Rev. **82**, 307 (1951).

[7] Ch. A. d'Adlau, Nuovo cimento **12**, 6, 859 (1954).

[8] Hinotani, Suda, and Tanaka, J. Phys. Soc. Jap. **9**, 883 (1954).

[9] W. E. Hazen, Phys. Rev. **99**, 911 (1955).

Translated by H. Kasha
243

OBSERVATION OF PARTICLES OF CHARGE $Z > 2$ IN DISINTEGRATIONS PRODUCED IN PHOTOGRAPHIC EMULSIONS BY HIGH-ENERGY NEUTRONS

V. M. SIDOROV and E. L. GRIGORIEV

Joint Institute for Nuclear Research

Submitted to JETP editor June 8, 1957

J. Exptl. Theoret. Phys. (U.S.S.R.) 33, 1179-1184 (November, 1957)

Experimental data are given on the observation of particles of charge $Z > 2$ in disintegrations produced in nuclear emulsion by high-energy neutrons. The neutrons had a broad energy distribution with a maximum in the 395 Mev region. Measurements have been made of the cross-section for the emission of heavy particles, their angular and energy distributions, and their charge distribution.

THE emission of heavy particles in nuclear interactions has been studied in many experiments both with cosmic rays and with artificially-accelerated particles.[1-6]. A considerable portion of the evidence concerning such heavy particles has been obtained from observations of the disintegration of nuclei in emulsions. Notwithstanding the known deficiencies of the photographic technique, it has been established by this method that the emission of heavy particles, especially those with high energies, occurs by a mechanism different from that connected with evaporation from an excited nucleus.

We present in this paper experimental data on particles with $Z > 2$, obtained from observations on nuclear disintegrations ("stars") produced by high energy neutrons in photographic emulsions.

A total of 10,037 stars were registered. The prongs of these stars included 19 hammer tracks, 16 pairs of α particles differing by very small angles, 2 emissions of 3 α particles within a narrow cone, 4 tracks of Be^8 decomposing in flight, 1 case of the emission of B^9 decomposing in flight, and 23 tracks of particles with $Z > 2$.

CONDITIONS OF THE EXPERIMENT AND THE METHOD OF CHARGE DETERMINATION

Photographic plates having emulsions of high sensitivity, 200 μ thick, were placed in a collimated neutron beam produced by 480 Mev protons bombarding a Be target. The energy distribution of the neutrons in the beam has been investigated in special experiments and has been reported previously.[7] The spectrum covers a large energy region and has a maximum in the region of 395 Mev. The scanning of the plates was carried out with a microscope having a magnification of 1350 ×.

The following were recorded: (1) all stars with more than 2 prongs, except those having centers at the surface of the glass or emulsion and those having a fast particle moving in the same direction as the neutron beam; (2) all single tracks that begin and end in the emulsion; (3) 2-prong stars (a) whose prongs make an angle less than 90° and (b) whose prongs differ in grain density.

The charge of the majority of particles was determined from the appearance of the disintegration (hammer tracks, pairs of α particles, etc.). In the remaining cases the charge Z was determined from measurements of the thinning-down length, L, using the relation $L = cZ^2$ (Ref. 8). The value $c = 0.8$ was found by counting the δ-electrons and measuring the length L of one of the fragments. It should be pointed out that this is not a very accurate way of determining charge and depends on the validity of the relation $L \sim Z^2$ and c = constant for all the charges measured. However, over the narrow range of Z values studied here, there are apparently no significant deviations from these relations. [This method yielded values $Z = 4$ (5 tracks) and $Z = 5$ and 6, (13 tracks).]

The magnitude of L was measured with an ocular micrometer at a total magnification of 2025. The thickness of the track was measured over 2.26 μ of its length. Another method was also used for the determination of L in the cases of stars lying in the plane of the emulsion. For these tracks the variation of the thickness with length was taken from photometric measurements of the tracks. The two methods give commensurate results.

STAR CHARACTERISTICS

The table shows the principal characteristics of the stars formed by 390 Mev neutrons in emulsions. The prong distribution is based on the measurement of a thousand stars. The average number of prongs per star is 3.8. From the table it is evident that the distribution by prongs of stars with heavy particles ($Z > 2$) is similar to the distribution of stars without such particles.

No. of Prongs	1	2	3	4	5	6	7	8	9	10
No. of stars, %	4.2	11.6	30.2	27.0	16.5	6.6	2.5	0.9	0.5	—
No. of stars with particles with Z>2, %	2	9	23	16	7	4	3	—	—	1
No. of stars with particles with Z>2, %	3.1	14.0	35.2	24.8	10.7	6.2	4.6	—	—	1.4

Li^8 EMISSION

Hammer tracks having an electron decay can be produced by either Li^8 or B^8 decaying according to the schemes:

$$Li^8 \rightarrow Be^{8*} + e^- + \nu; \quad B^8 \rightarrow Be^{8*} + e^+ + \nu$$
$$\hookrightarrow 2He^4 \qquad\qquad \hookrightarrow 2He^4$$

Owing to its larger charge, the emission of B^8 is less probable than the emission of Li^8. For this reason all the hammer tracks with electrons were assigned to Li^8. Those tracks which were not accompanied by electrons were attributed to Be^8 decaying, after slowing down, into two α particles. Since the efficiency of observation for electron tracks under our conditions depends on their orientation in the emulsion, it may be that a portion of the tracks assigned to Be^8 really belong to Li^8 whose decay electrons were missed. However, the measured efficiency for observing electron tracks, carried out by observations of the decay process $\mu^+ \rightarrow e^+ \ldots$, gave a high value for the efficiency, around 90%.

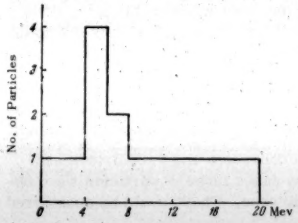

FIG. 1. Energy Distribution of Li^8

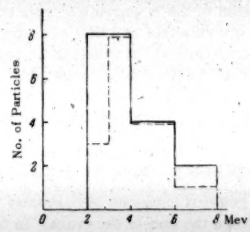

FIG. 2. Energy Distribution of α Particles. The dotted curve represents the data of Ref. 1

The kinetic energy of the Li nuclei was determined from a relation $R = f(E)$ for the emulsion, obtained from the range energy relation for α particles.[9] In this it was assumed* that $R(Li) = \frac{8}{9} \times R(\alpha)$.

The energy distribution of the Li^8 nuclei is shown in Fig. 1. From this it follows that Li^8 is most frequently emitted with an energy of ~ 5 Mev. Such a value for the most probable energy can be used as evidence that Li^8 in the majority of cases is emitted by light nuclei.[2] In support of this conclusion is also the fact that, with the exception of one case, all Li^8 nuclei observed are parts of stars having less than 5 prongs.

The energy spectrum of α particles found in the decay of Li^8 is shown in Fig. 2. The dotted curve is constructed from the data of Ref. 1. In spite of the relatively small number of cases found here, there is obviously agreement in the spectra. A similar agreement is also observed upon compariosn with the data of other authors.[9,11] The most probable energy of the α-particles is ~ 3 Mev and reflects the first excited state of Be^8 at 2.8 Mev.

In 14 out of 10,037 stars one of the prongs was found to be due to Li^8. The correction required to account for loss of Li^8 tracks from the emulsion is negligibly small, since all the tracks are much shorter than the emulsion thickness. Our value of the probability of the emission of Li^8 agrees satisfactorily with the value predicted by evaporation theory (~ 15 per 10^4 stars).[2]

*The energy of Li^8 obtained in this way agrees well with the value of the energy of Li as a function of its range, determined in the work of Ref. 10.

BERYLLIUM NUCLEI

It is known that the lifetime of a Be^8 nucleus in a ground state with even angular momentum is $\sim 10^{-16}$ sec. In this case the visible picture in a photographic plate will be 2 tracks of α particles coming out from the star center in the same direction. If the angular momentum of the Be^8 is large and odd and the emission of a γ-quantum requires a large change in angular momentum, the Be^8 lives a long time and stops in the emulsion prior to the radiation with subsequent decay into two α particles. In this case the emulsion shows a hammer track.

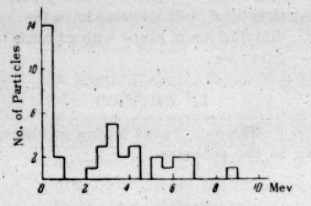

FIG. 3. Energy Distribution of α Particles from the Disintegration of Be^8

There were found 16 cases of the emission of two α particles within a narrow cone from the center of the star. The angle between such α particles was close to zero. The calculated probability of accidental occurrences that would lead to similar pairs of α particles is 5×10^{-4}. These pairs of α particles were attributed to decay of Be^8 which had not had time to leave a track in the emulsion. Knowing the energy of the α particles and the angle between them it is possible to find the energy of excitation ϵ of the Be^8 nucleus. The values of ϵ cluster about 85 kev, as expected from consideration of the mass defect of Be^8. Besides these 16 cases of α-particle pairs, there were found 5 hammer tracks attributable to the decay of Be^8 after stopping, and 4 cases of decay of Be^8 in flight. Evaluation of the lifetime of Be^8 based on measurements of the track lengths in these last four cases leads to $\tau = 10^{-12} - 10^{-13}$ sec.

Figure 3 shows the energy distribution of the α particles from the decay of Be^8. In the graph shows clearly the level corresponding to the ground state and that corresponding to a state of excitation of about 3 Mev. The distribution in the 4 – 7 Mev interval, in which there may be other excited states,[12,13,14] is less clearly defined. The absence here of detailed data concerning the highly excited states is due to the fact that, in these cases, the angle between the particles should be large and such pairs of α particles can thus be hidden among the α particles that have been emitted isotropically.*

PARTICLES WITH Z = 5 AND Z = 6

Sixteen cases were assigned to the general category of particles of charges 5 and 6. Thirteen had tracks with a sharply defined taper toward the end of the track. In two cases three α particles were observed to come out from the center of the star within a narrow angular cone. These could be considered as a disintegration of a carbon nucleus according to the scheme

$$C^{12} \rightarrow Be^{8*} + He^4$$
$$\qquad\quad \rightarrow 2He^4$$

However, it is not possible to say definitely that a C^{12} nucleus is involved since the excitation of the C^{12} as measured by the α-particle ranges and by the angle between Be^8 and He^4 was smaller than the energy of the disintegration (7.4 Mev).

DISTRIBUTION BY CHARGES

We present below data on the distribution of the 65 particles by charges:

Z	3	4	5	6	6 – 9
Number of Particles	18	30	9	7	1

As in disintegrations produced by cosmic rays, the distribution shows a preponderance of particles with

*The question of the levels of Be^8 is still not settled. Some experiments confirm the presence in Be^8 of several excited states, others show only the known state at approximately 3 Mev.[15]

Z = 4. Out of 65 particles, 15 were β-active; 14 of these show hammer type tracks (Li^8), one particle with Z = 5 was possibly the B^9 nuclide emitting an electron.

DISTRIBUTION BY ENERGIES

The distribution according to energy, as determined for 63 particles, is shown in Fig. 4 (one α pair has not been included in this since the range of the α particles did not stay in the emulsion; a particle whose charge was not accurately determined has similarly been omitted). The Li energies were determined from the range vs. energy curve of Ref. 7. The energies of Be^8, in the cases where it was emitted in the form of two α particles, and the energies of C^{12} were measured as the sum of the energies of the α particles. In all other cases the energy was determined from the relation

$$E = 0.262\, M\, (R\, Z_{\text{eff}}^2/M)^{0.575}\ \text{Mev},$$

which was obtained from the empirical relation

$$E = 0.262\, R^{0.575}\ \text{Mev}$$

valid for protons.[16] Taking into account the fact that the average range of the particles being studied here is approximately equal to the tapering-down length and assuming that the nuclei lose their charge smoothly, the magnitude of Z_{eff} was taken as Z/2.*

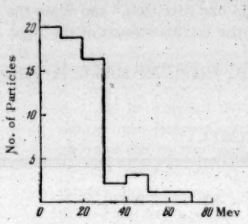

FIG. 4. Energy Distribution of Particles with Z > 2.

The great majority of the particles have energies less than the maximum electrostatic repulsion energy, which, for the particles considered, is about 30 Mev. Only very few particles are emitted with energies greater than this. Among these are four cases of the emission of Be^8 and one case of the emission of C^{12}. The analysis of the stars disclosed also very fast α particles having energies much higher than the Coulomb barrier of a heavy nucleus in the emulsion (30 α particles with energies greater than 60 Mev). Such α particles are easily distinguished from protons from the number of δ electrons in an equal region of the track. The α particle tracks had 5 — 7 δ electrons, the proton tracks 2 — 3 δ electrons. As has been shown earlier,[5,6] such cases of the emission of "higher than barrier" particles can hardly be explained as an evaporation from an excited nucleus. All the experimental data indicate that such particles arise in the primary interaction of the incident particle with the nucleus. However, the mechanism of their formation is still not clear.

ANGULAR DISTRIBUTION

From Fig. 5 it is evident that a considerable fraction of the heavy particles is emitted in the direction of motion of the incoming neutron. There are four times as many particles with Z > 2 in the forward hemisphere than in the backward one. An even greater anisotropy is observed for particles with Z > 4: out of 16 such particles, 15 go out into the forward hemisphere. Particles with one or two charges, however, have a significantly smaller anisotropy: only about twice as many of these are emitted in the forward hemisphere than in the backward one.

PRODUCTION CROSS-SECTIONS

The absolute cross-section for the emission of particles with charge Z > 2 was found, using the measured cross-section for star production, as determined in the same experiment. The number of neutrons passing through the photoemulsion during the time of irradiation was measured by counting the recoil protons with telescopes consisting of three proportional counters. The targets through which the neutron beam passed before impinging on the photographic plates were polyethlene and graphite. In order to determine the fraction in the beam of fast and slow neutrons of significantly different n—p scattering cross-sections, an absorber was placed before the third counter. This stopped the protons coming from neutrons having an energy less than 245 Mev.

*The energies calculated in these situations for the fragments agree satisfactorily with the values obtained for the same R, Z, and M in Ref. 8.

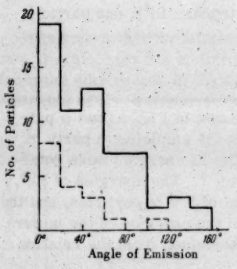

FIG. 5. Angular Distribution of Particles with Various Charges: Solid curve — Particles with $Z > 2$; dashed curve — Particles with $Z > 4$.

Using the values of the n–p scattering cross sections for the two energy groups, we found that a cross-section of $(0.43 \pm 0.2) \times 10^{-24}$ cm^2 for star production in the photographic plate for neutrons having the energy spectrum reported in Ref. 7. Using this value, the cross-section for the production of particles with $Z > 2$ was found to be $(2.8 \pm 1.4) \times 10^{-27}$ cm^2. The cross-sections for the emission Li^8 and Be^8 nuclei are $(0.8 \pm 0.4) \times 10^{-27}$ cm^2 and $(1.3 \pm 0.6) \times 10^{-27}$ cm^2 respectively.

The value of the cross section for the emission of Li^8 obtained here differs very little from the corresponding cross section found for the interaction of 340 Mev protons with carbon and nitrogen,[3] and from the cross section for the emission of Li^8 in the bombardment of the light nuclei of emulsion with 170 Mev protons.[1]

The authors are deeply grateful to V. B. Fliagin for help in carrying out this experiment.

[1] E. W. Titterton, Phil. Mag. **42**, 113 (1951).
[2] P. E. Hodgson, Phil. Mag. **42**, 207 (1951).
[3] S. C. Wright, Phys. Rev. **79**, 838 (1950).
[4] L. Marquez and I. Perlman, Phys. Rev. **80**, 953 (1951).
[5] D. H. Perkins, Proc. Roy. Soc. **203**, 399 (1950).
[6] S. O. C. Sörensen, Phil. Mag. **42**, 188 (1951).
[7] V. B. Fliagin, Report, Inst. for Nuclear Problems, Acad. of Sci., U.S.S.R. (1951).
[8] Freier, Lofgren, Ney, and Oppenheimer, Phys. Rev. **74**, 1818 (1948).
[9] E. Picup and Z. Voyvodic, Canad. Jour. Res. Sect. A, **28**, 616 (1950).
[10] J. P. Lonchamp, Jour. phys. et radium **14**, 433 (1953).
[11] E. W. Titterton, Nature **165**, 721 (1950).
[12] H. T. Richards, Phys. Rev. **59**, 796 (1941).
[13] Bennett, Banner, Richards, and Watt, Phys. Rev. **59**, 904 (1941).
[14] L. L. Green and W. M. Gibson, Proc. Phys. Soc. **A62**, 407 (1949).
[15] C. D. Moak and W. R. Wisseman, Phys. Rev. **101**, 1326 (1956).
[16] C. M. G. Lattes, Fowler, and Cüer, Proc. Phys. Soc. **A59**, 883 (1947).

Translated by A. Turkevich
244

SOVIET PHYSICS JETP VOLUME 6 (33), NUMBER 5 MAY, 1958

KNOCKOUT OF DEUTERONS FROM Li, Be, C, AND O NUCLEI BY PROTONS OF ENERGY 675 MEV*

L. S. AZHGIREI, I. K. VZOROV, V. P. ZRELOV, M. G. MESCHERIAKOV, B. S. NEGANOV, and A. F. SHABUDIN

Joint Institute for Nuclear Research, Academy of Sciences, U.S.S.R.

Submitted to JETP editor July 1, 1957

J. Exptl. Theoret. Phys. (U.S.S.R.) 33, 1185-1195 (November, 1957)

A study is made of the momentum spectra of charged particles emitted in the bombardment of deuterium, lithium, beryllium, carbon, and oxygen by 675-Mev protons. The investigation was carried out by the method of magnetic analysis at an angle of 7.6° to the proton beam. A group of deuterons of energy about 600 Mev is found to be emitted for all elements. In the case of deuterium the source of fast deuterons is elastic (p-d) scattering; in the remaining cases, deuterons are emitted in the reaction $p + (Z, A) \rightarrow d + p + (Z - 1, A - 2)$, which is proton scattering by quasi-deuteron groups inside the nuclei. With an accuracy of about 20%, the differential cross sections of this reaction are 2.9, 2.2, 3.7, and 4.6×10^{-27} cm^2/sterad for Li, Be, C, and O respectively. For the same nuclei, the mean energy of motion of the quasi-deuteron groups is evaluated at approximately 8, 11, 14, and 14 Mev. In the high momentum part of the spectra, no perceptible quantities of knocked out tritium nuclei have been detected.

The experiments that have been carried out show that in the passage of nucleons of a given energy through light nuclei, an essential role is played by the processes of three-particle interaction which are accompanied by large momentum transfer to the deuteron. The results obtained are in accord with the concept that underlies the high-momentum model of the nucleus.

1. INTRODUCTION

FROM the time of the early attempts to explain characteristics of the interaction of nucleons with nuclei at high energies (E > 100 Mev) one usually considers the process of the traversal of the nucleus by a nucleon as a series of successive collisions of the indicent nucleon with the individual nucleons located in its path. Such an approach to the problem of nucleon-nuclei interaction appears reasonable in the framework of the independent-particle model if the wavelength of the incident nucleon and the effective radius of the nucleon-nucleon interaction are small by comparison with the average distance between nucleons in the nucleus.

There is, however, reason to believe that the assumed existence of a cascade of two-particle collisions inside the nucleus give a rather rough approximation to reality. One should first mention that in the energy region from 100 to 1000 Mev the effective radius of the nucleon-nucleon interaction is only approximately one and one-half times less than the average distance between nucleons in densely packed nuclei. This circumstance by itself demonstrates that many-body interactions of nucleons in a cascade process are not rare. Nor should one overlook the fact that in the simplest form of the independent particle model the space correlation of nucleons inside the nucleus is not taken into account. Besides, as has been pointed out by Brueckner, Eden, and Francis,[1] the available experimental data show clearly that in a number of nuclear processes high-energy effects related to the space correlation of the nucleons play an appreciable role. Among these effects are the nuclear photoeffect, successfully described by the quasi-deuteron model of Levinger,[2] the absorption of mesons by nuclei, and the creation of mesons in nucleon-nuclei collision, the scattering of nucleons inside nuclei,[3-6] and also the capture of nucleons from nuclei by the incident nucleons with formation of deuterons.

*Communicated May 17, 1957 at the Second Session of the Scientific Council of the Joint Institute for Nuclear Research.

A particularly noteworthy feature of the last process, formed upon irradiation of different elements by neutrons and protons with energy of around 90 Mev,[7-10] is the emission of deuterons predominantly forward with energies only slightly less than the energy of the incident nucleon. The analysis of this process is based on the premise that the incident nucleon interacts simultaneously in the nucleus, only with one corresponding nucleon that moves approximately with the same momentum as that of the incident nucleon.[11] It was shown that the data obtained near 90 Mev on the angular distribution and yield of deuterons can be explained, at least qualitatively, by using for the nucleons in the nucleus a momentum distribution which extends much farther in the direction of large momenta than the distribution corresponding to the model of the Fermi gas of the non-interacting particles.[12,13] This corresponds to the admission that strong local interactions exist inside nuclei.

The formation of fast deuterons has also been observed under the action of 300-Mev protons and neutrons as the result of the capture of nucleons from nuclei not by directly-incident particles, but rather by relatively slow secondary nucleons which have undergone one or more collisions inside the nucleus.[14]

In this article some results are presented of experiments carried out with the aim of studying the collisions of protons with the tightly-bound strongly-interacting nucleons in the nuclei of Li, Be, C, and O at an energy of 675 Mev and particularly with quasi-deuteron groups. At the same time the results of another experiment on the observation of the elastic scattering of protons by free deuterons, at an energy of 675 Mev, is also presented. The comparison of data obtained under the same conditions on (p–d) elastic scattering, with the ejection of deuterons from light nuclei by protons, permits one to make definite conclusions on the character of the latter process. In the described experiment information was obtained concerning the following: (a) the momentum spectrum of the secondary charged particles emitted in p + Li, p + Be, and p + C collisions at 7.6 degrees relative to the beam of the primary protons; (b) the differential cross section of the processes of the direct ejection of deuterons from the nuclei, Li, Be, C, and O and also the differential cross section of elastic (p–d) scattering; (c) the average kinetic energy of the quasi-deuteron groups in the bombarded nuclei; (d) the upper limit of the value of the contribution of tritium nuclei in the yield of emitted deuterons.

2. METHOD OF INVESTIGATION

To detect the direct knockout of deuterons from light nuclei under the action of fast protons, we carried out experiments in which the momentum spectrum of the secondary particles was determined by the method of magnetic analysis. This method was already used by us in studying the momentum spectrum of the products of the reactions $p + p \rightarrow n + p + \pi^+$, $p + p \rightarrow p + p + \pi^0$, and $p + p \rightarrow d + \pi^+$ (Ref. 15). The placement of the analyzing magnet with poles of 100 cm diameter and with a 10-cm air gap relative to the primary beam and the concrete shield of the synchrocyclotron is shown on Fig. 1. The intensity H of the magnetic field in the gap of the magnet was measured by the method of nuclear absorption with an accuracy of 0.2% and remained constant within 0.2% with the help of an electronic stabilizer. The average radius of curvature, ρ, was 367.6 cm. The angle of deviation of the particles in the magnetic field was 19°.

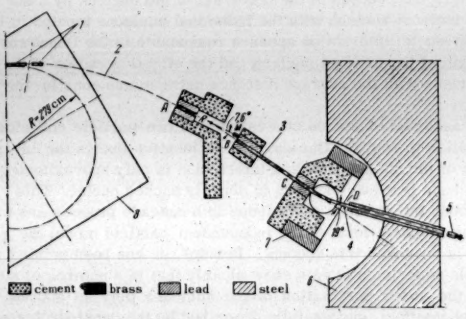

FIG. 1. Experimental setup: 1 — magnetic channel; 2 — proton beam; 3 — vacuum pipe; 4 — vacuum pump; 5 — telescope; 6 — shielding wall; 7 — magnet; 8 — synchrocyclotron chamber; R — target; M — monitor; A, B, C, D — collimators with slits 3 cm high and 1, 2, 3, and 1 cm wide, respectively.

A beam of unpolarized protons of 675 ± 6 Mev energy,* obtained from the 6-meter syn-

*This value of the average energy of the proton in the beam ejected in the atmosphere, after introducing several changes in the setup of the synchrocyclotron, was obtained in our laboratory by L. Soroko, O. Savchenko, and Iu. Akimov from measurements of the proton ranges in copper by a differential method.

chrocyclotron of the Joint Institute for Nuclear Research, was used in our experiment. The beam current at the location of the target was $\sim 3 \times 10^9$ protons/cm^2-sec. The intensity of the beam was controlled by an ionization chamber filled with helium. The brass collimator A determined the dimensions of the proton beam incident on the target. Alignment of the proton beam with the collimator A was attained by shifting the beam in the horizontal and vertical direction by means of an additional magnetic field made up of two movable steel bars, placed in the deflecting field of the accelerator at the point where the proton beam is ejected from the vacuum chamber. Secondary particles emitted from target R at an angle of 7.6° with respect to the primary beam, passed through collimators B and C, the analyzing field, and collimator D, and reached a telescope made up of four scintillation counters arranged for three and fourfold coincidence. The first three counters had as scintillators tolane crystals of dimensions 3×3, 2.5×2.5, and 4×4 cm, respectively, while the fourth counter had a liquid scintillator (a solution of terphenyl and phenylcyclohexane) of 10 cm diamter. The efficiency of the detection of the particles in the momentum interval investigated was approximately constant. The entire path of the particles from their entrance in collimator B until the telescope was in vacuum. Collimator D was used to decrease the importance of effects connected with the scattering and the slowing down of the particles in the walls of collimators B and C. Because of the high level of the irradiation near the synchrocyclotron, it was impossible to separate the beam of secondary particles ahead of the analyzing magnet by means of an array of scintillation counters.

TABLE I

Target	Height, cm	Width, cm	Thickness (g/cm^2)	ΔE, Mev	$\overline{\langle\theta^2\rangle^{1/2}}$, degree.
H_2O	6.0	1.5	1.18	2.78	0.18
D_2O	6.0	1.5	1.30	2.78	0.18
Li	2.5	1.0	1.11	2.30	0.08
Be	2.5	1.0	3.16	6.50	0.18
C	2.5	1.0	3.37	7.52	0.21

Chemically pure targets of Li, Be, and C were used. The elastic (p–d) scattering was observed from the difference in the effects with targets of D_2O (99.93% pure) and H_2O, poured in thin-walled aluminum containers. A target of H_2O was used in the observation on the direct knockout of deuterons from oxygen nuclei. The dimensions of the targets, and also the energy losses and the average angle of multiple scattering of 675-Mev protons in the targets, are displayed in Table I.

The resolving power $\Delta p/p$ of the spectrometer was approximately 3% for the targets used with the dimensions shown and for secondary-particle beam angle of $\sim 0.3°$.

3. ANALYSIS OF THE MEASUREMENT RESULTS

The ordinates of the momentum spectra were computed by dividing $H\rho$ into the number of coincidences corresponding to one and the same number of protons passing through the target. The background in the absence of a target was less than 2%. Upon computing the spectra, corrections were introduced as follows:

1. The absorption of secondary protons and deuterons in the target, in the scintillators, and in the foils covering the entrance and the exist of the vacuum pipe. This correction was at most 4%.

2. Counting errors in the detecting setup. This correction reached an appreciable value only in the narrow region where the peaks of the diffraction scattering of protons were located. When measuring the spectra in this region, the intensity of the beam was decreased sufficiently to keep the counting error below 10%.

The distortion of the forms of the spectra, due to variation of the angle of multiple scattering in the momentum interval examined and to the energy losses of the secondary particles in the target, was within the limits of experimental error.

In order to obtain the absolute value of the differential cross section $d^2\sigma/d\omega\,dp$, separate direct measurements were made of the cross section $d\sigma/d\omega$ of the emission of secondary charged particles with $H\rho > 1100 \times 10^3$ gauss-cm from p + Be and p + C collisions. The area under the curve representing spectra of charged particles with $H\rho > 1100 \times 10^3$ gauss-cm, were normalized to the corresponding experimental value $d\sigma/d\omega$. The accuracy of this procedure was approximately 20%. The ordinate of the spectra obtained with lithium and oxygen were determined by comparison with the yield of the secondary particles from these elements and carbon, and by the use of the known cross section for carbon. The same method was used to compute the ordinates of the peak corresponding to deuteron emissions in elastic (p–d) scattering at an angle of 7.6°.

4. EXPERIMENTAL RESULTS AND THEIR INTERPRETATION

The momentum spectra of the secondary particles from lithium, beryllium, and carbon for the interval from 3600×10^3 to 6200×10^3 gauss-cm are presented on Figs. 2, 3, and 4 together with the statistical errors of the measurements. The section of each spectrum from 4000×10^3 to 4500×10^3 gauss-cm consists of an intense peak, corresponding to protons diffraction-scattered by nuclei, and a closely adjoining projection to the left, corresponding to the lower part of the momentum distribution of the protons from the quasi-elastic scattering by nucleons inside the nucleus. In the case of elastic scattering of 675-Mev protons by nuclei of lithium, beryllium, and carbon, the diffraction peaks should be located at 4355×10^3, 4360×10^3, and 4370×10^3 gauss-cm respectively, while the peak corresponding to protons from elastic (p–d) scattering should be at 4300×10^3 gauss-cm. The experimentally-observed positions of the diffraction peaks differ by less than 0.5% from the computed values. The appearance of the spectra indicates that under the conditions of these experiments the emission of secondary protons is due chiefly to diffraction scattering by the nuclei.

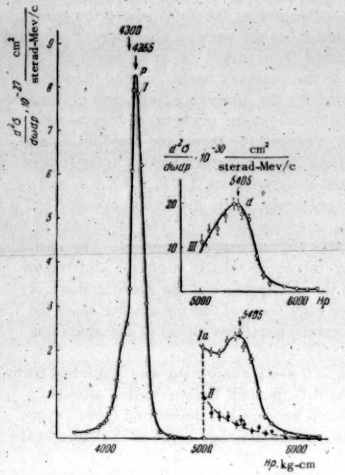

FIG. 2. Momentum spectrum of the secondary charged particles from (p + Li) collisions at an angle of 7.6°. I and Ia — total spectrum of secondary charged particles; II — proton spectrum (the ordinates of Ia and II represent $d^2\sigma/d\omega\,dp$ magnified 100 times); III — spectrum of particles stopped in the absorber.

The experiments in which deuterons were knocked out directly from light nuclei by 675-Mev protons were preceded by the observation of the deuteron yield from elastic (p–d) scattering at an angle of 7.6°. Figure 5 shows part of the spectrum of secondary particles from the (p–d) collision corresponding to this process. The distinct peak observed at 5405×10^3 gauss-cm is due to the recoil deuterons from elastic (p–d) collisions. The shape of this peak represents the experimental resolution curve of the spectrometer. The half width of this peak is approximately 150×10^3 gauss-cm. The value of the differential cross section of the elastic (p-d) scattering with emission of a deuteron at 7.6° to the primary beam is found to be $(0.55 \pm 0.12) \times 10^{-27}$ cm^2/sterad.*

Bearing in mind the results of the experiment on the elastic (p–d) scattering, we measured carefully the momentum spectra in the interval from 5000×10^3 to 6200×10^3 gauss-cm. The experiment was carried out with lithium, beryllium, carbon, and oxygen under an 18-cm copper absorber, sufficiently thick to stop the ejected deuterons completely, placed ahead of the fourth counter. The number of particles stopped by the absorber was obtained from the difference between the number of three and four-fold coincidences. At the same time, experimentally-determined corrections were introduced for the absorption and the scattering of the protons in the absorber and in the scintillators. The four-fold coincidences with absorber to the right of the diffraction peak, are due to diffraction-scattered protons subjected to additional scattering along their path in the spectrometer.

The observed results are shown in Figs. 2 – 4 and 6. In the momentum interval studied the ordinates of the spectra are magnified 100 times compared with the ordinates of the remaining part of the spectrum. Well resolved peaks near 5400×10^3 gauss-cm are observed on the spectra of the secondary particles from lithium and beryllium. In the same region of the carbon and oxygen spectra one notices characteristic tails to the right of the diffraction peak. No peculiarities were remarked in the spectra of the particles passing through the copper absorber. The experimentally observed spectra of the particles stopped in the absorber involved in all cases peaks with maxima around 5350×10^3, 5250×10^3, and 5230×10^3 gauss-cm for lithium, beryllium, carbon, and oxygen respectively.

*Results of experiments on the study of (p–d) collisions at an angle of 7.6° will be discussed in another communication.

From the spectra obtained by us it follows that 675-Mev protons interact with light nuclei to cause, with appreciable probability, emission of particles whose momentum is greater than the momentum of the protons diffraction-scattered by the nuclei. The momenta transferred to such particles are grouped around

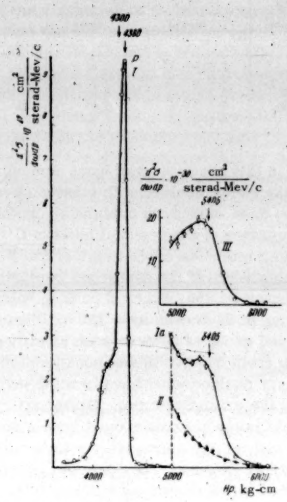

FIG. 3. Momentum spectrum of the secondary charged particles from (p + Be) collisions at an angle of 7.6°. I and Ia — total spectra of the secondary charged particles; II — proton spectrum (the ordinates of Ia and II represent $d^2\sigma/d\omega\,dp$ magnified 100 times); III — spectrum of the particles stopped in the absorber.

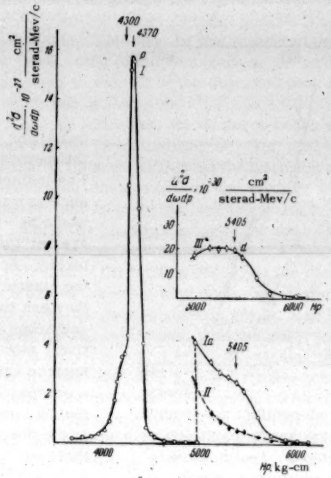

FIG. 4. Momentum spectrum of the secondary charged particles from (p + C) collisions at an angle of 7.6°. I and Ia — total spectrum of secondary charged particles; II — proton spectrum (the ordinates of Ia and II represent $d^2\sigma/d\omega\,dp$ magnified 100 times); III — spectrum of the particles stopped in the absorber.

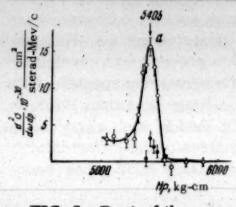

FIG. 5. Part of the momentum spectrum of secondary charged particles from (p + d) collisions with the peak of the elastically-scattered deuterons. ○ — results of measurements without absorber to stop the recoil deuterons; ● — the same with absorber.

values that are only slightly smaller than the momentum of the deuteron emitted in elastic (p–d) scattering. Like the recoil deuterons from elastic (p–d) scattering, the observed group of particles is completely stopped in 18 cm of copper. Under the conditions of these experiments, in the momentum region $H\rho > 5000 \times 10^3$ gauss-cm the only particles heavier than protons that could penetrate were deuterons and tritium nuclei. The latter could be emitted by quasi-elastic collision of the incident proton with a group of three strongly interacting nucleons and would have a momentum of approximately 6000×10^3 gauss-cm, which is appreciably greater than the momentum of the particles in the observed peaks.

The above experimental results evidence that 675-Mev protons sometimes knock out deuterons from light nuclei. This process is kinematically very similar to elastic (p–d) scattering. From the presence of such a correspondence between the two processes one can conclude that deuterons are knocked out as the result of almost elastic collision between the incident protons and quasi-deuteron groups inside the nuclei.

It should be emphasized that the observed group of deuterons could not result from capture of neutrons within the nuclei by the incident protons, i.e., in reactions of the type $p + (Z, A) \rightarrow d + (Z, A - 1)$. Indeed, the

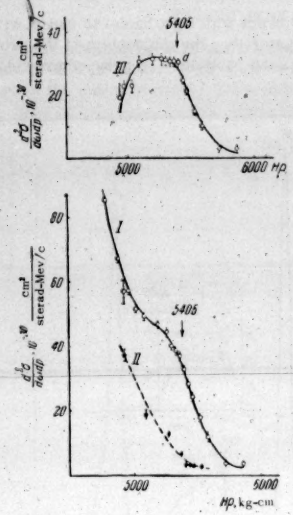

FIG. 6. Momentum spectrum of the secondary charged particles from (p+O) collisions. I — total spectrum of the secondary charged particles; II — proton spectrum; III — spectrum of the particles stopped in the absorber.

TABLE II

Element	$\left(\frac{d\sigma}{d\omega}\right)_t$, 10^{-27} cm²/sterad	$\left(\frac{d\sigma}{d\omega}\right)_d$, 10^{-27} cm²/sterad	$\left(\frac{d\sigma}{d\omega}\right)_d / Z$, 10^{-27} cm²/sterad	ΔE, Mev	Binding energy of the Deuteron, Mev
D	—	0.55±0.12	0.55	—	—
Li	—	2.9 ±0.6	0.97	10	9.5
Be	590±30	2.2 ±0.5	0.55	23	16.7
C	900±50	3.7 ±0.8	0.61	30	25.2
O	—	4.6 ±1.0	0.58	33	20.7

deuterons emitted in this process must have momenta greater than the momentum of the recoil deuterons in elastic (p–d) scattering. For instance, in the case of neutron capture by protons in the C^{12} nucleus without excitation of the residual nucleus C^{11}, deuterons would be emitted with momenta approximately 225×10^3 gauss-cm greater than the momentum of the deuterons in elastic (p–d) scattering. Actually, however, the observed peak is below the peak of the elastic scattering of deuterons by $\sim 150 \times 10^3$ gauss-cm. Neither can the observed group of deuterons be identified with the deuterons resulting from capture of nucleons from nuclei by relatively slow secondary nucleons that have become involved in the nuclear cascade by the primary proton. Deuterons emitted in such a process of indirect nucleon capture must have a smeared momentum spectrum without any correlation with the deuteron peak in the elastic (p–d) scattering. The observed peaks cannot furthermore be assigned to the deuterons formed in the reactions $p + p \rightarrow d + \pi^+$ and $p + n \rightarrow d + \pi^0$, which possibly take place inside the nuclei. The deuterons corresponding to these reactions would have to have momenta not more than 4560×10^3 gauss-cm, which is approximately 800×10^3 gauss-cm less than the studied region of the momentum spectrum. Finally, by virtue of the principle of detailed balance, one would expect to observe the production of deuterons in the reaction $p + n \rightarrow d + \gamma$, the inverse of the photodisintegration of the quasi-deuteron group in the nuclei. At an angle of observation of 7.6° and at a proton energy of 675 Mev, deuterons in this reaction must be emitted with momenta not greater than 4690×10^3 gauss-cm, which is almost 500×10^3 guass-cm lower than the observed region of the spectrum.

One can say thus that the peaks observed at the upper limits of the momentum spectra correspond actually only to deuterons ejected from nuclei by collision of protons with quasi-deuteron groups. An approximate estimate of the absolute magnitude of the differential cross section of this process was carried out by comparison of the areas, on one hand, under the diffraction and quasi-elastic scattering spectra of the protons and on the other hand under the peaks corresponding to particles with a range less than 18 cm in copper. The numerical values of the differential cross sections $(d\sigma/d\omega)_d$ obtained in such a way for the knock-out of deuterons are given in Table II, together with the corresponding values of the differential scattering $(d\sigma/d\omega)_t$ for the emission of secondary charged particles with $H\rho > 1100 \times 10^3$ gauss-cm from p + Be and p + C collisions.

In the case of Li, Be, and C the spectra were measured up to $H\rho = 6200 \times 10^3$ gauss-cm, which includes the region in which one would expect the occurrence of groups of tritons ejected from the nuclei. A study of the high-momentum component of the spectra showed that if the ejection of tritons from the nuclei occurred at all under the conditions of this experiment, their yield constituted less than 2 to 3% of the deuteron yield.

5. ANALYSIS OF THE DEUTERON PEAKS

A distinguishing feature of the spectra obtained is that the peaks corresponding to the ejected deuterons are appreciably wider than the peak observed in the case of the elastic (p–d) scattering. This difference

apparently results to a large extent from the momentum distribution of the quasi-deuteron groups inside the nuclei. The average kinetic energy of the quasi-deuteron groups in the nuclei can be estimated from data on the widths of the experimental peaks and from the resolution curve of the spectrometer, assuming the effect of the scattering of the deuterons as they leave the nuclei to be small. Simple computations have shown that the average kinetic energies of the quasi-deuteron groups are approximately 8, 11, 14, and 14 Mev for Li, Be, C, and O respectively.

The observed peaks are not clearly resolved on the left side. This may be due in part to energy loss of the protons and deuterons in the nuclei and in part to the slowing of the deuterons in the walls of the collimators. Nor can one exclude the possibility that adjacent to the left of the observed peak are smeared deuteron peaks from the possible reactions $p + p \rightarrow d + \pi^+$ and $p + n \rightarrow d + \pi^0$.

The experiment has demonstrated that in the spectra of light elements, the deuteron peaks are shifted slightly to the left of the peaks due to the deuterons from elastic (p–d) scattering. The next to the last column of Table II lists the difference between the energy of elastically-scattered deuterons and the average energy of the deuterons ejected from nuclei corresponding to the observed shift, while the binding energy of the deuterons in the nuclei is given in the last column of Table II. This difference represents principally the binding energy of the deuteron in the potential well due to the remaining nucleons. If the proton, after colliding with the quasi-deuteron group, also leaves the nucleus without further collisions, then the observed process can be envisioned as a reaction of the type $p + (Z, A) \rightarrow d + p + (Z - 1, A - 2)$. According to the data obtained, the recoil energy and the excitation of the residual nucleus $(Z - 1, A - 2)$ must not be large.

TABLE III

Nucleus	Li	Be	C	O
σ_d, 10^{-27} cm^2	~4.5	~6	~9	~12
σ_t, 10^{-27} cm^2	—	272±7	340±10	416±30

It is necessary to mention that the scattering of protons from quasi-deuteron groups with transfer of high momenta to the deuteron represents basically a process connected with three-particle interactions. For a given angle, the cross section of this process, as seen from Table II, increases with increasing dimension of the nuclear target. Normalized to one proton in the nucleus, the differential cross section for the ejection of a deuteron does not differ strongly from the cross section for elastic (p–d) scattering, observed under the same conditions. This fact apparently means that the character of the three-particle interaction is the same both in the collisions of protons with quasi-deuteron groups in light nuclei and in collisions of protons with free deuterons. Such a situation seems possible only if the other nucleons within the nucleus do not participate effectively in the interaction between the incident proton and the tight quasi-deuteron group.

The total cross section for the ejection of deuterons from the nuclei was estimated by assuming that the angular distributions of the recoil deuterons in elastic (p–d) collisions and in collisions of protons with quasi-deuteron groups are the same. The angular distribution of the cross section for elastic (p–d) scattering at an energy of 660 Mev was measured in our laboratory by Leksin[16] in the interval 40 — 150° in the proton-deuteron center-of-mass system. From these data it was estimated that the total cross section of elastic (p–d) scattering is approximately 1.5×10^{-27} cm^2. From this, assuming that the yield of deuterons is proportional to Z, we determined the total cross sections σ_d for the ejection of deuterons. Their values are listed in Table III. For comparison, this table contains also the values of the total cross section σ_t for the interaction of protons with the nuclei of the elements mentioned at an energy of 650 Mev.[17] The contribution of the three-nucleon collisions to the total cross section for the interaction of the protons with the nuclei must apparently be even greater because of the collisions between the protons and quasi pp and nn groups and also with pn groups in states other than $^3S_1$ and $^3D_1$.

6. CONCLUSION

The experiments carried out show that bombardment of Li, Be, C, and O by 675-Mev protons results with appreciable probability, in emission of deuterons with almost the same momentum as in elastic (p–d) scattering. Such a close relation between the processes named leads to the assumption that the deuterons are knocked out from light nuclei by collision of the incident protons with quasi-deuteron groups. Examination of the broadening of the deuteron peaks shows that the average kinetic energy of the quasi-deuteron groups in the potential well of the remaining nucleons in the nuclei is approximately 8, 11, 14, and 14 Mev for Li, Be, C, and O respectively. As suspected, the average kinetic energies of the quasi-deuteron groups

are less in lithium nuclei than in the nuclei of the other elements investigated. A similar result was obtained in Massachusetts[18] upon investigation of the photodisintegration of quasi-deuteron groups. From a comparison of the differential cross section of elastic scattering of protons by free deuterons and by quasi-deuteron groups, it follows that the character of the three-nucleon interactions in free (p-d) collisions and in collision of protons with quasi-deuteron groups do not differ in any noticeable way. If under the condition of these experiments, any tritons were knocked out at all by collisions between protons and tight three-nucleon groups, the yield of tritons comprised less than 2 to 3% of the yield of the ejected deuterons.

The results of these experiments can be considered as an important argument in favor of the nuclear model proposed by Brueckner and his colleagues[19-21] and recently analyzed by Bethe.[22] This model is based on the assumption that in nuclear matter strong short-range interactions exist between pairs of nucleons, in consequence of which the wave function of the ground state of the nucleus contains an appreciable admixture components corresponding to large momenta of individual nucleons. This is equivalent to assuming an appreciable correlation in the locations of the nucleons inside the nuclei or, in other words, to assuming short-lived formations of two or more strongly-interacting nucleons.

Within the framework of the high-momentum model of the nucleus, the ejection of deuterons from nuclei by high-energy protons can be considered either as the result of transfer of high momentum to the tight two-nucleon groups as a whole, or as the capture of a neutron from such a group with the formation of a deuteron emitted forward. The fact that the ejected particles do not include many tritons is apparent evidence of the relatively rare event whereby a three-nucleon group, capable of undergoing recoil as a whole, is formed inside the nucleus. An analogous result follows from the high-momentum model of the nucleus.[21,22]

The problem of the transfer of high energy from the incident nucleon to the nuclear fragment was investigated by Blokhintsev[23] under the assumption that short-lived tight clusters of nucleons, which can be ejected from nuclei in the form of separate particles upon collision with nucleons are formed inside the nuclei. Calculations based on such a picture show the dependence of the cross section for ejection of energetic deuterons on the atomic number and on the atomic weight of the nucleus to be of the form $Z^2A^{-1/3}$ for nuclei containing few nucleons, and of the form $ZA^{-1/3}$ for nuclei in which the effect of saturation of nuclear forces is already substantial. The probability of emission of tritons comprises only several percent of the yield of deuterons, which is not in disagreement with experiment. The absolute value of the cross section also appears to be in agreement with the results of these measurements.

It is impossible to say anything definite at this time on the nature of the forces acting between the incident proton and the quasi-deuteron group. At a given energy, the wavelength of the proton, in the center-of-mass system of the two nucleons is $\lambda = 0.35 \times 10^{-13}$ cm, which is only 1.7 times greater than the Compton wavelength of the nucleon, $\hbar/Mc$. The possibility is not excluded that such tight collisions of protons with quasi-deuteron groups are accompanied by a strong deformation of the meson cloud of the three colliding nucleons, and by an interaction which occurs through the simultaneous exchange of pairs of π mesons. From this point of view, the high-energy collisions of nucleons with quasi-deuteron groups, like three-body collisions appear as favorable for the observation of effects connected with three-body forces and therefore warrant further investigation.

In conclusion the authors express their thanks to D. I. Blokhintsev, G. A. Leksin, and V. I. Ogievets for discussions, and also to Iu. N. Denisov for help in the measurements of the magnetic field of the spectrometer.

[1] Brueckner, Eden, and Francis, Phys. Rev. 98, 1445 (1955).
[2] J. Levinger, Phys. Rev. 84, 43 (1951).
[3] Claidis, Hess, and Moyer, Phys. Rev. 87, 425 (1952).
[4] J. Wilcox and B. Moyer, Phys. Rev. 99, 875 (1955).
[5] P. Cüer and J. Combe, J. Phys. et radium 16, 298 (1955).
[6] McEwen, Gibson, and Duke, Phil. Mag. 2, 231 (1957).
[7] H. York, Phys. Rev. 75, 1467 (1949).
[8] K. Brueckner and W. Powell, Phys. Rev. 75, 1247 (1949).
[9] J. Hadley and H. York, Phys. Rev. 80, 345 (1950).
[10] W. Selove, Phys. Rev. 92, 1328 (1953); 101, 231 (1956).
[11] Cüer, Morand, and Van Roxsum, Compt. rend. 228, 481 (1949).

[12] G. Chew and M. Goldberger, Phys. Rev. 77, 470 (1950).
[13] J. Heidman, Phys. Rev. 80, 171 (1950).
[14] W. Hess and B. Moyer, Phys. Rev. 101, 337 (1956).
[15] Mescheriakov, Neganov, Vzorov, Zrelov, and Shabudin, Dokl. Akad. Nauk SSSR 109, 449 (1956), Soviet Phys. "Doklady" 1, 447 (1956).
[16] G. A. Leksin, J. Exptl. Theoret. Phys. (U.S.S.R.) 32, 440 (1957), Soviet Phys. JETP 5, 371 (1957).
[17] V. Moskalev and B. Gavrilovskii, Dokl. Akad. Nauk SSSR 110, 972 (1956), Soviet Phys. "Doklady" 1, 607 (1956).
[18] Wattenberg, Odian, Stein, Wilson, and Weinstein, Phys. Rev. 104, 1710 (1956).
[19] K. Brueckner and C. Levinson, Phys. Rev. 97, 1344 (1955).
[20] K. Brueckner, Phys. Rev. 97, 1353 (1955).
[21] K. Brueckner, Phys. Rev. 100, 36 (1955).
[22] H. Bethe, Phys. Rev. 103, 1354 (1956).
[23] D. Blokhintsev, J. Exptl. Theoret. Phys. (U.S.S.R.) 33, 1295 (1957), Soviet Phys. JETP, this issue, p. 995.

Translated by Fay Ajzenberg-Selove
245

SOVIET PHYSICS JETP VOLUME 6 (33), NUMBER 5 MAY, 1958

*A GROUP-THEORETICAL CONSIDERATION OF THE BASIS OF RELATIVISTIC QUANTUM MECHANICS. II. CLASSIFICATION OF THE IRREDUCIBLE REPRESENTATIONS OF THE INHOMOGENEOUS LORENTZ GROUP**

Iu. M. SHIROKOV

Moscow State University

Submitted to JETP editor December, 11, 1956

J. Exptl. Theoret. Phys. (U.S.S.R.) 33, 1196-1207 (November, 1957)

A classification is obtained for the states of a relativistic quantum system. The irreducible representations of the inhomogeneous Lorentz group are divided into four fundamental classes: P_m, P_Π, P_0, O_0. All the representations of classes P_m and P_Π, both unitrary and non-unitary, are found explicitly.

1. CLASSIFICATION OF THE STATES OF A RELATIVISTIC QUANTUM SYSTEM

WE have previously[1] found all the possible invariants of the inhomogeneous Lorentz group, and have noted that the classification of the irreducible representations of the group reduces to finding the eigenvalue spectra of these invariants. However, we as yet do not know the independent variables contained in the wave functions, which transform according to a particular irreducible representation. In order to find these variables and their domain of variation, we must select from among the operators of the group a complete set, i.e., a complete system of operators which commute with one another (but not with all the operators of the group). The choice of such a system of operators is, of course, not unique. This non-

*Notations used without explanation are the same as in Ref. 1. References like (I.8) are to the corresponding formula in Ref. 1.

uniqueness corresponds to the possibility of performing an equivalence transformation of type (I.8) on the particular representation. As such a system of operators, we might select the invariants of the homogeneous Lorentz group, $M_{\mu\nu}^2$ and $\epsilon_{\mu\nu\lambda\sigma}M_{\mu\nu}M_{\lambda\sigma}$, and in addition the square of the three-dimensional angular momentum M_i^2 and one of its projections, M_3. However, this classification is not convenient since it is not translationally invariant. The motion of the system as a whole is not separated out, so that the wave functions of individual states do not belong to a single value of energy and momentum. The most natural classification is one which is translationally invariant, in which the complete set selected consists of the four operators p_μ and one of the projections of Γ_σ, for example Γ_3. In a given irreducible representation, only three of the four operators p_μ are independent, since the eigenvalue of the invariant p_μ^2 is the same for all the functions of the irreducible representation. The set of eigenvalue spectra of the operators of the complete set (for example, p_1, p_2, p_3, Γ_3) also give us the complete system of independent variables and their domain of variation for the particular irreducible representation.

Let us summarize our results:

1. In order to find all the irreducible representations of the inhomogeneous Lorentz group, i.e., all the wave functions admissible in quantum mechanics, we must find the eigenvalues and simultaneous eigenfunctions of the operators p_1, p_2, p_3, p_0, Γ_σ^2, Γ_3, satisfying relations (I.41).

2. In a given irreducible representation, only those eigenfunctions can appear which belong to the same eigenvalues of the group invariants p_λ^2 and Γ_σ^2. As mentioned in Sec. 12 of Ref. 1, additional invariants may exist for certain classes of representations.

2. THE FOUR FUNDAMENTAL CLASSES OF REPRESENTATIONS OF THE GROUP G

The group of four-dimensional translations characterized by the operator p_μ is a commutative subgroup of the inhomogeneous Lorentz group. Its irreducible representations are one-dimensional and unitary.* Each representation is defined by the set of four numbers p_1, p_2, p_3, $p_0 = p_4/i$, which are eigenvalues of the operators $\hat{p}_1$, $\hat{p}_2$, $\hat{p}_3$, $\hat{p}_0$. The eigenvalues p_μ can be any real numbers. Only those functions can belong to the same irreducible representation of G which have the same value of p_μ^2. The irreducible representations of the whole group differ qualitatively from one another according as p_μ^2 is a negative number (timelike p_μ), positive (spacelike p_μ), or zero. In the last case, representations in which $p_\mu \neq 0$ (p_μ lies on the light cone) and in which $p_\mu = 0$ are qualitatively different. Accordingly, we get four classes of representations of the group G, which we shall investigate in turn:

I. Class P_m: p_μ is a timelike vector.

II. Class P_0: p_μ is a vector on the light cone.

III. Class P_Π: p_μ is a spacelike vector.

IV. Class O_0: $p_\mu = 0$.

For the unitary representations of the inhomogeneous Lorentz group, the division of the representations into these four classes was first done by Wigner by a different method. He also obtained the detailed classification of the unitary representations of classes P_m and P_0.[2] The complete system of irreducible representations of class O_0 coincides with the complete system of representations of the homogeneous Lorentz group which was found by Gel'fand and Naimark.[3]

3. CLASS P_m

For the class P_m, the sign of the energy, $S_H = p_0/|p_0|$, is an invariant of the group, so that for each set of eigenvalues of p_μ^2 and Γ_σ^2 there will be not one, but two irreducible representations, one for each sign of the energy. Instead of the energy, it is convenient to use the mass m defined as

$$m = (p_0/|p_0|)\sqrt{-p_\mu^2}, \tag{1}$$

*The group of translations also has non-unitary representations, corresponding to complex values of the components of the four-momentum. The representations of the inhomogeneous Lorentz group obtained from them belong to complex values of the invariants m and Π of the classes P_m and P_Π. Representations of this sort occur, for example, when we add an imaginary term to the mass in calculations with Green's functions.

and can be any real number except zero (since zero mass corresponds to classes P_0 and O_0). In each irreducible representation, only those functions can appear which belong to the same value of m. Therefore, of the four variables p_μ in the wave functions of the irreducible representation, only three (for example, p_1, p_2, p_3) will be independent, while the fourth, p_0, will be equal to

$$p_0 = \frac{m}{|m|} E_p \equiv \frac{m}{|m|} \sqrt{\mathbf{p}^2 + m^2}. \tag{2}$$

One can also proceed differently, by forming the 4-velocity vector

$$u_\mu = p_\mu / m, \; u_\mu^2 = -1, \; u_0 = u_4 / i = \sqrt{\mathbf{u}^2 + 1}. \tag{3}$$

In this case, for each value of m the functions of the irreducible representation will depend on the 4-velocity u_μ, which has three independent components.

To find the eigenvalues of Γ_σ^2, it is convenient to go over (for fixed p_μ, which is permissible since p_μ commutes with Γ_σ) to the rest frame in which

$$\mathbf{p} = 0, \; p_4 = im, \tag{4}$$

We then find from (I.39), (I.41) that

$$\Gamma_4 = 0, \; \Gamma_0^2 = \Gamma_i^2, \; [\Gamma_i, \; \Gamma_j]_- = im\varepsilon_{ijk}\Gamma_k. \tag{5}$$

Defining S_i by

$$\Gamma_i = mS_i, \tag{6}$$

we have

$$[S_i, \; S_j]_- = i\varepsilon_{ijk}S_k. \tag{7}$$

The commutators (7) define a three-dimensional Euclidean group of rotations, which is natural since $\Gamma_\sigma^2 = m^2 S_i^2$ represents the intrinsic angular momentum of the system. The irreducible representations of the three-dimensional rotation group are well known. All of them are unitary. Each is characterized by a positive integer or half-integer s, where

$$S^2\Omega_s = (\Gamma_0^2 / m^2)\,\Omega_s = s(s+1)\,\Omega_s, \tag{8}$$

and the operators S_i are $(2s+1)$-row matrices. For example, for $s = \frac{1}{2}$, $\mathbf{S} = \boldsymbol{\sigma}/2$, where $\boldsymbol{\sigma}$ is the Pauli matrix vector. The explicit form of the vector Γ_σ in an arbitrary coordinate system is obtained from (6) by Lorentz transformation:

$$\Gamma = m\mathbf{S} + \mathbf{p}(\mathbf{pS})/(|p_0| + m) = m\{\mathbf{S} + \mathbf{u}(\mathbf{uS})/(u_0 + 1)\}, \quad \Gamma_0 = \Gamma_4 / i = \mathbf{pS} = m\mathbf{uS}. \tag{9}$$

The commutation relations between the components Γ_σ, as defined by (7) and (9), coincide with (I.41).

For a complete description of the representation, we have only to find the explicit form of the operator g_μ. One can verify directly that the operator $g_\mu = (\mathbf{g}, ig_0)$, where

$$g_i = -(ip_i p_l \partial/\partial p_l) - (im^2\partial/\partial p_i) - 3ip_i + \varepsilon_{ijk}p_j S_k, \quad g_0 = (-ip_0 p_l \partial/\partial p_l) - 3ip_0 \tag{10}$$

satisfies the commutation relations (I.41).

By using (I.40), we can find from (9) and (10) the explicit form of the operator $M_{\mu\nu}$ for the 4-angular momentum:

$$\mathbf{M} = -i[\mathbf{p}\,\partial/\partial\mathbf{p}] + \mathbf{S} = -i[\mathbf{u}\,\partial/\partial\mathbf{u}] + \mathbf{S}, \; \mathbf{N} = ip_0\frac{\partial}{\partial\mathbf{p}} - \frac{[\mathbf{Sp}]}{p_0 + m} = iu_0\frac{\partial}{\partial\mathbf{u}} - \frac{[\mathbf{Su}]}{u_0 + 1}, \tag{11}$$

where $M_1 = M_{23}$ etc., $N_1 = M_{14}/i$. The square brackets denote the vector product. In this representation, the 4-momentum operator $\hat{p}_\mu$ has the form

$$\hat{p}_i = p_i, \; \hat{p}_0 = (m/|m|)\sqrt{\mathbf{p}^2 + m^2}, \text{ or } \hat{p}_\mu = mu_\mu. \tag{12}$$

Relations (11) were first used in the theory of elementary particles in Ref. 4.

Thus the irreducible representations of type P_m with timelike 4-momentum are characterized by two numbers: a real number m which is non-zero, and s which is integral or half-integral. The number m determines the rest mass of the system, and s its intrinsic angular momentum (i.e., the spin, in the case of an elementary particle). The wave functions $\Omega_{ms}(p_i)$ [or $\Omega_{ms}(u_i)$] corresponding to a par-

ticular representation are matrices of degree $2s + 1$, depending on three independent variables p_i defined over the whole real axis.

The probability density $\Omega^*_{ms}\Omega_{ms}$ is a scalar. In calculating mean values (or norms), the integration is carried out with respect to the invariant volume element

$$d_0 p = d^3p / |p_0| \quad \text{or} \quad d_0 u = d^3u / u_0,$$

$$\langle \Omega^* (p)\, \Omega (p) \rangle = \int d_0 p \Omega^* (p)\, \Omega (p), \tag{13}$$

$$\langle \Omega^* (u)\, \Omega (u) \rangle = \int d_0 u \Omega^* (u)\, \Omega (u). \tag{14}$$

We shall assign representations corresponding to positive and negative masses to different subclasses, and denote them by P_{+m} and P_{-m} respectively. Single-valued representations, corresponding to integer s, will be denoted by P^s_{+m} (P^s_{-m}), and two-valued representations with half-integer s by P'^s_{+m} (P'^s_{-m}). The results found for the classification of P_m coincide with Wigner's[2] results, and can be summarized in the following table:

Table of Representations of Class P_m

Representation	Unitarity Dimensionality in the spin variable	Fundamental invariants $m^2 = -p^2_\mu > 0$, $\Gamma^2_\sigma / m^2 = s(s+1)$, $s = \ldots$	Additional invariants, S_Π
P^s_{+m}	Unitary, finite-dimensional	0, 1, 2, ...	1
P'^s_{+m}	"	1/2, 3/2, ...	1
P^s_{-m}	"	0, 1, 2, ...	−1
P'^s_{-m}	"	1/2, 3/2 ...	−1

4. CLASS P_Π

For the class P_Π, the square of the 4-momentum

$$p^2_\mu = \Pi^2 \tag{15}$$

is positive, i.e., the vector p_μ is spacelike. The search for simultaneous eigenfunctions of the operators p_μ, Γ^2_σ, and one of the projections of Γ_σ, for example $\Gamma_0 = \Gamma_{4/1}$, is conveniently done in the coordinate system in which

$$p_\mu = (0,\ 0,\ \Pi,\ 0). \tag{16}$$

From (I.39) and (16) we find that in this coordinate system

$$\Gamma_3 = 0. \tag{17}$$

With the notation

$$\Gamma_1 + i\Gamma_2 = \Pi T^+,\ \Gamma_1 - i\Gamma_2 = \Pi T^-,\ \Gamma_0 = \Pi T_0 \tag{18}$$

the commutation relations (I.41) between the components Γ_σ, and the invariant Γ^2_σ become

$$[T^+,\ T_0]_- = -T^+,\ [T^-,\ T_0]_- = T^-, \tag{19}$$

$$[T^+,\ T^-]_- = -2T_0, \tag{20}$$

$$\Gamma^2_\sigma / \Pi^2 \equiv T^2 = T^- T^+ - T^2_0 - T_0. \tag{21}$$

The commutators (19), (20) define the group of rotations in three-dimensional pseudo-Euclidean space. All the unitary representations of this group were found by Bargmann.[5] T^2 in formula (21) is, of course, an invariant of this group. The wave functions satisfying (19), (20), are of the form $\Omega_{\alpha\beta}$, where α, β are the eigenvalues of T^2 and T_0 respectively:

$$T^2 \Omega_{\alpha\beta} = \alpha \Omega_{\alpha\beta},\ T_0 \Omega_{\alpha\beta} = \beta \Omega_{\alpha\beta}. \tag{22}$$

Only functions with the same value of α can appear in an irreducible representation. To determine the spectra of eigenvalues α, β, we operate on $\Omega_{\alpha\beta}$ with the first relation in (19):

$$[T, {}^{+}T_0]_{-}\Omega_{\varkappa\beta} = -(T^{+}\Omega_{\varkappa\beta}).$$

Using (22), we then get

$$T_0(T^{+}\Omega_{\varkappa\beta}) = (\beta + 1)(T^{+}\Omega_{\varkappa\beta}). \tag{23}$$

Similarly, from the second relation in (19) we find

$$T_0(T^{-}\Omega_{\varkappa\beta}) = (\beta - 1)(T^{-}\Omega_{\varkappa\beta}). \tag{24}$$

Thus the functions $(T^{+}\Omega_{\alpha\beta})$, $(T^{-}\Omega_{\alpha\beta})$ belong respectively to the eigenvalues $\beta \pm 1$. From this it follows that the spectrum of eigenvalues of T_0 is

$$\beta = \beta_0 + n, \tag{25}$$

where $1 > \beta_0 \geq 0$, $n = \ldots, -2, -1, 0, 1, 2, \ldots$, while the matrix T_0 is infinite-dimensional and has the form

$$(T_0)_{mn} = \beta_0\delta_{mn} + n\delta_{mn}. \tag{26}$$

We do not exclude the possibility that for certain values of β, $T^{+}\Omega_{\alpha\beta}$ (or $T^{-}\Omega_{\alpha\beta}$) may vanish. However, this case need not be treated specially, but will be obtained automatically from the general investigation.

The operator T_0 is the operator for an ordinary three-dimensional rotation in the hyperplane perpendicular to p_μ. The full rotation through 2π must either leave the function unchanged or (for a two-valued representation) multiply it by (-1). Thus β_0 can only be zero for single-valued representations, and $\frac{1}{2}$ for two-valued representations,

$$\beta_0 = 0, \ {}^1/_2, \tag{27}$$

since the matrix for a finite rotation through angle φ has the form

$$(\exp\{iT_0\varphi\})_{mn} = \delta_{mn}\exp\{i\beta_0\varphi + in\varphi\}. \tag{28}$$

To find the eigenvalues of the invariant T^2, we must determine the form of the matrices T^{+}, T^{-}. From (19) and (26) we get

$$T^{+}_{mn}(n - m + 1) = 0, \tag{29}$$

$$T^{-}_{mn}(n - m - 1) = 0, \tag{30}$$

so that

$$T^{+}_{mn} = a_n\delta_{m,\,n+1}, \tag{31}$$

$$T^{-}_{mn} = b_m\delta_{m+1,\,n}. \tag{32}$$

Substituting (31), (32), (22), and (26) in (21), we find

$$(T^2)_{mn} = \alpha\delta_{mn} = b_m a_n\delta_{m+1,\,n+1} - \delta_{mn}(n + \beta_0)(n + \beta_0 + 1) = \delta_{mn}\{a_n b_n - (n + \beta_0)(n + \beta_0 + 1)\},$$

i.e.,

$$a_n b_n = \alpha + (n + \beta_0)(n + \beta_0 + 1), \tag{33}$$

where, according to (27), β_0 is equal to 0 or $\frac{1}{2}$. We should mention that in (29) – (33) there is no summation over the repeated indices m, n.

Formula (33), expressing the coefficients a_m, b_n in terms of the eigenvalue α of the invariant, together with (26) essentially determines all the irreducible representations of the rotation group in three-dimensional pseudo-Euclidean space and all the irreducible representations of class P_{II} for the group G. Only the product $a_n b_n$ of the matrix elements is given uniquely by (33). The elements a_n, b_n themselves are not determined uniquely, which corresponds to the possibility of subjecting the system of operators T^{+}, T^{-}, T_0 to an equivalence transformation using an arbitrary non-degenerate diagonal matrix V, which leaves the operator T_0 unchanged. Formulas (26), (31), (32), and (33) can be rewritten as

$$(T_0)_{m'n'} = \delta_{m'n'}n', \quad (T^+)_{m'n'} = a_{n'}\delta_{m', n'+1}, \quad (T^-)_{m'n'} = b_{m'}\delta_{m'+1, n'}, \tag{34}$$

$$a_{n'}b_{n'} = \alpha + n'(n'+1), \tag{35}$$

Here the indices m', n' are assumed to run through all integral (half-integral) values for single-valued (double-valued) representations.

Now we must first see for which values of α a representation of the whole group corresponds to the infinitesimal representation in the neighborhood of the identity. Secondly, we must check whether all the representations we have found are irreducible, since an additional splitting of the representations is possible, for example, with respect to a sign invariant. Thirdly, we must separate the representations into unitary, real non-unitary and complex representations. Finally, we must construct the operators Γ_σ and g_μ, or the operators $M_{\mu\nu}$.

In order to solve the problem of the continuity of the representations (34) and (35), we shall attempt to construct the operator for an arbitrary finite rotation in the three-dimensional pseudo-Euclidean space. The third axis of our space is the time axis, and a rotation about it is a space rotation. The first and second axes are space axes, while rotations about them are Lorentz transformations. As in ordinary Euclidean three-space, any rotation can in our case be represented as a product of rotations through three Euler angles: a space rotation about the third axis, a Lorentz rotation about the first axis, and a space rotation about the rotated third axis. The matrix for the rotation about the third axis was given in (28). It exists for any α. To get the operator for a rotation around the first axis, it is convenient to go over to the continuous spectrum, i.e., to take as the wave function not an infinite-dimensional matrix, but a continuous function $\Omega(\Phi)$ of a variable Φ which ranges from zero to 2π. Then the operators T^+, T^-, T_0 can be taken in the form:[5]

$$T_0 = (1/i)\partial/\partial\Phi, \tag{36}$$

$$T^+ = e^{i\Phi}\left(\frac{1}{i}\frac{\partial}{\partial\Phi} - l\right), \quad T^- = \left(\frac{1}{i}\frac{\partial}{\partial\Phi} + l + 1\right)e^{-i\Phi}, \tag{37}$$

where

$$\alpha = -l(l+1). \tag{38}$$

A direct check will show that the operators T_0, T^+, T^- defined by (36) and (37) satisfy (19) – (22). The transition from (36) and (37) to (34) and vice versa is accomplished by a Fourier transformation. In accordance with (35) and (38), we find for $a_{n'}$, $b_{n'}$ from (37),

$$a_{n'} = (n'-l), \quad b_{n'} = (n'+l+1). \tag{39}$$

Rotation through the angle φ around the third axis is accomplished in the new representation by using the operator $U(\varphi)$:

$$U(\varphi) = \exp(\varphi\,\partial/\partial\Phi), \quad U(\varphi)\Omega(\Phi) = \Omega(\Phi+\varphi). \tag{40}$$

The operator T_1 for the infinitesimal rotation around the first axis is

$$T_1 = (T^+ + T^-)/2 = -il\sin\Phi - i\cos\Phi\cdot\partial/\partial\Phi. \tag{41}$$

We find the eigenfunctions and eigenvalues of the operator T_1:

$$T_1\psi_{\Phi k} = k\psi_{\Phi k}. \tag{42}$$

After a simple integration we find that for any real k,

$$\psi_{\Phi k} = (4\pi)^{-1/2}(\cos\Phi)^l\left\{\tan\left(\frac{\Phi}{2} + \frac{\pi}{4}\right)\right\}^{ik}. \tag{43}$$

An arbitrary function $\Omega(\Phi)$ can be expanded in terms of the $\psi_{\Phi k}$:

$$\Omega(\Phi) = \int_{-\infty}^{\infty} dk\,\psi_{\Phi k}\Omega_k, \tag{44}$$

so that we may consider $\psi_{\Phi k}$ as the kernel of the operator of linear transformation from Φ to k, i.e.,

to the basis in which the operator T_1 is diagonal. The kernel of the operator reciprocal to $\psi_{\Phi k}$ is

$$\psi^{-1}_{k\Phi} = (4\pi)^{-1/2}(\cos\Phi)^{-l-1}\left\{\tan\left(\frac{\Phi}{2}+\frac{\pi}{4}\right)\right\}^{-ik}. \tag{45}$$

In fact, we can verify directly that

$$\int_0^{2\pi} d\Phi\, \psi^{-1}_{k\Phi}\psi_{\Phi k'} = \delta(k-k'), \tag{46}$$

$$\int_{-\infty}^{\infty} dk\, \psi_{\Phi k}\psi^{-1}_{k\Phi'} = \delta(\Phi-\Phi'). \tag{47}$$

For the wave function $\Omega(k)$ in the new representation, the operation of rotation through the Lorentz angle χ around the first axis is trivial, and reduces to simply multiplying $\Omega(k)$ by $e^{ik\chi}$:

$$U_k(\chi)\Omega(k) = e^{ik\chi}\Omega(k). \tag{48}$$

By using (43), (45), and (I.9), we can transform the operator $U_k(\chi)$ to the Φ-representation,

$$U_{\Phi\Phi'}(\chi) = \int_{-\infty}^{\infty} dk\,\psi_{\Phi k}e^{i\chi k}\psi^{-1}_{k\Phi'} = \delta(\ln\tan\theta - \ln\tan\theta'+\chi)\,\frac{(\cos\Phi)^l}{(\cos\Phi')^{l+1}} = \frac{\delta(\ln\tan\theta-\ln\tan\theta'+\chi)}{\sqrt{\cos\Phi\cos\Phi'}}\left(\frac{\cos\Phi}{\cos\Phi'}\right)^{\sqrt{1/4-\alpha}}, \tag{49}$$

where $\theta = \Phi/2+\pi/4$, $\theta' = \Phi'/2+\pi/4$. The rotation operation itself takes the form

$$\{U(\chi)\Omega\}_\Phi = \int_0^{2\pi} d\Phi' U_{\Phi\Phi'}(\chi)\,\Omega(\Phi') \tag{50}$$

or, in somewhat different form,

$$\{U(\chi)\Omega\}_\Phi = e^{l\chi}\left(\frac{1+\tan^2\theta}{1+e^{2\chi}\tan^2\theta}\right)^{-l}\Omega(\Phi'), \tag{51}$$

where

$$\tan\left(\frac{\Phi}{2}+\frac{\pi}{4}\right) = e^{\chi}\tan\left(\frac{\Phi'}{2}+\frac{\pi}{4}\right).$$

From (51) we see that the transformation for rotation around the first axis actually does exist for any finite values of α, χ. As we said earlier, we can construct the operator for any rotation by using (40) and (51), and this operator will exist for arbitrary α. The theorem we have just demonstrated is not trivial since, for example, for the group of three-dimensional Euclidean rotations there exist representations in the neighborhood of the identity which cannot be extended over the whole group.

We shall now select the real and unitary representations of class P_Π. According to Sec. 13 of Ref. 1, the representations will be complex for complex α and real for real α. For unitary representations, the operators T^+ and T^- must be Hermitean adjoint to one another. In this case, we find from (31) and (35) that

$$a_{n'} = b^*_{n'},\ |a_{n'}|^2 = \alpha + n'(n'+1). \tag{52}$$

From (52) it follows that a representation can be unitary only if the quantity $\alpha + n'(n'+1)$ is not negative for any integral (half-integral) values of n'. For integer n', the requirement that (52) be positive is satisfied for $\alpha = a > 0$. (The case of $\alpha = 0$ will be treated later and assigned to another subclass). The corresponding single-valued unitary representations will be denoted by P^a_Π. For half-integral n', (52) is positive for $\alpha = a > 1/4$ (the case of $\alpha = 1/4$ also will be assigned to another subclass). These two-valued representations will be denoted by P'^a_Π. However, the subclasses P^a_Π and P'^a_Π do not exhaust the unitary irreducible representations of class P_Π. The point is that for $\alpha = -s(s+1)$, where s is an integer (half-integer) for single-valued (double-valued) representations, the representation (34) ceases to be irreducible. For $n' = s$ and $n' = -s-1$, the coefficients $a_{n'}$, $b_{n'}$ in (34) and (35) vanish, and the matrices T_0, T^+, T^- simultaneously assume the "block" form.

In this case the representation (34) breaks up into three irreducible representations, two of which are infinite-dimensional and unitary, while the third is finite-dimensional and non-unitary. The matrix elements of the infinitesimal operators are given by formulas (34), (35) for all three cases. In one of the representations, the indices m', n' run through values from $-\infty$ to $-s-1$; in the second they go from $s+1$ to ∞, and in the third from $-s$ to s. These representations are respectively designated by P_{Π}^{-l}, P_{Π}^{+l}, P_{Π}^{s} for integral l, s, and by $P_{\Pi}^{\prime -l}$, $P_{\Pi}^{\prime +l}$, $P_{\Pi}^{\prime s}$ for half-integral l, s. The representations P_{Π}^{+l}, P_{Π}^{-l}, $P_{\Pi}^{\prime +l}$, $P_{\Pi}^{\prime -l}$ (and P_{Π}^{s}, for $s=0$) are unitary. For them the sign of T_0 is an invariant. The representations P_{Π}^{s} ($s \neq 0$) and $P_{\Pi}^{\prime s}$ are non-unitary. For them, the sign of T_0 is not an invariant. The indices l, s can take on the values:

$$\begin{aligned}
&\text{for representations } P_{\Pi}^{+l}\text{:} && l = 0,\ 1,\ 2,\ \ldots,\\
&\text{for representations } P_{\Pi}^{\prime \pm l}\text{:} && l = -\tfrac{1}{2},\ \tfrac{1}{2},\ \tfrac{3}{2},\ \tfrac{5}{2},\ \ldots,\\
&\text{for representations } P_{\Pi}^{s}\text{:} && s = 0,\ 1,\ 2,\ \ldots,\\
&\text{for representations } P_{\Pi}^{\prime s}\text{:} && s = \tfrac{1}{2},\ \tfrac{3}{2},\ \tfrac{5}{2},\ \ldots,
\end{aligned} \tag{53}$$

We may mention that the unitary representations P_{Π}^{+0}, P_{Π}^{-0}, and P_{Π}^{0} are all different. The first two are infinite-dimensional and correspond to the case of $\Gamma_\sigma^2 = 0$, $\Gamma_\sigma \neq 0$. The representation P_{Π}^{0} corresponds to the case of $\Gamma_\sigma = 0$.

A peculiarity of the subclass $P_{\Pi}^{\prime \pm l}$ is the presence of the representation with $l = -\frac{1}{2}$, corresponding to the case when (34) splits into two, instead of three, irreducible representations. The finite-dimensional (in the spin variable) non-unitary representations of the group of 3-rotations in pseudo-Euclidean space corresponding to the subclasses P_{Π}^{s} and $P_{\Pi}^{\prime s}$ can be gotten by Weyl's[6] unitary trick from the irreducible representations of the ordinary group of 3-rotations.

The real, infinite-dimensional, non-unitary representations, which are not included in the subclasses enumerated above, will be denoted by P_{Π}^{b} (for integer n'), and by $P_{\Pi}^{\prime b}$ (for half-integer n'); the complex representations will be assigned to P_{Π}^{α} (for integral n'), and $P_{\Pi}^{\prime \alpha}$ (for half-integral n').

To complete our treatment of class P_{Π} there remains only the construction of the components of the operator $M_{\mu\nu}$. This rather involved problem is probably solved most simply as follows. In treating the class P_m we had occasion to transform to the rest system, which explicitly singled out the time axis. Accordingly, formula (11) is symmetric with respect to the three space axes but not symmetric with respect to the time axis. In the present section, we explicitly distinguished the third space axis whereas the first two space axes and the time axis were essentially not distinguished. We may therefore expect that we will get formulas which are relatively simple and similar to (11) if we introduce three-dimensional vectors and tensors defined in the pseudo-Euclidean space x_1, x_2, x_4. We shall mark such vectors with a superior tilde. One of the components of each such vector is imaginary. For example, in this space the three-dimensional momentum will have the form

$$\tilde{p}_i = (p_1,\ p_2,\ ip_0), \tag{54}$$

while the component p_3 will be the three-dimensional scalar

$$p_3 = \pm\sqrt{\Pi^2 - \tilde{p}_i^2}. \tag{55}$$

From the operators T^+, T^-, T_0, we can form the vector

$$\tilde{T}_i = (iT_1,\ iT_2,\ T_0),\ T_1 = (T^+ + T^-)/2,\ T_2 = (T^+ - T^-)/2i. \tag{56}$$

Using (19), we can easily verify that the $\tilde{T}_i$ satisfy the covariant commutation relations

$$[\tilde{T}_i \tilde{T}_j]_- = i\varepsilon_{ijk}\tilde{T}_k. \tag{57}$$

We now note that the relations (11) can be rewritten as

$$M_i = {}^1/_2\varepsilon_{ijk}M_{jk} = -(i\varepsilon_{ijk}p_j\partial/\partial p_k) + S_i, \qquad M_{i4} = (ip_4\partial/\partial p_i) + \varepsilon_{ijk}S_j p_k/(p_4 + \sqrt{p^2 + p_4^2}). \tag{58}$$

where $p^2 + p_4^2 = -m^2 = \text{inv}$, and the three-dimensional vectors are "ordinary" vectors. The tensor $M_{\mu\nu}$, defined by (58), satisfies the commutation relations (I.31); in deriving this, we use only the relations (7) and

$$\partial p_\mu / \partial p_\nu = \delta_{\mu\nu}. \tag{59}$$

Since relations (7) are completely analogous to (57), it is obvious that the tensor $\widetilde{M}_{\mu\nu}$, expressed in terms of the vector $\widetilde{M}_{i3}$ and the pseudo-vector $\widetilde{M}_i$ in the pseudo-Euclidean 3-space (x_1, x_2, x_4)

$$\widetilde{M}_i = {}^1/_2 \widetilde{\varepsilon}_{ijk} \widetilde{M}_{jk} = -i \widetilde{\varepsilon}_{ijk} \widetilde{p}_j \frac{\partial}{\partial \widetilde{p}_k} + \widetilde{T}_i, \qquad \widetilde{M}_{i3} = i p_3 \frac{\partial}{\partial \widetilde{p}_i} - i \widetilde{p}_i \frac{\partial}{\partial p_3} + \widetilde{\varepsilon}_{ijk} \frac{\widetilde{T}_j \widetilde{p}_k}{p_3 + \Pi} \tag{60}$$

will satisfy (I.31). In Eq. (60),

$$i, j, k = 1, 2, 4, \quad p_4^2 = \Pi^2.$$

Writing (60) in terms of "ordinary" components, we get

$$M_1 = M_{23} = -i (p_2 \partial / \partial p_3 - p_3 \partial / \partial p_2) + (T_1 E_p + T_0 p_1) / (p_3 + \Pi),$$

$$M_2 = M_{31} = -i (p_3 \partial / \partial p_1 - p_1 \partial / \partial p_3) + (T_2 E_p + T_0 p_2) / (p_3 + \Pi), \quad M_3 = M_{12} = -i (p_1 \partial / \partial p_2 - p_2 \partial / \partial p_1) + T_0, \tag{61}$$

$$N_1 = M_{14}/i = (i E_p \partial / \partial p_1) - T_1, \quad N_2 = M_{24}/i = (i E_p \partial / \partial p_2) + T_2, \quad N_3 = M_{34}/i = (i E_p \partial / \partial p_3) + (T_2 p_1 - T_1 p_2) / (p_3 + \Pi).$$

In (61), $E_p = -ip_4 = \pm \sqrt{p^2 - \Pi^2}$. The independent continuous variables are p_1, p_2, p_3. Their domain of variation is limited by the condition $\infty > |p| \geq \Pi$. The energy is not an independent variable, but for given values of p_1, p_2, and p_3, its sign can be arbitrary within the representation. Thus the sign of the energy is a discrete independent variable which takes on two values, and relations (61) will give the correct commutation relations over the whole domain of definition of the independent variables only if this point is taken into account. The simplest way to take account of the two signs of the energy is to express the components of the 4-vector p_μ in terms of the four-dimensional polar angles φ, ϑ, χ:

$$p_1 = \Pi \cosh\chi \sin\vartheta \cos\varphi, \quad p_2 = \Pi \cosh\chi \sin\vartheta \sin\varphi, \quad p_3 = \Pi \cosh\chi \cos\vartheta, \quad p_0 = \Pi \sinh\chi,$$

$$2\pi \geqslant \varphi \geqslant 0, \ \pi \geqslant \vartheta \geqslant 0, \ \infty > \chi > -\infty. \tag{62}$$

The two-valuedness of the energy is then obtained automatically. The components of $M_{\mu\nu}$, expressed in terms of the angle variables, become

$$M_1 = i \sin\varphi \frac{\partial}{\partial\vartheta} + i \cot\vartheta \cos\varphi \frac{\partial}{\partial\varphi} + \frac{T_1 \sinh\chi + T_0 \cosh\chi \sin\vartheta \cos\varphi}{1 + \cosh\chi \cos\vartheta},$$

$$M_2 = -i \cos\varphi \frac{\partial}{\partial\vartheta} + i \cot\vartheta \sin\varphi \frac{\partial}{\partial\varphi} + \frac{T_2 \sinh\chi + T_0 \cosh\chi \sin\vartheta \sin\varphi}{1 + \cosh\chi \cos\vartheta}, \quad M_3 = -i\partial/\partial\varphi + T_0,$$

$$N_1 = i \sin\vartheta \cos\varphi \frac{\partial}{\partial\chi} + i \tanh\chi \cos\vartheta \cos\varphi \frac{\partial}{\partial\vartheta} - i \tanh\chi \frac{\sin\varphi}{\sin\vartheta} \frac{\partial}{\partial\varphi} - T_1, \tag{63}$$

$$N_2 = i \sin\vartheta \sin\varphi \frac{\partial}{\partial\chi} + i \tanh\chi \cos\vartheta \sin\varphi \frac{\partial}{\partial\vartheta} + i \tanh\chi \frac{\cos\varphi}{\sin\vartheta} \frac{\partial}{\partial\varphi} + T_2,$$

$$N_3 = i \cos\vartheta \frac{\partial}{\partial\chi} - i \tanh\chi \sin\vartheta \frac{\partial}{\partial\vartheta} + \frac{\cosh\chi \sin\vartheta (T_2 \cos\varphi - T_1 \sin\varphi)}{1 + \cosh\chi \cos\vartheta}$$

Formulas (62), (63), together with (34), (35) give the complete solution of the problem of finding all the irreducible representations of the class P_Π.

One may try to construct the tensor $M_{\mu\nu}$ by a procedure different from ours, by simply replacing the vector S_i in (11) [or, what amounts to the same thing, in (58)] by the vector T_i with components (iT_1, iT_2, T_0). This vector is analogous to the vector $\widetilde{T}_i$ of (56), but, unlike it, is defined in a Euclidean rather than a pseudo-Euclidean 3-space. The components of the angular momentum tensor formed in this way,

$$M_i = {}^1/_2 \varepsilon_{ijk} M_{jk} = -i (\varepsilon_{ijk} p_j \partial / \partial p_k) + T_i. \qquad M_{i4} = (i p_4 \partial / \partial p_i) + \varepsilon_{ijk} T_j p_k / (p_4 + \sqrt{p^2 + p_4^2}) \tag{64}$$

satisfy commutation relations (I.31), and one might get the impression that we have constructed repre-

sentations which are equivalent to (63). As a matter of fact, however, (64) is equivalent to (63) only for representations which are finite-dimensional in the spin variable. For infinite-dimensional matrices T_i, formulas (64) do not in general define a representation at all, since in this case it is impossible to construct a finite three-dimensional rotation about the x or y axes. This is apparent from the fact that the components of the vector T_i are infinite-dimensional and, at the same time, irreducible with respect to three-dimensional rotations; i.e., they constitute an infinite-dimensional irreducible representation of the group of Euclidean 3-rotations in the neighborhood of the identity. Such a representation cannot be built up over the whole group, since all the irreducible representations of the group of 3-rotations (and of any compact group) are finite-dimensional.

In conclusion we give a table of the irreducible representations of the class P_Π:

Representation	Unitarity. Dimensionality in the spin variable.	Fundamental Invariants $\Pi^s=P^s_\mu>0$, $\alpha=-s(s+1)+\Gamma_\alpha(\Pi^s$	Additional invariants
P^a_Π	Unitary infinite-dimensional	$\alpha=a>0$	—
P^a_Π	" "	$\alpha=a>\frac{1}{4}$	—
P^{+l}_Π	" "	$s=l=0,\ 1,\ 2,\ldots$	$S_{\Gamma_4}=1$
P^{-l}_Π	" "	$s=l=0,\ 1,\ 2,\ldots$	$S_{\Gamma_4}=-1$
P^{+l}_Π	" "	$s=l=-\frac{1}{2},\ \frac{1}{2},\ \frac{3}{2},\ldots$	$S_{\Gamma_4}=1$
P^{-l}_Π	" "	$s=l=-\frac{1}{2},\ \frac{1}{2},\ \frac{3}{2},\ldots$	$S_{\Gamma_4}=-1$
P^s_Π	Non-unitary; $2s+1$	$s=0,\ 1,\ 2,\ldots$	—
P'^s_Π	" "	$s=\frac{1}{2},\ \frac{3}{2}$	—
P^b_Π	Non-unitary infinite-dimensional	$\alpha=b<0$ $s\neq 1,\ 2,\ 3,\ldots$	—
P'^b_Π	" "	$\alpha=b<\frac{1}{4}$ $s\neq\frac{1}{2},\ \frac{3}{2},\ldots$	—
P^α_Π	" "	α = complex	—
P'^α_Π	" "	α = complex	—

[1] Iu. M. Shirokov, J. Exptl. Theoret. Phys. (U.S.S.R.) **33**, 861 (1957), Soviet Phys. JETP 6, 664 (1958).

[2] E. P. Wigner, Ann. of Math. 40, 149 (1939).

[3] I. M. Gel'fand and M. A. Naimark, Journ. of Phys. (U.S.S.R.) 10, 93 (1946); M. A. Naimark, Usp. Mat. Nauk 9, 19 (1954). (Translation in Amer. Math. Soc. Translations, Ser. 2, Vol. 6, 1957.)

[4] Iu. M. Shirokov, Dokl. Akad. Nauk SSSR 94, 857; 99, 737 (1954).

[5] V. Bargmann, Ann. of Math. 48, 568 (1947).

[6] H. Weyl, Classical Groups, Princeton University Press, 1946.

Translated by M. Hamermesh
246

SOVIET PHYSICS JETP VOLUME 6 (33), NUMBER 5 MAY, 1958

A GROUP-THEORETICAL CONSIDERATION OF THE BASIS OF RELATIVISTIC QUANTUM MECHANICS. III. IRREDUCIBLE REPRESENTATIONS OF THE CLASSES P_0 AND O_0, AND THE NON-COMPLETELY-REDUCIBLE REPRESENTATIONS OF THE INHOMOGENEOUS LORENTZ GROUP*

Iu. M. SHIROKOV

Moscow State University

Submitted to JETP editor December 11, 1956

J. Exptl. Theoret. Phys. (U.S.S.R.) 33, 1208-1214 (November, 1957)

All the unitary and non-unitary irreducible representations of class P_0 for the inhomogeneous Lorentz group are obtained in explicit form. The isomorphism of the representations of class O_0 and the representations of the homogeneous Lorentz group is discussed. We indicate certain non-completely-reducible representations of the inhomogeneous Lorentz group which are of importance for physics.

1. IRREDUCIBLE REPRESENTATIONS OF CLASS P_0 FOR THE INHOMOGENEOUS LORENTZ GROUP

THE representations of class P_0 are characterized by a non-vanishing 4-momentum having zero length

$$p_\mu^2 = 0, \quad p_\mu \neq 0.$$

In this case there is no system of coordinates in which all except one of the components of p_μ would vanish. We can, however, choose a system of coordinates so that

$$p_1 = p_2 = 0, \quad p_3 = p_4/i = p. \tag{1}$$

From (1) and (I.39) we find for the components of the intrinsic angular momentum operator Γ_σ:

$$\Gamma_3 = -i\Gamma_4 = \Gamma_0. \tag{2}$$

With the notation

$$\Gamma_1 + i\Gamma_2 = \Gamma^+, \quad \Gamma_1 - i\Gamma_2 = \Gamma^-, \quad \Gamma_0 = p\Gamma \tag{3}$$

the commutation relations (I.41) between the components Γ_σ, and the invariant Γ_σ^2 become

$$[\Gamma^+, \Gamma] = -\Gamma^+, \quad [\Gamma^-, \Gamma] = \Gamma^-, \tag{4}$$

$$[\Gamma^+, \Gamma^-] = 0, \tag{5}$$

$$\Gamma_\sigma^2 = \Gamma^+\Gamma^-. \tag{6}$$

The relations (4) have the same structure as (II.19), and Γ, like T_0 in (II.19), is the operator of an infinitesimal Euclidean rotation. Repeating word for word the derivation in Sec. 4 of Ref. 2 (formulas II.22 – 32), we find that the admissible wave functions have the form $\psi_{\alpha n}$, where α, n are the eigenvalues of Γ_σ^2, Γ:

$$\Gamma_\sigma^2\psi_{\alpha n} = \alpha\psi_{\alpha n}, \quad \Gamma\psi_{\alpha n} = n\psi_{\alpha n},$$

and n runs through all positive and negative integer (half-integer) values for single-valued (double-valued) representations. The operators Γ^+ and Γ^- respectively increase and decrease the index n by unity. Only those functions can appear in an irreducible representation which belong to the same eigen-

*Notations used without explanation are the same as in Refs. 1 and 2. References like (I.39) and (II.19) are to the corresponding formulas in Refs. 1 and 2.

value α of the invariant. The operator Γ has the form

$$\Gamma_{mn} = \delta_{mn} n, \tag{7}$$

where m, n = ... −2, −1, 0, 1, 2, ... for single-valued representations, and m, n = ... $-3/2$, $-1/2$, $1/2$, $3/2$ ... for double-valued representations.

The operators Γ^+, Γ^- satisfy

$$\Gamma^+_{mn}(n-m+1) = 0, \quad \Gamma^-_{mn}(n-m-1) = 0 \tag{8}$$

and have the form

$$\Gamma^+_{mn} = a_n \delta_{m,n+1}, \quad \Gamma^-_{mn} = b_m \delta_{m+1,n}. \tag{9}$$

At this point the analogy with the treatment for class P_{II} ends because of the difference between the commutation relations [(II.20) and (5)] and the expressions for the invariants [(II.33) and (6)]. Using (9) and (6) instead of (II.33) and (II.35), we now get

$$a_n b_n = \alpha. \tag{10}$$

For $\alpha \neq 0$ we can, without loss of generality, set

$$a_n = a, \quad b_n = b = \alpha / a. \tag{11}$$

for all n.

The sign of the energy is the invariant for representations of class P_0, so that to each value of α there correspond two irreducible representations, $P_{+0}(E > 0)$ and $P_{-0}(E < 0)$. For unitary representations,

$$(\Gamma^+)^* = \Gamma^- \tag{12}$$

and, consequently,

$$b = a^*, \quad \alpha = a^* a \geqslant 0, \tag{13}$$

i.e., the representations of class P_0 are unitary for real non-negative $\alpha = c \geqslant 0$. We shall designate such single-valued (double-valued) representations by $P^c_{\pm 0}$ ($P'^c_{\pm 0}$).

In the special case of $\alpha = 0$, we find from (13),

$$a = b = 0, \quad \Gamma^+ = \Gamma^- = 0, \quad \Gamma_1 = \Gamma_2 = 0. \tag{14}$$

From (1), (2), (3), and (14) it follows that for $\alpha = 0$,

$$\Gamma_\sigma = p_\sigma \Gamma, \tag{15}$$

i.e., in this case Γ is the additional invariant which was mentioned earlier in Sec. 12 of Ref. 1 (cf. I.46 and I.47). Because of the invariance of Γ, the representation which was infinite-dimensional in the spin variable splits up into one-dimensional representations. Thus, for $\alpha = 0$, for a given sign of the energy there correspond to each positive integral (half-integral) value Σ of the operator Γ the representations $P^{+\Sigma}_{\pm 0}$ and $P^{-\Sigma}_{\pm 0}$ ($P'^{+\Sigma}_{\pm 0}$ and $P'^{-\Sigma}_{\pm 0}$), where for the representation $P^{+\Sigma}_{\pm 0}$ ($P'^{+\Sigma}_{\pm 0}$)

$$\Gamma_\sigma = \Sigma p_\sigma, \tag{16}$$

while for the representation $P^{-\Sigma}_{\pm 0}$ ($P'^{-\Sigma}_{\pm 0}$)

$$\Gamma_\sigma = -\Sigma p_\sigma, \quad \Sigma = 0, 1, 2, \ldots \quad (1/2, 3/2, 5/2, \ldots). \tag{17}$$

For a representation of this type, the fundamental invariants p^2_μ and Γ^2_σ are equal to zero, but then there are three supplementary invariants: the sign of the energy, the sign of Γ_0, and the factor of proportionality between Γ_σ and p_σ.

All other irreducible representations of class P_0 are non-unitary. We shall denote the single-valued (double-valued) representations, corresponding to real negative $\alpha = -c$ by $P^{-c}_{\pm 0}$ ($P'^{-c}_{\pm 0}$). The remaining complex non-unitary single-valued (double-valued) representations, corresponding to complex α, will be denoted by $P^{\alpha}_{\pm 0}$ ($P'^{\alpha}_{\pm 0}$). By analogy with Sec. 4 of Ref. 2 we may assume that for each non-unitary

representation of class P_0 in the neighborhood of the identity we can construct a representation over the whole group, but this point, of course, requires a special proof.

For the representations $P^{\pm\Sigma}_{+0}$ which are one-dimensional in the spin variable; the operator $M_{\mu\nu}$ has the form

$$M_1 = -i(p_3\partial/\partial p_2 - p_2\partial/\partial p_3) \pm \Sigma p p_1/(p_1^2+p_2^2),$$
$$M_2 = -i(p_3\partial/\partial p_1 - p_1\partial/\partial p_3) \mp \Sigma p p_2/(p_1^2+p_2^2), \quad M_3 = -i(p_1\partial/\partial p_2 - p_2\partial/\partial p_1), \tag{18}$$
$$N_1 = ip\partial/\partial p_1 \mp \Sigma p_2 p_3/(p_1^2+p_2^2), \quad N_2 = ip\partial/\partial p_2 \pm \Sigma p_1 p_3/(p_1^2+p_2^2), \quad N_3 = ip\partial/\partial p_3.$$

With respect to the classification of the unitary representations, the results found here coincide with those of Wigner.[3] We give a table of all the irreducible representations of class P_0:

Representation	Unitarity. Dimensionality in the spin variable.	Fundamental Invariants $p_\mu^2=0$, $\Gamma_\sigma^1=\alpha$	Additional invariants.
$P^{\pm\Sigma}_{\pm 0}$	Unitary, one-dimensional	$\alpha=0$	$S_H=\pm 1, S_{\Gamma_4}=\pm 1, \Sigma=0,1,2,\ldots$
$P'^{\pm\Sigma}_{\pm 0}$	" "	$\alpha=0$	$S_H=\pm 1, S_{\Gamma_4}=\pm 1, \Sigma=1/2, 3/2,\ldots$
$P^{c}_{\pm 0}$	Unitary, infinite-dimensional	$\alpha=c>0$	$S_H=\pm 1$
$P'^{c}_{\pm 0}$	" "	$\alpha=c>0$	$S_H=\pm 1$
$P^{-c}_{\pm 0}$	Non-unitary, infinite-dimensional	$\alpha=-c<0$	$S_H=\pm 1$
$P'^{-c}_{\pm 0}$	" "	$\alpha=-c<0$	$S_H=\pm 1$
$P^{\alpha}_{\pm 0}$	" "	$\alpha=$ complex	$S_H=\pm 1$
$P'^{\alpha}_{\pm 0}$	" "	$\alpha=$ complex	$S_H=\pm 1$

2. THE CLASS O_0

Unlike the three and four-dimensional rotation groups, the inhomogeneous Lorentz group is not simple, but contains a normal divisor (invariant subgroup), the subgroup of translations.

We shall denote by b, b′, ... those elements of G which are in the subgroup of translations, and by a, a′, ... the remaining elements, which represent rotations about different points. By definition, a subgroup is a normal divisor if its right and left residue classes with respect to any of the elements of the group coincide, i.e., if the sets of elements ba, b′a, b″a ... and ab, ab′, ab″ ... coincide. In other words, for any a, b, there exists an element b′ such that ba = ab′, or

$$a^{-1}ba = b'. \tag{19}$$

We can verify directly that (19) is satisfied for the group G:

$$x_\mu = a_{\mu\nu}x'_\nu = a_{\mu\nu}(x'_\nu + b_\nu) = x''_\mu + a_{\mu\nu}b_\nu \equiv x'''_\mu + b'_\mu.$$

The classes corresponding to elements a_1, a_2, will be denoted by A_1, A_2. Geometrically, a class consists of rotations through the same angle about different points. Each of the elements of the group G is either in one (and only one) of the residue classes, or is in the translation subgroup B. If the product of the elements a_2, a_1, taken from classes A_2, A_1, belongs to the class A_3,

$$a_2a_1 = a_3, \tag{20}$$

then the product of any other pair of elements a'_2, a'_1, taken from these respective classes also will belong to A_3,

$$a'_2a'_1 = a_3. \tag{21}$$

We can therefore introduce an operation of class multiplication, defining the product of classes as the set of all possible elements of the form a_2a_1. All elements of this type are in class A_3, so that we may write

$$A_2A_1 = A_3. \tag{22}$$

The translation subgroup B plays the role of the identity in the class multiplication,

$$AB = BA = A.$$

Together with B, the set of residue classes A forms a group with respect to the multiplicative operation which we have introduced. This group, which we denote by L, is the factor group of G with respect to the invariant subgroup B. More detailed information concerning factor groups is given, for example, in Pontriagin's[4] book, where, in particular, proofs of all the above assertions are given.

The factor group L is isomorphic to the homogeneous Lorentz group. Now let us assume that we have found some representation of L, i.e., we have associated with each of the elements A_1, A_2, ... a matrix U_1, U_2, ... so that for each relation of type (22) we have

$$U_2U_1 = U_3. \tag{23}$$

It is not difficult to see that the matrices U will at the same time also give a representation of the group G, if we associate the matrix U_1 with all the elements a_1', a_1'', a_1''', ... in the class A_1, etc., and if the elements b, b', ... are associated with the unit matrix. Thus to each irreducible representation of the homogeneous Lorentz group there corresponds an irreducible representation of the inhomogeneous group, in which all the translations are associated with the unit operator, so that for these representations $p_\mu = 0$, and all of them belong to the class O_0. The invariants for the class O_0 are the invariants of the homogeneous Lorentz group:

$$F = {}^1/_2 M_{\mu\nu}^2 = \mathbf{M}^2 - \mathbf{N}^2, \tag{24}$$

$$W = (1/4i)\,\varepsilon_{\mu\nu\lambda\sigma} M_{\mu\nu} M_{\lambda\sigma} = \mathbf{MN}. \tag{25}$$

All the representations of the homogeneous Lorentz group were found by Gel'fand and Naimark,[5] and we shall not review them in detail. Each representation is defined by a pair of numbers (k_0, c), where k_0 is non-negative and integral or half-integral, and c is an arbitrary complex number. The representation is unitary and infinite-dimensional if c is pure imaginary (fundamental series), or if c is real and lies between zero and one, $1 > c \geq 0$ with $k_0 = 0$ (the complementary series). The invariants F, W are expressed in terms of k_0, c by

$$F = k_0^2 + c^2 - 1, \quad W = ik_0 c. \tag{26}$$

We give the operators **M**, **N** for the finite-dimensional non-unitary representations, which are the most interesting for physics, and which are obtained for $c = k_0 + n$, $n = -(2k_0 - 1), \ldots -1, 0, 1, 2, \ldots$ The symmetric undotted spinor of rank $2k_0$ transforms according to the representations $S_{k_0}^{k_0+1}$ $(c = k_0 + 1)$, for which $M_{\mu\nu}$ is

$$\mathbf{M} = \mathbf{S}, \quad \mathbf{N} = i\mathbf{S} \tag{27}$$

In (27) **S** is the operator for the three-dimensional angular momentum of magnitude k_0,

$$[S_i, S_j] = i\varepsilon_{ijk} S_k, \quad \mathbf{S}^2 \Omega_{i_1 \ldots i_{2k_0}} = k_0 (k_0 + 1)\, \Omega_{i_1 \ldots i_{2k_0}}. \tag{28}$$

The dotted spinor of rank $2k_0$ transforms according to the representation $S_{k_0}^{-k_0-1}$ $(c = -k_0 - 1)$, for which $M_{\mu\nu}$ is

$$\mathbf{M} = \mathbf{S}, \quad \mathbf{N} = -i\mathbf{S}. \tag{29}$$

All other finite-dimensional irreducible representations are found by taking direct products $S_{k_0'}^{1-k_0'} \times S_{k_0}^{k_0''+1}$ with all possible k_0', k_0''. For such irreducible representations the operator $M_{\mu\nu}$ has the form

$$\mathbf{M} = \mathbf{S}_1 + \mathbf{S}_2, \quad \mathbf{N} = i\mathbf{S}_1 - i\mathbf{S}_2, \tag{30}$$

where

$$\mathbf{S}_1^2 \Omega = k_0' (k_0' + 1)\, \Omega, \quad \mathbf{S}_2^2 \Omega = k_0'' (k_0'' + 1)\, \Omega. \tag{31}$$

A straightforward computation of the invariants of the representation (30) will show the validity of the relations

$$S^{1-k_0'}_{k_0'} \times S^{k_0''+1}_{k_0''} = S^{k_0'+k_0''+1}_{k_0''-k_0'} \quad (k_0'' > k_0'); \quad S^{1-k_0'}_{k_0'} \times S^{k_0''+1}_{k_0''} = S^{k_0''-k_0'}_{k_0''+k_0'+1} \quad (k_0'' \geqslant k_0'), \tag{32}$$

which show that we have obtained all the finite-dimensional irreducible representations of class O_0.

3. THE NON-COMPLETELY-REDUCIBLE REPRESENTATIONS OF THE INHOMOGENEOUS LORENTZ GROUP

The reducible representations which we have treated up to now were not only reducible, but also fully reducible. In mathematics, there occur, in addition, representations which are not fully reducible.* A representation is said to be non-completely-reducible if all its matrices can be brought simultaneously to the form

$$U = \begin{pmatrix} U^{(1)} & 0 \\ U^{(21)} & U^{(2)} \end{pmatrix}, \tag{33}$$

where $U^{(21)}$ is not identically zero. For the product of two matrices U_1, U_2, of type (33) we find

$$U_1 U_2 = U_3 = \begin{pmatrix} U_1^{(1)} & 0 \\ U_1^{(21)} U_1^{(2)} \end{pmatrix} \begin{pmatrix} U_2^{(1)} & 0 \\ U_2^{(21)} U_2^{(2)} \end{pmatrix} = \begin{pmatrix} U_1^{(1)} U_2^{(1)} & 0 \\ U_1^{(21)} U_2^{(1)} + U_1^{(2)} U_2^{(21)} & U_1^{(2)} U_2^{(2)} \end{pmatrix}, \tag{34}$$

from which we see that the matrices $U^{(1)}$ and $U^{(2)}$ also give representations of the group. The representation $U^{(1)}$ is either fully reducible, or non-completely-reducible, or irreducible. In the first case we can expand $U^{(1)}$ in irreducible representations, while in the second case we can use the procedure just described to separate out representations of lower dimension from $U^{(1)}$. Continuing this process until we obtain irreducible representations, we find that any non-completely-reducible representation is built up from irreducible representations in the sense that all its matrices can be brought to the form

$$U = \begin{pmatrix} U^{(1)} & 0 & 0 & \dots \\ U^{(21)} & U^{(2)} & 0 & \dots \\ U^{(31)} & U^{(32)} & U^{(3)} & \\ \dots & \dots & \dots & \end{pmatrix}, \tag{35}$$

where $U^{(1)}$, $U^{(2)}$, ... constitute irreducible representations, and $U^{(21)}$, $U^{(31)}$, ... are not all zero.

Non-completely-reducible representations have various features different from those of irreducible representations. In particular, whereas a matrix which commutes with all the matrices of an irreducible representation must be the unit matrix, for a matrix commuting with all the matrices of a non-completely-reducible representation we can only say that its eigenvalues are equal (cf. Ref. 6, p. 39). Thus the non-completely-reducible representations cannot be classified by means of the invariants defined in Ref. 1. All the non-completely-reducible representations are non-unitary.

One might get the impression that non-completely-reducible representations are of purely mathematical interest and have nothing to do with physics. This is not the case. The simplest example of a physical quantity transforming according to a non-completely-reducible representation is the non-relativistic 4-dimensional radius vector $(\mathbf{x}, t)$. This vector transforms according to the non-completely-reducible representation of the Galilei group:

$$t = t', \quad \mathbf{x} = \mathbf{x}' + \mathbf{v}t'. \tag{36}$$

In fact, (36) can be written as

$$x_\alpha = V_{\alpha\beta} x'_\beta, \tag{37}$$

where $\alpha, \beta = 0, 1, 2, 3$; $x_0 = t$; $x_\alpha = (t, x_1, x_2, x_3)$,

*Everywhere except in the present section we have, in order to simplify the terminology, used the term "reducible" for "fully reducible" representations, since both terms are equivalent for all questions in which we can disregard the existence of non-completely-reducible representations.

$$V_{\alpha\beta} = \begin{pmatrix} 1 & 0 & 0 & 0 \\ v_1 & 1 & 0 & 0 \\ v_2 & 0 & 1 & 0 \\ v_3 & 0 & 0 & 1 \end{pmatrix}. \tag{38}$$

The matrices $V_{\alpha\beta}$ are obviously not fully reducible.

Going on to the inhomogeneous Lorentz group,

$$x_\mu = a_{\mu\nu} x'_\nu + b_\mu, \tag{39}$$

we rewrite (39) in homogeneous coordinates $y_1, \ldots y_5$,

$$x_\mu = y_\mu / y_5. \tag{40}$$

We get

$$y_s = A_{ss'} y'_{s'}, \tag{41}$$

where $s, s' = 1, 2, 3, 4, 5$,

$$A_{ss'} = \begin{pmatrix} a_{\mu\nu} & b_\mu \\ 0 & 1 \end{pmatrix}. \tag{42}$$

The five-rowed matrices $A_{ss'}$ form a non-completely-reducible representation of the group G. (It is interesting that the representation (42) is not only finite-dimensional, but also faithful, i.e., different elements of the group correspond to different matrices.) Thus the relativistic radius vector, expressed in homogeneous coordinates, transforms according to a non-completely-reducible representation of the group G.

By considering direct products of the representation (42) with itself, we can get new non-completely-reducible representations of the group G.

The representation (42) is fully reducible with respect to rotations, while the matrices for translations have diagonal elements equal to unity. We may pose the problem of finding all possible representations of this type, for which the matrices of rotations and translations have the respective forms

$$\begin{pmatrix} U^{(1)} & 0 \\ 0 & U^{(2)} \end{pmatrix}, \qquad \begin{pmatrix} 1 & U^{(12)} \\ 0 & 1 \end{pmatrix}. \tag{43}$$

For such representations, the infinitesimal operators $M_{\mu\nu}$, p_λ have the form

$$M_{\mu\nu} = \begin{pmatrix} M^{(1)}_{\mu\nu} & 0 \\ 0 & M^{(2)}_{\mu\nu} \end{pmatrix}, \qquad p_\lambda = \begin{pmatrix} 0 & L_\lambda \\ 0 & 0 \end{pmatrix}, \tag{44}$$

while the commutation relations reduce to

$$[M^{(1)}_{\mu\nu} M^{(1)}_{\lambda\sigma}] = i\,(\delta_{\mu\sigma} M^{(1)}_{\lambda\nu} + \delta_{\mu\lambda} M^{(1)}_{\nu\sigma} + \delta_{\nu\sigma} M^{(1)}_{\mu\lambda} + \delta_{\lambda\nu} M^{(1)}_{\sigma\mu}), \qquad [M^{(2)}_{\mu\nu} M^{(2)}_{\lambda\sigma}] = i\,(\delta_{\mu\sigma} M^{(2)}_{\lambda\nu} + \delta_{\mu\lambda} M^{(2)}_{\nu\sigma} + \delta_{\nu\sigma} M^{(2)}_{\mu\lambda} + \delta_{\lambda\nu} M^{(2)}_{\sigma\mu}), \tag{45}$$

$$M^{(1)}_{\mu\nu} L_\lambda - L_\lambda M^{(2)}_{\mu\nu} = i\,(L_\nu \delta_{\mu\lambda} - L_\mu \delta_{\nu\lambda}). \tag{46}$$

In general the matrices $M^{(1)}_{\mu\nu}$, $M^{(2)}_{\mu\nu}$ have different dimensions, so that the matrices L_μ can be rectangular. According to (44),

$$p_\mu p_\nu \equiv 0, \tag{47}$$

and no requirements are imposed on the commutation relations between the matrices L_μ. For the special case of $M^{(1)}_{\mu\nu} = M^{(2)}_{\mu\nu}$, the matrices L_μ are square, and the relation (46) becomes

$$[M^{(1)}_{\mu\nu}, L_\lambda] = i\,(L_\nu \delta_{\mu\lambda} - L_\mu \delta_{\nu\lambda}). \tag{48}$$

On the other hand, we know that any relativistic equation for an elementary particle can be written in the form:[1]

$$\left(\frac{1}{i} L_\mu \frac{\partial}{\partial x_\mu} + \varkappa_0\right)\psi = 0, \tag{49}$$

where the L_μ are matrices satisfying (48). Thus the problem of finding the possible equations for elementary particles reduces to the problem of finding the possible non-completely-reducible representations of type (44) with $M^{(1)}_{\mu\nu} = M^{(2)}_{\mu\nu}$.

[1] Iu. M. Shirokov, J. Exptl. Theoret. Phys. (U.S.S.R.) **33**, 861 (1957), Soviet Phys. JETP **6**, 664 (1958).
[2] Iu. M. Shirokov, J. Exptl. Theoret. Phys. (U.S.S.R.) **33**, 1196 (1957), Soviet Phys. JETP, this issue, p. 919.
[3] E. P. Wigner, Ann. of Math. 40, 149 (1939).
[4] L. S. Pontriagin, Непрерывные группы (Continuous Groups), 2nd ed., Moscow, GITTL, 1954. (See also the English translation of the 1st edition: Topological Groups, Princeton University Press, 1946.)
[5] I. M. Gel'fand and A. M. Naimark, Journ. of Phys. (U.S.S.R.) 10, 93 (1946); M. A. Naimark, Usp. Mat. Nauk 9, 19 (1954), (Translation in Amer. Math. Soc. Translations, Ser. 2, Vol. 6, 1957.)
[6] F. D. Murnaghan, Theory of Group Representations, Johns Hopkins Press, 1938.
[7] I. M. Gel'fand and A. M. Iaglom, J. Exptl. Theoret. Phys. (U.S.S.R.) **18**, 703 (1948); H. J. Bhabha, Revs. Mod. Phys. **21**, 451 (1949).

Translated by M. Hamermesh
247

SOVIET PHYSICS JETP VOLUME 6 (33), NUMBER 5 MAY, 1958

EQUATIONS FOR THE GREEN'S FUNCTIONS OF A SYSTEM OF FUNDAMENTAL PARTICLES

V. G. SOLOV'EV

Joint Institute for Nuclear Research

Submitted to JETP editor May 3, 1957

J. Exptl. Theoret. Phys. (U.S.S.R.) **33**, 1215-12250 (November, 1957)

Green's functions for fundamental particles are introduced. On the basis of Lagrangians describing all strong interactions of mesons and baryons, closed systems of equations for the Green's functions are obtained in variational derivatives with respect to the external currents, in both three-dimensional and four-dimensional isotopic spin space.

THE scheme of Gell-Mann[1] for the description of heavy mesons and hyperons is well confirmed by the experimental data. On the basis of this scheme d'Espagnat and Prentki,[2,3] Salam,[4] Matthews and Salam,[5] and others have constructed Lagrangians that describe all the strong interactions of the fundamental particles.

The purpose of the present work is to obtain a complete system of equations for the Green's functions of the fundamental particles.

1. THE INTERACTION LAGRANGIAN. THE GREEN'S FUNCTIONS

Let us consider all the strong interactions of mesons and baryons. Let the spinors $\Lambda(x)$, $\Sigma(x)$, $\Xi(x)$, and $N(x)$ describe Λ, Σ, and Ξ hyperons and nucleons, and let the pseudoscalar $\varphi(x)$ and the scalar $k_1(x)$ describe π and K mesons, respectively. Furthermore we assume that in the isotopic spin space Λ is a scalar, $\varphi = \begin{pmatrix}\varphi_1\\ \varphi_2\\ \varphi_3\end{pmatrix}$ and $\Sigma = \begin{pmatrix}\Sigma_1\\ \Sigma_2\\ \Sigma_3\end{pmatrix}$ are pseudovectors, $N = \begin{pmatrix}p\\ n\end{pmatrix}$ and $k_1 = \begin{pmatrix}k^+\\ k^0\end{pmatrix}$ are

spinors of the first kind, and $\Xi = \begin{pmatrix} \Xi^0 \\ \Xi^- \end{pmatrix}$ are spinors of the second kind.[2]

On the basis of Ref. 4 we write the interaction Lagrangian in the following form:

$$L(x) = g_1 : \overline{N}^\tau(x)\gamma_5\tau^l\varphi^l(x)N(x): + g_2 : \overline{\Lambda}(x)\gamma_5\varphi^l(x)\Sigma^l(x) + \overline{\Sigma}^l(x)\varphi^l(x)\gamma_5\Lambda(x): + g_3\tfrac{1}{2i}\,\mathrm{Tr}\,(\tau^l\tau^k\tau^l) : \overline{\Sigma}^l(x)\gamma_5\varphi^k(x)\Sigma^l(x):$$
$$+ g_4 : \overline{\Xi}^\tau(x)\gamma_5\tau^l\varphi^l(x)\Xi(x): + g_5 : \overline{N}^\tau(x)\theta(x)\Lambda(x) + \overline{\Lambda}(x)\theta^{*\tau}(x)N(x): + g_6 : \overline{N}^\tau(x)\tau^l\Sigma^l(x)\theta(x) + \theta^{*\tau}(x)\overline{\Sigma}^l(x)\tau^l N(x):$$
$$+ g_7 : \overline{\Xi}^\tau(x)\tau_2\theta^*(x)\Lambda(x) + \overline{\Lambda}(x)\theta^\tau(x)\tau_2\Xi(x): + g_8 : \overline{\Xi}^\tau(x)\tau_2\tau^l\Sigma^l(x)\theta^*(x) + \theta^\tau(x)\tau^l\overline{\Sigma}^l(x)\tau_2\Xi(x):, \qquad (1)$$

where $\overline{\Psi} = \Psi^+\gamma_4$, the sign $^\mathrm{T}$ means transposition in the isotopic spin space, * means the complex conjugate, and the matrices γ are those of Feynman; θ and θ^* are constructed from $k_1 = \begin{pmatrix} k^+ \\ k^0 \end{pmatrix}$ and $\tilde{k}_1 = \begin{pmatrix} \tilde{k}^0 \\ \tilde{k}^- \end{pmatrix}$.[3] The summation over Latin indices is taken from 1 to 3, that over Greek indices from 1 to 4. The sign Sp means that the trace of the Dirac matrices is to be taken, and Tr means the trace of the isotopic spin matrices.

Let us also add to the Lagrangian (1) terms containing external currents, $l^l(x)$ for the π-meson field, and $\eta(x)$ and $\eta^*(x)$ for the K-meson field, namely the terms

$$L'(x) = l^l(x)\varphi^l(x) + \theta^{\tau*}(x)\eta_1(x) + \eta_1^{*\tau}(x)\theta(x). \qquad (2)$$

Besides the ordinary Green's functions

$$G_N(x, y) = i\langle T\{N(x)\overline{N}^\tau(y)S\}\rangle_0 / \langle S\rangle_0 \qquad (3)$$

and so on, let us introduce generalized Green's functions in which the external lines belong to different particles, namely

$$G_{N\Lambda}(x, y) = i\langle T\{N(x)\overline{\Lambda}(y)S\}\rangle_0 / \langle S\rangle_0 \qquad (4)$$

and so on.

The variational derivatives of these generalized Green's functions with respect to the external fields determine the cross-sections for the corresponding processes. For example, the transition amplitude for the process $\pi^- + p \to \Lambda + K_0$ is proportional to[6]

$$\int_{C_1} dp_1^0 \int_{C_2} dp_2^0 \overline{U}(p_2)\left\{\frac{\delta^2 G_{\Lambda N}(-p_1, -p_2)}{\delta\Phi^*(-k_1)\delta\theta(k_2)}\right\}_{\Phi=\theta=0} U(p_1), \qquad (5)$$

where the integration with respect to p_1^0 and p_2^0 is carried out along closed contours enclosing the points $p_1 = [p_1^2 + m_N^2]^{\frac{1}{2}}$ and $p_2 = [p_2^2 + m_\Lambda^2]^{\frac{1}{2}}$ and $\overline{U} = U^+\gamma_4$ and U are spinor functions. The variational derivatives are taken with respect to the external fields, which we define as follows:

$$\Phi^l(x) = \langle T\{\varphi^\tau(x)S\}\rangle_0 / \langle S\rangle_0, \qquad (6)$$
$$\Theta(x) = \langle T\{\theta(x)S\}\rangle_0 / \langle S\rangle_0. \qquad (6')$$

2. THE COMPLETE SYSTEM OF EQUATIONS FOR THE GREEN'S FUNCTIONS

In the derivation of the equations for the Green's functions we use the generalization given by N. N. Bogoliubov of Wick's theorem on the development of T-products of field operators. We assume that the spinors describing different fields anticommute. Confining ourselves to the strong interactions given by Eq. (1), we find the following system of equations for the Green's functions in variational derivatives with respect to the external currents:

$$\left(-i\gamma_\mu\frac{\partial}{\partial x_\mu} + m_N - g_1\gamma_5\tau^l\left(\Phi^l(x) - i\frac{\delta}{\delta J^l(x)}\right)\right)G_N(x, y) = \delta(x - y)$$
$$- g_5\left(\Theta(x) - i\frac{\delta}{\delta\eta_1^{*\tau}(x)}\right)G_{\Lambda N}(x, y) - g_6\tau^l\left(\Theta(x) - i\frac{\delta}{\delta\eta_1^{*\tau}(x)}\right)G^l_{\Sigma N}(x, y); \qquad (7)$$

$$\left\{-i\gamma_\mu\frac{\partial}{\partial x_\mu}+m_\Xi-g_4\gamma_5\tau^l\left(\Phi^l(x)-i\frac{\delta}{\delta l^l(x)}\right)\right\}G_\Xi(x,y)=\delta(x-y)$$
$$-g_7\tau_2\left(\Theta^*(x)+i\frac{\delta}{\delta\eta^\tau(x)}\right)G_{\Lambda\Xi}(x,y)-g_8\tau_2\tau^l\left(\Theta^*(x)+i\frac{\delta}{\delta\eta^\tau(x)}\right)G^l_{\Sigma\Xi}(x,y); \quad (8)$$

$$\left\{\left(-i\gamma_\mu\frac{\partial}{\partial x_\mu}+m_\Sigma\right)\delta_{il}-\frac{g_5}{2i}\,\mathrm{Tr}\,(\tau^i\tau^m\tau^l)\,\gamma_5\left(\Phi^m(x)-i\frac{\delta}{\delta l^m(x)}\right)\right\}G^{lk}_\Sigma(x,y)=\delta(x-y)+g_5\gamma_5\left(\Phi^l(x)-i\frac{\delta}{\delta l^l(x)}\right)G^k_{\Lambda\Sigma}(x,y)$$
$$-g_6\left(\Theta^{*\tau}(x)+i\frac{\delta}{\delta\eta(x)}\right)\tau^iG^k_{N\Sigma}(x,y)-g_8\left(\Theta^\tau(x)-i\frac{\delta}{\delta\eta^*(x)}\right)\tau^i\tau_2G^k_{\Xi\Sigma}(x,y); \quad (9)$$

$$\left\{-i\gamma_\mu\frac{\partial}{\partial x_\mu}+m_\Lambda\right\}G_\Lambda(x,y)=\delta(x-y)+g_5\gamma_5\left(\Phi^l(x)-i\frac{\delta}{\delta l^l(x)}\right)G^l_{\Sigma\Lambda}(x,y)$$
$$+\left(\Theta^{*\tau}(x)+i\frac{\delta}{\delta\eta(x)}\right)[g_5G_{N\Lambda}(x,y)+g_7\tau_2G_{\Xi\Lambda}(x,y)]; \quad (10)$$

$$\left\{-i\gamma_\mu\frac{\partial}{\partial x_\mu}+m_N-g_4\gamma_5\tau^l\left(\Phi^l(x)-i\frac{\delta}{\delta l^l(x)}\right)\right\}G_{N\Lambda}(x,y)$$
$$=g_5\left(\Theta(x)-i\frac{\delta}{\delta\eta^{*\tau}(x)}\right)G_\Lambda(x,y)+g_6\tau^l\left(\Theta(x)-i\frac{\delta}{\delta\eta^{*\tau}(x)}\right)G^l_{\Sigma\Lambda}(x,y)]; \quad (11)$$

$$\left\{-i\gamma_\mu\frac{\partial}{\partial x_\mu}+m_N-g_4\gamma_5\tau^k\left(\Phi^k(x)-i\frac{\delta}{\delta l^k(x)}\right)\right\}G^l_{N\Sigma}(x,y)$$
$$=g_5\left(\Theta(x)-i\frac{\delta}{\delta\eta^{*\tau}(x)}\right)G^l_{\Lambda\Sigma}(x,y)+g_6\tau^k\left(\Theta(x)-i\frac{\delta}{\delta\eta^{*\tau}(x)}\right)G^{kl}_\Sigma(x,y); \quad (12)$$

$$\left\{-i\gamma_\mu\frac{\partial}{\partial x_\mu}+m_\Lambda\right\}G^l_{\Lambda\Sigma}(x,y)=g_5\gamma_5\left(\Phi^k(x)-i\frac{\delta}{\delta l^k(x)}\right)G^{kl}_\Sigma(x,y)+g_5\left(\Theta^{*\tau}(x)+i\frac{\delta}{\delta\eta(x)}\right)G^l_{N\Sigma}(x,y)$$
$$-g_7\left(\Theta^\tau(x)-i\frac{\delta}{\delta\eta^*(x)}\right)\tau_2G^{l'}_{\Xi\Sigma}(x,y); \quad (13)$$

$$\left\{-i\gamma_\mu\frac{\partial}{\partial x_\mu}+m_\Xi-g_4\gamma_5\tau^l\left(\Phi^l(x)-i\frac{\delta}{\delta l^l(x)}\right)\right\}G_{\Xi\Lambda}(x,y)$$
$$=g_7\tau_2\left(\Theta^*(x)+i\frac{\delta}{\delta\eta^\tau(x)}\right)G_\Lambda(x,y)+g_8\tau_2\tau^l\left(\Theta^*(x)+i\frac{\delta}{\delta\eta^\tau(x)}\right)G^l_{\Sigma\Lambda}(x,y); \quad (14)$$

$$\left\{-i\gamma_\mu\frac{\partial}{\partial x_\mu}+m_\Xi-g_4\gamma_5\tau^k\left(\Phi^k(x)-i\frac{\delta}{\delta l^k(x)}\right)\right\}G^l_{\Xi\Sigma}(x,y)$$
$$=g_7\tau_2\left(\Theta^*(x)+i\frac{\delta}{\delta\eta^\tau(x)}\right)G^l_{\Lambda\Sigma}(x,y)+g_8\tau_2\tau^k\left(\Theta^*(x)+i\frac{\delta}{\delta\eta^\tau(x)}\right)G^{kl}_\Sigma(x,y); \quad (15)$$

$$(\Box-\mu_\pi^2)\,\Phi^l(x)=-I^l(x)+ig_1\,\mathrm{Sp}\,\mathrm{Tr}\,\gamma_5\tau^lG_N(x,x)-ig_2\,\mathrm{Sp}\,\mathrm{Tr}\,\gamma_5G^l_{\Sigma\Lambda}(x,x)-ig_2\,\mathrm{Sp}\,\mathrm{Tr}\,\gamma_5G^l_{\Lambda\Sigma}(x,x)$$
$$-\frac{g_5}{2}\,\mathrm{Tr}\,(\tau^i\tau^l\tau^k)\,\mathrm{Sp}\,\mathrm{Tr}\,\gamma_5G^{kl}_\Sigma(x,x)-ig_4\,\mathrm{Sp}\,\mathrm{Tr}\,\gamma_5\tau^lG_\Xi(x,x); \quad (16)$$

$$(\Box-\mu_K^2)\Theta(x)=-\eta_l(x)-ig_5\,\mathrm{Sp}\,G_{N\Lambda}(x,x)-ig_6\,\mathrm{Sp}\,\tau^lG^l_{N\Sigma}(x,x)-ig_7\,\mathrm{Sp}\,\tau_2G^{(\tau)}_{\Lambda\Xi}(x,x)+ig_8\,\mathrm{Sp}\,\tau_2\tau^lG^{l(\tau)}_{\Sigma\Xi}(x,x). \quad (17)$$

The equations for $G_{\Lambda N}(x,y)$, $G^\ell_{\Sigma\Xi}(x,y)$, $G^\ell_{\Sigma\Lambda}(x,y)$, $G_{\Lambda\Xi}(x,y)$, and $G^\ell_{\Sigma\Xi}(x,y)$ are analogous to Eqs. (11), (12), (13), (14), and (15). It is not hard to obtain them if we apply the appropriate operators acting from the right on the variable y; for example, we find the equation for $G_{\Lambda N}(x,y)$ in the form

$$G_{\Lambda N}(x,y)\left\{i\gamma_\mu\frac{\overleftarrow{\partial}}{\partial y_\mu}+m_N-g_1\gamma_5\tau^l\left(\Phi^l(y)-i\frac{\delta}{\delta l^l(y)}\right)\right\}=\left(\Theta^{*\tau}(y)+i\frac{\delta}{\delta\eta(y)}\right)[g_5G_\Lambda(x,y)+g_6\tau^lG^l_{\Lambda\Sigma}(x,y)]. \quad (11')$$

The functions $G^{(T)}_{\Xi\Lambda}(x,y)=i\langle T\{\Xi^T(x)\Lambda(y)S\}\rangle_0/\langle S\rangle_0$, $G^{(T)}_{\Lambda\Xi}(x,y)$, $G^{\ell(T)}_{\Xi\Sigma}(x,y)$, and $G^{\ell(T)}_{\Sigma\Xi}(x,y)$ satisfy equations obtained from Eqs. (14) and (15) by carrying out transpositions in the isotopic spin space.

The system of equations (7) – (17) is a closed one. This system of equations is exact; it does not involve any approximations.

The system (7) – (17) must be supplemented if in addition to the scalar θ mesons there are also pseudoscalar τ mesons. Some of the equations are considerably changed in case the hyperons (for example Σ) turn out to have spin greater than $\frac{1}{2}$.

It is easy to obtain from the complete system of equations (7) – (17) the partial closed system essential to the treatment of any given concrete process, if one confines oneself to part of the terms of the Lagrangian (1).

3. THE EQUATIONS FOR THE GREEN'S FUNCTIONS IN THE FOUR-DIMENSIONAL ISOTOPIC SPIN SPACE

The system of equations (7) – (17) for the Green's functions not only is very cumbersome, but also contains eight independent interaction constants. To reduce the number of coupling constants, Matthews and Salam[5] have formally expressed all the strong interactions in a four-dimensional isotopic spin space, without making any essential change in the d'Espagnat-Prenkti formulation of the Gell-Mann scheme. We shall use the interaction Lagrangian obtained in Ref. 5 to find the equations for the Green's functions in a compact form containing only three independent coupling constants.

For this purpose we introduce the following isotopic spinors

$$\Psi = \begin{pmatrix} N \\ \Xi \end{pmatrix}, \quad \mathscr{R} = \begin{pmatrix} \theta \\ \tilde{\theta} \end{pmatrix},$$

and tensors $\Sigma_{\mu\nu} = \begin{pmatrix} \Lambda & -i\Sigma_3 & i\Sigma_2 & 0 \\ i\Sigma_3 & \Lambda & -i\Sigma_1 & 0 \\ -i\Sigma_2 & i\Sigma_1 & \Lambda & 0 \\ 0 & 0 & 0 & \Lambda \end{pmatrix}$,

$$\pi_{\mu\nu} = \begin{pmatrix} 0 & -i\varphi_3 & i\varphi_2 & 0 \\ i\varphi_3 & 0 & -i\varphi_1 & 0 \\ -i\varphi_2 & i\varphi_1 & 0 & 0 \\ 0 & 0 & 0 & 0 \end{pmatrix},$$

where $\theta = \begin{pmatrix} \theta_1 \\ \theta_2 \end{pmatrix}$, $\tilde{\theta} = \begin{pmatrix} \theta_2^* \\ \theta_1^* \end{pmatrix}$.

We write the interaction Lagrangian in the form

$$L(x) = \frac{f_1}{2} : \overline{\Psi}^{\tau}(x)\,\Gamma_4\Gamma_\mu\Gamma_\nu\,\mathscr{R}(x)\,\Sigma_{\mu\nu}(x) + \overline{\Sigma}_{\nu\mu}(x)\,\mathscr{R}^{*\tau}(x)\,\Gamma_\nu\Gamma_\mu\Gamma_4\Psi(x) : + \frac{f_2}{2} : \overline{\Psi}^{\tau}(x)\,\Gamma_4\Gamma_\mu\Gamma_\nu\gamma_5\Psi(x) : \pi_{\mu\nu}(x)$$
$$+ \frac{f_3}{2}\,\mathrm{Sp}\,\gamma_\mu\gamma_\nu\gamma_\rho\gamma_\sigma\gamma_\alpha\gamma_\beta : \overline{\Sigma}_{\mu\nu}(x)\,\gamma_5\Sigma_{\rho\sigma}(x)\,\pi_{\alpha\beta}(x) : + \frac{1}{2}\,I_{\mu\nu}(x)\,\pi_{\mu\nu}(x) + H^{*\tau}(x)\,\mathscr{R}(x) + \mathscr{R}^{*\tau}(x)\,H(x). \qquad (18)$$

Here the Γ are matrices in the four-dimensional isotopic spin space, and

$$\Gamma_\mu\Gamma_\nu + \Gamma_\nu\Gamma_\mu = \delta_{\mu\nu}, \quad \Gamma_k = \begin{pmatrix} \tau^k & 0 \\ 0 & \tau^k \end{pmatrix}, \quad \Gamma_4 = \begin{pmatrix} I & 0 \\ 0 & -I \end{pmatrix}.$$

We determine the Green's functions from

$$G(x,y) = i\,\langle T\{\Psi(x)\,\overline{\Psi}^{\tau}(y)\,S\}\rangle_0 / \langle S\rangle_0 = i\,\frac{1}{\langle S\rangle_0}\,\langle T\left\{\begin{pmatrix} N(x)\,\overline{N}^{\tau}(y) & N(x)\,\overline{\Xi}^{\tau}(y) \\ \Xi(x)\,N^{\tau}(y) & \Xi(x)\,\overline{\Xi}^{\tau}(y) \end{pmatrix} S\right\}\rangle_0; \qquad (19)$$

$$G_{\mu\nu;\rho\sigma}(x,y) = i\,\langle T\{\Sigma_{\mu\nu}(x)\,\overline{\Sigma}_{\rho\sigma}(y)\,S\}\rangle_0 / \langle S\rangle_0; \qquad (20)$$

$$G^{\mu\nu}_{\Psi\Sigma}(x,y) = i\,\langle T\{\Psi(x)\,\overline{\Sigma}_{\mu\nu}(y)\,S\}\rangle_0 / \langle S\rangle_0; \qquad (21)$$

$$G^{\mu\nu}_{\Sigma\Psi}(x,y) = i\,\langle T\{\Sigma_{\mu\nu}(x)\,\overline{\Psi}^{\tau}(y)\,S\}\rangle_0 / \langle S\rangle_0; \qquad (21')$$

$$\Pi_{\mu\nu}(x) = \langle T\{\pi_{\mu\nu}(x)\,S\}\rangle_0 / \langle S\rangle_0; \qquad (22)$$

$$K(x) = \langle T\{\mathscr{L}(x)S\}\rangle_0 / \langle S\rangle_0; \tag{23}$$

$$K^*(x) = \langle T\{\mathscr{L}^*(x)S\}\rangle_0 / \langle S\rangle_0. \tag{23'}$$

We obtain the complete system of equations for the Green's functions of the fundamental particles in the following form:

$$\left\{-i\gamma_{\mu'}\frac{\partial}{\partial x_{\mu'}} + M - \frac{f_2}{2}\Gamma_4\Gamma_\mu\Gamma_\nu\gamma_5\left(\Pi_{\mu\nu}(x) - 2i\frac{\delta}{\delta l_{\mu\nu}(x)}\right)\right\} G(x,y) = \delta(x-y) - \frac{f_1}{2}\Gamma_4\Gamma_\mu\Gamma_\nu\left(K(x) - i\frac{\delta}{\delta H^{*\tau}(x)}\right) G^{\mu\nu}_{\Sigma\Psi}(x,y); \tag{24}$$

$$\left\{-i\gamma_{\mu'}\frac{\partial}{\partial x_{\mu'}} + M - \frac{f_2}{2}\Gamma_4\Gamma_\rho\Gamma_\sigma\gamma_5\left(\Pi_{\rho\sigma}(x) - 2i\frac{\delta}{\delta l_{\rho\sigma}(x)}\right)\right\} G^{\mu\nu}_{\Psi\Sigma}(x,y) = \frac{f_1}{2}\Gamma_4\Gamma_\rho\Gamma_\sigma\left(K(x) - i\frac{\delta}{\delta H^{*\tau}(x)}\right) G_{\rho\sigma;\mu\nu}(x); \tag{25}$$

$$G^{\mu\nu}_{\Sigma\Psi}(x,y)\left\{i\gamma_{\mu'}\frac{\partial}{\partial y_{\mu'}} + M - \frac{f_2}{2}\Gamma_4\Gamma_\rho\Gamma_\sigma\gamma_5\left(\Pi_{\rho\sigma}(y) - 2ii\frac{\delta}{\delta l_{\rho\sigma}(y)}\right)\right\} = \frac{f_1}{2}\left(K^{*\tau}(y) + i\frac{\delta}{\delta H(y)}\right)\Gamma_\rho\Gamma_\sigma\Gamma_4 G_{\mu\nu;\rho\sigma}(x,y); \tag{25'}$$

$$\left\{\left(-i\gamma_{\mu'}\frac{\partial}{\partial x_{\mu'}} + M_1\right)\delta_{\alpha\beta} - \frac{f_3}{2}\mathrm{Sp}\left(\gamma_\pi\gamma_\tau\gamma_i\gamma_\varkappa\gamma_\beta\right)\gamma_5\left(\Pi_{\pi\tau}(x) - 2i\frac{\delta}{\delta l_{\pi\tau}(x)}\right)\right\} G_{\varkappa\beta,\rho\sigma}(x,y)$$
$$= 4\delta_{\rho\sigma}\delta(x-y) + 8f_1\left(K^{*\tau}(x) + i\frac{\delta}{\delta H(x)}\right)\Gamma_4 G^{\rho\sigma}_{\Psi\Sigma}(x,y); \tag{26}$$

$$\left\{\left(-i\gamma_{\mu'}\frac{\partial}{\partial x_{\mu'}} + M_1'\right)(\Gamma_\alpha\Gamma_\beta - \delta_{\alpha\beta}) + \frac{f_3}{16}(\Gamma_m\Gamma_n - \delta_{mn})\,\mathrm{Sp}\left[(\gamma_m\gamma_n - \delta_{mn})\gamma_\pi\gamma_\tau\gamma_\alpha\gamma_\beta\right]\gamma_5\left(\Pi_{\pi\tau}(x) - 2i\frac{\delta}{\delta l_{\pi\tau}(x)}\right)\right\} G_{\varkappa\beta;\rho\sigma}(x,y)$$
$$= 2(\delta_{\rho\sigma} - \Gamma_\rho\Gamma_\sigma)\delta(x-y) - 2f_1\Gamma_n\left(K^{*\tau}(x) + i\frac{\delta}{\delta H(x)}\right)\Gamma_n G^{\rho\sigma}_{\Psi\Sigma}(x,y), \tag{26'}$$

$$(\Box - \mu_n^2)\Pi_{mn}(x) = -I_{mn}(x) - if_2\,\mathrm{Sp}\,\mathrm{Tr}\,\Gamma_4\Gamma_m\Gamma_n\gamma_5 G(x,x) + \frac{i}{16}f_3\,\mathrm{Sp}\,\gamma_\alpha\gamma_\beta\gamma_\sigma\gamma_\tau\gamma_m\gamma_n\cdot\mathrm{Sp}\,\mathrm{Tr}\,\gamma_5 G_{\rho\sigma;\varkappa\beta}(x,x); \tag{27}$$

$$(\Box - \mu_K^2)K(x) = -H(x) - i\frac{f_1}{2}\,\mathrm{Sp}\,\Gamma_\nu\Gamma_\mu\Gamma_4 G^{\nu\mu}_{\Psi\Sigma}(x,x). \tag{28}$$

On going over from the four-dimensional to the three-dimensional isotopic spin space the system of equations (24) – (28) goes over into a system closely similar to Eqs. (7) – (17), if in the latter we express the interaction constants g_i in terms of the f_i by the formulas:

$$2g_5 = -2g_7 = g_6 = -g_8 = f_1, \quad g_1 = -g_4 = f_2, \quad g_3 = g_2 = f_3.$$

[1] M. Gell-Mann and A. Pais, Proceedings of Glasgow Conference on Nuclear and Meson Physics, p. 342, 1954.

[2] B. d'Espagnat and J. Prentki, Phys. Rev. 99, 328 (1955).

[3] B. d'Espagnat and J. Prentki, Phys. Rev. 102, 1684 (1956); Nuclear Physics 1, 33 (1956).

[4] A. Salam, Nuclear Physics 2, 173 (1956).

[5] P. Matthews and A. Salam, Nuclear Physics 2, 582 (1956).

[6] V. G. Solov'ev, Dissertation, Moscow State University, 1956.

Translated by W. H. Furry
248

THE INTERACTION OF SLOW π MESONS WITH NUCLEI

A. M. BALDIN and A. I. LEBEDEV

P. N. Lebedev Physics Institute, Academy of Sciences, U.S.S.R.

Submitted to JETP editor May 4, 1957

J. Exptl. Theoret. Phys. (U.S.S.R.) 33, 1221-1226 (November, 1957)

The influence of the interaction of charged mesons with a nucleus on the cross section of the production of mesons on nuclei is considered for the case in which the meson wavelength exceeds the size of the nucleus. A relation is obtained connecting the cross section of photoproduction of mesons with the shifts and widths of mesoatomic levels. Comparison with experimental data permits some conclusions concerning the interaction of mesons with groups of nucleons and the mechanism of the photoproduction of mesons on nuclei.

1. INTRODUCTION

THE interaction of the meson field with groups of nucleons is of decided interest. Information concerning this interaction is obtained from the analysis of data on the scattering and the production of mesons on nuclei.[1] However, these works are usually concerned with the interaction of rather energetic mesons. The interpretation of the data is then strongly dependent on the model representations, and in particular on the form of the effective potential of the meson-nucleus interaction. In order to talk about the interaction of the meson field with a group of nucleons, it is reasonable to consider effects in which the meson wavelength is considerably greater than the size of the nucleon group. One such effect is radiation during mesoatomic transitions.[2] Along this line are the great advances in the measurement of the shifts and the evaluation of the widths of the mesoatomic levels, which may be interpreted in terms of the specifically nuclear interaction between the meson and the nucleus.

The purpose of the present work is the investigation of effects which may yield similar information. We have in mind the scattering and creation on nuclei of mesons whose wavelengths are greater than the nuclear dimensions. These effects have their own peculiarities. The most important role is played by the meson-nucleus Coulomb interaction. It is true that these effects are less "pure" than radiation during mesoatomic transitions. However, they still have some advantages, namely, the possibility of varying the meson wavelength within known limits, and the possibility of studying the interactions between mesons of various signs and nuclei of all the elements in the periodic system. Moreover, on the basis of the study of these effects, conclusions may be drawn with regard to the mechanism of the creation of mesons on the nucleus. As regards the possibilities for the experimental study of these effects, there is at present already some data on the photoproduction of slow mesons,[3,4] which we will discuss below in comparison with our theory.

2. THE INTERACTION OF π MESONS WITH NUCLEI

The wave function of the relative motion of the meson and the nucleus, outside the nucleus, will be a linear combination of regular and non-regular eigenfunctions of the Hamiltonian H_0, which in the case of charged π mesons contains the Coulomb interaction Ze^2/r in addition to the kinetic energy operator. For a definite angular momentum l, the wave function has the form

$$\psi_l(kr) = \sqrt{\frac{2}{\pi}}\frac{1}{kr}\{AF_l(kr) + BG_l(kr)\}, \tag{1}$$

where the constants A and B may be determined by using a concrete model for the meson-nucleus interaction potential for $r \leq r_Z$ [$r_Z = (\hbar/\mu c)A^{1/3}$ is the radius of a nucleus with atomic number Z], or they may be expressed by the shifts and widths of the mesoatomic levels by considering the interaction potential v' inside the nucleus to be a perturbation v on the Hamiltonian H_0.

The wave function φ of a meson interacting with a nucleus must satisfy the following integral equation:

$$\psi^{\pm} = \chi + \frac{1}{E \pm i\varepsilon - H_0} v\psi^{\pm}. \tag{2}$$

Limiting ourselves to the first order perturabtion theory and writing Eq. (2) in the $|r|, l, m$ representation, we find

$$\psi_l^{+}(kr) \approx \chi_l(kr) + \int \frac{\int \chi_l^{*}(kr')\, v(r')\, \chi_l(k'r')\, r'^2\, dr'}{E_k \pm i\varepsilon - E_{k'}} \chi_l(k'r')\, k'^2\, dk', \tag{3}$$

where ϵ is an infinitely small quantity and $\chi_l(kr) = \sqrt{2/\pi} F_l(kr)/kr$ is the regular eigenfunction of the operator H_0 with the eigenvalue E_k. For charged π mesons, $\chi_l(kr)$ is expressed by a hypergeometric function and as $r \to \infty$ has the form

$$\chi_l(kr)_{r\to\infty} = \sqrt{\frac{2}{\pi}} \frac{1}{kr} \sin\left(kr - \alpha \ln 2kr - \frac{l\pi}{2} + \eta_l\right).$$

Integrating Eq. (3) with $r \to \infty$ and letting ϵ approach zero, we obtain the following asymptotic form for the function $\varphi_l^{\pm}(kr)$:

$$\psi_l^{\pm}(kr)_{r\to\infty} = \sqrt{\frac{2}{\pi}} \frac{1}{kr} \left\{\left(1 \pm iI_l\right) \sin\left(kr - \alpha \ln 2kr - \frac{l\pi}{2} + \eta_l\right) + I_l \cos\left(kr - \alpha \ln 2kr - \frac{l\pi}{2} + \eta_l\right)\right\}, \tag{4}$$

where

$$I_l = -\frac{\pi\mu k}{\hbar^2} \int_0^{\infty} |\chi_l(kr)|^2\, v(r)\, r^2\, dr = -\frac{2\mu}{k\hbar^2} \int_0^{\infty} |F_l(kr)|^2\, v(r)\, dr. \tag{5}$$

Remembering that in Eq. (1)

$$G_l(kr)_{r\to\infty} = \cos\left(kr - \alpha \ln 2kr - \frac{l\pi}{2} + \eta_l\right),$$

and comparing the asymptotic forms of Eqs. (1) and (4), we find that $A = 1 \pm iI_l$ and $B = I_l$. If I_l is small, then

$$\psi_l^{\pm}(kr) \approx \sqrt{\frac{2}{\pi}} \frac{1}{kr} e^{\pm iI_l} \{F_l(kr) + I_l G_l(kr)\}. \tag{6}$$

In the remainder of this section we will limit ourselves to the case $l = 0$ and will consider the interactions of π^- mesons with light nuclei ($Z < 15$), for which $r_Z \ll R$, where $2R = a$ is the radius of the lowest mesonic orbit: $R = \hbar^2/2\mu Ze^2$. We will express I_0 through the shift and width ΔE of the 1S level of the mesoatom.* In the first order of perturbation theory we have

$$\Delta E \approx \frac{1}{2R^2} \int v(r)\, r^2\, dr. \tag{7}$$

Since we are considering slow mesons ($kr \ll 1$), the functions $F_0(kr)$ and $G_0(kr)$ in a region of the order of the dimensions of the nucleus will have the form

$$F_0(kr) \approx C_0 kr, \quad G_0(kr) \approx \frac{1}{C_0}\left\{1 - \frac{r}{R}\left[\ln\frac{r}{R} + 2\gamma - 1 + h(\alpha)\right]\right\};$$
$$h(\alpha) = \alpha^2 \sum_{n=1}^{\infty} \frac{1}{n(n^2+\alpha^2)} - \ln|\alpha| - \gamma; \quad C_0^2 = \frac{2\pi|\alpha|}{1 - e^{-2\pi|\alpha|}}; \quad \alpha = -\frac{Ze^2}{\hbar c}\sqrt{\frac{\mu c^2}{2E_\pi}}; \quad \gamma = 0.5772\ldots \tag{8}$$

Now, using Eq. (5), we obtain

$$I_0 = -\frac{2\mu C_0^2 k}{\hbar^2} \int v(r)\, r^2\, dr = -\frac{4\mu C_0^2 kR^3}{\hbar^2} \Delta E. \tag{9}$$

*ΔE is a complex quantity. Im(ΔE) (width of mesoatomic level) is connected with the interaction that leads to meson absorption. The level shift Re(ΔE) is due to nuclear as well as to non-nuclear interactions. The part of Re(ΔE) which arises from a specifically nuclear interaction has been measured experimentally.[2]

3. PRODUCTION OF SLOW MESONS

If the interaction leading to meson production is either weak (for example, photoproduction) or very strong (production during collisions of nucleons with nuclei), the production matrix element may be written in the form[5]

$$T \approx (\varphi^-, U\psi^{0+}), \tag{10}$$

where φ^- is the wave function of the final state, U is the interaction leading to meson production, and the wave function ψ^{0+} is independent of the interaction in the final state. Summing and integrating over all variables in this expression, with the exception of the meson-nucleus relative coordinate, we find that the corss section for meson production is

$$\sigma = W \left| \int \varphi^- (kr)\, T(\mathbf{r})\, d\mathbf{r} \right|^2. \tag{11}$$

where W is the usual factor connecting the square of the transition amplitude with the transverse cross section, and $T(\mathbf{r})$ differs from zero in the region where meson production occurs, i.e., in a region on the order of the nuclear dimensions.

Using the theorem of the mean, we take the wave function $\varphi^-(\mathbf{kr})$ at some mean point of the interval $0 \leq r_m \leq r_Z$ out in Eq. 11:

$$\sigma = W \left| \frac{\varphi^- (kr_m)}{\varphi^0 (kr_m)} \right|^2 \left| \int \varphi^0 (kr)\, T(\mathbf{r})\, d\mathbf{r} \right|^2 = \left| \frac{\varphi^- (kr_m)}{\varphi^0 (kr_m)} \right|^2 \sigma^0, \tag{12}$$

where σ^0 is the production cross section without taking account of the interaction in the final state, and $\varphi^0(\mathbf{kr})$ is the wave function for free motion.

Let us suppose that $r_m = r_Z$. Then the function in Eq. (1) may be used as $\varphi^-(\mathbf{kr})$, if production occurs in a state with definite momentum ℓ. In the case of S-production of slow π^- mesons, this function is

$$\varphi_0^- (kr) = \sqrt{\frac{2}{\pi}} \frac{1}{kr} \{AF_0(kr) + BG_0(kr)\}. \tag{13}$$

For light nuclei, the functions $F_0(\mathbf{kr})$ and $G_0(\mathbf{kr})$ have the form of Eq. (8). The factor $|\varphi_0^-(\mathbf{kr}_Z)/\varphi_0^0(\mathbf{kr}_Z)|^2$ is expressed in this case ($\varphi_0^0(\mathbf{kr}) = \sqrt{2/\pi}\ \sin kr/kr$) by the width and shift of the mesoatomic level. If data were available at present regarding the cross section of the production of slow mesons on light nuclei as a function of Z, and also regarding the widths and shifts of the mesoatomic levels, the above relations could be used to draw conclusions regarding the mechanism of meson production on nuclei. The functions $F_0(\mathbf{kr})$ and $G_0(\mathbf{kr})$ presented above are not suitable for heavier nuclei ($Z > 15$), because in this case the radius of the Bohr orbit becomes comparable to the radius of the nucleus. For the case of a Coulomb field of repulsion, expansions of $F_\ell(\mathbf{kr})$ and $G_\ell(\mathbf{kr})$ with respect to kr are known[6] which do not use the smallness of r/R. These expansions are easily obtained for an attractive field by changing the sign of R and going to Bessel functions with imaginary arguments. Then for $\ell = 0$, we have

$$F_0(kr) = C_0 kr \left\{ \left(\frac{r}{R}\right)^{1/2} J_1\left[2\left(\frac{r}{R}\right)^{1/2}\right] - \frac{(kr)^2}{3}\left(\frac{r}{R}\right)^{-1} J_2\left[2\left(\frac{r}{R}\right)^{1/2}\right] + \cdots \right\}, \quad G_0(kr) = \frac{1}{C_0}\left\{ -\left(\frac{r}{R}\right)^{1/2} \pi Y_1\left[2\left(\frac{r}{R}\right)^{1/2}\right] \right.$$
$$\left. - h(\alpha)\left(\frac{r}{R}\right)^{1/2} J_1\left[2\left(\frac{r}{R}\right)^{1/2}\right] + \frac{(kr)^2}{3}\left[\left(\frac{r}{R}\right)^{-1/2} J_1\left[2\left(\frac{r}{R}\right)^{1/2}\right] + \pi Y_2\left[2\left(\frac{r}{R}\right)^{1/2}\right] + h(\alpha) J_2\left[2\left(\frac{r}{R}\right)^{1/2}\right]\right] - \cdots \right\}, \tag{14}$$

where J_1, J_2, Y_1 and Y_2 are Bessel functions of the first and second order, of the first and second kinds, respectively. The factor $|\varphi_0^-(\mathbf{kr}_Z)/\varphi_0^0(\mathbf{kr}_Z)|^2$ is determined for all nuclei by the constants A and B, which may be determined by joining the logarithmic derivatives at the boundary of the nucleus.

4. MODEL OF THE MESON-NUCLEUS INTERACTION POTENTIAL FOR $\ell = 0$

Since we are considering the interactions of mesons with wavelengths much greater than the dimensions of the region in which nuclear forces act, we may expect that our conclusions will depend only weakly on the model, i.e., on the form of the potential. We will therefore consider it to be constant: $V' = V_0 + iK + V'$, where $V_0 + iK$ is the specifically nuclear interaction between the π meson and the nucleus, and V' contains all the non-nuclear interactions, among which we will consider only the electrostatic potential,

since the calculated results do not depend critically on the magnitude of the real part of the potential. For the same reason, we will consider V' equal to the value of the Coulomb potential at the boundary of the nucleus. For the potential V_0, we will use a value ~ 5 Mev, which corresponds to the magnitude and sign of the shift of the 1s level ($\mathrm{Re}(\Delta E)_{\mathrm{nucl}}$) in mesoatoms.[7-9] The quantity K must have a value of 1 – 2 Mev in order to conform to the observed width of the mesoatomic level.[10-12]

The potential v' is independent of meson energy for small energies.

5. PHOTOPRODUCTION OF SLOW π MESONS

Using the proposed model, it was possible to interpret the experimental data[3,4] on the photoproduction of very slow π^- mesons (with mean energy of 2 Mev) on nuclei of various elements (see also Ref. 13). Since in this case, the mesons are produced in the form of an S-wave, the production cross section based on Eqs. (12) and (13) is*

$$\sigma_Z = \left|\frac{\sin kr_Z}{kr_Z}\right|^{-2} \sigma^0 \{[F_0(kr_Z)\, b_Z r_Z - r_Z F_0'(kr_Z)]^2 + [r_Z G_0'(kr_Z) - G_0(kr_Z)\, b_Z r_Z]^2\}^{-1};$$

$$b = \frac{\beta \sinh 2\beta r + \gamma \sin 2\gamma r}{\cosh 2\beta r - \cos 2\gamma r} + i\,\frac{\gamma \sinh 2\beta r - \beta \sin 2\gamma r}{\cosh 2\beta r - \cos 2\gamma r}; \qquad (15)$$

$$\beta = \left(\frac{\mu}{\hbar^2}\right)^{1/2}\left[\sqrt{(V_0 + V' - E_\pi)^2 + K^2} + (V_0 + V' - E_\pi)\right]^{1/2}; \quad \gamma = \left(\frac{\mu}{\hbar^2}\right)^{1/2}\left[\sqrt{(V_0 + V' - E_\pi)^2 + K^2} - (V_0 + V' - E_\pi)\right]^{1/2}.$$

It follows from Eq. (15) that the finite dimensions of the nucleus have a very strong effect on the influence of the Coulomb field of the nucleus on the photoproduction of mesons. In fact, if the nucleus was a point ($r_2 \to 0$), then $\sigma = C_0^2\, \sigma^0$. For slow mesons, C_0^2 is a large quantity, depending sharply on Z. The photoproduction cross section would then increase very rapidly with increasing atomic number, which is not observed experimentally.[3,4] For ~ 2 Mev mesons, for example, the factor C_0^2 leads to a transverse cross section for heavy nuclei 20 – 40 times greater than that for light nuclei, while the ratio σ_Z/σ_L calculated by Eq. (15) is only 2.5 – 5. Experiment gives 4.0 ± 1.0 for this ratio.[3]

Let us assume volume photoproduction of mesons,

$$\sigma^0 = \text{const}\ (A - Z)\ \sigma^0_{\mathrm{nucl}} \qquad (16)$$

We shall try to explain the experimentally observed Z-dependence of the π^--meson yield by reabsorption, i.e., we shall pick a value for K which yields agreement between the calculated and the observed dependence of σ on Z.

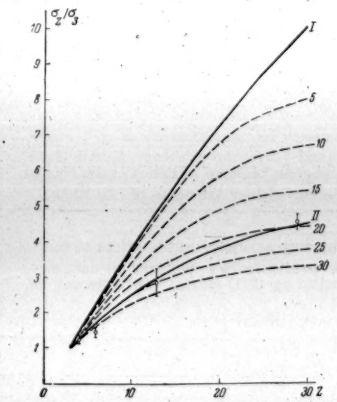

The Z-dependence of the ratio σ_Z/σ_3. The solid curves I and II were calculated for K = 0 from Eq. (15) for the case of volume and surface meson production, respectively. The dotted curves were calculated for volume production, taking account of self-absorption; the corresponding values of K are indicated alongside each curve. The experimental points were taken from Ref. 4.

The experimentally obtained Z-dependence of the ratio σ_Z/σ_3 of the photoproduction cross sections for slow mesons, and also curves calculated from Eq. (15) taking account of Eq. (16), are shown in the figure. As is clear from the figure, the magnitude of the imaginary part of the potential must be taken as K = 15 – 20 Mev in order to explain the experimental data. This value disagrees sharply with the value of K = 1 – 2 Mev obtained from mesoatom data.[10-12]

Thus, assumption (16) does not correspond to reality.

On the other hand, the curve calculated on the assumption of surface photoproduction of mesons with K = 0 (the curve calculated with K = 1.5 Mev practically coincides with this curve) agrees well with experiment.

*The primes on F(kr) and G(kr) denote differentiation with respect to r.

6. CONCLUSIONS

(a) According to the theory presented here, the mechanism of meson reabsorption cannot explain the dependence of the photoproduction cross section on atomic number. Some mechanism must be introduced to forbid meson production inside the nucleus. This result was obtained on the basis of a concrete model of the meson-nucleus interaction potential. However, since the interaction of mesons with wavelengths considerably greater than the nuclear dimensions are considered, the results do not depend critically on the choice of the model.*

(b) Without referring to a model of the potential, the same result may be obtained on the basis of the material presented in Sec. 2, if data on the photoproduction of mesons of low energy on light nuclei ($Z < 15$) and on the shifts and widths of mesoatomic levels are accumulated.

(c) The finite dimensions of the nucleus have a great influence on the photoproduction of slow mesons by sharply changing the action of the Coulomb field.†

[1] Frank, Gamel, and Watson, Phys. Rev. **101**, 891 (1956).
[2] M. Stearns and M. B. Stearns, Phys. Rev. **103**, 1534 (1956).
[3] E. G. Gorzhevskaia and N. M. Panova, Dokl. Akad. Nauk SSSR **111**, 1205 (1956). Soviet Phys. "Doklady" **1**, 757 (1956).
[4] Belousov, Popova, Semashko, Shitov, Tamm, Veksler, and Iagudina, Proc. CERN Symp. Geneva **2**, 288 (1956).
[5] K. M. Watson, Phys. Rev. **88**, 1163 (1952).
[6] J. D. Jackson and J. M. Blatt, Revs. Mod. Phys. **22**, 77 (1950).
[7] H. A. Bethe and R. R. Wilson, Phys. Rev. **83**, 690 (1951).
[8] H. A. Bethe and F. de Hoffman, Mesons and Fields, Vol 2, Sec. 33h, New York, 1955.
[9] Deser, Goldberger, Baumann, and Thirring, Phys. Rev. **96**, 774 (1955).
[11] D. West and E. F. Bradley, Phil. Mag. **1**, 97 (1956).
[12] R. Karplus and F. Halpern, Proc. Sixth Rochester Conf., IX-33, 1956.
[13] A. M. Baldin, Proc. CERN Symp. Geneva **2**, 272 (1956).

Translated by D. Lieberman
249

*Effects connected with the increase of the yield of low-energy mesons because of the rescattering of higher-energy mesons lead only to an increase of the slow meson output with an increase of Z. Thus, these effects will not influence our conclusions.

†The ratio of the yields of positive and negative mesons, which is very sensitive to the effect of the Coulomb interaction, is described well by Eq. (15) (according to the preliminary experimental data of Popova, Semashko, and Iagudina, private communication).

OSCILLATIONS OF A FERMI-LIQUID IN A MAGNETIC FIELD

V. P. SILIN

P. N. Lebedev Physics Institute, Academy of Sciences, U.S.S.R.

Received by JETP editor May 6, 1957

J. Exptl. Theoret. Phys. (U.S.S.R.) 33, 1227-1234 (November, 1957)

A study is made of the spin oscillations of a paramagnetic Fermi-liquid (He^3) placed in a constant magnetic field at low temperatures, where collisions can be ignored.

LANDAU, using a phenomenological theory,[1] has carried out an investigation of the oscillations of a Fermi-liquid[2] by generalizing certain results obtained earlier for a gas with weak interactions[3,4] (also see Ref. 5). In particular, he has shown that it is apparently possible for neutral sound waves to be propagated in actual liquid He^3 at low temperatures, but not for spin waves.

The present paper is devoted to a study of spin oscillations in a Fermi-liquid placed in a magnetic field. In formulating the relevant kinetic equation, Landau[1] ignored the presence of a magnetic field; consequently in the first section of this report we derive a kinetic equation which takes it into account.[6] In Sec. 2 we investigate spin oscillations for the isotropic case and obtain the characteristic frequencies of these oscillations. These frequencies appear to be the limiting values of the spin-wave frequencies when the wavelength goes to infinity. Section 3 is devoted to a study of spin waves. Here it is shown, in contrast with the results of Landau quoted above, that it is possible for spin waves to be propagated in actual liquid He^3 in the presence of a constant magnetic field.

1. THE KINETIC EQUATIONS

To obtain the kinetic equations which describe the quasi-particles of a Fermi-liquid in the presence of a magnetic field, we start from the equation for the density matrix

$$\hbar \frac{\partial}{\partial t} \rho_{mn}(\mathbf{r}', \mathbf{r}; t) = H_{mn'}\rho_{n'n}(\mathbf{r}', \mathbf{r}; t) - H^{*}_{n'n}\rho_{mn'}(\mathbf{r}', \mathbf{r}; t), \tag{1.1}$$

where ρ is the density matrix, whose subscripts indicate the spin properties of the quasi-particle (we shall actually concern ourselves later on with the case of spin $\frac{1}{2}$). H is the Hamiltonian operator of a quasi-particle. The possibility that such a Hamiltonian exists is tied in with the possibility of being able to speak in general of quasi-particles. Transforming to a mixed representation for the density matrix,

$$n_{mn}(\mathbf{p}, \mathbf{r}, t) = (2\pi)^{-3} \int d\tau e^{-i\tau\mathbf{p}} \rho_{mn}\left(\mathbf{r} - \frac{\hbar\tau}{2}, \mathbf{r} + \frac{\hbar\tau}{2}, t\right), \tag{1.2}$$

we can rewrite equation (1.1) as follows:

$$\frac{\partial}{\partial t} n_{mn}(\mathbf{p}, \mathbf{r}, t) = \frac{1}{(2\pi)^6} \frac{i}{\hbar} \int d\tau\, d\mathbf{k}\, d\boldsymbol{\eta}\, d\mathbf{q} \exp\{i[\tau(\boldsymbol{\eta} - \mathbf{p}) + \mathbf{k}(\mathbf{q} - \mathbf{r})]\},$$
$$\times \left[\varepsilon_{mn'}\left(\boldsymbol{\eta} + \frac{\hbar\mathbf{k}}{2}, \mathbf{q} - \frac{\hbar\tau}{2}\right) n_{n'n}(\boldsymbol{\eta}, \mathbf{q}, t) - \varepsilon_{n'n}\left(\boldsymbol{\eta} - \frac{\hbar\mathbf{k}}{2}, \mathbf{q} + \frac{\hbar\tau}{2}\right) n_{mn'}(\boldsymbol{\eta}, \mathbf{q}, t)\right]. \tag{1.3}$$

Here $\epsilon_{mn}(\mathbf{p}, \mathbf{r})$ has the same functional dependence on the c-numbers $\mathbf{p}$ and $\mathbf{r}$ as the Hamiltonian H has on the momentum and coordinate operators.

The equation of the quasi-classical approximation can be obtained by expanding (1.3) in powers of $\hbar$. However, Eq. (1.3) does not take account of effects described by the collision integral in the usual Boltzmann equation. In Eq. (1.1) it is assumed that there is a Hamiltonian operator for each individual quasi-particle, different from the Hamiltonian of a free particle in that there is a certain self-consistent field of the other particles. The Hamiltonian does not depend explicity on the coordinates of these other particles, however, and in this sense does not take into account the interaction between them. It is possible in principle to take such an interaction into consideration. On the other hand, it is clear that the collisions

which have been ignored in Eq. (1.3) are the result of such an interaction. We consequently add a collision integral J_{mn} to the terms obtained from (1.3) in the equation of the quasi-classical approximation:

$$\frac{\partial n}{\partial t} - \frac{i}{\hbar}[\varepsilon,\ n] + \frac{1}{2}\left(\frac{\partial \varepsilon}{\partial \mathbf{p}}\frac{\partial n}{\partial \mathbf{r}} + \frac{\partial n}{\partial \mathbf{r}}\frac{\partial \varepsilon}{\partial \mathbf{p}}\right) - \frac{1}{2}\left(\frac{\partial \varepsilon}{\partial \mathbf{r}}\frac{\partial n}{\partial \mathbf{p}} + \frac{\partial n}{\partial \mathbf{p}}\frac{\partial \varepsilon}{\partial \mathbf{r}}\right) = J, \tag{1.4}$$

where $[\epsilon, n]$ is the commutator of ϵ and n, which are matrices with respect to the spin variable.

It is convenient to get rid of the matrices and to introduce instead of n a distribution function f of the particles in phase space and a vector function σ of the spin density in phase space, determined by the relations:

$$f(\mathbf{p}, \mathbf{r}, t) = \mathrm{Sp}_\sigma n; \quad \sigma(\mathbf{p}, \mathbf{r}, t) = \mathrm{Sp}_\sigma \hat{\sigma} n. \tag{1.5}$$

Here the $\hat{\sigma}$ are the Pauli spin matrices.

Then, noting that $\epsilon(\mathbf{p}, \mathbf{r})$ can be written in the form

$$\varepsilon_{mn} = \delta_{mn}\varepsilon_1 + \hat{\sigma}_{mn}\boldsymbol{\varepsilon}_2, \tag{1.6}$$

we obtain the following equations for the functions f and σ:

$$\frac{\partial f}{\partial t} + \frac{\partial \varepsilon_1}{\partial \mathbf{p}}\frac{\partial f}{\partial \mathbf{r}} - \frac{\partial \varepsilon_1}{\partial \mathbf{r}}\frac{\partial f}{\partial \mathbf{p}} + \frac{\partial \varepsilon_2}{\partial p_j}\frac{\partial \boldsymbol{\sigma}}{\partial r_j} - \frac{\partial \boldsymbol{\varepsilon}_2}{\partial r_j}\frac{\partial \boldsymbol{\sigma}}{\partial p_j} = J; \tag{1.7}$$

$$\frac{\partial \boldsymbol{\sigma}}{\partial t} + \left(\frac{\partial \varepsilon_1}{\partial \mathbf{p}}\frac{\partial}{\partial \mathbf{r}}\right)\boldsymbol{\sigma} - \left(\frac{\partial \varepsilon_1}{\partial \mathbf{r}}\frac{\partial}{\partial \mathbf{p}}\right)\boldsymbol{\sigma} + \frac{2}{\hbar}[\boldsymbol{\varepsilon}_2\boldsymbol{\sigma}] + \left(\frac{\partial f}{\partial \mathbf{r}}\frac{\partial}{\partial \mathbf{p}}\right)\boldsymbol{\varepsilon}_2 - \left(\frac{\partial f}{\partial \mathbf{p}}\frac{\partial}{\partial \mathbf{r}}\right)\boldsymbol{\varepsilon}_2 = \mathbf{J}. \tag{1.8}$$

Here the quantities J and $\mathbf{J}$ denote $\mathrm{Sp}_\sigma \hat{J}$ and $\mathrm{Sp}_\sigma \hat{\sigma}\hat{J}$, respectively.

The functions ϵ_1 and $\boldsymbol{\epsilon}_2$ depend on the space coordinates because of the fact that they are functionals of $n(\mathbf{p}, \mathbf{r})$. Actually, if there is no magnetic field, then according to Landau

$$\delta\varepsilon_{mn}(\mathbf{p}, \mathbf{r}) = \mathrm{Sp}_{\sigma'}\int \hat{f}_{nn'}(\mathbf{p}, \mathbf{p}')\,\delta n_{n'm}(\mathbf{p}', \mathbf{r})\,d\mathbf{p}'. \tag{1.9}$$

If we ignore the small spin-orbit coupling in the expression for $\epsilon(\mathbf{p}, \mathbf{r})$, then in the presence of a magnetic field

$$\delta\varepsilon(\mathbf{p}, \mathbf{r}) = -\frac{1}{2}\beta(\hat{\boldsymbol{\sigma}}\mathbf{H}) + \mathrm{Sp}_{\sigma'}\int \{\varphi(\mathbf{p}, \mathbf{p}') + (\boldsymbol{\sigma}\boldsymbol{\sigma}')\psi(\mathbf{p}, \mathbf{p}')\}\,\delta n(\mathbf{p}', \mathbf{r})\,d\mathbf{p}', \tag{1.10}$$

which, according to (1.6), permits us to write down the following expressions:

$$\delta\varepsilon_1(\mathbf{p}, \mathbf{r}) = \int \varphi(\mathbf{p}, \mathbf{p}')\,\delta f(\mathbf{p}', \mathbf{r})\,d\mathbf{p}', \tag{1.11}$$

$$\delta\boldsymbol{\varepsilon}_2(\mathbf{p}, \mathbf{r}) = -\frac{1}{2}\beta\mathbf{H} + \mathrm{Sp}_{\sigma'}\int \psi(\mathbf{p}, \mathbf{p}')\,\delta\boldsymbol{\sigma}(\mathbf{p}', \mathbf{r})\,d\mathbf{p}'. \tag{1.12}$$

Furthermore, because of the fact that

$$\frac{\partial \varepsilon}{\partial \mathbf{p}} = \frac{\mathbf{p}}{m} + \mathrm{Sp}_{\sigma'}\int \hat{f}(\mathbf{p}, \mathbf{p}')\frac{\partial n(\mathbf{p}', \mathbf{r})}{\partial \mathbf{p}'}\,d\mathbf{p}', \tag{1.13}$$

we have

$$\frac{\partial \varepsilon_1}{\partial \mathbf{p}} = \frac{\mathbf{p}}{m} + \int \varphi(\mathbf{p}, \mathbf{p}')\frac{\partial f(\mathbf{p}', \mathbf{r})}{\partial \mathbf{p}'}\,d\mathbf{p}', \tag{1.14}$$

$$\frac{\partial \boldsymbol{\varepsilon}_2}{\partial p_j} = \int \psi(\mathbf{p}, \mathbf{p}')\frac{\partial \boldsymbol{\sigma}(\mathbf{p}', \mathbf{r})}{\partial p_j'}\,d\mathbf{p}'. \tag{1.15}$$

In Eq. (1.8) it is necessary to know not only the derivatives of the functions ϵ_1 and $\boldsymbol{\epsilon}_2$ but the entire function $\boldsymbol{\epsilon}_2$. Regarding the magnetic field as negligibly small, or , to be more precise, considering that

$$\beta(\boldsymbol{\sigma}\mathbf{H}) \ll \varepsilon(\mathbf{p}, \mathbf{r}), \tag{1.16}$$

we can also consider the quantity $\boldsymbol{\sigma}(\mathbf{p}, \mathbf{r})$ to be small, and therefore drop the δ operation in Eq. (1.12). At the same time we ignore quantities of second order in expansions in powers of the magnetic field (H/ϵ).

2. SPIN OSCILLATIONS FOR AN ISOTROPIC DISTRIBUTION

When there is no spatial anisotropy, then, according to the results of the preceding section, it is possible to write (1.8) in the following form:

$$\frac{\partial \sigma}{\partial t} + \frac{2}{\hbar}\int d\mathbf{p}'\,\psi(\mathbf{p},\mathbf{p}')\,[\sigma(\mathbf{p}')\,\sigma(\mathbf{p})] + \frac{\beta}{\hbar}[\sigma\times\mathbf{H}] = \mathbf{J}. \tag{2.1}$$

In particular, we can obtain from (2.1) an equation describing the time rate of change of the magnetization density

$$\mathbf{M} = (\beta/2)\int \sigma\, d\mathbf{p}. \tag{2.2}$$

Integrating (2.1) over $d\mathbf{p}$ and noting that $\psi(\mathbf{p},\mathbf{p}')$ is a symmetric function of $\mathbf{p}$ and $\mathbf{p}'$, we obtain

$$\partial\mathbf{M}/\partial t + (\beta/\hbar)[\mathbf{M}\times\mathbf{H}] = (\beta/2)\int \mathbf{J}\, d\mathbf{p}, \tag{2.3}$$

which for the appropriate approximation of the collision integral agrees with the ordinary Bloch equation. Thus, given a certain constant magnetic field $\mathbf{H}_0$, we find that if we disregard collisions, which, generally speaking, lead to attenuation, the principal frequency of oscillations of the magnetization turns out to be

$$\Omega_0 = \beta H_0/\hbar. \tag{2.4}$$

However, in contrast with the corresponding results for a gas, the frequency Ω_0 here will not be the only frequency characterizing spin oscillations.

We consider a state, slightly out of equilibrium, in which there is a constant uniform field $\mathbf{H}_0$. Then

$$\sigma = \sigma_0(p) + \sigma_1(\mathbf{p}, t);\quad \mathbf{H} = \mathbf{H}_0 + \mathbf{H}_1(t);\quad \sigma_0 \parallel \mathbf{H}_0;\quad H_0 \gg H_1;\quad \sigma_0 \gg \sigma_1. \tag{2.5}$$

Resolving σ_1 into components parallel ($\sigma_\parallel$) and perpendicular ($\sigma_\perp = \sigma_x\mathbf{i} + \sigma_y\mathbf{j}$) to $\mathbf{H}_0$, we obtain in the linear approximation the following equations for $\sigma_\parallel$ and for $\sigma^{(\pm)} = \sigma_x \pm i\sigma_y$:

$$\partial\sigma_\parallel/\partial t = \mathbf{J}_\parallel, \tag{2.6}$$

$$\frac{\partial}{\partial t}\sigma^{(\pm)} \mp i\Omega_0\sigma^{(\pm)} \mp i\,\frac{2}{\hbar}\int d\mathbf{p}'\,\{\sigma_0(p)\,\sigma^{(\pm)}(\mathbf{p}') - \sigma_0(p')\,\sigma^{(\pm)}(\mathbf{p})\} \pm i\,\frac{\beta}{\hbar}\,\sigma_0(p)(H_{1x} \pm iH_{1y}) = J^{(\pm)}, \tag{2.7}$$

from which it is clear that only the component of σ lying in a plane perpendicular to $\mathbf{H}_0$ can oscillate.

Noting that

$$\sigma_0(p) = {}^1\!/_2\,\beta H_0\,\partial f_0/\partial\varepsilon, \tag{2.8}$$

where f_0 is the Fermi distribution function, so that σ_0 has the form of a δ-function, we can express the solution of (2.7) in the form

$$\sigma^{(\pm)}(\mathbf{p}) = (\partial f_0/\partial\varepsilon)\,\zeta^{(\pm)}(\theta,\varphi,t). \tag{2.9}$$

Then, introducing the notation

$$\Psi(\cos\chi) = 4\pi\,\frac{2}{(2\pi\hbar)^3}\,\frac{p_0^2}{v_0}\,\psi(\mathbf{p}_0,\mathbf{p}_0'), \tag{2.10}$$

where $\mathbf{p}_0$ and $\mathbf{v}_0$ are the momentum and velocity of the particles on the Fermi surface and χ is the angle between the vectors $\mathbf{p}_0$ and $\mathbf{p}_0'$, we obtain from (2.7) the following equation for $\zeta^{(\pm)}$:

$$\frac{\partial\zeta^{(\pm)}}{\partial t} \mp i\Omega_0\zeta^{(\pm)} \pm i\Omega_0\int\frac{d\sigma'}{4\pi}\,\Psi(\cos\chi)\,\{\zeta^{(\pm)}(\theta',\varphi') - \zeta^{(\pm)}(\theta,\varphi)\} \pm i\Omega_0 H_\pm = \bar{J}_\pm. \tag{2.11}$$

The solution of (2.11) can be written as an expansion in spherical harmonics:

$$\zeta^{(\pm)}(\theta,\varphi,t) = \sum_{n,m} C_{n,m}^{(\pm)}(t)\,\frac{e^{im\varphi}}{\sqrt{2\pi}}\,P_n^m(\cos\theta)\left(\frac{2n+1}{2}\,\frac{(n-m)!}{(n+m)!}\right)^{1/2}. \tag{2.12}$$

If we now represent the function $\Psi(\cos\chi)$ as a series of Legendre polynomials

$$\Psi(\cos\chi) = \sum_{n=0}^{\infty}\alpha_n P_n(\cos\chi), \tag{2.13}$$

we obtain from (2.11) the following equations:

$$\text{for } n=0: \quad \frac{\partial}{\partial t} C_{0,0}^{(\pm)} \mp i\Omega_0 C_{0,0}^{(\pm)} \pm i\Omega_0 H_\pm \sqrt{2\pi} = J_{0,0}^{(\pm)}, \tag{2.14}$$

$$\text{for } n\neq 0: \quad \frac{\partial}{\partial t} C_{n,m}^{(\pm)} \mp i\Omega_0 C_{n,m}^{(\pm)} \left(1+\alpha_0 - \frac{2\alpha_n}{2n+1}\right) = J_{n,m}^{(\pm)}. \tag{2.15}$$

Here $J^{\pm}_{n,m}$ denote the appropriate coefficients of the expansion in spherical harmonics.

It is easy to see that (2.14) corresponds to the Bloch equation and agrees with the linearized equation (2.3). In the absence of an external field and with no allowance made for collisions, this equation describes spin oscillations with frequencies $\pm\Omega_0$. If collisions are ignored in Eq. (2.15), then

$$C^{\pm}_{n,m} \sim \exp(\pm i\omega_n t), \text{ where } \omega_n = \Omega_0\left(1+\alpha_0 - \frac{2\alpha_n}{2n+1}\right). \tag{2.16}$$

The frequency of all such oscillations coincides with Ω_0 for an ideal gas. One can say that the presence of a self-consistent field in which the quasi-particles move about removes such a degeneracy.

3. SPIN WAVES

In Fermi-liquids, because of the presence of exchange interactions, the propagation of spin waves is possible in principle.[2,4] However, a detailed analysis of this possibility carried out by Landau for He^3, has shown that such waves can apparently not be propagated in real helium.[2] This result was obtained under the assumption that there was no magnetic field. Below we shall study the problem of the propagation of spin waves in a Fermi-liquid placed in a magnetic field.

We are interested in states which depart slightly from equilibrium, and for which the magnetic field is constant and uniform. In the linear approximation Eqs. (1.7) and (1.5) can be written in the following way (neglecting collisions):

$$\frac{\partial f_1}{\partial t} + \left(\mathbf{v}\frac{\partial}{\partial \mathbf{r}}\right) f_1 - \frac{\partial f_0}{\partial \mathbf{p}} \int d\mathbf{p}'\, \varphi(\mathbf{p},\mathbf{p}') \frac{\partial f_1(\mathbf{p}',\mathbf{r})}{\partial \mathbf{r}} + v_{i,j} \frac{\partial \sigma_{1i}}{\partial r_j} - \frac{\partial \sigma_{0i}}{\partial p_j} \frac{\partial}{\partial r_j} \left\{ \int d\mathbf{p}'\, \psi(\mathbf{p},\mathbf{p}')\, \sigma_{1i}(\mathbf{p}',\mathbf{r}) - \frac{1}{2}\beta H_{1i}(\mathbf{r}) \right\} = 0; \tag{3.1}$$

$$\frac{\partial \sigma_{1i}}{\partial t} + \left(\mathbf{v}\frac{\partial}{\partial \mathbf{r}}\right)\sigma_{1i} - \int d\mathbf{p}'\, \varphi(\mathbf{p},\mathbf{p}') \left(\frac{\partial f_1(\mathbf{p}',\mathbf{r})}{\partial \mathbf{r}} \frac{\partial}{\partial \mathbf{p}}\right) \sigma_{0i} + v_{i,j} \frac{\partial f_1}{\partial r_j} + \frac{2}{\hbar} \int d\mathbf{p}'\, \psi(\mathbf{p},\mathbf{p}') \{[\boldsymbol{\sigma}_0(p')\times\boldsymbol{\sigma}_1(\mathbf{p},\mathbf{r})]_i + [\boldsymbol{\sigma}_1(\mathbf{p}',\mathbf{r})\times\boldsymbol{\sigma}_0(p)]_i\}$$
$$- \left(\frac{\partial f_0}{\partial \mathbf{p}}\frac{\partial}{\partial \mathbf{r}}\right) \left\{ \int d\mathbf{p}'\, \psi(\mathbf{p},\mathbf{p}')\, \sigma_{1i}(\mathbf{p}',\mathbf{r}) - \frac{1}{2}\beta H_{1i}(\mathbf{r}) \right\} - \frac{\beta}{\hbar}[\mathbf{H}_0\times\boldsymbol{\sigma}_1]_i - \frac{\beta}{\hbar}[\mathbf{H}_1\times\boldsymbol{\sigma}_0]_i = 0, \tag{3.2}$$

where

$$\mathbf{v} = \frac{\partial \varepsilon_{1a}}{\partial \mathbf{p}} = \frac{\mathbf{p}}{m} + \int \varphi(\mathbf{p},\mathbf{p}') \frac{\partial f_0(p')}{\partial \mathbf{p}'} d\mathbf{p}', \tag{3.3}$$

$$v_{i,j} = \int \psi(\mathbf{p},\mathbf{p}') \frac{\partial \sigma_{0i}(p')}{\partial p_j'} d\mathbf{p}'. \tag{3.4}$$

Noting that $\boldsymbol{\sigma}_0$ is parallel to $\mathbf{H}_0$, we can represent $\boldsymbol{\sigma}_1$ as the sum of components parallel and perpendicular to the field $\mathbf{H}_0$, as we did in Sec. 2. Introducing the notation

$$\sigma^{(\pm)} = \sigma_x \pm i\sigma_y = (\partial f_0/\partial\varepsilon)\zeta^{(\pm)}(\mathbf{r};\theta,\varphi,t),$$

we have the following equation for the perpendicular part:

$$\frac{\partial}{\partial t}\zeta^{(\pm)} + \left(\mathbf{v}_0\frac{\partial}{\partial \mathbf{r}}\right)\zeta \mp i\Omega_0\zeta^{(\pm)} \pm i\Omega_0 H_\pm \mp i\Omega_0 \int \frac{d\sigma'}{4\pi} \Psi(\cos\chi)\{\zeta^{(\pm)}(\mathbf{r},\theta',\varphi') - \zeta^{(\pm)}(\mathbf{r},\theta,\varphi)\}$$
$$= -\left(\mathbf{v}\frac{\partial}{\partial \mathbf{r}}\right)\left\{\frac{\beta}{2}H_\pm + \int \frac{d\sigma'}{4\pi}\Psi(\cos\chi)\zeta^{(\pm)}(\mathbf{r},\theta',\varphi')\right\}, \tag{3.5}$$

where $\mathbf{v}_0$ is the velocity at the Fermi surface.

It follows from Eq. (3.5) that the transverse spin waves are not connected with acoustic oscillations. The longitudinal spin waves are, however, related to sound waves; but, as we can easily convince ourselves, a constant magnetic field leads only to a change in the sound velocity, and thus in the velocity of propagation of the longitudinal spin waves, which in order of magnitude is $\sim H_0^2$. Therefore in what follows we limit our study to transverse spin waves, corresponding to oscillations of $\boldsymbol{\sigma}$ in a plane perpendicular to $\mathbf{H}_0$ and described by Eq. (3.5).

If we suppose that there is no varying external field, we can set the solution of (3.5) proportional to $\exp(-i\omega t + i\mathbf{k}\cdot\mathbf{r})$. Equation (3.5) can then be rewritten

$$(kv_0\cos\theta-\omega)\zeta^{(\pm)}(\theta,\varphi)\mp\Omega_0\left(1-\int\frac{d\sigma'}{4\pi}\Psi(\cos\chi)\right)\zeta^{(\pm)}(\theta,\varphi)+(kv_0\cos\theta\mp\Omega_0)\int\frac{d\sigma'}{4\pi}\Psi(\cos\chi)\zeta^{(\pm)}(\theta';\varphi')=0. \tag{3.6}$$

We now investigate the solution of (3.6) under the assumption that $\Psi(\cos\chi)$ is a constant. If such an assumption is made for actual liquid He^3, the constant appears to be negative. For our case we obtain from (3.6), with Ψ constant, the following relation between the frequency ω and the wave vector k of the spin waves:

$$1+\frac{1}{2}\Psi\int_0^\pi d\theta\sin\theta\,\frac{kv_0\cos\theta\mp\Omega_0}{kv_0\cos\theta\mp\Omega_0(1-\Psi)-\omega}=0. \tag{3.7}$$

Carrying out the integration, we obtain the following result:

$$1+\frac{\omega\mp\Psi\Omega_0}{2kv_0}\frac{\Psi}{1+\Psi}\ln\frac{\omega\pm\Omega_0(1-\Psi)-kv_0}{\omega\pm\Omega_0(1-\Psi)+kv_0}=0. \tag{3.8}$$

If the constant magnetic field is zero, then (3.8) takes the form[2]

$$1+\frac{\omega}{2kv_0}\frac{\Psi}{1+\Psi}\ln\frac{\omega-kv_0}{\omega+kv_0}=0. \tag{3.9}$$

This last expression admits of real values for the ratio ω/kv_0 only for positive Ψ. Since Ψ is not positive for He^3, there can be no spin waves propagated in the absence of a magnetic field.

If the magnetic field is not zero, but the frequency of the spin waves is much greater than Ω_0, (3.8) agrees approximately with (3.9), so one can say that spin waves cannot be propagated at such high frequencies as well.

Let us investigate this question in some detail. We set

$$\omega=\mp\Omega_0\rho,\quad u_0=v_0/\Omega_0; \tag{3.10}$$

and obtain from (3.8)

$$1=\frac{\rho+\Psi}{2ku_0}\frac{\Psi}{1+\Psi}\ln\frac{\rho-1+\Psi+ku_0}{\rho-1+\Psi-ku_0}. \tag{3.11}$$

In the region of long waves, a solution of (3.11) can be obtained from an expansion in powers of (ku_0), from which we obtain

$$\rho=1+(1+\Psi^{-1})(ku_0)^2,\quad ku_0\ll 1. \tag{3.12}$$

Thus for positive Ψ the absolute value of the frequency increases with increasing k. The same thing occurs for negative Ψ provided that $1+1/\Psi>0$. However if $1+1/\Psi<0$, as might conceivably occur for actual liquid He^3, the absolute value of the frequency decreases with an increase in the wave vector of the spin waves.

It is easy to show that for $\Psi<0$ there is no real value of ρ, corresponding to unattenuated spin waves, if

$$\rho>1-\Psi-ku_0\quad(ku_0>1). \tag{3.13}$$

Let us explain under what conditions the inequality (3.13) sets the limit for ρ. To do this we set

$$\rho=1-\Psi-ku_0-\Delta,\quad\text{where } 1\gg\Delta>0. \tag{3.14}$$

From Eq. (3.11) we obtain

$$\Delta=2ku_0\exp\left(\frac{1+\Psi}{\Psi}\frac{2ku_0}{1-ku_0}\right). \tag{3.15}$$

From this it follows that a solution of the form (3.14) is possible if

$$-(1+\Psi^{-1})2ku_0/(1-ku_0)\gg 1. \tag{3.16}$$

For the case $1+1/\Psi<0$ this condition is satisfied when

$$u_0^{-1}-k\ll-2k(1+\Psi)/\Psi. \tag{3.17}$$

Thus one can say that as the wave vector approaches the value u_0^{-1} the absolute value of the frequency of the spin waves decreases and

$$\rho = \rho_{\lim} = -\Psi \quad \text{for} \quad k = k_{\lim} = u_0^{-1} = \Omega_0 / v_0. \tag{3.18}$$

Thus for $1 + 1/\Psi < 0$ the absolute value of the frequency of the spin waves decreases with increasing value of the wave vector in the region of small k, in accordance with (3.12), but for values of the wave vector equal to Ω_0/v_0, it attains a minimum value equal to $|\Psi\Omega_0|$.

We note that for the case $1 + 1/\Psi > 0$ the condition (3.16) also leads to (3.18), but only if the wave vector approaches Ω_0/v_0 from the side of large values.

When the function $\Psi(\cos\chi)$ does not reduce to a constant, Eq. (3.6) leads to a whole series of spin waves whose frequencies coincide, in the limit of infinite wave length, with the corresponding frequencies obtained in the preceding section. It is necessary to point out that for spin oscillations corresponding to isotropic distributions, it follows from Eqs. (2.14) and (2.15) that an external magnetic field can excite oscillations of the magnetization only at a frequency Ω_0. Conversely, for spin waves corresponding to arbitrary functions $\Psi(\cos\chi)$, the individual spherical harmonics [see (2.12)] no longer appear to be solutions of the problem; indeed, the solutions of (3.5) appear to be determined by superpositions of the different spherical functions, among them the one corresponding to $n = m = 0$ [see (2.12)]. Upon integration over all angles, only this spherical harmonic gives a non-zero result, and consequently it alone corresponds to a magnetization. It is clear that an external field leads to a change of just the magnetization. Consequently, in the case of spin waves, an external magnetic field in any solution of (3.5) can lead to changes in the zero-order term of the expansion in spherical harmonics. Furthermore, in view of the fact that the relation between all the terms of the expansion is completely determined, the magnetic field leads to a change of the entire solution, or in other words to the excitation of spin waves. It is clear that as the wavelength of the spin waves increases, the amplitude of forced oscillation of all the waves except those going over into oscillations of the magnetization (2.14) must decrease. Conversely, in the region of wavelengths of the order of v_0/Ω_0, the amplitudes of forced oscillation of all the possible spin waves will have the same order of magnitude.

In conclusion we would like to express our appreciation to V. L. Ginsburg for his interest in this work.

[1] L. D. Landau, J. Exptl. Theoret. Phys. (U.S.S.R.) **30**, 1058 (1956), Soviet Phys. JETP **3**, 920 (1956).

[2] L. D. Landau, J. Exptl. Theoret. Phys. (U.S.S.R.) **32**, 59 (1957), Soviet Phys. JETP **5**, 101 (1957).

[3] Iu. L. Klimontovich and V. P. Silin, J. Exptl. Theoret. Phys. (U.S.S.R.) **23**, 151 (1952); V. P. Silin, (Trans. Phys. Inst. Acad. Sci.) **6**, 199 (1955).

[4] V. P. Silin, Физика металлов и металловедение (Phys. of Metals and Metal Res.) 3, 193 (1956).

[5] I. M. Khalatnikov and A. A. Abrikosov, J. Exptl. Theoret. Phys. (U.S.S.R.) **33**, 110 (1957), Soviet Phys. JETP **6**, 84 (1958).

[6] V. P. Silin, J. Exptl. Theoret. Phys. (U.S.S.R.) **33**, 495 (1957), Soviet Phys. JETP **6**, 387 (1958).

Translated by W. M. Whitney
250

INVESTIGATION OF THE EQUILIBRIUM FORM OF ATOMIC NUCLEI

B. L. BIRBRAIR

A. I. Herzen Leningrad State Pedagogical Institute

Submitted to JETP editor May 7, 1957

J. Exptl. Theoret. Phys. (U.S.S.R.) **33**, 1235-1247 (November, 1957)

It is shown that the experimentally observed abrupt transition from the spherical equilibrium form of atomic nuclei to the ellipsoidal form is explained by the influence of pair interactions of nucleons. If the magnitude of the difference between the pair energies in the ellipsoidal and spherical states is estimated from experimental data on the nuclear binding energies, then the theoretical regions of prolate nuclei coincide with those observed in experiment.

INTRODUCTION

THE concept of the independent motion of nucleons in the mean effective field of the nucleus is basic to contemporary nuclear models. As a first approximation, a spherically symmetric field was assumed,[1] which made it possible to explain the existence of nuclear shells, with consideration of strong spin-orbit coupling. The scheme of bound states in a spherical nucleus, which we call the Mayer scheme, allowed us to understand a number of regularities observed in the spectra of single particle excitations of the nuclei.

Along with single-particle excitations in atomic nuclei, collective excitations, which possess a rotational or vibrational character have been discovered. Nuclei with a rotational spectrum of collective motion have a prolate equilibrium shape, which also follows from the data on quadrupole moments. The spins and parities of single particle states in these nuclei do not satisfy the Mayer scheme. Therefore it was hypothesized that the effective field in these nuclei does not have spherical symmetry.[2,3] In this case, the energies of the bound states of the nucleons are functions of the deformation (by deformation of the nucleus, we mean the departure of the nuclear field $U(\mathbf{r})$ from spherically symmetric form), and the nucleonic configuration, together with the equilibrium deformation of the given nucleus, is determined from the condition of a minimum in its total energy.[4]

The field acting on the given nucleon is the average of its interaction with all the remaining nucleons, and therefore the symmetry of the potential $U(\mathbf{r})$ is determined by the spatial distribution of the nucleons in the nucleus. Inasmuch as the latter is isotropic for filled shells, then, strictly speaking, only the magic nuclei can satisfy the Mayer scheme. It can be expected that the remaining nuclei will be deformed, and their single particle states will satisfy the scheme of bound states in a deformed nucleus, which we call the Nilsson scheme.

However, the Nilsson scheme agrees with experiment only in three well known regions of rotational excitation: (1) the rare earths in the range $_{60}Nd^{150} - _{76}Os^{190}$, (2) the heavy nuclei, beginning with $_{88}Ra^{222}$, and (3) the light nuclei in the region of $_{12}Mg^{24}$. For nuclei outside the stated intervals, there is no indication of the presence of a deformation, and their single particle states satisfy the usual Mayer scheme.

To clarify the existence of sharp limits within which the nuclei are prolate, the conditions of transition to the deformed equilibrium form are investigated in the present research. For this purpose, we first consider the establishment of equilibrium deformation in the independent particle approximation; the role of pair interaction in the process under investigation is then explained and, finally, the results are applied to finding the limits of prolateness of the nuclei; finally, comparison is made with experiment

1. EQUILIBRIUM DEFORMATION IN THE INDEPENDENT-PARTICLE APPROXIMATION

The Hamiltonian of a nucleon in a spherical nucleus has the form

$$\hat{H}_M = -\frac{\hbar^2}{2m}\Delta + V(r) + \frac{C}{r}\frac{dV}{dr}\hat{\mathbf{l}}\hat{\mathbf{s}}. \qquad (1)$$

The solution of the Schrödinger equation with the Hamiltonian (1) gives the wave functions and the energies of the bound states or the nucleons in the spherical nucleus. The state $|Nlj\rangle$ is characterized by a principal quantum number N, an orbital angular momentum l and a total angular momentum j. For the proper choice of the spin-orbit coupling constant C, the energy spectrum of the system reproduces the experimentally observed order of levels in the spherical nucleus.[5] The nucleonic configuration of the nucleus is determined by the numbers of nucleons in the filled states, and the total energy of the nucleus in the independent particle approximation is the sum of the energy of the nucleons for a given configuration.

In a deformed nucleus, one can always find a surface

$$r'(\vartheta, \varphi) = r\left[1 + \sum_{\lambda,\mu} \alpha_{\lambda\mu} Y_{\lambda\mu}(\vartheta, \varphi)\right], \tag{2}$$

on which the potential of the nucleus $U(\mathbf{r})$ has a constant value. Denoting $U(\mathbf{r}') = V(\mathbf{r})$ and limiting ourselves to terms of second order in the expansion (2), we get

$$U(\mathbf{r}) = V(r) + \frac{5}{8\pi}\beta^2 r^2 \frac{d^2V}{dr^2} - r\frac{dV}{dr}\sum_{\mu} \alpha_{2\mu} Y_{2\mu}(\vartheta, \varphi), \tag{3}$$

where $\beta \sim \Delta R/R$ is the deformation parameter of the nucleus, and is related to α_μ by the expression $\beta^2 = \sum_\mu |\alpha_\mu|^2$.

In the case of axially symmetric deformations, the Hamiltonian of the nucleon has the form

$$\hat{H}_N \hat{H}_0 + \hat{H}_\beta = -\frac{\hbar^2}{2m}\Delta + V(r) + \frac{5}{8\pi}\beta^2 r^2 \frac{d^2V}{dr^2} + \frac{C}{r}\frac{dV}{dr}\hat{\mathbf{l}}\hat{\mathbf{s}} - r\frac{dV}{dr}\beta Y_{20}; \quad \hat{H}_\beta = \frac{C}{r}\frac{dV}{dr}\hat{\mathbf{l}}\hat{\mathbf{s}} - r\frac{dV}{dr}\beta Y_{20}. \tag{4}$$

Solution of the Schrödinger equation with the Hamiltonian (4) gives the wave functions and the energies of the bound states in the deformed nucleus. The state $|\Omega\rangle$ is now characterized by the projection Ω of the total angular momentum on the axis of deformation (we choose this to be the z axis) and by its parity. For $\beta = 0$, as is evident from (1) and (4), the schemes of Mayer and Nilsson coincide. Under the action of $\hat{H}_\beta$, each spherical state with given j is split into $(2j + 1)/2$ states with $|\Omega| = \frac{1}{2}, \frac{3}{2}, \ldots, j$. The states with $|\Omega| \ll j$ have a prolate orbit in the direction of the deformation axis and their completion contributes to the elongation of the nucleus. The states with $|\Omega| \approx j$ have an orbit which is perpendicular to the axis of deformation and upon its completion the nucleus is flattened. Therefore, for $\beta > 0$, the levels are separated from the bottom upward in the order of increase of $|\Omega|$, while for $\beta < 0$ the order of splitting is reversed.

Upon increase in the deformation, a crossing of levels takes place which arises as the result of the splitting of the spherical terms with different j. Therefore, for small deformations, the Nilsson scheme is strongly dependent on the order of the levels for $\beta = 0$, and also on the form of the potential $V(\mathbf{r})$. We shall show that in the limiting case of large deformations, the Nilsson scheme depends slightly on these factors. For this purpose, we recall that the order of the levels for $\beta = 0$ is determined on the basis of the magnitude of the spin-orbit coupling, and can change with variation of the constant C. In the case of large deformations, the spin-orbit coupling is greatly reduced, and the order of the levels is determined on the basis of the factor βY_{20}, by which the weak dependence of the Nilsson scheme on the form of the potential is also explained (cf. Refs. 2, 3). Actually, we can represent a state with given Ω in the form of a superposition of spherical states

$$|\Omega\rangle = \sum_{j=\Omega}^{N+1/2} C_j |Nlj\Omega\rangle, \quad \sum_j |C_j|^2 = 1, \tag{5}$$

where all the states of the N-th shell give, at large deformations, almost identical contributions ($C_\Omega \approx C_{\Omega+1} \approx \ldots \approx C_{N+\frac{1}{2}}$). Then the matrix element of spin-orbit coupling is equal to

$$|\langle\Omega|2\hat{\mathbf{l}}\hat{\mathbf{s}}|\Omega\rangle| = |\sum_j |C_j|^2 \langle lj|2\hat{\mathbf{l}}\hat{\mathbf{s}}|lj\rangle| = |\sum_l \{|C_{l+1/2}|^2 l - |C_{l-1/2}|^2 (l+1)\}|, \tag{6}$$

which is much smaller than the same matrix element in the spherical state [after exclusion of a few levels with $\Omega = N + \frac{1}{2}$, when only a single term enters into the expansion (5)]. Since, aside from (6), the relation

$$|\langle\Omega|\frac{C}{r}\frac{dV}{dr}\hat{l}\hat{s}|\Omega\rangle| \ll |\langle\Omega|r\frac{dV}{dr}\beta Y_{20}|\Omega\rangle|,$$

is satisfied for all Ω, the independence of the Nilsson scheme of the spin-orbit coupling for large deformations is thus shown.

The ground state of the nucleus is determined by the nucleonic configuration which corresponds to the smallest energy.

For nuclei with filled shells, the configurations in the Nilsson and Mayer schemes coincide, and the equilibrium deformation is equal to zero. In the presence of external nucleons, the Nilsson scheme gives the lower energy, since the energy of the lowest deformed state is less than the energy of the corresponding spherical terms. (For example, for positive deformations, the states with $|\Omega| \ll j$ are filled first; their energy for $\beta > 0$ is less than for $\beta = 0$.) The Coulomb energy, which is included in the total energy of the nucleus, and has the form

$$E_C = \frac{3}{5}\frac{Z^2e^2}{R}\left(1 - \frac{4}{45}\varepsilon^2\right), \quad \varepsilon = \frac{3}{2}\sqrt{\frac{5}{4\pi}}\beta, \tag{7}$$

is also less in the deformed state. The difference $E_N - E_M = \Delta E(A)$ between the energies of the nucleus in the deformed and spherical states is always negative and can serve as a measure of the equilibrium deformation (for a filled shell, $\Delta E = 0$). With increase in the number of nucleons (or holes) outside a filled shell, $\Delta E(A)$ increases in absolute value, reaches a maximum when the shell is half filled, and then decreases to zero. The equilibrium deformation, correspondingly, changes continuously from nucleus to nucleus, and thus there is no jump in the equilibrium form.

2. CONSIDERATION OF PAIR INTERACTION OF NUCLEONS

Apart from the sum of the single particle energies of the nucleons and the Coulomb energy, the energy of the remaining interactions also enters into the total energy of the nucleus. The latter is introduced in the single particle model theory of shells, in order to take into account the experimentally observed spin dependence of the nuclear forces (the state of the system of independent particles is degenerate in the total spin).

We consider the contribution to the energy which gives the interaction of nucleons in the same quantum state, the so-called pair interaction. We shall consider the pair forces to be extremely short range and choose the operator of interaction in the form

$$\hat{W}(1.2) = -g\delta(\mathbf{r}_1 - \mathbf{r}_2). \tag{8}$$

Inasmuch as the pair interaction in the form (8) reproduces the empirical rule of spins, then it can be assumed that (8) correctly describes the qualitative regularities connected with the effect of pair forces, even if it does not pretend to yield quantitative agreement with experiment.

The energy of two monoenergetic nucleons in a spherical state with total angular momentum I is equal to[6]

$$w(j^2I) = {}^1/_2(2j+1+I)(2j-I)!\,I!^2(j-{}^1/_2+{}^1/_2I)!^2[(2j+I)!\,({}^1/_2I)!^4(j-{}^1/_2-{}^1/_2I)!^2]^{-1}F^0, \tag{9}$$

where j is the individual angular momentum of the nucleon,

$$F^0 = -\frac{g}{4\pi}\int_0^\infty R_{Nl}^4 r^3 dr,$$

and R_{Nl} is the radial part of the wave function. The state with momentum I = 0 corresponds to a minimum in the pair energy. For all j encountered in the periodic system,

$$w(j^2 2)/w(j^2 0) < {}^1/_4, \quad w(j^2 4)/w(j^2 0) < {}^1/_7, \quad w(j^2 6)/w(j^2 0) < {}^1/_{11},$$

etc.

We shall now show that the pair energy in the deformed state of the nucleus is always greater than the minimum energy in the spherical state. For this purpose, we expand the wave function in spherical states with definite total angular momentum [see Eqs. (5) – (7) in the Appendix]:

$$\Psi_\Omega(1,2)=\sum_{\nu=0}^{2j-1} D_\Omega^I \Psi_{jI}(1,2), \qquad \sum_{I=0}^{2j-1} |D_\Omega^I|^2 = 1, \tag{10}$$

where

$$\Psi_\Omega(1,2)=\frac{1}{\sqrt{2}}[\Psi_{j,\Omega}(1)\Psi_{j,-\Omega}(2)-\Psi_{j,-\Omega}(1)\Psi_{j,\Omega}(2)], \quad \Psi_{jI}(1,2)=\sum_{\Omega=-j}^{j} C_{\Omega,-\Omega}^{I0}\Psi_{j,\Omega}(1)\Psi_{j,-\Omega}(2). \tag{11}$$

Then the pair energy in the deformed state of the nucleus is equal to

$$w_\Omega=\sum_{I=0}^{2j-1}|D_\Omega^I|^2 w(j^2I) > w(j^20)\left\{|D_\Omega^0|^2+\frac{1}{4}|D_\Omega^2|^2+\ldots\right\} > w(j^20). \tag{12}$$

The relation (12) is a consequence of the fact that the deformed state of the system is not an eigenstate of the total angular momentum.

In Table I we have listed the experimental values for the pair energy in the regions of heavy and light nuclei, obtained from data on the binding energies.[7,8] As can be seen, the pair energy decreases in absolute value in the transition to an elongated nucleus. In the region of heavy nuclei, the average value of the pair energy changes by 0.5 Mev in transition to elongated nuclei. In the region of light nuclei, the corresponding change amounts to 2 Mev. In the region of rare earths, the binding energies are not measured accurately, and cannot be used to determine the change in the pair energy in the transition. In this region, the energy ought to be somewhat higher than in the heavy nuclei, since the pair energy is an almost monotonically decreasing function of the mass number. For this region, we have taken the value 0.7 Mev, which is evidently close to the correct one.

TABLE I

Protons		Neutrons	
pair	w, Mev	pair	w, Mev
Spherical nuclei		Spherical nuclei	
83—84	—1.373	127—128	—1.418
85—86	—1.689	129—130	—1.518
87—88	—1.784	131—132	—1.778
		133—134	—1.875
		135—136	—1.875
		137—138	—1.988
Prolate nuclei		Prolate nuclei	
89—90	—1.068		
91—92	—1.030		
93—94	—1.024		
95—96	—0.996		
97—98	—1.027	133—134	—1.359
99—100	—1.050	135—136	—1.268
		137—138	—1.389
		139—140	—1.340
		141—142	—1.186
		143—144	—1.074
		145—146	—1.132
		147—148	—1.107
		149—150	—1.092
		151—152	—1.100
Vicinity of Mg^{24}; nucleons			
Spherical nuclei			
9—10	—5.5		
Prolate nuclei			
11—12	—3.5		
13—14	—3.5		

The energy of pair interaction is equal to the sum of the pair energies in all pairs of nucleons. The difference $W_N - W_M - \Delta W(A)$[6] between the pair energies of the nucleus in the deformed and spherical states depends on the number of nucleons (or holes) outside a filled shell, but, in contrast to the difference $\Delta E(A)$ of single particle energies, they are always positive. If $\Delta E(A)$ is smaller than $\Delta W(A)$ in absolute magnitude, then the transition to the deformed equilibrium form is energetically forbidden. However, the nucleus has a spherical equilibrium form if the sum $\Delta E + \Delta W$ is positive.

Transition to the deformed equilibrium form is achieved upon filling those nucleonic levels in which the difference between the energies in the deformed and spherical states exceeds the difference of pair energies. Upon their filling, the sum $\Delta E + \Delta W$ changes sign and the nucleus acquires a deformed equilibrium form. Since the change of sign of the sum comes about for sufficiently large $\Delta E(A)$, then the equilibrium deformation of the nucleus in this case changes abruptly from zero to a value of 0.2 — 0.3.

3. DETERMINATION OF THE POSSIBLE STATES OF PROLATENESS

Up to the present time, it has not been possible to make any assumptions as to the dependence of the nuclear potential on the distance, and our conclusions do not depend on the form of $V(r)$. Now let us

TABLE II

Nucleus	β	Proton configuration	Neutron configuration	$E(A), \hbar\omega_0^0$	ΔE, Mev	ΔW	ΔE + ΔW
$_{60}Nd^{146}_{86}$	0.3	$g^{10}_{9/2}; g^4_{7/2}\left(\frac{1}{2}+,\frac{3}{2}+\right); d^2_{5/2}\left(\frac{1}{2}+\right); h^4_{11/2}\left(\frac{1}{2}-,\frac{3}{2}-\right);$	$h^{10}_{11/2}\left(\frac{1}{2}--\frac{9}{2}-\right); f^4_{7/2}\left(\frac{1}{2}-,\frac{3}{2}-\right); h^2_{9/2}\left(\frac{1}{2}-\right);$	699.311	−12.364	12.6	+0.236
	0	$g^{10}_{9/2}; g^8_{7/2}; d^2_{5/2};$	$h^{12}_{11/2}; f^6_{7/2};$	700.899			
$_{60}Nd^{148}_{88}$	0.3		$h^{10}_{11/2}; f^4_{7/2}\left(\frac{1}{2}-,\frac{3}{2}-\right); h^2_{9/2}\left(\frac{1}{2}-\right); i^2_{13/2}\left(\frac{1}{2}+\right);$	710.758	−17.835	13.3	−4.535
	0		$h^{12}_{11/2}; f^6_{7/2};$	713.059			
$_{60}Nd^{150}_{90}$	0.3		$h^{10}_{11/2}; f^4_{7/2}\left(\frac{1}{2}-,\frac{3}{2}-\right); h^2_{9/2}\left(\frac{1}{2}-\right); i^4_{13/2}\left(\frac{1}{2}+,\frac{3}{2}+\right);$	722.387	−21.854	14	−7.854
	0		$h^{12}_{11/2}; f^8_{7/2};$	725.219			
$_{62}Sm^{148}_{86}$	0.3	$g^{10}_{9/2}; g^4_{7/2}\left(\frac{1}{2}+,\frac{3}{2}+\right); d^2_{5/2}\left(\frac{1}{2}+\right); h^6_{11/2}\left(\frac{1}{2}-,\frac{3}{2}-,\frac{5}{2}-\right);$		713.846	−13.084	12.6	−0.484
	0	$g^{10}_{9/2}; g^8_{7/2}; d^4_{5/2};$		715.534			
$_{62}Sm^{150}_{88}$	0.3			725.294	−18.513	13.3	−5.213
	0			727.694			
$_{62}Sm^{152}_{90}$	0.3			736.924	−22.511	14	−8.511
	0			739.854			

Table II continued

Nucleus	β	Proton configuration	Neutron configuration	$E(A), \hbar\omega_0^0$	ΔE, Mev	ΔW	ΔE + ΔW
$_{76}Os^{186}_{110}$	0.2	$g^{10}_{9/2}; g^8_{7/2}; d^6_{5/2}; h^{10}_{11/2}\left(\frac{1}{2}--\frac{9}{2}-\right); d^2_{3/2}\left(\frac{1}{2}+\right);$	$h^{12}_{11/2}; f^8_{7/2}; h^8_{9/2}\left(\frac{1}{2}--\frac{7}{2}-\right); i^{10}_{13/2}\left(\frac{1}{2}+,-\frac{9}{2}+\right); p^2_{3/2}\left(\frac{1}{2}-\right);$	970.857	−10.523	7.7	−2.823
	0	$g^{10}_{9/2}; g^8_{7/2}; d^6_{5/2}; h^{12}_{11/2};$	$h^{12}_{11/2}; f^8_{7/2}; h^{10}_{9/2}; i^{10}_{13/2};$	972.322			
$_{76}Os^{188}_{112}$	0.2		$h^{12}_{11/2}; f^8_{7/2}; h^8_{9/2}\left(\frac{1}{2}--\frac{7}{2}-\right); i^{10}_{13/2}\left(\frac{1}{2}+,-\frac{9}{2}+\right); p^2_{1/2}\left(\frac{1}{2}-\right); f^2_{5/2}\left(\frac{1}{2}-\right);$	983.748	−7.758	7	−0.758
	0		$h^{12}_{11/2}; f^8_{7/2}; h^{10}_{9/2}; i^{12}_{13/2};$	984.832			
$_{76}Os^{190}_{114}$	0.2		$h^{12}_{11/2}; f^8_{7/2}; h^8_{9/2}\left(\frac{1}{2}--\frac{7}{2}-\right); i^{10}_{13/2}\left(\frac{1}{2}+,-\frac{9}{2}+\right); p^4_{1/2}; f^2_{5/2}\left(\frac{1}{2}-\right);$	996.673	−4.772	6.3	+1.528
	0		$h^{12}_{11/2}; f^8_{7/2}; h^{10}_{9/2}; i^{14}_{13/2};$	997.342			
$_{76}Os^{192}_{116}$	0.1		$h^{12}_{11/2}; f^8_{7/2}; h^{10}_{9/2}; i^{10}_{13/2}\left(\frac{1}{2}+,-\frac{9}{2}+\right); p^4_{1/2}; f^2_{5/2}\left(\frac{1}{2}-\right);$	1009.619	−3.788	5.6	+1.812
	0		$h^{12}_{11/2}; f^8_{7/2}; h^{10}_{9/2}; i^{14}_{13/2}; p^2_{3/2};$	1010.152			

undertake the determination of the regions of deformation, making use of the entire scheme of bound states which are taken into account by starting from a model of an "oscillator potential well".[2]

Change in sign of the sum ΔE + ΔW can be brought about by filling the lowest levels of the N-th shell. Actually, for $\beta = 0$, these levels have the highest j, equal to $N + \frac{1}{2}$, thanks to spin-orbit coupling, and

usually enter into the constitution of the $(N-1)$-st shell (for example, the level $i_{13/2}$ which enters into the constitution of the fifth oscillator shell). The state with $\Omega = \frac{1}{2}$, which is produced in the splitting of the term $j_{max} = N + \frac{1}{2}$, has an orbit which is elongated in comparison with the states of the $(N-1)$-st shell, and its filling can lead to the formation of an interval of elongated nuclei In similar fashion, the filling of states with $\Omega = j_{max}$ can lead to the formation of an interval of oblate nuclei.

For determination of the sign of the deformations, we compare the energy of the lowest levels for $\beta > 0$ and $\beta < 0$. The energy of the level for large deformations in the model of the oscillator potential well is equal to

$$E_\Omega = \hbar\omega_0^0(1 + {}^1/_3\varepsilon^2)[N + {}^3/_2 + {}^1/_3\varepsilon(N - 3n_z)] - C_{N\Omega n_z}, \tag{13}$$

where n_z is the oscillator quantum number along the z axis, $C_{N\Omega n_z}$ is a small constant of the state (on the order of magnitude of $0.1\,\hbar\omega_0^0$), which is independent of the deformation. The lowest states for $\epsilon > 0$ have $\Omega = \frac{1}{2}$, $n_z = N$ and $\Omega = {}^3/_2$, $n_z = N - 1$. Their energies are respectively equal to

$$E_{1/2} = \hbar\omega_0(\varepsilon)[N + {}^3/_2 - {}^2/_3\varepsilon N] - C_{1/2}, \quad E_{3/2} = \hbar\omega_0(\varepsilon)[N + {}^3/_2 - {}^1/_3\varepsilon(2N - 3)] - C_{3/2}. \tag{14}$$

The lowest states for $\epsilon < 0$ have

$$\Omega = N + {}^1/_2,\ n_z = 0 \text{ and } \Omega = N - {}^1/_2,\ n_z = 1.$$

Their energies are respectively equal to

$$E_{N+1/2} = \hbar\omega_0(\varepsilon)[N + {}^3/_2 - {}^1/_3|\varepsilon|N] - C_{N+1/2}, \quad E_{N-1/2} = \hbar\omega_0(\varepsilon)[N + {}^3/_2 - {}^1/_3|\varepsilon|(N - 3)] - C_{N-1/2}. \tag{15}$$

As comparison of (14) with (15) shows, for large $|\epsilon|$,

$$E_{1/2} < E_{N+1/2}, \quad E_{3/2} < E_{N-1/2}.$$

In other words, for large deformations, an elongated equilibrium shape is more advantageous and, since the transition is accomplished precisely for large deformations, the absence of nuclei with negative quadrupole moments can be explained on these grounds.

The finding of the possible intervals of elongation has been carried out by comparison of the total energies of the nuclei for $\beta = 0$ and $\beta > 0$.

(a) Region of rare earths (even-even isotopes $_{60}Nd^{146} - {}_{76}Os^{192}$, Table II). For each nucleus, the nucleonic configurations of the ground states were found for $\beta = 0$ and $\beta > 0$, and the sums of the single particle energies were computed in terms of the oscillator quantum $\hbar\omega_0^0 \approx 41A^{-1/3}$ Mev. The difference in the one-particle energies ΔE is equal to the difference between the pair energies in the spherical and deformed states. The latter is proportional to the number of pairs of monoenergetic nucleons, if the shell is less than half filled, and correspondingly, to the number of hole pairs if the shell is more than half filled, since, for filling the shell, the pair energies in the spherical and deformed states are identical, while the energy states of a given number of nucleons outside a filled shell are analogous to the states of the same number of holes.

The sum $\Delta E + \Delta W$ changes sign in the transition form $N = 86$ to $N = 88$, which corresponds to the filling of the neutron state $i_{13/2}(\frac{1}{2}+)$. The value obtained for the lower limit of prolateness agrees with the experimental values for the filling of the neutron states $i_{13/2}(\frac{1}{2}+, {}^3/_2+)$. In the filling of each of these states, ΔE changes by a quantity far exceeding the difference in the pair energies, which produces a transition to the prolate equilibrium form.

In the region of the lower boundary of the lower limit of prolateness, the proton subshell $Z = 64$ is close to being filled, as a consequence of which the protons do not affect the establishment of the prolate equilibrium form.

The inverse transition to the spherical equilibrium form is achieved for $Z = 76$, $N = 116$, which corresponds to a filling of the proton state $h_{11/2}({}^9/_2-)$ and the neutron states $p_{3/2}({}^3/_2-)$ and $h_{9/2}({}^9/_2-)$. The value found for the upper limit of prolatenes agrees with the experimental value $Z = 76$, $N = 114$. In contrast to the lower limit, the transition here is determined by the filling of both the neutron and the proton states, inasmuch as now both shells are close being filled.

(b) Region of heavy nuclei (Table III). The rotational region found in the heavy elements begin with the nucleus $_{88}Ra^{222}$. Inasmuch as $N = 134$ corresponds to filling of five oscillator shells, the neutrons do not exhibit any noticeable effect on the transition to the prolate equilibrium shape. Therefore, energy comparison is carried out for isotones with $N = 134$, since the problem consists of searching for proton states which govern the transition.

TABLE III

Nucleus	β	Proton configuration	Neutron configuration	$E'(A)\hbar\omega_0^0$	ΔE, ΔW, Mev	$\Delta E+\Delta W$
$_{84}Po^{218}_{134}$	0.3	$h^{10}_{11/2}; f^2_{7/2}\left(\frac{1}{2}-\right); i^2_{13/2}\left(\frac{1}{2}+\right);$ $h^{12}_{11/2}; f^2_{7/2};$	$i^{12}_{13/2}; g^6_{9/2}\left(\frac{1}{2}+,\frac{3}{2}+,\frac{5}{2}+\right); i^4_{13/2}\left(\frac{1}{2}+\frac{3}{2}+\right)$ $i^{14}_{13/2}; g^8_{9/2}$	1196.094	−4.980	+4.020
	0			1196.825	9	
$_{86}Rn^{220}_{134}$	0.3	$h^{10}_{11/2}; f^2_{7/2}\left(\frac{1}{2}-\right); h^2_{9/2}\left(\frac{1}{2}-\right); i^2_{13/2}\left(\frac{1}{2}+\right);$ $h^{12}_{11/2}; f^4_{7/2};$		1213.152	−10.954	−1.454
	0			1214.765	9.5	
$_{88}Ra^{222}_{134}$	0.3	$h^{10}_{11/2}; f^2_{7/2}\left(\frac{1}{2}-\right); h^2_{9/2}\left(\frac{1}{2}-\right); i^4_{13/2}\left(\frac{1}{2}+,\frac{3}{2}\right);$ $h^{12}_{11/2}; f^6_{7/2};$		1230.327	−17.063	−7.063
	0			1232.847	10	

With this aim, we constructed the Nilsson scheme for states of the proton shell 82 — 126 (see drawing). The construction was performed by the same method which was used in Ref. 2. For the state of the fifth oscillator shell, we assumed the same constant of spin-orbit coupling κ which was used in Ref. 2 for the state of the fourth proton shell (see also Ref. 4). For the states of the sixth oscillator shell, the constant of spin-orbit coupling was increased several fold in order to obtain better agreement with experiment (the values $\kappa_5 = 0.0613$, $\kappa_6 = 0.058$ were taken in place of the value $\kappa_6 = 0.05$ of Nilsson). In Table IV, the spins and parities of the ground state of nuclei with an odd number of protons are compared with the experimental values of these quantities. Agreement with experiment can be regarded as satisfactory.

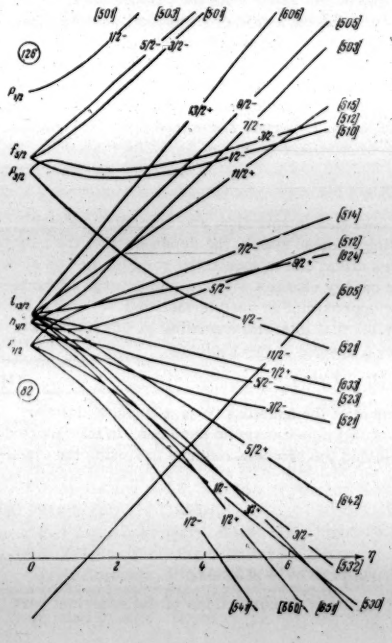

The calculation carried out with the use of the drawing shows that the transition to the prolate equilibrium form is determined by filling of the proton states $i_{13/2}$ ($\frac{1}{2}$ +, $\frac{3}{2}$+), i.e., the same states which produce the transition in the region of the rare earths. The limit of the region of prolateness corresponds to Z = 88 and agrees with experiment.

TABLE IV

Chemical Symbol	Z	Theoretical value of the spin	Experimental value
Ac	89	$^3/_2-$, $^3/_2+$	$^3/_2-$
Pa	91	$^3/_2-$, $^{11}/_2-$, $^5/_2+$	$^3/_2-$
Np	93	$^5/_2+$, $^5/_2-$	$^5/_2+$
Am	95	$^5/_2-$, $^5/_2-$	$^5/_2-$
En	99	$^7/_2+$, $^{11}/_2-$	$(^7/_2)$

(c) Nuclei in the region of Mg^{24}. According to the given calculation, for this region, the transition to the prolate equilibrium form is achieved by filling the state $d_{5/2}$ ($\frac{1}{2}$+) which corresponds to N, Z = 10. The reverse transition takes place upon filling of the state $d_{5/2}$ ($^5/_2$+), which corresponds to N, Z = 14. The value thus found for the lower limit of prolateness does not agree with experiment, since the rotational region begins with the nucleus $_{11}Na^{23}$. The upper limit is determined more precisely, apparently. Thus, for this region of the nuclei, the agreement of the theory with experiment is

worse than in the first two; however, even here the observed rotational nuclei do not exceed the limits computed theoretically.

(d) The existence of all three intervals of elongation is brought about, as we have seen, by filling of the the lowest states of the oscillator shells. In the regions of the rare earths and heavy nuclei, the lowest states filled are ths sixth, while in the region of Mg^{24}, it is the second oscillator shell. We can expect that in the filling of the lowest states, the third, fourth and fifth shells will also produce a region of elongated nuclei. However, calculation carried out for these regions shows that the difference between the single particle energies in the deformed and spherical states does not exceed the difference of the energies of pair interaction (for the difference of pair energies we have assumed the value 1 Mev, which is the lower limit of this quantity in the regions lying about Mg^{24} and the rare earths), and consequently there are no prolate nuclei in these states.

Thus, in addition to the regions of the rare earths and of heavy nuclei, and to the region about Mg^{24}, the theory does not give other regions of prolateness, a result that agrees with the available experimental data.

CONCLUSIONS

(1) As we can see from the results of the investigation just carried out, the role of the remaining interaction of nucleons at a distance is not confined to an account of the spin dependence of nuclear forces. It is shown that the jump change of the equilibrium form of atomic nuclei, observed in experiment, is determined by the effect of the pair energy, which favors the transition to the deformed equilibrium form if number of nucleons outside the shell is small.

(2) If the difference between the pair energies in the deformed and spherical states is estimated from experimental data, than all three known regions of prolate nuclei are obtained, while the theoretical boundaries for the prolate nuclei are in agreement with the experimental data. The theory gives no evidence for the existence of other regions of prolate nuclei that do not arise from the present data.

(3) The use of the oscillator potential for the calculation of the nucleonic energies and the potential for the pair interaction does not restrict the generality of the results, inasmuch as the Nilsson scheme depends only slightly on the choice of the potential, while experimental values are used for the pair energy.

In conclusion, I consider it my pleasant duty to thank Professor L. A. Sliv for his unflagging interest in the work and for a number of valuable suggestions given during its undertaking. The author also thanks his coworkers in the Department of Theoretical Physics of the A. I. Herzen Leningrad State Pedagogical Institute for discussion of the results of the research.

APPENDIX

In Sec. 2 we determined the limiting values of the pair energies in spherical and deformed nuclear states. In the comparison with the energy of pair interaction in these states, the dependence of the pair energy on the deformation was not considered, although this effect can influence the results. Let us show that, in the case of limitingly short-range forces, the pair energy changes within a small range of variation of β between the limiting values, and consequently the approximation used is justified.

For this purpose, let us consider a system of two particles that interact according to Eq. (8). The Hamiltonian of the nucleon is expressed by Eq. (4), and for a system of two nucleons,

$$\hat{H}(1,2) = \hat{H}_N(1) + \hat{H}_N(2) + \hat{W}(1,2). \tag{1}$$

We limit ourselves to the case in which the individual moment of the nucleons j is a quantum number (the so-called j-approximation), and consider the system of two monoenergetic nucleons. In this approximation, the operator of spin-orbit coupling can be inserted, and the problem reduces to finding the eigenvalues of the equation

$$\hat{O}\Psi = u\Psi, \tag{2}$$

where

$$\hat{O} = \hat{V} + \hat{W}, \quad \hat{V} = -\beta\left[r_1 \frac{dV}{dr_1} Y_{20}(\theta_1) + r_2 \frac{dV}{dr_2} Y_{20}(\theta_2)\right], \quad W = -g\delta(\mathbf{r}_1 - \mathbf{r}_2). \tag{3}$$

We seek a solution of Eq. (2) in the form of a linear combination of eigenfunctions of the spherical part of the Hamiltonian (1)

$$\Psi = \sum_{\Omega=1/2}^{j} B_\Omega \Psi_\Omega, \tag{4}$$

$$\Psi_\Omega = R_{Nl}(r_1) R_{Nl}(r_2) \frac{1}{\sqrt{2}} [Y_{j,\Omega}(1) Y_{j,-\Omega}(2) - Y_{j,-\Omega}(1) Y_{j,\Omega}(2)], \tag{5}$$

$Y_{j,\Omega}$ are the well known spherical harmonics in the spin. The matrix elements $\hat{V}$ and $\hat{W}$ are equal to

$$\langle \Omega_1 | \hat{V} | \Omega_2 \rangle = \sqrt{\frac{5}{\pi}} \beta \langle Nl \left| r \frac{dV}{dr} \right| Nl \rangle \frac{3(\Omega - 1/2)(\Omega + 1/2) - (j - 1/2)(j + 3/2)}{2j(2j+2)} \delta_{\Omega_1 \Omega_2}; \tag{6}$$

$$\langle \Omega_1 | \hat{W} | \Omega_2 \rangle = \sum_{I=0}^{2j-1} D^I_{\Omega_1} D^I_{\Omega_2} w(j^2 I), \tag{7}$$

where $D^I_\Omega = \sqrt{2} C^{I0}_{\Omega;-\Omega}$; $C^{I0}_{\Omega;-\Omega}$ are the Clebesh-Gordan coefficients, and $w(j^2 I)$ is expressed by Eq. (9) of Sec. 2.

For determination of the eigenvalues of Eq. (2), we must solve a secular equation of degree $(2j + 1)/2$. We do this in the case $j = 3/2$, making use of the model of the oscillator potential well, and for definiteness setting $N = 4$, $l = 2$, although N and l do not play an essential role in the choice of $V(r)$. The eigenvalues of (2) are then determined from the expressions

$$\begin{vmatrix} -1.4\beta - 0.18a - u & 0.12a \\ 0.12a & 1.4\beta - 0.18a - u \end{vmatrix} = 0, \tag{8}$$

where $a = g\alpha^3/4\pi\hbar\omega$ is the ratio of the constant in the energy of pair interaction to the energy of the oscillator quantum, $\alpha = \sqrt{m\omega/\hbar}$. The energy of the ground state is equal to

$$u = -0.18a - \sqrt{0.0144a^2 + 1.96\beta^2}. \tag{9}$$

in units of $\hbar\omega$. The corresponding wave function is

$$\Psi = \cos(\varphi/2)\Psi_{1/2} - \sin(\varphi/2)\Psi_{3/2}, \quad \tan\varphi = 0.12a/1.4\beta. \tag{10}$$

As is easily seen, for $\beta \to 0$

$$\Psi \to -[-\Psi_{1/2} + \Psi_{3/2}]/\sqrt{2} = -\Psi_{I=0,0}, \tag{11}$$

i.e., the total momentum $\beta = 0$ corresponds to the spherical ground state of the system for $I = 0$. For sufficiently large deformations, we can neglect the pair energy (in the limit $a \to 0$), and $\Psi \to \Psi_{1/2}$, i.e., $\Omega = \frac{1}{2}$ corresponds to the deformed ground state.

In order to obtain the pair energy as a function of the deformation, we subtract from (9) the purely deformation energy, which is obtained from (8) in the absence of the pair energy. As a result, we have

$$w(\beta) = -0.18a - 1.4[\sqrt{\beta^2 + (0.12/1.4)^2 a^2} - |\beta|]. \tag{12}$$

In the spherical state, $w = -0.3\,a$; in the deformed state, $w = -0.18\,a$. As is seen from (12), the pair energy is practically equal to the deformation value at $\beta \approx 0.1$, and for further increase of β, it is independent of the deformation.

[1] M. G. Mayer and J. H. Jensen, Elementary theory of nuclear shell structure, (New York, London, 1955).

[2] S. G. Nilsson, Dan Med. Fys. Medd. 29, No. 16 (1955).

[3] K. Gottfried, Phys. Rev. 103, 1017 (1956).

[4] B. Mottelson and S. Nilsson, (Probl. of Mod. Phys.) 1, 486 (1956) [presumably a translation of Z. Physik 141, 217 (1955)].

[5] P. F. A. Klinkenberd, Revs. Mod. Phys. 24, 63 (1952).

[6] N. Zeldes, Nucl. Phys. 2, 1-64 (1956).

[7] J. R. Huizenga, Physica 21, 410 (1955).

[8] A. H. Wapstra, Physica 21 367 (1956).

Translated by R. T. Beyer
251

*DIFFRACTION SCATTERING AND NUCLEON STRUCTURE**

S. Z. BELEN'KII†

P. N. Lebedev Physics Institute, Academy of Sciences, U.S.S.R.

Submitted to JETP editor May 17, 1957

J. Exptl. Theoret. Physics (U.S.S.R.) 5, 1248-1250 (November, 1957)

The scattering of high-energy particles, such as the collision of two nucleons or the collision of a π meson with a nucleon, is analyzed. It is shown that, at high energies, each of these processes is characterized by a single scattering amplitude. Only the imaginary part of this amplitude plays an essential role, and, generally speaking, it can be determined from experiments on diffraction scattering.

1. Elastic meson-nucleon and nucleon-nucleon scattering is in general a very complicated affair. The functions characterizing the scattering amplitudes have both real and imaginary parts. They differ for states of different isotopic and ordinary spin. A phase-shift analysis is very difficult to carry out even at moderate energies, and its relation to the structure of nucleons is quite uncertain. It is possible, however, to make the following statement: When the scattered particles carry large energies, the analysis becomes simplified, only one scattering amplitude plays an essential role, and in general only its imaginary part. In that case only one real function is unknown, and it can be fully and completely determined from meson-nucleon and nucleon-nucleon diffraction scattering experiments. This function leads to definite conclusions about the size and form-factor (structure) of nucleons.

The proof of this statement is based on the following three conditions: (1) the isotopic invariance of nuclear interaction, (2) the high probability of multiple production of π mesons at high energies; (3) the fact that at high energies the total interaction cross section tends to a value σ_0 which differs from zero and is independent of energy (and equal, furthermore, to that for the interaction of π^+ and π^- mesons with nucleons). It should be noted that an attempt has already been made[1] to obtain some information on the nucleon "radius" from experimental data on the elastic and non-elastic scattering of π mesons having energies of 1.4 Bev and greater. This analysis, however, was based on a crude model of the nucleon represented by a sphere of constant density with abrupt boundaries. As was shown earlier,[2] the problem of determining the nucleonic structure can be treated more consistently by starting from the general scattering theory for particles which can also be absorbed by the scattering center. In that case the spatial distribution of the scattering and absorbing field may be obtained from experimental data on the elastic and inelastic scattering of π mesons by nucleons, if these data are sufficiently detailed.

Essential to this proof is the premise that in the imaginary part of the scattering amplitude is considerably smaller than the real part in the corresponding energy region.[3] These questions will be considered here in greater detail.

2. We consider first the scattering of a proton by a proton (pp) and of a proton by a neutron (pn). We denote the wave function of the isotopic state as follows:

$$(pp) = \chi_{1,1}, \quad (nn) = \chi_{1,-1}, \quad (pn) = (\chi_{0,0} - \chi_{1,0})/\sqrt{2}, \quad (np) = (\chi_{0,0} - \chi_{1,0})/\sqrt{2}. \tag{1}$$

The first index denotes the total isotopic spin T, and the second index its z-component T_z.

The following three basic processes may occur in elastic scattering:[3]

$$\begin{aligned} &1)\ p + p \to p + p, (pp) \to (pp);\\ &2)\ p + n \to p + n, (pn) \to (pn);\\ &3)\ p + n \to n + p, (pn) \to (np). \end{aligned} \tag{2}$$

*Prepared for publication by V. P. Silin and E. L. Feinberg from notes found among the manuscripts of S. Z. Belen'kii. This work was reported at a seminar of the Theoretical Division of the Physics Institute, Academy of Sciences, September 7, 1956.

†Deceased.

The last process includes an exchange of nucleons (exchange scattering).

The differential cross section for these reactions is obtained from the scattering amplitudes in the state $T = 1$ and $T = 0$, denoted[3] by f and g, as follows:

$$\sigma_1 = |f|^2, \quad \sigma_2 = {}^1/_4|f+g|^2, \quad \sigma_3 = {}^1/_4|f-g|^2. \tag{3}$$

At small energies, say on the order of 10^8 ev, it is well known that there is a considerable amount of exchange scattering. This means that σ_2 and σ_3 are of the same order of magnitude. In that case σ_1 is also of the same order of magnitude. Therefore, $|f| \gg |g|$.

At large energies, where the main process consists of meson production, i.e. an inelastic interaction, the elastic exchange scattering is relatively small, i.e. $\sigma_3 \ll \sigma_{\text{inel}}$. As for σ_2, the elastic scattering cross section with no charge exchange, it is always of the order of σ_{inel}, since it contains diffraction scattering which is considerable even for a "gray" nucleus. Thus, at large energies, $\sigma_3 \ll \sigma_2$ while $\sigma_2 \sim \sigma_1$, i.e.

$$|f-g| \ll |f|, \quad |f| \sim |g|, \tag{4}$$

and all the scattering processes are characterized by a single function f, which may thus be related to the structure of the nucleon.

3. Similar considerations apply to the interaction of π mesons with nucleons. Five basic processes are now possible, and their cross sections can similarly be expressed in terms of two scattering amplitudes for isotopic spins $T = {}^3/_2$ (amplitude f) and $T = {}^1/_2$ (amplitude g):

$$\begin{aligned}
&1)\ \pi^+ + p \to \pi^+ + p, && \sigma_1 = |f|^2;\\
&2)\ \pi^0 + p \to \pi^0 + p, && \sigma_2 = {}^1/_9|2f+g|^2;\\
&3)\ \pi^0 + p \to \pi^+ + n, && \sigma_3 = \sigma_5 = {}^2/_9|f-g|^2;\\
&4)\ \pi^- + p \to \pi^- + p, && \sigma_4 = {}^1/_9|f+2g|^2;\\
&5)\ \pi^- + p \to \pi^0 + n, && \sigma_5 = \sigma_3
\end{aligned} \tag{5}$$

(these, of course, are not the same f and g as for the nucleon-nucleon scattering). At small energies, the scattering cross sections for π^+ and π^- mesons are different. At high energies, inelastic processes come into play. In comparison with these, the charge-exchange scattering cross section σ_5 is small, while σ_1, σ_2 and σ_4, which include diffraction scattering, are of the same order of magnitude as σ_{inel}, i.e., $\sigma_1 \sim \sigma_2 \sim \sigma_4 \sim \sigma_0$, $\sigma_3 \sim \sigma_5 \ll \sigma_0$, or

$$|f-g| \ll |f|, \quad |f| \sim |g|, \tag{6}$$

as in the case of nucleon-nucleon collisions. For mesons too, therefore, all the essential processes of elastic scattering are determined at high energies by a single function f. In other words, the scattering does not depend upon the isotopic spin.

4. We now show, on the basis of general considerations, that the imaginary part of the scattering amplitude f is large compared with its real part, so that all the scattering processes can be described at high energy by one real function.

In order to distinguish among the five types of pion-nucleon scattering processes, we introduce the complex scattering amplitudes $f_i(k)$, $i = 1, \ldots, 5$, as functions of the meson momentum k. Then $f_1(k) \equiv f(k)$ and $f_4(k) = [f(k) + 2g(k)]/3$, and therefore $g(k) = [3f_4(k) - f_1(k)]/2$. It follows then that

$$f_5(k) = \frac{\sqrt{2}}{3}(f_1 - g) = \frac{1}{\sqrt{2}}(f_1 - f_4).$$

Separating the real and imaginary parts $D(k)$ and $A(k)$ of $f_1(k)$ and $f_4(k)$ respectively, we may write

$$f_1(k) = D_+(k) + iA_+(k), \quad f_4(k) = D_-(k) + iA_-(k). \tag{7}$$

The imaginary part of the forward scattering amplitude is related to the total cross section σ_0 by a formula which, inasmuch as the total cross sections for π^+ and π^- mesons practically coincide at large energies, may be written as

$$A_+(k) \approx A_-(k) = k\sigma_0/4\pi. \tag{8}$$

Therefore

$$f_5 = (f_1 - f_4)/\sqrt{2} = (D_+(k) - D_-(k))/\sqrt{2}. \tag{9}$$

One may further apply the relation [see, for example, Ref. (4)] $D_-(k) = D_+(-k)$, which we gave for energies much larger than the rest mass of the meson. Eq. (9) then takes the following form:

$$f_s = (D_+(k) - D_+(-k))/\sqrt{2}. \tag{10}$$

It is easily seen from the dispersion relations that link the real part of the forward scattering amplitude with the total scattering cross section,[4] that within given limits, the total cross sections at high energies $D_\pm(k)$ cannot increase faster than the first power of k. Thus, even if $D_+(k) = \alpha k$, where α is a constant, $D_-(k) = D_+(-k) = -\alpha k$, and therefore, $f_s(k) = \sqrt{2\alpha k} = \sqrt{2}\, D_+(k)$. Owing to the fact that at large energies, from Eq. (6), $|f_s| \ll |f_1|$, and $f_1 = D_+ + iA_+$, the following inequality holds:

$$|D_+(k)| \ll |A_+(k)|. \tag{11}$$

Note that according to Eq. (8), $A_+(k)$ increases with energy as the first power of k as long as σ_0 does not vanish, thus if $D_+(k)$ increases more slowly, Eq. (11) is fulfilled all the more.

[1] Eisberg, Fowler, Lea, Shephard, Shutt, Thorndike, and Whittemore, Phys. Rev. **97**, 797, (1955).
[2] S. Z. Belen'kii, J. Exptl. Theoret. Phys. (U.S.S.R.) **30**, 983, (1956), Soviet Phys. JETP **3**, 813 (1956).
[3] L. B. Okun' and I. Ia. Pomerantchuk, J. Exptl. Theoret. Phys. (U.S.S.R.) **30**, 424 (1956), Soviet Phys. JETP **3**, 307 (1956).
[4] Goldberger, Miyazawa, and Oehme, Phys. Rev. **99**, 986 (1955).

Translated by M. A. Melkanoff
252

SOVIET PHYSICS JETP VOLUME 6 (33), NUMBER 5 MAY, 1958

INVERSE DISPERSION RELATIONS

V. Z. BLANK and D. V. SHIRKOV

Joint Institute of Nuclear Research

Submitted to JETP editor May 17, 1957

J. Exptl. Theoret. Phys. (U.S.S.R.) **33**, 1251-1253 (November, 1957)

"Inverse" dispersion relations express the imaginary part of a scattering amplitude as a Cauchy integral of the real part. The integral over the unphysical region is evaluated by making use of ordinary "direct" dispersion relations. The forward scattering amplitudes for charged pions on nucleons are discussed in detail. The inverse dispersion relations for this case are written out explicitly in a form in which no unobservable quantities appear.

STARTING from quantum field theory, various authors[1,2] have derived dispersion relations for the scattering of pions and photons on nucleons and for the photoproduction of pions. These relations express the real part D(E) of the amplitude as a Cauchy integral of the imaginary part A(E), thus

$$D(E) = \frac{1}{\pi} \mathrm{P} \int_{-\infty}^{\infty} \frac{A(E')}{E' - E} dE'. \tag{1}$$

The negative part of the energy range can be eliminated by using symmetry properties, and for forward scattering the part of the integral arising from unphysical positive energies can be computed explicitly. This reflects the fact that in the unphysical region the function A(E) can be represented as a sum of δ-functions. The integral over the unphysical range then depends only on the coupling constants of the relevant interactions.

The dispersion relations for pion-nucleon scattering have been tested experimentally, and satisfactory agreement between theory and experiment has been found, over the range of energies now accessible.[3] A test of dispersion relations at higher energies would be of great interest. The derivations of dispersion relations all assume the validity of microscopic causality,[2,4] and if there is a failure of microscopic causality the relations should be altered in a definite way. However, dispersion relations of the form (1) may be unsuited for such a test. They will be inconvenient if at high energies the real part of the scattering amplitude becomes small compared with the imaginary part, and already there are some indications[5] that this will happen. If so, the relations equate a small quantity on the left side of Eq. (1) to an integral of a large quantity of variable sign on the right side. In this case, the already considerable experimental errors in the determination of A will produce an enormous overall effect. As a result, the experimental test of dispersion relations of the form of Eq. (1) at high energy may be very difficult, and the experimental observation of a fundamental length may be hindered.

If these difficulties prove to be real, it will be much more convenient to use inverse dispersion relations of the form

$$A(E) = -\frac{1}{\pi} \mathrm{P} \int_{-\infty}^{\infty} \frac{D(E')}{E'-E} dE', \tag{2}$$

which do not suffer from the same disadvantages. The problem then arises, that in order to use Eq. (2) we must determine the function D(E) in the unphysical range of positive energies. This problem has not yet been solved, and Eq. (2) has consequently not been studied.

We can overcome the difficulty as follows. Bogoliubov[4] has shown that the direct dispersion relation (1) holds even when E lies in the unphysical region. The function D in the integrand of Eq. (2) can therefore be replaced in the unphysical positive-energy region by the expression (1), and all unobservable quantities are thereby eliminated from the equation. The double integral which results from this substitution can be reduced to a single integral by interchanging the order of integration.

Consider the amplitude for forward pion-nucleon scattering in the laboratory system,

$$f(E) = \delta_{\rho\rho'} f_1^1 + 2i\,(\sigma\,[\mathbf{q}\times\mathbf{q}'])\,\delta_{\rho\rho'} f_2^1 + \frac{[\tau_{\rho'}, \tau_\rho]}{2} f_2^1 + i\,(\sigma\,[\mathbf{q}\times\mathbf{q}'])\,[\tau_{\rho'}, \tau_\rho]\, f_2^2 \tag{3}$$

The scalar coefficients f_j^i satisfy the following inverse dispersion relations

$$A_i^l(E) = \frac{D_i^l(E) - D_i^l(\mu)}{\pi} \ln\frac{E+\mu}{E-\mu} - \frac{2E(E^2-\mu^2)}{\pi} \int_\mu^\infty \frac{dE'}{(E'^2-E^2)(E'^2-\mu^2)} \left\{ D_i^l(E') - D_i^l(\mu) + \frac{A_i^l(E')}{\pi} \ln\frac{E'+\mu}{E'-\mu} \right\}$$

$$- C_i \frac{f^2}{\pi} \frac{2E(E^2-\mu^2)}{E^2-(\mu^2/2M)^2} \ln\left(\frac{1+\mu/2M}{1-\mu/2M}\right) \Big/ [\mu^2 - (\mu^2/2M)^2] \quad (i = 1,2); \tag{4}$$

$$A_i^k(E) = -\frac{2}{\pi}(E^2-\mu^2) \int_\mu^\infty \frac{dE'}{(E'^2-E^2)(E'^2-\mu^2)} \left\{ E' D_i^k(E') - \mu D_i^k(\mu) + \frac{A_i^k(E')}{\pi} \ln\frac{E'+\mu}{E'-\mu} \right\}$$

$$+ \left(D_i^k(E) - \frac{\mu}{E} D_i^k(E) \right) \frac{1}{\pi} \ln\frac{E+\mu}{E-\mu} - C_i \frac{f^2}{\pi} \frac{\mu^2}{M} \frac{E^2-\mu^2}{E^2-(\mu^2/2M)^2} \ln\left(\frac{1+\mu/2M}{1-\mu/2M}\right) \Big/ [\mu^2 - (\mu^2/2M)^2] \tag{5}$$

Here $(i \neq k;\ i,\ k = 1,2).$

$$C_1 = 1, \quad C_2 = -1/\mu^2. \tag{6}$$

In the usual way we derive from Eq. (4) and (5) the more interesting dispersion relations for the scattering of charged pions by protons,

$$A_+(E) = -\frac{E^2-\mu^2}{\pi} \int_\mu^\infty \frac{dE'}{E'^2-\mu^2} \mathrm{P} \frac{1}{E'-E} \left\{ D_+(E') - D_+(\mu) + \frac{A_+(E')}{\pi} \ln\frac{E'+\mu}{E'-\mu} \right\}$$

$$+ \frac{E^2-\mu^2}{\pi} \int_\mu^\infty \frac{dE'}{E'^2-\mu^2} \frac{1}{E'+E} \left\{ D_-(E') - D_-(\mu) + \frac{A_-(E')}{\pi} \ln\frac{E'+\mu}{E'-\mu} \right\} + \frac{1}{\pi} \left\{ D_+(E) - \frac{E+\mu}{2E} D_+(\mu) - \frac{E-\mu}{2E} D_-(\mu) \right\} \ln\frac{E+\mu}{E-\mu}$$

$$+ \frac{2f^2(E^2-\mu^2)}{\pi(E-\mu^2/2M)} \ln\left(\frac{\mu-\mu^2/2M}{\mu+\mu^2/2M}\right) \Big/ [\mu^2 - (\mu^2/2M)^2]; \tag{7}$$

$$A_-(E) = -\frac{(E^2-\mu^2)}{\pi} \int_\mu^\infty \frac{dE'}{E'^2-\mu^2} \mathrm{P} \frac{1}{E'-E} \left\{ D_-(E') - D_-(\mu) + \frac{A_-(E')}{\pi} \ln\frac{E'+\mu}{E'-\mu} \right\} + \frac{(E^2-\mu^2)}{\pi} \int_\mu^\infty \frac{dE'}{E'^2-\mu^2} \frac{1}{E'+E}$$

$$\times \left\{ D_+(E') - D_+(\mu) + \frac{A_+(E')}{\pi} \ln\frac{E'+\mu}{E'-\mu} \right\} + \frac{1}{\pi} \left\{ D_-(E) - \frac{E+\mu}{2E} D_-(\mu) - \frac{E-\mu}{2E} D_+(\mu) \right\} \ln\frac{E+\mu}{E-\mu}$$

$$+ \frac{2f^2}{\pi} \left(\frac{E^2-\mu^2}{E+\mu^2/2M} \right) \ln\left(\frac{1-\mu/2M}{1+\mu/2M}\right) \Big/ [\mu^2 - (\mu^2/2M)^2]. \tag{8}$$

The "large" function A appears on the right side of these relations. It might seem that the problem of obtaining relations in which only the small function appears in the integrals has not been completely solved. But in fact the "large" functions A occur in the integrals multiplied by a small logarithm, which drastically reduces their effect. Thus, supposing that the total charged pion-proton cross-sections at high energy are constant and (for example) equal to $3 \cdot 10^{-26}$ cm^2, but that the functions D_+ and D_- are constant at high energy and approximately equal to $(0 \cdot 3/\mu)$, we find that the contribution of the imaginary part to the integral is five times smaller than that of the real part. These numbers are in agreement with Sternheimer's estimates.[5]

The authors thank L. I. Lapidus for calling their attention to the importance of inverse dispersion relations, and N. N. Bogolyubov for much helpful advice.

[1] Gell-Mann, Goldberger and Thirring, Phys. Rev. **95**, 1612 (1954); M. Goldberger, Phys. Rev. **97**, 508 (1955) and **99**, 979 (1955); R. Karplus and M. Ruderman, Phys. Rev. **98**, 771 (1955); Goldberger, Miyazawa and Oehme, Phys. Rev. **99**, 986 (1955); E. Corinaldesi, Nuovo cimento **4**, 1384 (1956); Logunov, Stepanov, and Tavkhelidze, Dokl. Akad. Nauk. SSSR **112**, 45 (1957), Soviet Phys. "Doklady" **2**, 12 (1957); A. A. Logunov and B. M. Stepanov, Dokl. Akad. Nauk SSSR **110**, 368 (1956), Soviet Phys. "Doklady" **1**, 552 (1956); N. N. Boboliubov and D. V. Shirkov, Dokl. Akad. Nauk SSSR **113**, 487 (1957).

[2] R. Oehme, Phys. Rev. **100**, 1503 (1955).

[3] Anderson, Davidon and Kruse, Phys. Rev. **100**, 339 (1955); U. Haber-Schaim, Phys. Rev. **104**, 1113 (1956); W. Davidon and M. Goldberger, Phys. Rev. **104**, 1119 (1956); A. I. Mukhin and B. M. Pontecorvo, J. Exptl. Theoret. Phys. (U.S.S.R.) **31**, 550 (1956), Soviet Phys. JETP **4**, 373 (1957).

[4] N. N. Bogoliubov, report to the Seattle International Conference on Theoretical Physics, September 1956. See also Bogoliubov, Medvedev, and Polivanov, Вопросы теории дисперсионных соотношений (Problems of the Theory of Dispersion Relations) (Gostekhizdat, in press); N. N. Bogoliubov and D. V. Shirkov, Введение в теорию квантованных полей (Introduction to Quantum Field Theory) (Gostekhizdat, Moscow, 1957), Chapter 9.

[5] R. Sternheimer, Phys. Rev. **101**, 384 (1956).

Translated by F. J. Dyson
253

ELECTRON LOSSES DUE TO PHASE OSCILLATIONS INDUCED BY RADIATION FLUCTUATIONS IN SYNCHROTRONS

A. N. MATVEEV

Moscow State University

Submitted to JETP editor May 17, 1957

J. Exptl. Theoret. Phys. (U.S.S.R.) **33**, 1254-1260 (November, 1957)

An effective method is given for calculating electron losses due to phase oscillations induced by radiation. An approximate method is given for accounting for nonlinear effects by means of the appropriate boundary conditions in the linear theory.

1. INTRODUCTION

IT is well known that the quantum nature of radiation causes both phase[1] and betatron oscillations.[2,3] These oscillations lead to electron losses when electrons go out of phase with the accelerating voltage and when they collide with the walls of the synchrotron vacuum chamber. In the operation of a synchrotron it is the electron losses due to phase oscillations which are of most importance.

The mean-square deviation of phase oscillations in a weak-focusing synchrotron has been calculated by Sands.[1] Kolomenskii and the present author[4-6] have generalized these results to strong-focusing synchrotrons, and elsewhere the present author[7] has emphasized the importance of nonlinear effects in the theory of synchrotron oscillations induced by radiation. It has been shown in Ref. 6 how to obtain the formula for the smallest losses. By the use of this formula one can merely assert that "the losses are greater than some given quantity," but not how much greater. Because the smallest losses are quite large, a practical investigation of this phenomenon is necessary.

The present article describes an effective method for obtaining a formula which gives the electron losses to any previously determined accuracy, and gives an evaluation of this accuracy.

In addition, it is shown how to formulate the boundary conditions so that the nonlinear effects, as previously derived,[7] can be accounted for.

2. STOCHASTIC EQUATION AND FORMULATION OF THE PROBLEM

To derive stochastic equations for the phase oscillations induced by radiation fluctuations, we shall start with the obvious relation

$$\delta E = E - E_s = \sum eV_0 (\cos\varphi - \cos\varphi_s) + \int_0^t W_s dt - \sum \varepsilon_i. \tag{1}$$

In this equation ϵ_i is the energy of the radiated photons, eV_0 is the high-frequency field amplitude, φ is the phase with which an electron passes through the accelerating gap, and W_S is the equilibrium power radiated. It is clear that in this problem the excitation of energy in betatron oscillations need not be accounted for.

We define the packing factor α of a synchrotron by the relation

$$\delta \langle R \rangle / \langle R \rangle = \alpha \delta E / E. \tag{2}$$

We then obviously have

$$\delta E / E = (\lambda / k\omega\alpha)\dot{\Psi}, \tag{3}$$

where k is the number of the accelerating harmonic of the high-frequency field; $\Psi = \varphi - \varphi_S$ is the deviation of the particle phase from equilibrium, ω is the angular frequency of rotation of a particle in the synchrotron, $\lambda = 1 + L/2\pi R_0$, and L is the total length of the linear sections of the synchrotron per

revolution. Intensive phase oscillations are excited by radiation fluctuations only in the last stage of acceleration. Therefore we can neglect quantities proportional to the variation of the equilibrium energy and the energy in betatron oscillations in obtaining the stochastic equation. With the aid of (3) and well known formulas for the power radiated, Eq. (1) leads to the nonlinear stochastic equation[7]

$$\ddot{\Psi} + \gamma\dot{\Psi} + f^2[\cos\varphi_s - \cos(\varphi_s + \Psi)] = (k\omega\alpha/\lambda E_s)\,[W - \sum_i \varepsilon_i \delta(t - t_i)], \tag{4}$$

where

$$f^2 = (k\omega^2\alpha/2\pi\lambda)\,eV_0/E_s,\quad \gamma = (4-\alpha)(2\omega r_0/3R_0)(E_s/m_0c^2)^3,\quad r_0 = e^2/m_0c^2,\quad W = (2ce^2/3R^2)(E/m_0c^2)^4.$$

If the phase deviation Ψ is considered small, Eq. (4) can be linearized and leads to the linear stochastic equation[6]

$$\ddot{\Psi} + \gamma\dot{\Psi} + \Omega^2\Psi = (k\omega\alpha/\lambda E_s)\Big[W - \sum_i \varepsilon_i \delta(t - t_i)\Big],\quad \Omega^2 = f^2\sin\varphi_s. \tag{5}$$

We have already treated[7] the excitation of phase oscillations according to the nonlinear equation (4). We have shown that a particle in the potential well is "heated" basically the same way according to either the linear or the nonlinear theory. The main differences are due to the depth of the potential well. If the maximum allowable phase deviation from equilibrium is taken from the nonlinear theory, the potential well which will give the same deviation in the linear theory must be much greater than that of the nonlinear theory. This indeed is why the linear theory predicts lower electron losses than does the nonlinear one, as was previously shown.[7] We can therefore account for this fundamentally nonlinear effect by means of the linear theory if we proceed as follows. The potential-well depth is taken from the nonlinear theory, and the allowable limits of deviation in the linear theory are obtained from the requirement that the well depth in both theories be equal. This will account for the nonlinear effects.

Thus in solving the problem we shall proceed from the linear stochastic equation (5) and shall account for nonlinearity only in the boundary conditions.

It is convenient first to change in (5) to a new independent variable ζ defined by

$$\zeta = \int^t \Omega dt.$$

Then (5) becomes

$$\Psi'' + \beta\Psi' + \Psi = (k\omega\alpha/\lambda E_s\,\Omega)\,[W_\zeta - \sum \varepsilon_i \delta(\zeta - \zeta_i)],\quad \beta = \gamma/\Omega + \Omega'/\Omega, \tag{6}$$

where the primes denote differentiation with respect to ζ.

Let $W(\Psi, \Psi', \zeta)$ be the coordinate and velocity distribution function in the (Ψ, Ψ') phase plane. Then by using standard methods we obtain the equation

$$\frac{\partial W}{\partial\zeta} + \Psi'\frac{\partial W}{\partial\Psi} - \Psi\frac{\partial W}{\partial\Psi'} = \frac{\beta}{2}\left(\Psi\frac{\partial W}{\partial\Psi} + \Psi'\frac{\partial W}{\partial\Psi'}\right) + \beta W + q\left(\frac{\partial^2 W}{\partial\Psi^2} + \frac{\partial^2 W}{\partial\Psi'^2}\right),\quad q = (k\omega\alpha/2\lambda E_s\Omega)^2\langle\varepsilon^2\rangle_\zeta.$$

for this distribution function. This equation can be greatly simplified by the following considerations.

It is seen from (6) that the decay time of phase oscillations is much greater than the oscillation period, and that the extent to which the oscillations are excited in a single period is insignificant. This means that in the (Ψ, Ψ') phase plane the distribution is axially symmetric to a good approximation, or that it depends only on $r = \sqrt{\Psi^2 + \Psi'^2}$. Therefore the equation for the distribution function $W(r, \zeta)$ becomes

$$\frac{\partial W}{\partial\zeta} = \frac{\beta}{2} r\frac{\partial W}{\partial r} + \beta W + q\left(\frac{\partial^2 W}{\partial r^2} + \frac{1}{r}\frac{\partial W}{\partial r}\right). \tag{7a}$$

The initial distribution for $\zeta = 0$ can obviously also be taken to be axially symmetric, so that

$$W(r, 0) = W_0(r) \tag{7b}$$

with the normalization

$$\int_0^{a_0} W_0(r)\, r\, dr = 1, \tag{7c}$$

where a_0 is the maximum allowable oscillation amplitude at $\zeta = 0$. As for the boundary condition, we have already indicated how it can be used to account for the nonlinear effects. The corresponding analytic expression will be given below. At present we shall assume only that the maximum allowable amplitude at time ζ is given by $a(\zeta)$. This function depends on ζ because the equilibrium phase changes during an acceleration cycle, so that the maximum allowable amplitude changes also. On the basis of the above, and accounting for the fact that when a particle attains the boundary it leaves the accelerating cycle, we obtain the boundary condition

$$W(a(\zeta), \zeta) = 0. \tag{7d}$$

for Eq. (7a). Solution of (7a) with boundary conditions (7b) and (7d) gives the fraction $N(\zeta)/N(0) = F(\zeta)$ of the particles that are not lost by dropping out of phase. From the normalization condition (7c), the function $F(\zeta)$ is given by

$$F(\zeta) = \int_0^{a(\zeta)} W(r, \zeta)\, r dr. \tag{8}$$

The problem of the theory is to perform the calculation indicated in (8).

An exact analytic solution of (7a) with boundary conditions (7b) and (7d) would seem to be impossible. Furthermore, this exact analytic solution is impossible even if one sets $\beta = 0$, thus neglecting damping, since (7d) is given on a moving boundary.

We shall describe a method for finding a majorizing solution, which is an analytical method for effectively solving the problem to any arbitrary prescribed accuracy, and which evaluates the magnitude of the error.

3. MAJORIZING SOLUTION

Let us change in (7a) to a new independent variable ξ and to a new function Φ according to

$$\xi = r \exp\left(\frac{1}{2}\int_0^{\zeta} \beta\, d\zeta\right), \quad \Phi = W \exp\left(-\int_0^{\zeta} \beta\, d\zeta\right). \tag{9}$$

Then (7a) and boundary conditions (7b) and (7d) become

$$\frac{\partial \Phi}{\partial \zeta} = \varphi\left(\frac{\partial^2 \Phi}{\partial \xi^2} + \frac{1}{\xi}\frac{\partial \Phi}{\partial \xi}\right), \quad \varphi = q \exp\left[\int_0^{\zeta} \beta\, d\zeta\right]; \tag{10}$$

$$\Phi(\xi, 0) = W_0(\xi), \quad \Phi(A(\zeta), \zeta) = 0, \quad A(\zeta) = a(\zeta) \exp\left(\frac{1}{2}\int_0^{\zeta} \beta\, d\zeta\right). \tag{10a}$$

Note that

$$F(\zeta) = \int_0^{a(\zeta)} W r\, dr = \int_0^{A(\zeta)} \Phi \xi\, d\xi. \tag{11}$$

Let the functions Φ_i be the solutions of (10) with identical initial conditions

$$\Phi_i(\xi, 0) = W_0(\xi)$$

and with homogeneous boundary conditions on the different boundaries $A_i(\zeta)$, i.e.,

$$\Phi_i(A_i(\zeta), \zeta) = 0.$$

Let, further,

$$F_i(\zeta) = \int_0^{A_i(\zeta)} \Phi_i \xi\, d\xi.$$

Under these conditions it can be shown that if for all ζ we have

$$A_i(\zeta) \leqslant A(\zeta) \leqslant A_j(\zeta), \tag{12}$$

then it follows that

$$F_i(\zeta) \leqslant F(\zeta) \leqslant F_j(\zeta), \tag{13}$$

and the equalities in (13) are attained if and only if the corresponding equalities hold in (12) identically for all ζ.

We prove this assertion as follows. Let $P(A_i(\zeta), \xi_0, \zeta) = P_i$ be the probability that, starting a stochastic process from the point ξ_0 at $\zeta = 0$, a particle will not reach the boundary $A_i(\zeta)$ during the time interval $(0, \zeta)$. If the $A_i(\zeta)$ satisfy (12), we may immediately write the obvious relation

$$P_i \leqslant P \leqslant P_j, \tag{14}$$

which is valid for arbitrary equal initial positions ξ_0 of the particle.

Actually these relations express the obvious fact that a particle can reach boundary $A_i(\zeta)$ without reaching $A(\zeta)$, but cannot reach $A(\zeta)$ without reaching $A_i(\zeta)$. A similar statement holds for the relation between the boundaries $A(\zeta)$ and $A_j(\zeta)$. This is true for any initial position ξ_0. But this means that (13) is simply another way of stating (14), or that the validity of (13) follows immediately from that of (14). This proves relation (13).

Let us divide the interval $(0, \zeta)$, with which we are dealing, into several segments at the points ζ_n (where $n = 0, 1, 2, \ldots$). Further, let us set

$$A_n^{(+)} = A(\zeta_{n+1}), \quad A_n^{(-)} = A(\zeta_n).$$

To be specific let us consider the case in which

$$A_n^{(-)} \leqslant A(\zeta) \leqslant A_n^{(+)}, \quad \zeta_n \leqslant \zeta \leqslant \zeta_{n+1}. \tag{15}$$

Let $\Phi_{n,\,n+1}^{(\pm)}$ be the function Φ that satisfies Eq. (10), but whose boundary conditions are given in the intervals (ζ_n, ζ_{n+1}) on the broken lines $A_n^{(\pm)}$, which means that this function is defined for

$$\zeta_n \leqslant \zeta \leqslant \zeta_{n+1}, \quad 0 \leqslant \xi \leqslant A_n^{(\pm)}. \tag{16}$$

Solving Eq. (10) for these conditions, we obtain

$$\Phi_{n,\,n+1}^{(\pm)}(\xi, \zeta) = 2\,(A_n^{(\pm)})^{-2} \sum_i \frac{J_0(\lambda_{n,\,i}^{(\pm)} \xi)}{J_1^2(\lambda_i)}\, b_{n,\,i}^{(\pm)} \exp\left\{-(\lambda_{n,\,i}^{(\pm)})^2 \int_{\zeta_n}^{\zeta} \varphi\, d\zeta\right\}; \tag{17}$$

$$b_{n,\,i}^{(\pm)} = \int_0^{A_{n-1}^{(\pm)}} \Phi_{n-1,\,n}^{(\pm)}(\xi, \zeta_n)\, J_0(\lambda_{n,\,i}^{(\pm)} \xi)\, \xi\, d\xi, \quad \lambda_{n,\,i}^{(\pm)} = \lambda_i / A_n^{(\pm)}, \tag{17a}$$

where J is the Bessel function of order one, and the λ_i are the roots of the equation $J_0(\lambda_i) = 0$. Since the $(\pm)$ superscripts enter the formulas symmetrically, we may suppress them for simplicity.

Inserting (17) into (17a) and performing the integration, we obtain the following formula for $b_{n,\,i}$:

$$b_{n,\,i} = \frac{2J_0(\lambda_{n,\,i} A_{n-1})}{A_{n-1}} \sum_j [J_0'(\lambda_j)]^{-1} b_{n-1,\,j} \exp\left(-\lambda_{n-1,\,j}^2 \int_{\zeta_{n-1}}^{\zeta_n} \varphi\, d\zeta\right) \frac{\lambda_{n-1,\,j}}{\lambda_{n,\,i}^2 - \lambda_{n-1,\,j}^2}. \tag{18}$$

From (17) and (11), we see that the desired quantity $F_{n,\,n+1}$ can be written in the form

$$F_{n,\,n+1} = \int_0^{A_n} \Phi_{n,\,n+1} \xi\, d\xi = 2 \sum_i [b_{n,\,i} / \lambda_i J_1(\lambda_i)] \exp\left(-\lambda_{n,\,i}^2 \int_{\zeta_n}^{\zeta} \varphi\, d\zeta\right). \tag{19}$$

From (15) and from (12) and (13) we have

$$F_{n,\,n+1}^{(-)}(\zeta) \leqslant F(\zeta) \leqslant F_{n,\,n+1}^{(+)}(\zeta), \quad \zeta_n \leqslant \zeta \leqslant \zeta_{n+1}, \quad n = 0, 1, 2, \ldots \tag{20}$$

Thus the $F_{n,\,n+1}^{\pm}$ are majorizing solutions for the exact solution $F(\zeta)$. By choosing the points ζ_n at which we break up the line so as to make the majorizing solutions sufficiently close to each other, we find the exact solution $F(\zeta)$ to the desired accuracy and know the magnitude of the error involved. This

makes it possible to obtain analytic solutions for the problem to any arbitrary prescribed accuracy. The effectiveness of this analytic method can be traced to two causes. First, the series in the recursion formulas (18) converge extremely rapidly, a small number of terms is sufficient for the calculations, depending, of course, on the accuracy desired. Second, in view of the fact that energetic oscillations are excited only towards the end of the accelerating cycle, a solution which is sufficiently accurate for all practical purposes can be obtained by breaking up the $(0, \zeta)$ interval into only a small number of segments. Thus a few simple calculations based on the above formulas yield all the necessary results to the desired accuracy, together with an accurate evaluation of the error admitted. This indeed makes the method of majorizing solutions effective in our case.

4. BOUNDARY CONDITIONS

To have a complete solution of the given problem, we must have an explicit expression for the function q of Eq. (7a), as well as for $a(\zeta)$ the function used to specify the boundary conditions.

To obtain an explicit expression for q we must calculate $\langle\epsilon\rangle_\zeta^2$. Noting that

$$\langle\varepsilon^2\rangle_\zeta = \Omega^{-1}\langle\varepsilon^2\rangle_t \tag{21}$$

and making use of well known formulas for the probability of emitting a photon of energy ϵ, we obtain the expression

$$\langle\varepsilon^2\rangle_t = (55/24\sqrt{3})(\hbar c^2 e^2/\lambda R^3)(E/m_0c^2)^7. \tag{22}$$

Together with (21), this gives the explicit expression for q in (7a).

To set up the boundary conditions for the present problem we must know the maximum allowable phase deviation from equilibrium. These maximum allowable deviations are not the same in both directions. Within the framework of the linear theory, however, they must be equal. This condition alone makes it impossible to introduce the boundary conditions exactly and uniquely in the given problem, so that some arbitrariness remains. For arbitrary boundary conditions, however, the above method of majorizing solutions is equally applicable to all cases.

We shall now show how to state the boundary conditions in a way which would seem to take fullest account of the nonlinear effects. In so doing we make use of the previous results.[7]

We have already noted above that the main difference between the results of the linear and nonlinear theories is due to the different potential-well depths. If the well depth is taken from the nonlinear theory and the maximum allowable deviation in the linear theory is chosen as that corresponding to this well depth, then the linear theory will have accounted for the fundamental nonlinear effect. On the basis of this concept, Eqs. (4) and (5) give the following expression for the quantity entering boundary condition (7d):

$$a(\zeta) = 2(1 - \varphi_s \cot\varphi_s)^{1/2}. \tag{23}$$

5. SUMMARY

The formulas presented above give an explicit analytic solution of the problem under consideration. It is not necessary to illustrate the application of these formulas to any particular example chosen at random. We make only two remarks. First, the equations of the present work again emphasize the practical importance of the phenomenon under consideration even for electron energies of the order of 1 Bev. Second, they show the unavoidability of strong focusing at electron energies of several Bev.

[1] M. Sands, Phys. Rev. **97**, 470 (1955).
[2] A. A. Sokolov and I. M. Ternov, Dokl. Akad. Nauk SSSR **92**, 537 (1953); J. Exptl. Theoret. Phys. (U.S.S.R.) **25**, 698 (1953).
[3] A. S. Sokolov and I. M. Ternov, Dokl. Akad. Nauk SSSR **97**, 823 (1954); J. Exptl. Theoret. Phys. (U.S.S.R.) **28**, 432 (1955), Soviet Phys. JETP **1**, 227 (1955).
[4] A. A. Kolomenskii, J. Exptl. Theoret. Phys. (U.S.S.R.) **30**, 207 (1956), Soviet Phys. JETP **3**, 132 (1956).
[5] A. N. Matveev, Dokl. Akad. Nauk SSSR **108**, 432 (1956), Soviet Phys. "Doklady" **1**, 321 (1956).
[6] A. N. Matveev, Dokl. Akad. Nauk SSSR **109**, 495 (1956), Soviet Phys. "Doklady" **1**, 443 (1956).
[7] A. N. Matveev, J. Exptl. Theoret. Phys. (U.S.S.R.) **33**, 913 (1957), Soviet Phys. JETP **6**, 702 (1958).

Translated by E. J. Saletan
254

NONLINEAR EFFECTS IN METALS AT LOW TEMPERATURES

M. I. KAGANOV and V. G. PESCHANSKII

Institute for Technical Physics, Academy of Sciences, Ukrainian S.S.R.

Submitted to JETP editor May 20, 1957

J. Exptl. Theoret. Phys. (U.S.S.R.) **33**, 1261-1263 (November, 1957)

We investigate the possibility of observing deviations from Ohm's law in metals at low temperatures.

In order to observe deviations from Ohm's law in all metals (apart from bismuth[1]) it is necessary to have huge current densities of the order of 10^8 to 10^9 amp/cm^2. This is connected with the fact that the energy gained by an electron between collisions is small. Since on decreasing the temperature the mean free path increases considerably, we can expect that the observation of nonlinear effects should, as a matter of course, be done at low temperatures. The present article is thus devoted to an analysis of this possibility.

1. At large current densities it is not possible to assume that the symmetrical part of the electron distribution function agrees with the Fermi equilibrium function. However, one can successfully approximate the symmetric part of the electron distribution function by the Fermi function, be it at a temperature different from the lattice temperature,[2,4] in those circumstances where the time between collisions between the electrons, which is given by the equation

$$\tau_{ee} = \frac{1}{q_e n v}\left(\frac{\zeta}{\Theta}\right)^2,$$

(where q_e is the cross section for electron collisions ($q_e \sim 10^{-15}$ cm^2), n is the number of electrons per unit volume, ζ the Fermi energy, v the velocity at the Fermi level, and Θ the temperature of the electron gas[2,3]), is considerably less than the time t_{rel} necessary to transfer energy from the electrons to the lattice. We calculate t_{rel} using the value of the heat transfer $\overline{U}$ found in Ref. 4.

$$\overline{U} \approx (ms^2 n/\tau_0 T_0^5)(\Theta^5 - T^5); \quad \Theta, T \ll T_0 \tag{1}$$

(here and henceforth we omit numerical factors of the order of unity; see Ref. 2). In Eq. (1) m is the electron mass, s the velocity of sound, T the lattice temperature, T_0 the Debye temperature, and τ_0 the relaxation time of the electrons at $T = T_0$ (putting $\Theta = T$).

The heat balance equations are of the form

$$C_e \partial\Theta/\partial t = -(ms^2 n/\tau_0 T_0^5)(\Theta^5 - T^5), \quad C_{ph}\partial T/\partial t = (ms^2 n/\tau_0 T_0^5)(\Theta^5 - T^5), \tag{2}$$

where $C_e \approx n\Theta/\zeta$ is the electronic heat capacity and $C_{ph} \approx n(T/T_0)^3$ the phonon heat capacity (we consider temperatures well below T_0).

Taking into account that $\Theta \approx T$ we have from equations (2)*

$$t_{rel} \approx \begin{cases} \tau_0 T_0^2/ms^2 T & (T \ll T_0\sqrt{T_0/\zeta}), \\ \tau_0 T_0^5/ms^2 \zeta T^3 & (T \gg T_0\sqrt{T_0/\zeta}). \end{cases} \tag{3}$$

Comparing these expressions with τ_{ee}, we can satisfy ourselves that the time to produce the electronic Fermi distribution is less than t_{rel} down to temperatures of the order of 0.1 to 1°K (depending on the metal). This enables us to use as the electronic distribution function the quasi-equilibrium function $f_0(\Theta)$ ($\Theta \neq T$) down to sufficiently low temperatures.

2. In calculating the resistance of a metal one usually assumes that $\Theta = T$. This is natural if one is not interested in nonlinear effects. If $\Theta \neq T$ the conductivity depends both on the phonon (lattice) tem-

*In Ref. 4 we gave only the second equation of (3) and the region of applicability of this equation was not indicated.

perature and on the electron temperature. One can easily show that

$$\sigma = (ne^2\tau(\Theta, T)/m)\{1 - \pi^2\Theta^2/12\zeta^2\}, \tag{4}$$

where

$$1/\tau(\Theta, T) = 1/\tau_{imp} + 1/\tau_{ep}(T, \Theta) + 1/\tau_{ee}(\Theta). \tag{5}$$

In equation (5) τ_{imp}, τ_{ep} and τ_{ee} are the relaxation times referring respectively to collisions with impurities, with phonons, and with electrons.

The quantity τ_{imp} does not depend at all on the temperature, and τ_{ee} depends only on the electron temperature (see Sec. 1). The evaluation of the temperature dependence of τ_{ep} proceeds in the usual way (see, for instance, Ref. 5) with only one difference, namely that we assume the electron and phonon temperatures to be different ($\Theta \neq T$). The result is

$$\frac{1}{\tau_{ep}(\Theta, T)} = \frac{1}{\tau_{ep}(T)}\left\{1 + \frac{4(\Theta^5 - T^5)}{5T^5}\right\}. \tag{6}$$

Here $\tau_{ep}(T)$ is the value of this relaxation time in the isothermal model.

To determine the electron temperature it is natural to use the heat balance equation

$$\rho j^2 = \overline{U}, \tag{7}$$

where ρ is the total resistivity which is practically equal to the impurity resistivity, $\rho \approx m/ne^2\tau_{imp}$. From Eqs. (7) and (1) it follows that

$$\Theta^5 = T^5 + (j/nes)^2(\tau_{imp}/\tau_0)T_0^5 \tag{8}$$

or

$$\frac{\Delta T}{T} \approx (j/nes)^2(\tau_{imp}/\tau_0)(T_0/T)^5. \tag{9}$$

Using expressions (4), (6), and (9), and the value of $\tau_{ee}(\Theta)$ we find the way the resistance depends on the current density (we assume that $\Delta T \ll T$),

$$\Delta\rho/\rho \approx (j/nes)^2\{1 + l_{ep}(T)/2l_{ee}(T)\}. \tag{10}$$

The l's in this equation are connected to the τ through the relation $l = v\tau$. We see from this equation that nonlinear effects increase with the ratio l_{ep}/l_{ee}, which in turn increases as T^{-3} with decreasing temperature.

Our considerations are no longer correct at very low temperatures since the condition $\Delta T \ll T$ is no longer satisfied. We shall consider another limiting case, namely, $T = 0$. We have then from Eq. (8)

$$\Theta = T_0(\tau_{imp}/\tau_0)^{1/5}(j/nes)^{1/5},$$

and thus for $T = 0$

$$\Delta\rho/\rho \approx (j/nes)^2 + (\tau_{ee}^{2/5}\tau_{imp}^{3/5}/\tau_{0ee})(j/nes)^{4/5} \tag{11}$$

(where $\tau_{0ee} = \tau_{ee}(T_0)$) where the first term corresponds to the creation of phonons and the second one to electron-electron collisions.*

We notice that Eq. (11) is, strictly speaking, only justified for those current densities which produce an increase of the electron temperature to 0.1 to 1.0°K (see Sec. 1). If the current density is less, it is impossible to speak about two temperatures; and Eq. (11) must be assumed to give a purely qualitative description.

Finally we note that we must apparently look for nonlinear effects at low temperatures in those metals, for which a large part of the resistivity is due to electron-electron interactions.

If $l_{ep}/l_{ee} \sim 10^3$ to 10^4, we can expect an increase in the resistivity of one per cent for currents of the order of 10^5 to 10^6 amp/cm^2.

Apart from the paper by Ginzburg and Shabanskii, the papers by Shabanskii[6,7,8] are also devoted to a theoretical discussion of nonlinear effects in metals. In those papers the author has tried to extend the Fokker-Planck method to the case of a temperature well below the Debye temperature. It seems to us,

*If we assume that the metal does not contain any impurities, we have at $T = 0$,

$$\rho = \rho_{ee},\ \rho_{ee}/\rho_{0ee} = (\tau_0/\tau_{0ee})^{2/5}(j/nes)^{4/5}.$$

however, that one can make serious objections to an application of this method to these cases. The trouble is that the terms which are neglected in the expansion of the collision integral for $T \ll T_0$ are of the same order of magnitude as the terms which are left in [see Ref. 6, Eq. (4)].

The inapplicability of the Fokker-Planck method to the problem under consideration can clearly be seen from the fact that the directly calculated coefficients A_1 and A_2 (see Ref. 6) do not agree with the values obtained by the author from the condition $S(f_0) = 0$. Apart from that, the author arrives in Ref. 7 at the paradoxical conclusion that the resistivity of a metal must go to infinity as $T \to 0$.

We shall not compare here all our results with the analogous equations of Refs. 6, 7, 8, although several of them agree in order of magnitude with the equations of those papers, in the case of small temperature differences ($\Delta T \ll T$).

The authors would like to use this opportunity to thank I. M. Lifshitz and E. S. Borovik for discussions of the problem considered in this paper.

[1] E. S. Borovik, Dokl. Akad. Nauk SSSR **91**, 771 (1953).
[2] V. L. Ginzburg and V. P. Shabanskii, Dokl. Akad. Nauk SSSR **100**, 445 (1955).
[3] L. D. Landau and I. Ia. Pomeranchuk, J. Exptl. Theoret. Phys. (U.S.S.R.) **7**, 379 (1937).
[4] M. I. Kaganov, I. M. Lifshitz, and L. V. Tanatarov, J. Exptl. Theoret. Phys. (U.S.S.R.) **31**, 232 (1956), Soviet Phys. JETP **4**, 173 (1957).
[5] A. H. Wilson, The Theory of Metals, Cambridge Univ. Press, 1953.
[6] V. P. Shabanskii, J. Exptl. Theoret. Phys. (U.S.S.R.) **27**, 142 (1954).
[7] V. P. Shabanskii, J. Exptl. Theoret. Phys. (U.S.S.R.) **27**, 147 (1954).
[8] V. P. Shabanskii, J. Exptl. Theoret. Phys. (U.S.S.R.) **31**, 657 (1956), Soviet Phys. JETP **4**, 497 (1957).

Translated by D. ter Haar
255

SOVIET PHYSICS JETP VOLUME 6 (33), NUMBER 5 MAY, 1958

INVARIANT REPRESENTATIONS OF THE SCATTERING MATRIX

V. I. RITUS

P. N. Lebedev Physical Institute, Academy of Sciences, U.S.S.R.

Submitted to JETP editor May 24, 1957

J. Exptl. Theoret. Phys. (U.S.S.R.) **33**, 1264-1267 (November, 1957)

The scattering matrix S for the reaction $a + b \to a' + b'$ is expressed in terms of a finite number of spin operators Q_i, each invariant under rotations and reflections. A method for constructing the Q_i is given, and their number is determined for a reaction with given initial and final spins. The restrictions placed upon the form and number of the Q_i by the condition that the scattering matrix be invariant under time reversal are considered. Examples are given in which S is represented by the Q_i for several reactions.

THE scattering matrix $S(\mathbf{k}', \mathbf{k})$ for the reaction $a + b \to a' + b'$ is an operator in the space defined by the spins of the incident and scattered particles, and is a function of their relative momenta $\mathbf{k}, \mathbf{k}'$. Since S is invariant under rotation, it can be written in the form

$$S(\mathbf{k}', \mathbf{k}) = \sum A_i(\mathbf{k}'\mathbf{k})\, Q_i(\mathbf{k}', \mathbf{k}, \mathbf{T}), \tag{1}$$

where the $Q_i(\mathbf{k}', \mathbf{k}, \mathbf{T})$ are invariant operators that depend on the vectors $\mathbf{k}', \mathbf{k}$ and on the matrices $\mathbf{T}$

(Ref. 1) which take the system from its initial spin state into its final one. The $A_i(\mathbf{k}'\mathbf{k})$ are invariant function of the scalar product $(\mathbf{k}'\mathbf{k})$ and the total energy of the system. The representation (1) is convenient to use in studying the general properties of scattering matrices, investigating reactions with polarized particles, carrying out phase analyses, and similar problems.

In the following we examine the representation (1), find the connection between the operators Q_i and the angular operators $L(\mathbf{k}', \mathbf{k})$[2], give a general method for constructing the operators Q_i, and determine the number of operators for a given reaction.

In Ref. 2, the matrix $S(\mathbf{k}', \mathbf{k})$ was written as a series

$$S(\mathbf{k}', \mathbf{k}) = \sum S^{fi}_{Jl's'ls} L_{Jl's'ls}(\mathbf{k}', \mathbf{k}) \tag{2}$$

over invariant angular operators L. The coefficients $S^{fi}_{Jl's'ls}$ in the expansion are functions of the total energy only. The operators L are matrices whose elements $L(\alpha', \alpha)$ are given by the formula

$$L_{Jl's'ls}(\mathbf{k}'\alpha', \mathbf{k}\alpha) = \sum_{M\mu\mu'} C^{l'M-\mu'; s'\mu'}_{JM} C^{lM-\mu; s\mu}_{JM} Y_{l'M-\mu'}(\mathbf{k}') Y^{*}_{lM-\mu}(\mathbf{k}) Q_{s'\mu'}(\alpha') Q^{*}_{s\mu}(\alpha) \tag{3}$$

(for notation, see Ref. 2). Upon choosing the x, y, and z axes to be in the directions of the vectors $\mathbf{x} = \frac{(\mathbf{k}\times\mathbf{k}')\times\mathbf{k}}{\sqrt{1-(\mathbf{k}'\mathbf{k})^2}}$, $\mathbf{y} = \frac{\mathbf{k}\times\mathbf{k}'}{\sqrt{1-(\mathbf{k}'\mathbf{k})^2}}$, $\mathbf{z} = \mathbf{k}$ it is not hard to see that (3) becomes

$$L(\mathbf{k}'\alpha', \mathbf{k}\alpha) = \sum_{\mu'\mu} L^{\mu'\mu}_{Jl's'ls}(\mathbf{k}'\mathbf{k}) Q^{\mu'\mu}_{s's}(\alpha', \alpha), \tag{4}$$

where $L^{\mu'\mu}_{Jl's'ls}(\mathbf{k}'\mathbf{k}) = \sqrt{2l+1}\, C^{l'\mu-\mu'; s'\mu'}_{J\mu}\, C^{l0; s\mu}_{J\mu}\, \theta_{l'\mu-\mu'}(\mathbf{k}'\mathbf{k})$ are invariant functions of $(\mathbf{k}'\mathbf{k}) \equiv \cos\theta$ and $Q^{\mu'\mu}_{s's}(\alpha', \alpha) = Q_{s'\mu'}(\alpha') Q^{*}_{s\mu}(\alpha)$ are invariant spin operators which take the spin of the system from s, μ to s', μ'. These operators (matrices in α', α) are equal to $\delta_{\alpha'\mu'}\delta_{\mu\alpha}$ and can be expressed as invariant functions of the matrices T (Ref. 1) and the vectors $\mathbf{k}, \mathbf{k}'$. For example if $s = s' = \frac{1}{2}$, then $T = \sigma$ and $Q^{\frac{1}{2}\frac{1}{2}}_{\frac{1}{2}\frac{1}{2}}(\alpha', \alpha) = \frac{1}{2}(1 + \sigma_z)_{\alpha'\alpha} = \frac{1}{2}[1 + (\sigma\mathbf{k})]_{\alpha'\alpha}$. In the general case, the operators $Q^{\mu'\mu}_{s's}$ can be written in terms of Racah's spin-tensor $T^{(n)}_{m}$ through the relation

$$Q^{\mu'\mu}_{s's} = \sum_{n=|s'-s|}^{s'+s} (-1)^{n+s'+\mu} (2n+1)^{1/2} C^{s'-\mu'; s\mu}_{n\mu-\mu'} T^{(n)}_{\mu'-\mu}.$$

From the properties of the T matrices, it follows that the operators $Q_{s's}$ are polynomials of degree $s + s'$ in the components of T. Hence, $Q^{\mu'\mu}_{s's} = Q^{\mu'\mu}_{s's}(\mathbf{k}', \mathbf{k}, \mathbf{T})$. Each angular operator $L(\mathbf{k}', \mathbf{k})$ can therefore be expanded into $(2s' + 1)(2s + 1)$ spin operators, with coefficients which are known functions of $(\mathbf{k}'\mathbf{k})$. Actually, however, there are fewer than $(2s' + 1)(2s + 1)$ spin operators in (4) because parity is conserved in the reaction $a + b \to a' + b'$.

Indeed, from the symmetry of the Clebsch-Gordan coefficients and the properties of the functions θ_{lm} it follows that

$$L^{-\mu', -\mu}_{Jl's'ls}(\mathbf{k}'\mathbf{k}) = (-1)^{l'-l+s'-s+\mu'-\mu} L^{\mu'\mu}_{Jl's'ls}(\mathbf{k}'\mathbf{k}). \tag{5}$$

Hence (4) can be written

$$L_{Jl's'ls}(\mathbf{k}', \mathbf{k}) = \sum_{\mu'>0,\, \mu} L^{\mu'\mu}[Q^{\mu'\mu} + \xi Q^{-\mu'-\mu}] + \sum_{\mu'=0,\, \mu>0} L^{\mu'\mu}[Q^{\mu'\mu} + \xi Q^{-\mu'-\mu}] + L^{00}Q^{00}, \tag{6}$$

where $\xi = (-1)^{l'-l+s'-s+\mu'-\mu}$. Since parity is conserved, $l'-l$ must be even or odd according to whether the intrinsic parity of the system changes or not during the reaction. Hence ξ and the operators shown in brackets in (6) do not depend on l, l'. We choose these operators to be the $Q_i(\mathbf{k}', \mathbf{k}, T)$. From (6) it follows that if the spins s, s' are half-integral, then the terms with $\mu' = 0$ or $\mu = 0$ in (6) are absent and $L(\mathbf{k}', \mathbf{k})$ is expressed in terms of $\frac{1}{2}(2s' + 1)(2s + 1)$ operators Q_i. If s, s' are integers, then all terms are present in (6). In this case, if $l'-l+s'-s$ is odd, from (5) it follows that $L^{00} = 0$ and $L(\mathbf{k}', \mathbf{k}_0$ is expressed in terms of $2s's + s' + s$ operators Q_i. If, on the other hand, $l'-l+s'-s$ is

even, then $L^{00} \neq 0$ and $L(k', k)$ is expressed in terms of $2S'S + S' + S + 1$ operators Q_i.

In this way, the angular operators $L(k', k)$, and with them the scattering matrix $S(k', k)$, are written in terms of a finite number r of independent operators $Q_i(k', k, T)$. For half-integral spins, $r = \frac{1}{2}(2S' + 1)(2S + 1)$, while for integer spins $r = 2S'S + S' + S + 1$ or $r = 2S'S + S' + S$ depending on whether the number $l' - l + S' - S$ is even or odd.

It is clear that instead of choosing the r independent operators Q_i to be as given by formula (6), one could equally well have chosen any linear combination of these (with functions of $(k' k)$ as coefficients), in particular the first r angular operators $L(k', k)$.

In addition to being invariant under rotations and reflections, the matrix S must be invariant under time reversal, i.e., the matrix elements between states $\psi_{S\mu k}$ and $\psi_{S'\mu' k'}$ must be equal to the matrix elements between the time-reflected states $\psi_{S'-\mu'-k'}$, $\psi_{S-\mu-k}$. This leads to the condition $KSK^{-1} = S^+$ (Ref. 3), or in detail

$$(KSK^{-1})_{k'\alpha', k\alpha} = S^*(k\alpha, k'\alpha'), \tag{7}$$

where K is the Wigner time reversal operator,[4] including complex conjugation. The angular operators L must satisfy relation (7), which now becomes

$$(KL_{Jl'S'lS}K^{-1})_{k'\alpha', k\alpha} = L^*_{Jl'S'lS}(k\alpha, k'\alpha'). \tag{8}$$

Hence (7) establishes a connection between the coefficients $S^{fi}_{Jl'S'lS}$ and $S^{if}_{Jl'S'lS}$ in the expansion (2), i.e., between the direct and time-reversed reactions.

$$S^{fi}_{Jl'S'lS} = S^{if}_{Jl'S'lS}. \tag{9}$$

For inelastic processes ($i \neq f$), or processes involving spin change ($S' \neq S$), (9) does not restrict the matrix S. However, for elastic scattering ($i = f$, $S' = S$), (9) becomes a relation between the coefficients of one and the same reaction. Hence the operators Q_i now appear in the matrix S only in the combination $Q_i(k', k, T) + Q_i^+(k, k', T)$, and the number of independent operators $Q_i(k', k, T)$ decreases by the number t of relations $S^{ii}_{Jl'S'lS} = S^{ii}_{Jl'S'lS}$ where $l' \neq l$. For half-integral spin, $t = S^2 - 1/4$, while for integer spin, $t = S^2$. Hence for purely elastic reactions, the number of spin invariants is $(S + 1)^2 - 1/4$ or $(S + 1)^2$, depending on whether the spin is half-integral or integral.

As an example, we write out the matrices $S(k', k)$ in terms of the operators Q_i for several reactions, the + and − signs indicating whether the intrinsic parity is conserved or not.

1. $S = S' = 1/2$, $+.\ S(k', k) = A + i(\sigma n)B$,
$-.\ S(k', k) = (\sigma k')A + (\sigma k)B$.

2. $S = S' = 1$, $+.\ S(k', k) = A + i(Sn)B + [(Sk')(Sk) + (Sk)(Sk')]C +$
$+ (Sk')^2 D + (Sk)^2 E$, for purely elastic processes, $E = D$
$-.\ S(k', k) = (Sk')A + (Sk)B + i(Sk')(Sn)C + i(Sk)(Sn)D$.

3. $S = 1$, $S' = 0$ and $S = 0$, $S' = 1$. $+.\ S(k', k) = i(Tn)A$,
$-.\ S(k', k) = (Tk')A + (Tk)B$.

4. $\gamma + b \to a' + b'$, $S = S' = 1/2$.
$S(k', k) = i(ne)A + (\sigma e)B + (\sigma k')(k'e)C + (\sigma k)(k'e)D$.

5. $\gamma + b \to \gamma' + b'$, $S = S' = 1/2$.
$S(k', k) = (e'e)A + (s's)B + i(\sigma [e'e])C + i(\sigma [s's])D + i(\sigma k)(s'e)E +$
$+ i(\sigma k')(e's)F + i(\sigma k')(s'e)G + i(\sigma k)(e's)H$,

for purely elastic processes, $F = -E$, $H = -G$. In these formulas $n = k' \times k$, $e = k \times e$, A, B, ..., H are functions of $(k' k)$ and the energy of the system. As mentioned above, invariants other than those given above could have been chosen, for example, a corresponding number of angular operators L^2.

[1] E. Condon and G. Shortley, The Theory of Atomic Spectra, Cambridge Univ. Press, 1935.
[2] V. I. Ritus, J. Exptl. Theoret. Phys. (U.S.S.R.) 32, 1536 (1957), Soviet Phys. JETP 5, 1249 (1957).
[3] K. Watson, Phys. Rev. 88, 1163 (1952).
[4] E. P. Wigner, Gott. Nachr. 31, 546 (1932).

Translated by R. Krotkov
256

APPLICATION OF DISPERSION RELATIONS FOR THE DETERMINATION OF BOUND STATES*

V. I. SERDOBOL'SKII

P. N. Lebedev Physics Institute, Academy of Sciences, U.S.S.R.

Submitted to JETP editor May 24, 1957

J. Exptl. Theoret. Phys. (U.S.S.R.) 33, 1268-1270 (November, 1957)

Dispersion relations are discussed in the framework of nonrelativistic theory. It is shown that the energies, parities, and certain spectral coefficients characterizing the bound states of the system can be determined on the basis of scattering data. Some characteristics of the deuteron are determined by using the n—p scattering data.

THE dispersion relations for the scattering amplitude are usually formulated on the basis of relativistic field theory. This leads to a number of difficulties, which with few exceptions preclude the obtaining of applicable results. We shall discuss dispersion relations in the framework of nonrelativistic theory.

In order for dispersion relations to exist, it is necessary that the scattering amplitude be an analytic function of the complex energy and be bounded for $E \to \infty$. However, in the nonrelativistic case, the scattering amplitude behaves like e^{-2ikR} for $k \to \infty$, where k is the wave number, and R_0 is a radius beyond which the interaction vanishes. Dispersion relations can be written only for the function $F(k) = f(k, \theta, \varphi)\, e^{2ikR}$, $R > R_0$. Let us denote

$$F_0(k) = \operatorname{Re} f(k, \vartheta, \varphi) \cos 2kR - \operatorname{Im} f(k, \vartheta, \varphi) \sin 2kR, \quad F_1(k) = \operatorname{Re} f(k, \vartheta, \varphi) \sin 2kR + \operatorname{Im} f(k, \vartheta, \varphi) \cos 2kR.$$

From the Cauchy theorem we then have:

$$F_0(k) = \frac{1}{\pi} \int_0^\infty \frac{2k'dk'}{k'^2 - k^2} F_1(k') - \sum_\lambda \frac{\nu_\lambda}{k^2 + |k_\lambda|^2} e^{-2|k_\lambda| R},$$

$$F_1(k) = -\frac{1}{\pi} \int_0^\infty \frac{2kdk'}{k'^2 - k^2} F_0(k') + \sum_\lambda \frac{k\nu_\lambda}{|k_\lambda| (k^2 + |k_\lambda|^2)} e^{-2|k_\lambda| R}.$$

Here k_λ are the poles of the scattering amplitude that lie on the upper half of the imaginary axis, and $\nu_\lambda = -\operatorname{Res} f$, the residues at the points $E = E_\lambda$. The following integral relations also hold

$$\frac{2}{\pi} \int_0^\infty dk F_0(k) = -\sum_\lambda \frac{\nu_\lambda}{|k_\lambda|} e^{-2|k_\lambda| R}; \quad \frac{2}{\pi} \int_0^\infty kdk F_1(k) = -\sum_\lambda \nu_\lambda e^{-2|k_\lambda| R}.$$

The coefficient ν_λ is connected with the asymptotic part of the wave function of the stationary state. To show this we write the (elastic) scattering equation in the form

$$T = V + V(E - H)^{-1} V, \quad \operatorname{Im} E > 0. \tag{1}$$

Here T is the scattering operator introduced by Lippman and Schwinger.[1] We now investigate the scattering of a particle by a nucleus in state A. Let Φ_a be a normalized wave function for channel a

$$\Phi_a = (2\pi)^{-3/2} e^{i\mathbf{k}_a \mathbf{r}} \varphi_{Aa}, \quad (\Phi_{a'}, \Phi_a) = \delta(\mathbf{k}_a - \mathbf{k}_{a'}) \delta_{AA'} \delta_{aa'}.$$

We designate by Ψ_a the solution of the scattering problem

*The first conjecture that the bound states can be found from scattering data by analytic continuation of the S matrix is due to Heisenberg

$$\Psi_a = \Phi_a + (E - H_0)^{-1} V \Psi_a.$$

The scattering amplitude for the transition from state a into state a′ is given by

$$f_{a \to a'}(k, \theta, \varphi) = -2\pi^2 (\Phi_{a'}, T\Phi_a). \tag{2}$$

The integral equation (1) allows an analytical continuation into the complex E plane. From (1) and (2) one can easily obtain the residue of the scattering amplitude

$$[\mathrm{Res}\, f_{a \to a'}]_{E_\lambda} = -2\pi^2 \sum_{\lambda \in E_\lambda} (\Phi_{a'}, V\Psi_\lambda)(\Psi_\lambda, V\Phi_a).$$

Here the summation is over all quantum numbers λ characterizing the state with energy E_λ. The functions $\Phi_{a'}$ and Φ_a are the appropriate analytical continuations of the respective plane waves. At large r, where the interaction vanishes and where the angular factor becomes insignificant, the wave function has the form $\exp(-|k_\lambda| r)\, g_\lambda / r$. The factor g_λ depends on angular, spin, and other variables. For the scalar products we obtain

$$(\Phi_{a'}, V\Psi_\lambda) = -(2/\pi)^{1/4} g'_\lambda, \qquad (\Psi_\lambda, V\Phi_a) = -(2/\pi)^{1/4} I_\lambda g_\lambda.$$

The number I_λ, which equals ± 1, characterizes the parity of the state λ. In the particular case of elastic forward scattering $a = a'$, $\vec{k} = \vec{k}'$ and

$$\nu_\lambda = \pi I_\lambda \sum_{\lambda \in E_\lambda} g_\lambda^2.$$

This shows that the sign of ν_λ determines the parity of the bound state λ. The absolute value of ν_λ is proportional to the virtual decay, i.e., to the probability that the bound particles of the system separate to a distance larger than the range of the forces.

We now apply the dispersion relations to the concrete problem of neutron-proton scattering. We utilize the fact that the n − p interaction can be well represented by the potential function $\hat{V} = V(\mathbf{r})\, \delta(\mathbf{r} - \mathbf{r}')$. One can show (we shall not give the proof here) that the forward-scattering amplitude for this potential, as a function of the complex energy, is bounded for $E \to \infty$ and approaches the limit

$$f(\infty) = -\frac{1}{4\pi} \int V(\mathbf{r})\, d\mathbf{r}.$$

Cauchy's theorem can be applied to the difference $f(k) - f(\infty)$, where $f(k)$ is the forward scattering amplitude. Let $f_t(k)$ and $f_s(k)$ be the triplet and singlet scattering amplitudes respectively. Let further

$$f_0(k) = \mathrm{Re}\left[\frac{3}{4} f_t(k) + \frac{1}{4} f_s(k)\right],$$

and let the cross section be $\sigma = {}^3/_4\, \sigma_t + {}^1/_4\, \sigma_s$. The dispersion relations then become

$$f_0(k) - f_0(0) = \frac{k^2}{2\pi^2} \int_0^\infty \frac{\sigma(k')\, dk'}{k'^2 - k^2} + \frac{3}{4} \frac{k^2 \nu_1}{k_1^2 (k^2 + k_1^2)}.$$

Here ν_1 is the spectral coefficient and k_1 the reciprocal of the deuteron radius: $k_1 = 1/R_D$; $R_D = 4.314 \times 10^{-13}$ cm. The n − p scattering cross section is known with good accuracy up to high energies. We performed the integration to an upper limit corresponding to 70 Mev. The contribution from the discarded part of the integral does not exceed a fraction of one per cent. The computation was performed for values of k corresponding to 1, 2, and 5 Mev in the laboratory system. The coefficient ν_1 was obtained from the dispersion relations and found to be roughly the same for all energies, $(7.5 \pm 0.4) \times 10^{12}$ cm^{-1}.

The positive sign of the spectral coefficient indicates the even parity of the wave function of the deuteron. The spectral coefficient can be obtained independently from a model of the deuteron. For example, in the approximation of effective-range theory one obtains the expression $\nu_1 = 2/(R_D - r_{0t})$ which gives a value 7.7×10^{12} cm^{-1}. The discrepancy between this value and the value obtained from the dispersion relations is small and well within the limits of possible errors.

In conclusion the author wishes to thank Professor A. S. Davidov for his interest in this work.

[1] B. A. Lippman and J. Schwinger, Phys. Rev. 79, 469 (1950).

Translated by M. Danos
257

THE QUANTUM STATES OF PARTICLES COUPLED WITH ARBITRARY STRENGTH TO A HARMONICALLY OSCILLATING CONTINUUM. II. THE CASE OF TRANSLATIONAL SYMMETRY

V. M. BUIMISTROV and S. I. PEKAR

Physics Institute, Academy of Sciences, Ukranian S.S.R.

Submitted to JETP editor, May 25, 1957

J. Exptl. Theoret. Phys. (U.S.S.R.) 33, 1271-1276 (November, 1957)

The method developed in the preceding paper[1] is extended to the case of a system with translational symmetry (there is no external potential field and the particle is not localized). The variational method is used to calculate the lowest energy levels and wave functions of the system described by the Hamiltonian of Eqs. (1) and (2). The trial function is chosen in the form given by Eqs. (5) and (6). This method is applied to the polaron problem. In the limiting cases of weak and strong coupling between the particle and oscillations the calculated energy agrees with the exact result of perturbation theory (in the second approximation) and approaches Feynman's result for strong coupling.[2]

In a previous article[1] we have treated particles interacting with a harmonically oscillating continuum while in a particle-localizing external potential field. This latter field removed the translational symmetry. In the present article we shall treat the problem without this external field, so that the particle may move through all space. It is assumed that the Hamiltonian of the system is of the form

$$H = -\frac{\hbar^2}{2m}\Delta + \frac{1}{2}\sum_{\varkappa}\hbar\omega_{\varkappa}(q_{\varkappa}^2 - \partial^2/\partial q_{\varkappa}^2) + \sum_{\varkappa} c_{\varkappa} q_{\varkappa}\chi_{-\varkappa}(\mathbf{r}). \tag{1}$$

Here $\mathbf{r}$ is the radius vector of the particles, m is its mass, the $\omega_{\varkappa}$ are the natural frequencies of the continuum, $\varkappa$ is the wave vector of the continuum oscillation, the $q_{\varkappa}$ are the normal coordinates of these oscillations, the $c_{\varkappa}$ are the coupling constants of the particle with these oscillations, and

$$\chi_{\varkappa}(\mathbf{r}) = \sqrt{2/V}\sin(\varkappa\mathbf{r} + \pi/4). \tag{2}$$

The $\chi_{\varkappa}(\mathbf{r})$ form a complete system of orthonormal functions in the fundamental volume V of the periodicity, a volume chosen in the form of a cube. Such a Hamiltonian is obtained, for instance, when the motion of a conduction electron interacting with crystal lattice vibrations is considered. A similar Hamiltonian occurs for a particle interacting with a quantized field.

1. CHOICE OF THE TRIAL FUNCTION AND DETERMINATION OF THE FUNCTIONAL $\overline{H}$

Ordinarily, the continuum oscillations with wave vectors $\varkappa$ and $-\varkappa$ have the same frequency and coupling constant, so that we may write $c_{\varkappa} = c_{-\varkappa}$ and $\omega_{\varkappa} = \omega_{-\varkappa}$. The normal coordinates $q_{\varkappa}$ are usually the coefficients of the Fourier expansion of the deformation of the medium or field. In the present case we shall expand in terms of the basis functions given in Eq. (2). Let the translation operator $T_{\mathbf{a}}$ denote the following change in the configuration of the system: the particle and the whole deformation of the medium undergo a space translation by the vector $\mathbf{a}$. Explicitly, the definition of $T_{\mathbf{a}}$ is

$$T_{\mathbf{a}} f(\mathbf{r}, q_{\varkappa}, q_{-\varkappa}) = f(\mathbf{r} + \mathbf{a}, q_{\varkappa}\cos\varkappa\mathbf{a} - q_{-\varkappa}\sin\varkappa\mathbf{a}, q_{-\varkappa}\cos\varkappa\mathbf{a} + q_{\varkappa}\sin\varkappa\mathbf{a}). \tag{3}$$

It is easily shown that H is invariant under such a translation. Thus the exact wave functions of the system may be chosen, as is well known, so that they be eigenfunctions of all the $T_{\mathbf{a}}$ (with all possible $\mathbf{a}$) that satisfy the equations

$$T_{\mathbf{a}}\Phi_{\mathbf{k}} = e^{i\mathbf{k}\mathbf{a}}\Phi_{\mathbf{k}}. \tag{4}$$

It is well known that the total momentum of the system is represented by the operator $\mathbf{P} = -i\hbar(\nabla_{\mathbf{a}} T_{\mathbf{a}})_{\mathbf{a}=0}$. The $\Phi_{\mathbf{k}}$ are then eigenfunctions of this operator belonging to the eigenvalues $\hbar\mathbf{k}$.

The trial functions we choose for this system are

$$\Phi_{\mathbf{k}} = A\int \exp\{-i\mathbf{k}\xi_3\}\, T_{\xi}\Psi\,(d\xi_3), \tag{5}$$

$$\Psi = (2\beta/\pi)^{3/4}\exp\left\{-\beta r^2 - \frac{1}{2}\sum_{\varkappa}\left(x_{\varkappa}^2 + \frac{1}{2}\ln\pi\right)\right\},\quad x_{\varkappa} = q'_{\varkappa} + s_{\varkappa},\quad q'_{\varkappa} = q_{\varkappa} - a_{\varkappa}\chi_{-\varkappa}(\mathbf{r}). \tag{6}$$

The form of (6) is taken from our previous work,[1] and the a_K, s_K, and β are to be the variation parameters. For arbitrary real $\mathbf{k}$ the function of Eq. (5) is an exact simultaneous eigenfunction of $T_{\mathbf{a}}$ and $\mathbf{P}$. Since the $\Phi_{\mathbf{k}}$ with different $\mathbf{k}$ belong to different momentum eigenvalues, they are mutually orthogonal.

According to the variational method in quantum mechanics, we must obtain an extremum of the functional

$$\overline{\overline{H}} = \int \Phi_{\mathbf{k}}^* H \Phi_{\mathbf{k}}\, d\tau,$$

with the subsidiary condition $\int \Phi_{\mathbf{k}}^*\Phi_{\mathbf{k}}\,d\tau = 1$. It is easily shown that

$$\overline{\overline{H}} = AA^*\int d\tau \iint \exp\{i\mathbf{k}(\xi_1 - \xi_2)\}\,(d\xi_1)\,(d\xi_2)\, T_{\xi_1}\Psi^* H T_{\xi_2}\Psi = \dot{A}A^* V\int d\tau \int \exp\{i\mathbf{k}\xi_3\}\, T_{\xi}\Psi^* H \Psi\,(d\xi_3). \tag{7}$$

This is done by applying $T_{-\xi_2}$ to the whole integrand in (7) (this does not change the value of the integral) and making use of the invariance of H under translation. The normalizing integral can be similarly transformed.

After changing from the variables $\mathbf{r}, \ldots, q_K, \ldots$ to the new variables $\mathbf{r}, \ldots, q'_K, \ldots$ the Hamiltonian can be written in the form

$$H = \sum_{l=1}^{8} I_l,\quad I_1 = -\frac{\hbar^2}{2m}\Delta,\quad I_2 = \frac{\hbar^2}{m}\sum_{\varkappa}(\nabla q_{\varkappa 0}\cdot\nabla)\frac{\partial}{\partial q'_{\varkappa}},\quad I_3 = -\frac{\hbar^2}{2m}\sum_{\varkappa,\varkappa_1}(\nabla q_{\varkappa 0}\cdot\nabla q_{\varkappa_1 0})\frac{\partial^2}{\partial q'_{\varkappa}\partial q'_{\varkappa_1}},\quad I_4 = \frac{\hbar^2}{2m}\sum_{\varkappa}\Delta q_{\varkappa 0}\frac{\partial}{\partial q'_{\varkappa}},$$
$$I_5 = \frac{1}{2}\sum_{\varkappa}\hbar\omega_{\varkappa}q'^2_{\varkappa},\quad I_6 = \sum_{\varkappa}(\hbar\omega_{\varkappa}a_{\varkappa} + c_{\varkappa})\,q'_{\varkappa}\chi_{-\varkappa}(\mathbf{r}),\quad I_7 = \sum_{\varkappa}\left(\frac{1}{2}\hbar\omega_{\varkappa}a_{\varkappa}^2 + c_{\varkappa}a_{\varkappa}\right)\chi^2_{-\varkappa}(\mathbf{r}),\quad I_8 = -\frac{1}{2}\sum_{\varkappa}\hbar\omega_{\varkappa}\frac{\partial^2}{\partial q'^2_{\varkappa}}. \tag{8}$$

The value of the Jacobian of the transformation indicated in (7) is just unity. The integration over the new variables can be performed exactly. We introduce the notation

$$\overline{f} = \frac{1}{I}\int \exp\left\{-\sum_{\varkappa}\frac{s_{\varkappa}^2}{2}(1-\cos\mathbf{x}_3^{\varkappa}) - \frac{\beta\xi_3^2}{2}\right\} f(\xi_3)\cos\mathbf{k}_3^{\xi}\,(d\xi_3), \tag{9}$$

where

$$I = \int \exp\left\{-\sum_{\varkappa}\frac{s_{\varkappa}^2}{2}(1-\cos\mathbf{x}_3^{\varkappa}) - \frac{\beta\xi_3^2}{2}\right\}\cos\mathbf{k}_3^{\xi}\,(d\xi_3), \tag{10}$$

and then the result can be written

$$\overline{\overline{H}} = \sum_{l=1}^{8}\overline{\overline{I}}_l,\quad \overline{\overline{I}}_1 = \frac{3\hbar^2\beta}{2m} - \frac{\hbar^2\beta^2}{2m}\overline{\xi^2},\quad \overline{\overline{I}}_2 = -\frac{\hbar^2\beta}{mVV}\sum_{\varkappa}a_{\varkappa}s_{\varkappa}e^{-\varkappa^2/8\beta}\,\overline{(\mathbf{x}_3^{\xi}/2)\sin(\mathbf{x}_3^{\xi}/2)},$$
$$\overline{\overline{I}}_3 = \frac{\hbar^2}{4mV}\sum_{\varkappa}a_{\varkappa}^2\varkappa^2 - \frac{\hbar^2}{2mV}\sum_{\varkappa,\varkappa_1}a_{\varkappa}a_{\varkappa_1}s_{\varkappa}s_{\varkappa_1}(\boldsymbol{\varkappa}\boldsymbol{\varkappa}_1)\,e^{-(\varkappa-\varkappa_1)^2/8\beta}\,\overline{\sin(\mathbf{x}_3^{\xi}/2)\sin(\mathbf{x}_1^{\xi}/2)},$$
$$\overline{\overline{I}}_4 = 0,\quad \overline{\overline{I}}_5 = \frac{1}{4}\sum_{\varkappa}\hbar\omega_{\varkappa}(1+s_{\varkappa}^2) + \frac{1}{4}\sum_{\varkappa}\hbar\omega_{\varkappa}s_{\varkappa}^2\,\overline{\cos\mathbf{x}_3^{\xi}},\quad \overline{\overline{I}}_6 = -V^{-1/2}\sum_{\varkappa}(\hbar\omega_{\varkappa}a_{\varkappa} + c_{\varkappa})\,s_{\varkappa}e^{-\varkappa^2/8\beta}\,\overline{\cos(\mathbf{x}_3^{\xi}/2)}, \tag{11}$$
$$\overline{\overline{I}}_7 = \frac{1}{V}\sum_{\varkappa}\left(\frac{1}{2}\hbar\omega_{\varkappa}a_{\varkappa}^2 + c_{\varkappa}a_{\varkappa}\right),\quad \overline{\overline{I}}_8 = \frac{1}{4}\sum_{\varkappa}\hbar\omega_{\varkappa}(1-s_{\varkappa}^2) + \frac{1}{4}\sum_{\varkappa}\hbar\omega_{\varkappa}s_{\varkappa}^2\,\overline{\cos\mathbf{x}_3^{\xi}}.$$

In obtaining (11), the a_K and s_K are restricted by $a_K = a_{-K}$ and $s_K = s_{-K}$. For the a_K and s_K we shall use, for simplicity, expressions previously obtained[1] by minimizing $\overline{\overline{H}}$ in the approximation without translational symmetry, namely

$$a_{\varkappa} = -\frac{c_{\varkappa}(1-e^{-\varkappa^2/4\beta})}{(\hbar^2\varkappa^2/2m) + \hbar\omega_{\varkappa}(1-e^{-\varkappa^2/4\beta})},\quad s_{\varkappa} = \left(a_{\varkappa} + \frac{c_{\varkappa}}{\hbar\omega_{\varkappa}}\right)V^{-1/2}e^{-\varkappa^2/8\beta}. \tag{12}$$

Somewhat more exact but more complicated results could have been obtained by determining the a_K and

s_κ from the extremum condition of the functional $\overline{\overline{H}}$ given by (11).

It follows from (11) and (12) that

$$\overline{\overline{H}} = \sum_\kappa \frac{1}{2}\hbar\omega_\kappa + \frac{3\hbar^2\beta}{2m} - \frac{1}{2V}\sum_\kappa \frac{c_\kappa^2}{\hbar\omega_\kappa} e^{-\varkappa^2/4\beta} - \frac{1}{2V}\sum_\varkappa \frac{c_\varkappa^2 (1-e^{-\varkappa^2/4\beta})^2}{(\hbar^2\varkappa^2/2m)+\hbar\omega_\varkappa(1-e^{-\varkappa^2/4\beta})}$$

$$- \frac{\hbar^2\beta^2}{2m}\frac{1}{\gamma^2} - \frac{\hbar^2\beta}{mV}\sum_\kappa a_\kappa s_\kappa e^{-\varkappa^2/8\beta}\overline{(\boldsymbol{\varkappa}\boldsymbol{\xi})\sin(\boldsymbol{\varkappa}\boldsymbol{\xi}/2)} + \sum_\kappa \frac{1}{2}\hbar\omega_\kappa s_\kappa^2\left[\overline{\cos(\boldsymbol{\varkappa}\boldsymbol{\xi})} - 2\overline{\cos(\boldsymbol{\varkappa}\boldsymbol{\xi}/2)}\right] \qquad (13)$$

$$+ \sum_\kappa \frac{1}{2}\hbar\omega_\kappa s_\kappa^2 - \frac{\hbar^2}{2mV}\sum_{\kappa,\kappa_1} a_\kappa a_{\kappa_1} s_\kappa s_{\kappa_1} (\boldsymbol{\varkappa}\boldsymbol{\varkappa}_1) e^{-(\varkappa-\varkappa_1)^2/8\beta}\overline{\sin(\boldsymbol{\varkappa}\boldsymbol{\xi}/2)\sin(\boldsymbol{\varkappa}_1\boldsymbol{\xi}/2)}.$$

Here the first four terms agree with the previously obtained expression for $\overline{\overline{H}}$ in the absence of the additional external field $V(\mathbf{r})$. The remaining terms in (13) arise as a result of the transition to translational symmetry in the trial functions of (5) and (6). These are the only terms which depend on the momentum of the system.

2. DEPENDENCE OF THE ENERGY ON THE MOMENTUM AND ENERGY OF THE POLARON GROUND STATE

In an attempt to make the problem more specific and to perform some numerical calculations, let us henceforth consider the particular case of a polaron when there is no dispersion of the optical lattice vibrations ($\omega_\kappa = \omega$). In this case we have

$$c_\varkappa = -e\sqrt{4\pi\hbar\omega_\kappa c}/|\varkappa|, \quad c = 1/n^2 - 1/\varepsilon. \qquad (14)$$

Here ϵ is the static dielectric constant of the crystal, n is the index of refraction, and e is the electron charge. In Eq. (1) m is the effective mass of a band electron.

Let us first consider the limiting case of strong coupling between the electron and polar crystal vibrations, that is the case of large c. We replace $\mathbf{k}$ and c by the dimensionless wave vector $\mathbf{k}'$ and the dimensionless coupling constant α given by

$$\mathbf{k}' = -\frac{\mathbf{k}}{e}\left(\frac{3\pi^{1/2}\hbar\omega}{c\beta_0^{1/2}}\right)^{1/3}, \quad \beta_0 = \frac{m^2e^4c^2}{9\pi\hbar^4}, \quad \alpha = \frac{e^2c}{\hbar^{3/2}}\left(\frac{m}{2\omega}\right)^{1/2}. \qquad (15)$$

Let us now expand $\overline{\overline{H}}$ as given by (13) in a power series in $\mathbf{k}$, retaining terms of order $\mathbf{k}^0$, $\mathbf{k}^2$, and $\mathbf{k}^4$. We then expand each coefficient of this series in inverse powers of α, retaining terms of order α^2, α^0, and α^{-2}. To do this we expand the trigonometric functions of $(\kappa\xi)$ in the last four terms of the integrand of (13) in powers of $(\kappa\xi)$ up to terms of order $(\kappa\xi)^4$ inclusive. The result so obtained can be simplified by averaging over angles in κ-space, which leads to

$$\overline{\overline{H}} = R(\beta) + \overline{\xi^2}\left[-\frac{\hbar^2\beta^2}{2m} - \frac{\hbar^2\beta}{6mV}\sum_\kappa a_\kappa s_\kappa e^{-\varkappa^2/8\beta}\varkappa^2 - \frac{\hbar\omega}{24}\sum_\kappa s_\kappa^2\varkappa^2 - \frac{\hbar^2}{24mV}\sum_{n=0}^{\infty}\frac{1}{(n+3)\,n!}\Big(\sum_\kappa a_\kappa s_\kappa e^{-\varkappa^2/8\beta} y^n\varkappa^2\Big)^2\right]$$
$$(n-\text{even})$$

$$+ \overline{\xi^4}\left[\frac{\hbar^2\beta}{240mV}\sum_\kappa a_\kappa s_\kappa e^{-\varkappa^2/8\beta}\varkappa^4 + \frac{7\hbar\omega}{1920}\sum_\kappa s_\kappa^2\varkappa^4 + \frac{\hbar^2}{480mV}\sum_{n=0}^{\infty}\frac{1}{n!\,(n+3)}\sum_\kappa a_{\kappa_1} s_\kappa e^{-\varkappa^2/8\beta} y^n\varkappa^4 \sum_{\kappa_1} a_{\kappa_1} s_{\kappa_1} e^{-\varkappa_1^2/8\beta}\, y_1^n\varkappa_1^2\right], \qquad (16)$$

$$y = \varkappa_\kappa/2\sqrt{\beta}, \quad y_1 = \varkappa_1/2\sqrt{\beta}.$$

Here $R(\beta)$ is the sum of the first four terms of (13). It is now necessary to calculate $\overline{\xi^2}$ and $\overline{\xi^4}$ with the required accuracy. This is done by expanding the arguments of the exponential in (9) and (10) in powers of $(\kappa\xi)$, leaving the term of order $(\kappa\xi)^2$ in the exponent, and writing the exponential containing higher powers of $(\kappa\xi)$ in the form of a series. We then obtain

$$\overline{\xi^2} = \delta^{-1}\left[\frac{3}{2} + \frac{15}{2}\gamma\delta^{-2} + k^2\left(-\frac{1}{4}\delta^{-1} - \frac{15}{4}\gamma\delta^{-3}\right) + \frac{1}{4}k^4\gamma\delta^{-4}\right]; \quad \overline{\xi^4} = \delta^{-2}\left[\frac{15}{4} - \frac{5}{4}\delta^{-1}k^2 + \frac{1}{16}\delta^{-2}k^4\right], \qquad (17)$$

where

$$\delta = \frac{1}{12}\sum_\kappa s_\kappa^2\varkappa^2 + \frac{1}{2}\beta, \quad \gamma = \frac{1}{240}\sum_\kappa s_\kappa^2\varkappa^4.$$

If we now calculate all the sums over κ by replacing them by integrals in κ-space, then (16) leads to

$$\frac{\bar{\bar{H}}}{\hbar\omega} = \sum_{\kappa} \frac{1}{2} + \frac{\alpha^2}{3\pi}(\zeta - 2\zeta^{1/2}) - 3(2-\sqrt{2})\zeta^{-1/2} + \frac{27\pi \cdot 0.096}{2\alpha^2} + \left[\frac{3}{2} + \frac{81\pi}{8\alpha^2} + k'^2\left(-\frac{1}{4}\zeta^{-1/2} - \frac{9\pi \cdot 2.29}{4\alpha^2}\right) + k'^4 \frac{27\pi}{80\alpha^2}\right] \tag{18}$$

$$\times\left(1 + \frac{9\pi}{\alpha^2}\,0.043\right)\left[-\frac{1}{2}\zeta^{1/2} + 0.086 - 0.235\zeta^{-1/2} + \frac{9\pi}{\alpha^2}\,0.098\right] + \frac{9\pi}{5\alpha^2}\,0.649\left[\frac{15}{4} - \frac{5}{4}k'^2 + \frac{1}{16}k'^4\right], \quad \zeta = \beta/\beta_0.$$

The value of ζ is found from the condition that $\bar{\bar{H}}$ be a minimum. The expansion of ζ in powers of α is of the form

$$\zeta = 1 + 6\pi\alpha^{-2}(-0.68 + 0.21\,k'^2). \tag{19}$$

Inserting (19) into (18) we obtain

$$\frac{\bar{\bar{H}}}{\hbar\omega} = -\frac{1}{3\pi}\alpha^2 - 2.73 - \frac{8.6}{\alpha^2} + k'^2\left[0.16 + \frac{10.8}{\alpha^2}\right] - k'^4\,\frac{1.28}{\alpha^2}. \tag{20}$$

$$\bar{\bar{H}} = -\left(0.106\alpha^2 + 2.73 + \frac{8.6}{\alpha^2}\right)\hbar\omega + \frac{P^2}{2M} + \frac{P^4}{2N}, \quad M = 155\left(\frac{\alpha}{10}\right)^4\left[1 + \frac{67}{\alpha^2}\right]^{-1} m, \quad N = -9.7\cdot 10^4\left(\frac{\alpha}{10}\right)^{10} m^2\hbar\omega. \tag{21}$$

In the limiting case of weak coupling Eq. (13) leads quite simply to the first terms in the series for the ground state energy and effective mass by setting $s_\kappa = 0$ and

$$a_\kappa = -c_\kappa\left[(\hbar^2\kappa^2/2m) + \hbar\omega\left(1 - e^{-\kappa^2/4\beta}\right)\right]$$

(these are the asymptotic values of the s_κ and the a_κ as given by (12) in the limit as $c \to 0$). The result $\bar{\bar{H}} = -\alpha\hbar\omega + P^2/2m$ coincides with the exact one. We have not calculated further terms in the series. Allcock[3] summarizes the results of various authors' calculations of the polaron ground state energy and effective mass. Comparison of these results shows that in the intermediate-coupling region ($\alpha \sim 5$) Feynman[2] obtains the most accurate result. Expression (20) obtained here gives a somewhat lower ground state energy for $\alpha = 5$ (at least by 7% if the term of order c^{-2} in Feynman's expression for the energy is positive, as he himself supposes).

The convergence of the power series in $1/\alpha^2$ for the ground state energy is much better than that of the analogous series for the effective mass. It is therefore desirable to obtain the subsequent terms in the power series in α^{-2} for the effective mass for real ionic crystals ($\alpha \sim 8$).

Nevertheless, let us give the effective mass of the polaron in NaCl as calculated according to (21). This is $M = 49$ m (if we assume[4] that $\alpha^2 = 77$ in NaCl). The Feynman-Allcock formula[4] (the first two terms in Feynman's expansion) gives $M = 40.8$ m in this case. For a polaron kinetic energy equal to about $\hbar\omega$ in NaCl, the $P^4/2N$ term is about 20% of the $P^2/2M$ term.

The authors express their gratitude to Iu. L. Mentkovskii, who checked the calculations.

[1] V. M. Buimistrov and S. I. Pekar, J. Exptl. Theoret. Phys. (U.S.S.R.) **32**, 1193 (1957), Soviet Phys. JETP **5**, 970 (1957).

[2] R. P. Feynman, Phys. Rev. **97**, 660 (1955).

[3] G. R. Allcock, Advances in Physics **5**, 412 (1956).

[4] S. I. Pekar, Исследования по электронной теории кристаллов (Investigations in the Electron Theory of Crystals), Gostekhizdat, 1951.

Translated by E. J. Saletan
258

ON THE PROBLEM OF THE EXCITED STATES OF NUCLEONS

N. F. NELIPA

Physical Institute of the Academy of Sciences, S.S.S.R.

Submitted to JETP editor, May 29, 1957

J. Exptl. Theoret. Phys. (U.S.S.R.) **33**, 1277-1281 (1957)

It is shown that within the limits of the Markov equation,[1] two different classes of excited states exist for the nucleon: short lived (nuclear times) and long lived ($\sim 10^{-10}$ sec). These states may be identified with hyperons. Taking account of the latter in intermediate states leads to resonance effects. The scattering of π mesons by protons is used as a methodological example. The calculated maxima in the total scattering cross sections are quite close to the experimentally observed values.

1. Markov[1] has proposed a nonlocal equation for the description of excited nucleons. We wish to point out an interesting peculiarity of the Markov equation. It appears that two very different classes of excited states exist within the framework of this equation:* short lived (nuclear times) and relatively long lived ($\sim 10^{-10}$ sec). Generally speaking, the excited states of the nucleon may be identified with heavy particles.[1] Then unstable and relatively stable heavy particles will correspond to these classes of excited states. Taking account of these particles, similar to isobars,[2] may lead to resonance effects in intermediate states. As an example having methodological significance, the scattering of π mesons by protons is considered. If the first excited state of the nucleon is taken[3,4] to be a Λ^0 particle, for example, calculations lead to the presence of maxima in the total $\pi^- - p$ scattering cross sections at π^--meson energies close to those found experimentally. Thus, in principle, a new possibility emerges for the explanation of experimental facts.

2. The Markov equation is[1]

$$\{\gamma_\nu \partial / \partial X_\nu + a\,[\partial^2 / \partial \zeta_\nu \partial \zeta_\nu + V(\zeta_\nu \zeta_\nu)]^n + m_0 + W(x')\}\,\psi = 0, \tag{1}$$

where $\zeta_\nu = r_\nu / r_0$ is a dimensionless internal degree of freedom, r_0 is a constant with the dimensions of length, X_ν is the coordinate of the "center of mass" of the particle, $W(x')$ is the energy operator of the interaction between the meson and the nucleon fields, and a and m_0 are constants.

It is characteristic of Eq. (1) that the interaction $W(x')$ is considered to be point-like, but displaced with respect to the "center of mass" of the particle (in the simplest case, $x'_\nu = X_\nu + r_\nu$); quanta of the field (for example, mesons) may be emitted and absorbed at any point of space surrounding the nucleon.

The choice of a concrete form of Eq. (1) is quite arbitrary because of the indefiniteness of the expression for $V(\zeta_\nu \zeta_\nu)$ and the value of n. However, to elucidate the possibilities of Eq. 1, we may limit ourselves to the case of $n = 1$ and

$$V(\zeta_\nu \zeta_\nu) = \zeta_\nu \zeta_\nu + 2\,\frac{(k_\nu \partial / \partial \zeta_\nu)^2 - k_\nu \zeta_\nu}{k_\nu k_\nu}. \tag{2}$$

Then the wave function of the unexcited Eq. 1 will have the form

$$\psi = u(X)\,\chi_{n_1 n_2 n_3 n_4}(\zeta_\nu). \tag{3}$$

The function χ describes the internal states of the particle. The set of numbers (n_1, n_2, n_3, n_0) characterize the degree of excitation of the nucleon. For the excited state of a nucleon with nonvanishing momentum **p**,

$$\chi_{n_1 n_2 n_3 n_4} = N H_{n_1}(\zeta_1)\,H_{n_2}(\zeta_2)\,H_{n_3}(\zeta_3)\,H_{n_4}(\zeta_0)\,\exp\left\{-\frac{1}{2}\,[\zeta_\nu \zeta_\nu + 2\,(p_\nu \zeta_\nu)^2 / M_0^2]\right\}, \tag{4}$$

where N is a normalization factor, $H_n(\xi)$ is a Chebyshev-Hermite polynomial, and M_0 is the mass of the unexcited nucleon.

* This results from the existence of definite selection rules for the matrix elements over internal variables.

The function u(X) in Eq. (3) describes the motion of the "center of mass," and is a solution of the usual Dirac equation with mass

$$M_n = m_0 + a(n_1 + n_2 + n_3 + n_0 + 2) = M_0 + a(n_1 + n_2 + n_3 + n_0). \tag{5}$$

The constant a characterizes the energy spacing between two excitations of the nucleon and is determined by experiment. The equidistant spectrum is due to the coice of $V(\xi_\mu, \xi_\nu)$ in the form of Eq. (2).

It is clear that the Markov equation yields an increasing mass spectrum, Eq. (5), and is thus essentially different from other relativistic equations for excited elementary particles (see, for example, Ref. 5).

3. We shall show now that definite selection rules exist for the matrix elements over internal variables, which leads to two classes of excited states of nucleons: short lived (allowed transitions) and relatively long lived (forbidden transitions).

For definiteness, let us consider the matrix element of the transition of a nucleon with momentum $\mathbf{p}_0$ and any (n_1, n_2, n_3, n_0) into a state with momentum $\mathbf{p}'$ and any (n_1', n_2', n_3', n_0'), with absorption of a meson with momentum $\mathbf{k}_0$ (so that $\mathbf{p}' = \mathbf{p}_0 + \mathbf{k}_0$). To simplify the calculations, we transform to the center-of-mass system of the meson and nucleon, (i.e., set $\mathbf{p}_0 + \mathbf{k}_0 = 0$). The momentum of the nucleon in the intermediate state in the c.m.s. is zero in this case, and therefore the form of the function χ is simplified. Moreover, we orient the x-axis along the nucleon momentum in the c.m.s. and limit ourselves to the case of pseudoscalar interaction between the meson and nucleon with pseudoscalar coupling. Then, bearing Eq. (4) in mind, the transition matrix element over the internal variables may be written in the present case in the c.m.s.,

$$I_{nn'} = N \int_{-\infty}^{+\infty} H_{n_1}(\zeta_1) \dots H_{n_0'}(\zeta_0)\, e^B d\zeta_1 d\zeta_2 d\zeta_3 d\zeta_0, \tag{6}$$

where N is the normalization constand for the Chebyshev-Hermite polynomials,

$$B = -\zeta_1^2 - \zeta_2^2 - \zeta_3^2 - M_0^{-2}(q_1\zeta_1 + E\zeta_0)^2 - i(q_1\zeta_1 - \varepsilon\zeta_0) r_0, \qquad q = |\mathbf{p}_0| = |\mathbf{k}_0|,$$

$\mathbf{q}_1$ is the projection of the vector $\mathbf{q}$ on the x-axis, ϵ is the meson energy, and E is the energy of the nucleon.

We evaluate the integral in Eq. (6) by generalizing somewhat a method which we have used previously.[6] We start with the equalities[7]

$$\exp\{-t_1^2 + 2t_1\zeta_1\} = \sum_{n_1=0}^{\infty} \frac{1}{n_1!} H_{n_1}(\zeta_1)\, t_1^{n_1}, \dots \tag{7}$$

$$\exp\{-t_1'^2 + 2t_1'\zeta_1\} = \sum_{n_1'=0}^{\infty} \frac{1}{n_1'!} H_{n_1'}(\zeta_1)\, t_1'^{n_1'} \dots \tag{8}$$

We multiply both sides of Eqs. (7) and (8) term by term and then multiply both sides of the result by e^B. Then we integrate both sides over ξ_1, ξ_2, ξ_3, ξ_0 from $-\infty$ to $+\infty$ and obtain

$$N\pi^2 \frac{M_0}{E} \exp\left[-\frac{1}{4} r_0^2 \left(q_1^2 + \varepsilon^2 + 2\frac{\varepsilon}{E} q_1^2\right)\right] [-\alpha(t_1 + t_1') + \beta(t_0 + t_0') - 2\frac{q_1}{E}(t_1 + t_1')(t_0 + t_0') + 2(t_1 t_1' + t_0 t_0')]$$
$$= \sum_{n_1=0}^{\infty} \dots \sum_{n_0'=0}^{\infty} I_{nn'} \frac{1}{n_1!} \dots \frac{1}{n_0'!} t_1^{n_1} \dots t_0'^{n_0'}, \tag{9}$$

where

$$\alpha = ir_0(q_1 + q_1\varepsilon/E), \quad \beta = ir_0(q_1^2/E + \varepsilon). \tag{10}$$

Equation (9) is the expansion of the exponent in a Maclaurin series in powers of t and t', the coefficients of which are the desired integrals. By the general rule for finding the coefficients of the expansion of a function in a Maclaurin series, we obtain

$$I_{nn'} = N\pi^2 \frac{M_0}{E} \exp\left[-\frac{1}{4} r_0^2\left(q_1^2 + \varepsilon^2 + 2\frac{\varepsilon}{E} q_1^2\right)\right] \frac{\partial^{n_1+\ldots+n_0'}}{\partial t_1^{n_1} \ldots \partial t_0'^{n_0'}} \exp\left[-\alpha(t_1+t_1') + \beta(t_0+t_0') - 2\frac{q_1}{E}(t_1+t_1')(t_0+t_0') + 2(t_1t_1' + t_0t_0')\right]_{t_1=t_2=\ldots=t_0'=0}. \quad (11)$$

In the case of an arbitrary orientation of the vector $\mathbf{q}$, we must replace q_1 by q in Eq. (11), adding the corresponding terms in t. In particular, if $n_1 = n_2 \ldots = n_0' = 0$, then

$$I_{00} = \frac{M_0}{E} \exp\left[-\frac{1}{4} r_0^2\left(q^2 + \varepsilon^2 + 2\frac{\varepsilon}{E} q^2\right)\right]. \quad (12)$$

If $N \equiv n_1 + n_2 + n_3 = 0$, $n_0 = 0$ and $N' = 1$, $n_0' = 0$, then

$$I_{01} = \frac{1}{\sqrt{2}} I_{00} i r_0 \left[1 + \frac{\varepsilon}{E}\right] q, \quad (13)$$

For $N = n_0 = 0$ and $N' = n_0' = 1$,

$$I_{02} = \frac{1}{2} I_{00}\left[-2\frac{q}{E} + r_0^2\left(1 + \frac{\varepsilon}{E}\right)\left(\frac{q^2}{E} + \varepsilon\right)q\right]. \quad (14)$$

If $r_0 a \sim r_0/\lambda \ll 1$, Eq. (13) is considerably smaller than Eq. (14). Using Eq. (11), it is easy to convince ourselves that generally speaking, if

$$N' = n_0', \quad (15)$$

then $I_{nn'}$ will contain terms independent of $r_0 q$, i.e., $I_{nn'}$ will be relatively large; in the other cases, $I_{nn'}$ will be a relatively small quantity, of the order of $r_0 q$. Consequently, condition (15) corresponds to allowed transitions. For the case $N' \neq n_0'$, the transitions will be less probable.*

Since t and t' enter symmetrically into Eq. (11), the selection rules for N and n_0 will be the same as for N' and n_0'.

4. As an example having methodological significance, we will consider the scattering of π^- mesons on nucleons within the framework of Eq. (1). For simplicity, we will limit ourselves to calculations of the pseudoscalar theory, with pseudoscalar coupling between the meson and the nucleon.

We will first consider the scattering of π^- mesons by protons:

$$\pi^- + p \to \pi^- + p. \quad (I)$$

We use non-covariant perturbation theory for the calculations. The sequences of events shown in the figure correspond to process I in the first nonvanishing approximation. The lower sequence corresponds to all cases in which an excited state of the nucleon is formed in the intermediate state.

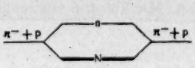

In the c.m.s. the transition matrix element corresponding to the first sequence may be written

$$\frac{H_{An}H_{nF}}{E - E'} = \frac{2\pi g^2}{\varepsilon} \frac{(u_0^* \beta\gamma_5 u')(u'^* \beta\gamma_5 u)}{E + \varepsilon - E'} I_0; \quad (16)$$

$$I_0 = \int \chi_{0000}(\zeta_v, q_v)\, e^{iq_v\zeta_v r_a} \chi_{0000}(\zeta_v, p_v')\, d\zeta_v \int \chi_{0000}(\zeta_v, p')\, e^{-iq_v'\zeta_v'} \chi_{0000}(\zeta_v, q_v')\, d\zeta_v. \quad (17)$$

Here, the nucleon momentum in the intermediate state $p' = 0$. The transition matrix element

$$\frac{H_{AN}H_{NF}}{E - E_N} = \frac{2\pi g^2}{\varepsilon} \frac{(u_0^* \beta\gamma_5 u_N)(u_N^* \beta\gamma_5 u)}{E + \varepsilon - E_N} I_n. \quad (18)$$

corresponds to the second sequence. We will assume that nucleons in excited states interact with mesons in the same way as protons and neutrons.[3]

The concrete form of I_n in Eq. (18) is determined by the degree of excitation of the nucleon in the

*The same selection rules were obtained by L. G. Zastavenko in another way, see Ref. 4.

intermediate state, i.e., by the values of the numbers $n_1', \ldots$. If we consider only those excitations in the intermediate state for which $N' \equiv n_1' + n_2' + n_3' = 1$, $n_0' = 1$, then three terms will enter into I_2, corresponding to the triple degeneracy of the sequence with excited nucleons in the intermediate state.*

The differential scattering cross section in the c.m.s. of the meson and nucleon can now be written

$$d\sigma/d\Omega = (g^4/2W^2)\{[(E_\varepsilon + q^2)^2 + M_0^2\varepsilon^2 + (W^2 - M_0^2)\, q^2 \cos\vartheta]\,(\Phi_0 + \Phi_2)^2 + [E^2 - q^2\cos\vartheta + M_0^2]\, a^2\Phi_2^2 - 2M_0 a\Phi_2\,(\Phi_0 + \Phi_2)\,[2E_\varepsilon + q^2(1+\cos\vartheta)]\}, \tag{19}$$

where ϵ and E are the energies of the meson and nucleon, respectively, $W = E + \epsilon$, and

$$\Phi_0 = I_0/(M^2 - W_0^2),\ \Phi_2 = I_2/(W^2 - M_2^2),\ I_0 = M_0^2/E^2,\ I_2 = (M_0^2q^2/E^4)\cos\vartheta.$$

To obtain the expressions for I_0 and I_2, we assumed that the excited state of the nucleon is a particle with a lifetime of the order of 10^{-10} sec (for example, Λ^0, etc.). Then[4] $r_0 \sim 10^{-13}$ cm and the exponential factor entering into I_0 and I_2 may be replaced by unity for practically all possible momenta. It is clear that in this case the magnitude of r_0 does not play an essential role.

Integrating Eq. (10) over the angles, we obtain the total cross section of process (I):

$$\sigma^- = (2\pi g^4/W^2)\,\Phi_0^2\,[(E_\varepsilon + q^2)^2 + M_0^2\varepsilon^2] + (4\pi g^4/3W^2)\,F_2\Phi_0\,[(W^2 - M_0^2)\,q^2 - 2M_0 a q^2] + (2\pi g^4/3W^2)\,F_2^2[(E_\varepsilon + q^2)^2 + M_0^2\varepsilon^2 + a^2(E^2 + M_0^2) - 2M_0 a\,(2E_\varepsilon + q^2)], \tag{20}$$

where $F_2 = M_0^2q^2/E^4(W^2 - M_2^2)$.

The most interesting thing in this expression is the presence of maxima in the cross section at $W^2 = M_2^2$, or more generally, at $W^2 = M_n^2$. The value of M_n is determined by the magnitude of a, i.e., the energy spacing between two excitations of the nucleon. If we assume that the excited state of the nucleon is, for example, a Λ^0-particle, then a $\sim$ 180 Mev, and the cross section will have maxima at kinetic energies of the scattered π^- mesons of $\sim$ 300, 910 and 1570 Mev in the laboratory system for M_2, M_4 and M_6, respectively. This discloses, in principle, a new possibility of explaining the experimentally-observed maxima in the scattering of π^- mesons by nucleons, occurring, as is well known,[8] at meson energies $\sim$ 200 and 900 Mev. To draw more definite conclusions, it is necessary to study the same problem in the theory of damping, and also to keep in mind that our considerations are based on the assumption that $V(\xi_\nu \xi_\nu)$ has the form of Eq. (2), and that $n = 1$.

5. Evidently, the presence of maxima in the scattering cross section of π^- mesons by nucleons is due to a term of the type $1/(W^2 - M_n^2)$. It is easy to see that for the process

$$\pi^+ + p \to \pi^+ + p \tag{II}$$

this factor appears only if it is admitted that an excited doubly charged particle appears in the intermediate state.† Therefore, process II requires additional study.

In conclusion, I wish to thank Prof. M. A. Markov for suggesting this topic, and for helpful advice during the work.

[1] M. A. Markov, Dokl. Akad. Nauk SSSR 101, 51, 449 (1955); Suppl. Nuovo cimento 4, 760 (1956).

[2] Tamm, Gol'fand and Fainberg, J. Exptl. Theoret. Phys. (U.S.S.R.) 26, 649 (1954).

[3] M. A. Markov, О систематике элементарных частиц (Classification of Elementary Particles), Acad. Sci. Press, Moscow, 1955.

[4] P. S. Isaev and M. A. Markov, J. Exptl. Theoret. Phys (U.S.S.R) 29, 111 (1955), Soviet Phys. JETP 2, 84 (1956).

[5] I. Gel'fand and A. Iaglom, J. Exptl. Theoret. Phys. (U.S.S.R.) 18, 703 (1948).

[6] N. F. Nelipa, Dissertation, Phys. Inst. Acad. Sci., Moscow, (1952).

[7] V. Smirnov, Курс высшей математики (Course of Higher Mathematics), vol. 3, (1939).

[8] H. Bethe and F. de Hoffman, Mesons and Fields Vol. 2, New York, (1955).

Translated by D. Lieberman
259

*The less interesting case $N' = 1$, $n_0' = 0$ was considered by a Filiukov (Dissertation, Moscow State University, 1955).

†A similar situation occurs in the theory of isobaric states (see Ref. 2).

ON THE THEORY OF THE ANOMALOUS SKIN EFFECT IN METALS

V. P. SILIN

P. N. Lebedev Physics Institute, Academy of Sciences, U.S.S.R.

Submitted to JETP editor June 2, 1957; resubmitted July 11, 1957

J. Exptl. Theoret. Phys. (U.S.S.R.) 33, 1282-1286 (November, 1957)

The anomalous skin effect is considered, using Landau's theory of a Fermi liquid, as extended by the author[1] to the case of a degenerate electron fluid. We show that the information we get about the Fermi surface by measuring the surface impedance does not depend on whether we consider the conduction electrons to be a gas or to be a degenerate fluid. We discuss the problem of how to define the parameters for an isotropic model of a metal.

1. It is well known that in the region of the anomalous skin effect[2] it is impossible to use such macroscopic characteristics of the metal as conductivity, and that it becomes necessary to use some model for the behavior of the electron conductivity in a metal. It is therefore usual in the theory of the anomalous skin effect[3] to use the model of an electron gas, although in actual fact the interaction between the conduction electrons in a metal is relatively strong. In this connection one should consider this phenomenon by starting from the theory of Fermi-liquids.[4]

If we confine our interest to the case of weak fields, we may assume that the electron distribution differs only slightly from its equilibrium value,

$$f = f_0 + f_1(\mathbf{p}, \mathbf{r}), \quad f_1 \ll f_0 = \frac{2}{(2\pi\hbar)^3}\left\{\exp\left[\frac{\epsilon_0(\mathbf{p}) - \mu}{kT}\right] + 1\right\}^{-1},$$

where $\epsilon_0(\mathbf{p})$ is the electron energy in the equilibrium state. We find then from Eq. (14) of Ref. 1 (see also Ref. 4) that

$$\frac{\partial f_1}{\partial t} + \mathbf{v}_0 \frac{\partial f_1}{\partial \mathbf{r}} - \frac{\partial f_0}{\partial \mathbf{p}} \int d\mathbf{p}' \frac{\partial f_1(\mathbf{p}', \mathbf{r})}{\partial \mathbf{r}} \Phi(\mathbf{p}, \mathbf{p}') + e\mathbf{E}\frac{\partial f_0}{\partial \mathbf{p}} = -\frac{1}{\tau} f_1, \tag{1}$$

where $\mathbf{v}_0 = \partial\epsilon_0/\partial\mathbf{p}$, τ is the relaxation time and $\Phi(\mathbf{p}, \mathbf{p}')$ describes the correlation of the particles.

To develop a theory of the anomalous skin effect it is necessary to solve Eq. (1) combined with the Maxwell equations. In that case the current density is, according to Landau,

$$\mathbf{j} = e\int \frac{\partial \epsilon}{\partial p} f d\mathbf{p} = e\int\left(\frac{\partial \epsilon_0}{\partial p} f_1 + \frac{\partial \epsilon_1}{\partial p} f_0\right) d\mathbf{p} = e\int d\mathbf{p}\left\{\mathbf{v}_0 f_1 - \frac{\partial f_0}{\partial p}\int d\mathbf{p}'\, \Phi(\mathbf{p}, \mathbf{p}') f_1(\mathbf{p}')\right\}. \tag{2}$$

2. Let the metal occupy the half-space $z \geq 0$. The function f_1 can then be written as follows

$$f_1(\mathbf{p}, z, t) = e\frac{\partial f_0}{\partial \epsilon}\psi(\mathbf{n}, z)\, e^{i\omega t} \quad (\mathbf{n} = \mathbf{v}_0/v_0). \tag{3}$$

The transport equation (1) and the equation for the electric field can now be written

$$\frac{1}{l_{\text{eff}}}\psi(\mathbf{n}, z) + \mathbf{kn}\frac{\partial}{\partial z}\left\{\psi(\mathbf{n}, z) + \int dS' F(\mathbf{n}, \mathbf{n}')\psi(\mathbf{n}', z)\right\} + \mathbf{nE} = 0, \tag{4}$$

$$\mathbf{E}' + \epsilon_0\left(\frac{\omega}{c}\right)^2 \mathbf{E} = -\frac{8\pi i\omega e^3}{c^3(2\pi\hbar)^3}\int dS\mathbf{n}\left\{\psi(\mathbf{n}, z) + \int dS' F(\mathbf{n}, \mathbf{n}')\psi(\mathbf{n}', z)\right\}, \tag{5}$$

where $\mathbf{k}$ is a unit vector in the direction of the z-axis, dS is an element of the Fermi surface, ϵ_0 the dielectric constant, excluding the contribution from the conduction electrons, $l_{\text{eff}} = \mathbf{v}_0\tau/(1 + i\omega\tau)$, and finally

$$F(\mathbf{n}, \mathbf{n}') = [2/(2\pi\hbar)^3]\,\Phi(\mathbf{p}, \mathbf{p}')/v_0(\mathbf{n}) \tag{6}$$

Solving (4) and (5), we can find an experimentally measured quantity, namely the surface impedance of the metal.

3. In the region of the normal skin effect, where the inhomogeneity of the electron distribution in space is not important, the solution of Eq. (4) is of the form $\psi = -l_{\text{eff}}(\mathbf{n}\cdot\mathbf{E})$. This leads to the following expression for the current,

$$j_\alpha = 2e^2(2\pi\hbar)^{-3}\int dS l_{\text{eff}}\left\{n_\alpha n_\beta + \int dS' F(\mathbf{n}', \mathbf{n}) n'_\alpha n_\beta\right\} E_\beta = \sigma_{\alpha\beta}E_\beta. \tag{7}$$

Using expression (7) we can write down an expression for the conductivity tensor or, more generally, the complex dielectric constant ($\epsilon' = \epsilon_0 - i4\pi\sigma/\omega$).

Assuming the metal to be isotropic, we can write Eq. (7) in the following form,

$$\mathbf{j} = \sigma\mathbf{E} = \frac{8\pi e^2 p_0^2 l_{\text{eff}}}{3(2\pi\hbar)^3}\left\{1 + p_0^2\int d\Omega \cos\chi F(\cos\chi)\right\}\mathbf{E}. \tag{8}$$

In the region of low frequencies ($\omega\tau \ll 1$) the complex dielectric constant is determined by static conductivity,

$$\sigma_0 = \frac{8\pi e^2 p_0^2 v_0 \tau}{3(2\pi\hbar)^3}\left\{1 + p_0^2\int d\Omega \cos\chi F(\cos\chi)\right\} \equiv \frac{8\pi e^2 p_0^2 l}{3(2\pi\hbar)^3}, \tag{9}$$

where $l = v_0\tau\{1 + p_0^2\int d\Omega \cos\chi F(\cos\chi)\}$ plays the role of the electron mean free path. On the other hand, in the region of high frequencies ($\omega\tau \gg 1$), the dielectric constant has the form

$$\varepsilon = \varepsilon_0 - 4\pi e^2 N/m\omega^2, \tag{10}$$

where

$$N = \frac{8\pi p_0^2 v_0 m}{3(2\pi\hbar)^3}\left\{1 + p_0^2\int d\Omega \cos\chi F(\cos\chi)\right\}. \tag{11}$$

4. To solve the transport equation (4) in the region of the anomalous skin effect, where the spatial inhomogeneity plays an essential role, it is necessary to introduce a boundary condition at the metal surface.[5] We introduce such a condition for the function

$$\Psi(\mathbf{n}, z) = \psi(\mathbf{n}, z) + \int dS' F(\mathbf{n}, \mathbf{n}')\psi(\mathbf{n}', z), \tag{12}$$

which determines the particle current as can be seen from Eq. (5). We assume that on the metal surface

$$\Psi(n, z=0)|_{\mathbf{kn}>0} = q\Psi(n_x, n_y, -n_z, z=0)|_{\mathbf{kn}<0}. \tag{13}$$

We can then easily obtain from Eq. (4) an integral equation for $\psi(\mathbf{n}, z)$, using Eq. (13) and taking into account the fact that as $z \to \infty$ $\Psi(\mathbf{n}, z)$ tends to zero. In the limit of a sharply expressed anomalous skin effect ($l_{\text{eff}} \to \infty$), this equation simplifies considerably and has the form

$$\Psi(\mathbf{n}, z) \equiv \psi(\mathbf{n}, z) + \int dS' F(\mathbf{n}, \mathbf{n}')\psi(\mathbf{n}', z) = \psi_0(\mathbf{n}, z). \tag{14}$$

Here

$$\mathbf{kn} > 0: \quad \psi_0(\mathbf{n}, z) = -\int_0^z dz' \exp\left(-\frac{1}{l_{\text{eff}}}\left|\frac{z'-z}{\mathbf{kn}}\right|\right)\frac{\mathbf{nE}(z')}{\mathbf{nk}} - q\int_0^\infty dz' \exp\left(-\frac{z'+z}{l_{\text{eff}}\,\mathbf{kn}}\right)\frac{\mathbf{nE}(z')}{\mathbf{nk}}, \tag{15}$$

$$\mathbf{kn} < 0: \quad \psi_0(\mathbf{n}, z) = \int_z^\infty dz' \exp\left(-\frac{1}{l_{\text{eff}}}\left|\frac{z'-z}{\mathbf{kn}}\right|\right)\frac{\mathbf{nE}(z')}{\mathbf{nk}}, \tag{16}$$

where we have neglected the z-component of the electrical field, since it gives a negligibly small contribution. The function $\psi_0(\mathbf{n}, z)$ is the corresponding solution of the usual theory of the anomalous skin effect.[6]

In our considerations the function Ψ plays the same role in determining the current as the function ψ in the usual theory. We can therefore confirm, according to (15), that in the limit, as $l_{\text{eff}} \to \infty$, the expression which we obtain for the surface impedance coincides with the corresponding expression of the usual theory.

We must note that this result is obtained when we satisfy the boundary condition (13). This boundary condition for the function Ψ differs, generally speaking, from the usual boundary condition[3,5,6] imposed upon the

function ψ. One can show, however, that if condition (13) is imposed upon the function $\psi(\mathbf{n}, z)$, the result just obtained is not changed.

The anomalous skin effect is an important means of studying the form of the Fermi surface. In that respect one can summarize the situation and say that if we consider instead of an electron gas a degenerate electron fluid, no complications arise in the analysis of the Fermi surface. Such an analysis can also be conducted using the methods of Kaganov and Azbel'.

5. We consider now some problems connected with the application of the above theory to an analysis of experimental results in the case where we can use an isotropic model of the metal to discuss the experiments (see, for instance, Ref. 7). The expression for the surface impedance in the case of a sharply expressed anomalous skin effect ($l_{\text{eff}} \to \infty$) is of the form[3]

$$Z_\infty = (\sqrt{3}\pi\omega^2 l/c^4\sigma_0)(1 + \sqrt{3}i), \tag{17}$$

where l is the mean free path of the electrons and where

$$\sigma_0/l = {}^2/_3\, 4\pi e^2 p_0^2 (2\pi\hbar)^{-3}. \tag{18}$$

Using the isotropic model, we can try to determine from the experimental data the quantity

$$A = p_0^2 \int d\Omega \cos\chi F(\cos\chi), \tag{19}$$

by which (9) to (11) differ from the corresponding formulae of the usual theory. We should also use experimental data on the electronic heat capacity, on the dielectric constant (in the region of infrared radiation), and on σ_0/l as determined from the anomalous skin effect. The measurement of the electronic heat capacity ($c_e = \gamma T$) gives us the quantity[4]

$$\gamma = \frac{2\pi^2 k^2}{3(2\pi\hbar)^3} \int \frac{dS}{v(n)} = \frac{2\pi^2}{3} k^2 \frac{4\pi p_0^2}{(2\pi\hbar)^3 v_0}, \tag{20}$$

where k is Boltzmann's constant. The determination of the dielectric constant in the infrared region of the spectrum, at frequencies much larger than the collision frequencies of the electrons but much smaller than the frequencies of the natural absorption, enables us to find the quantity N determined by equation (11).

The state of the electrons in the isotropic model of a metal is characterized by three parameters, a natural choice for which is the velocity v_0 of the electrons at the Fermi surface, their momentum p_0, and the quantity A [see Eq. (19)]. These quantities can all be determined with the above mentioned measurements, according to the following equations,

$$v_0 = \frac{\pi^2 k^3 (\sigma_0/l)}{e^2\gamma}; \quad p_0^2 = \frac{3(2\pi\hbar)^3 \sigma_0}{8\pi e^2 l}; \quad 1 + A = \frac{e^4}{\pi^2\hbar^3 m} \frac{\gamma N}{(\sigma_0/l)}. \tag{21}$$

In the table we give the values of N, γ and σ_0/l for several metals[7,8,9] and the value of the parameter A determined from Eq. (21); this parameter characterizes the difference between a Fermi fluid and a gas. As can be seen from the table, this parameter is not small compared to unity. If we consider the use of an isotropic model for a metal as legitimate, this fact can be considered to indicate that the conduction electrons are considerably different from a gas. We note that among the different equations given in Ref. 7 for the velocity v_0 of the electrons at the Fermi surface, assuming the metal to be isotropic, the correct value under those assumptions agrees with our determination according to Eq. (21). The corresponding value of v_0 is given in the table.

	$\gamma\cdot10^{-3}$ (erg-cm^{-3}-deg.$^{-2}$)	$N\cdot10^{-22}$	$(\sigma_0/l)\ 10^{-22}$ (Ref. 8)	A according to (21)	$v_0\cdot10^{-8}$ from (21)
Cu	1.02	3.3	13.9±0.4	−0.46	1.11
Ag	0.65	5.2	7.8±0.4	+0.9	1.04
Au	~0.65	5.1	7.6±0.4	+0.8	~1.0
Sn	1.03	<3.5	8.6±0.7	<+0.5	0.68
Al	1.46	5.4	18.4±1.4	+0.28	0.31

6. In this way we can estimate effects caused by the difference between an electron fluid and a gas, if we assume that the isotropic model of a metal is justified. In those cases, however, where the Fermi surface differs appreciably from a sphere, it is considerably more complicated to obtain a similar estimate. At any rate, we can say that, in order to determine the role of the correlation between particles, it is necessary to study the dielectric permeability tensor in the infrared range of the spectrum,

$$\varepsilon_{\alpha\beta} = \varepsilon_{\alpha\beta}^{(0)} - \frac{1}{\omega^2} \frac{8\pi e^2}{(2\pi\hbar)^3} \int dS v(\mathbf{n}) \left\{ n_\alpha n_\beta + \int dS' F(\mathbf{n}, \mathbf{n}') n'_\alpha n_\beta \right\}. \tag{22}$$

One can now hope that one can also elucidate the role of the function $F(\mathbf{n}, \mathbf{n}')$ in the case of an anisotropic metal, by using also data on the electronic heat capacity and on the form of the Fermi surface, obtained in particular from the anomalous skin effect.

The role of the correlation between particles can also be elucidated by studying phenomena in a magnetic field. The transport equation is in that case

$$\frac{\partial}{\partial t}\psi + \left\{\mathbf{v}\frac{\partial}{\partial \mathbf{r}} + \frac{e}{c}[\mathbf{v}\times\mathbf{H}]\frac{\partial}{\partial \mathbf{p}}\right\}\left\{\psi + \int dS' F(\mathbf{n}, \mathbf{n}')\psi(\mathbf{n}', \mathbf{r}')\right\} + e\mathbf{v}\mathbf{E} = I(\psi). \tag{23}$$

This equation is practically the quasi-classical Schrödinger equation for the electron state, which differs only slightly from its equilibrium state. In particular, we can thus determine the quasi-classical spectrum of the electronic energy levels in a magnetic field from the equation

$$i\omega\psi + \frac{e}{c}[\mathbf{v}\times\mathbf{H}]\frac{\partial}{\partial \mathbf{p}}\left\{\psi + \int dS' F(\mathbf{n}, \mathbf{n}')\psi(\mathbf{n}')\right\} = 0. \tag{24}$$

The presence of the function F in Eq. (24) considerably affects the determination of the eigenfrequencies of the electrons. In the case of the isotropic model the solution of Eq. (24) can easily be found by expanding $e^{ik\varphi}P_n^k(\cos\theta)$ in spherical harmonics. The eigenfrequencies are then $\omega_n^k = k(eHv_0/cp_0)\{1 + 4\pi A_n/(2n+1)\}$, where A_n is the expansion coefficient of the function $F(\cos\chi)$ in Legendre polynomials. The fact that the spectrum of the electronic energy levels in a magnetic field depends strongly on the function F enables us to state that, for instance, the de Haas-Van Alphen effect can be used to determine the shape of this function. On the other hand, the determination of the Fermi surface is apparently very difficult. This is also true for the case of diamagnetic resonance (bismuth). The change in the eigenfrequencies of the electrons in a constant magnetic field, caused by the correlation between particles, can also influence considerably the interpretation of resonance frequencies in the case of cyclotron resonance, which is observed in the region of the anomalous skin effect. We note finally that in the case of galvanomagnetic phenomena the difference between Eq. (23) and the usual one consists in fact only in a redefinition of the collision integral. The results of the usual theory of galvanomagnetic and magnetothermal phenomena remain thus practically the same.

In conclusion I wish to express my deep gratitude to V. L. Ginzburg for his interest in this paper and for discussing its results, and also to L. D. Landau for useful suggestions.

[1] V. P. Silin, J. Exptl. Theoret. Phys. (U.S.S.R.) 33, 495 (1957), Soviet Phys. JETP 6, 387 (1958).
[2] A. B. Pippard, Physica 15, 45 (1949).
[3] G. E. H. Reuter and E. H. Sondheimer, Proc. Roy. Soc. A195, 336 (1948).
[4] L. D. Landau, J. Exptl. Theoret. Phys. (U.S.S.R.) 30, 1058 (1956), Soviet Phys. JETP 3, 920 (1956).
[5] K. Fuchs, Proc. Camb. Phil. Soc. 34, 100 (1938).
[6] M. I. Kaganov and M. Ia. Azbel', Dokl. Akad. Nauk SSSR 102, 49 (1956).
[7] V. L. Ginzburg and G. P. Motulevich, Usp. Fiz. Nauk 55, 469 (1955), Fortschr. d. Phys. 3, 309 (1955).
[8] R. G. Chambers, Proc. Roy. Soc. A215, 481 (1952).
[9] G. P. Motulevich and A. A. Shubin, Оптика и спектроскопия (Optics and Spectroscopy), 2, 633 (1957).

Translated by D. Ter Haar
260

AGING EQUATION FOR GAMMA QUANTA

B. V. NOVOZHILOV

Institute of Chemical Physics, Academy of Sciences, U.S.S.R.

Submitted to JETP editor June 6, 1957

J. Expti. Theoret. Phys. (U.S.S.R.) 33, 1287-1289 (November, 1957)

An equation is derived for the distribution function of multiply-scattered low energy γ-quanta ($E \ll m_0c^2$), analogous to the aging equation for neutrons. The spatial and wavelength distributions obtained for the quanta are in satisfactory agreement with the numerical solutions of the Boltzmann equation.

In the neutron attenuation theory one frequently employs the so-called aging equation,[1] derived on the assumption that all neutrons of specified initial energy behave identically in the sense of energy loss. This is true when the energy lost by a neutron in one collision is considerably smaller than its initial energy, i.e., when the neutrons are moderated in a medium whose nuclei have a mass much greater than the neutron mass.

An approximation analogous to the aging approximation for neutrons can be devised also for γ quanta moving in a scattering and absorbing medium. In this case the criterion of applicability of the aging equation will be the inequality $E \ll m_0c^2$, where E is the energy of the γ quanta and m_0c^2 is the rest energy of the electron. Actually, the change in the wavelength $\lambda = m_0c^2/E$ of a quantum, in the case of Compton scattering by an angle θ, is

$$\lambda' - \lambda = 1 - \cos\theta, \tag{1}$$

where λ and λ' are the wavelengths before and after scattering. In order for the inequality $\Delta\lambda \ll \lambda$ to be satisfied, as required for the derivation of an aging equation, we must have $\lambda \gg 1$, i.e., $E \ll m_0c^2$. If we denote by $\xi(\lambda)$ the average wavelength change $\overline{\lambda' - \lambda}$ resulting from a single Compton scattering event, we can write

$$\xi(\lambda) = 1 - \overline{\cos\theta}, \tag{2}$$

where the average cosine of the scattering angle is

$$\overline{\cos\theta} = \frac{\pi r_0^2}{\sigma(\lambda)}\lambda\left[6\lambda^2 + 6\lambda - 2 + \frac{2}{(\lambda+2)^3} + (1 - \lambda - 6\lambda^2 - 3\lambda^3)\ln\frac{\lambda+2}{\lambda}\right], \tag{3}$$

[$\sigma(\lambda)$ is the Compton cross section, and r_0 is the classical radius of the electron]. We list below several values of $\xi(\lambda)$.

λ	$\xi(\lambda)$	λ	$\xi(\lambda)$
1	0.708	12	0.940
2	0.786	15	0.947
4	0.859	17	0.950
6	0.904	20	0.955
8	0.924	∞	1.000
10	0.935		

In the derivation of the aging equation we assume that the source emits quanta of wavelength λ_0, and that the angular distribution of the quanta is spherically symmetrical (for the energies considered here, this is true already after a few collisions). Assuming that the wavelength of the quantum changes continuously, and not jumpwise, we can write

$$d\lambda = \mu(\lambda)\xi(\lambda)cdt, \tag{4}$$

where $d\lambda$ is the change in the wavelength of the quantum during the time dt, and $\mu(\lambda)$ is the linear coefficient of absorption for the Compton process. An exact connection is thus established between the wavelength of the γ quantum and the time elapsed from the instant of its emission.

Let $n(\mathbf{r}, t)\,dt$ be the density at the point $\mathbf{r}$, of the quanta whose diffusion time ranges from t to $t+dt$. For the distribution function $n(\mathbf{r}, t)$ one can write a balance equation

$$\frac{\partial n(\mathbf{r}, t)}{\partial t} = -\operatorname{div}\mathbf{j}(\mathbf{r}, t) - \mu_{ph}(t)\,n(\mathbf{r}, t)\,c. \tag{5}$$

The first term in the right half, which takes into account the escape of the quanta, will be replaced by $D\nabla^2 n(\mathbf{r}, t)$, where the diffusion coefficient is

$$D = c/3\ \mu(1 - \overline{\cos\theta}). \tag{6}$$

The second term describes the absorption of the quanta as a result of the photoeffect; $\mu_{ph}(t)$ is the linear absorption coefficient for the photoeffect, taken at a wavelength corresponding to the diffusion time t. Changing from the temporal distribution function $n(\mathbf{r}, t)$ with respect to time to the wavelength distribution function $n(\mathbf{r}, \lambda)$ through the use of the relation $n(\mathbf{r}, t) = n(\mathbf{r}, \lambda)\,d\lambda/dt$, and replacing the differentiation with respect to time by differentiation with respect to λ, we get

$$c\mu(\lambda)\xi(\lambda)\frac{\partial[cn(\mathbf{r}, \lambda)\mu(\lambda)\xi(\lambda)}{\partial\lambda} = D\nabla^2[n(\mathbf{r}, \lambda)\mu(\lambda)\xi(\lambda)c] - \mu_{ph}(\lambda)\mu(\lambda)c\xi(\lambda)n(\mathbf{r}, \lambda). \tag{7}$$

Introducing the symbols

$$q(\mathbf{r}, \lambda) = n(\mathbf{r}, \lambda)\mu(\lambda)\xi(\lambda)c, \quad \tau = \frac{1}{3}\int_{\lambda_0}^{\lambda} d\lambda\,[\mu(\lambda)\xi(\lambda)]^{-2}, \quad \varkappa = 3\mu_{ph}(\lambda)\mu(\lambda)\xi(\lambda) \tag{8}$$

the aging equation can be written as

$$\partial q(\mathbf{r}, \tau)/\partial\tau = \nabla^2 q(\mathbf{r}, \tau) - \varkappa(\tau)\,q(\mathbf{r}, \tau). \tag{9}$$

In analogy with neutron attenuation, τ can be called the age of the γ quantum, and $q(\mathbf{r}, \tau)$, the attenuation density.

Let us consider a point source in an infinite medium. If the source is placed at the origin and emits S quanta per unit time, Eq. (9) is augmented by the initial condition

$$q(\mathbf{r}, 0) = S\delta(\mathbf{r}), \tag{10}$$

and the solution of the equation becomes

$$q(\mathbf{r}, \tau) = S(4\pi\tau)^{-3/2}\exp\left[-\frac{r^2}{4\tau} - \int_0^{\tau}\varkappa d\tau\right]. \tag{11}$$

Let us note that

$$\int_0^{\tau}\varkappa d\tau = \int_{\lambda_0}^{\lambda} d\lambda\,\mu_{ph}(\lambda)/\mu(\lambda)\xi(\lambda).$$

The literature contains no experimental data on the gamma spectrum with which to compare the distribution (11). There is merely a mention[2] of an investigation of the spectrum of γ-quanta from Hg^{203} ($E_0 = 0.275$ Mev) in water.

However, the distribution (11) can be compared with the results of a numerical solution of the kinetic equation for the distribution function of the quanta.[3] The results of these comparisons are shown in the figure. The ordinates represent the energy I transported by the quanta in all directions per unit time, across a unit area, within a unit energy interval. The source energy is $E_0 = 0.25$ Mev ($\lambda = 2$). The quanta propagate in water, and their distance from the source is four mean free paths of quanta of energy E_0. The solid curve is obtained from Eq. (11), while the crosses indicate the results of Goldstein and Wilkins.[3] The discrepancy at small wavelengths is attributed to the fact that the aging equation is not valid at energies close to the source energy. The discrepancy over the remaining interval is due first to errors in Ref. 3, which are estimated by the authors to be 10 — 15%, and second to the rather high initial energy of the quanta ($\lambda_0 = 2$, while the condition for the validity of the approximation is $\lambda \gg 1$).

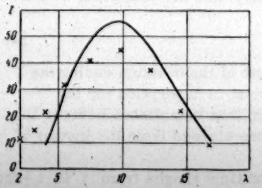

Translated by J. G. Adashko
261

[1] A. I. Akhiezer and I. Ia. Pomeranchuk. Некоторые вопросы теории ядра (Certain Problems in the Theory of the Nucleus) GTTL, 1950.

[2] M. M. Weiss and W. Bernstein. Phys. Rev. 92, 1264 (1954).

[3] H. Goldstein and J. Wilkins, Calculations of the Penetration of γ Rays. Final report, NYO-3075. 1954.

SATURATION EFFECT IN A SYSTEM WITH THREE ENERGY LEVELS

V. M. FAIN

Gor'kiy Radiophysics Research Institute

Submitted to JETP editor June 10, 1957

J. Exptl. Theoret. Phys. (U.S.S.R.) 33, 1290-1294 (November, 1957)

The response of a system with three levels (E_1, E_2, and E_3) to an alternating field with harmonics $\omega_{31} = (E_3 - E_1)/\hbar$, $\omega_{21} = (E_2 - E_1)/\hbar$, and $\omega_{32} = (E_3 - E_2)/\hbar$ is examined. An expression which can be used in the theory of quantum oscillators or amplifiers, is derived for the dielectric constant (or magnetic permeability).

MUCH attention has lately been paid in radio spectroscopy to various kinds of quantum-mechanical amplifiers and oscillators (see, for example, Refs. 1—10). One proposed system employs three paramagnetic-resonance energy levels.[1] It is therefore interesting to consider the effect of an alternating high-frequency field on a system with three energy levels.

Let the system considered have levels E_1, E_2, and E_3 and let $E_1 < E_2 < E_3$. Furthermore, let the system be under the influence of high-frequency field F, whose spectral expansion includes harmonics with the following frequencies:

$$\omega_{21} = (E_2 - E_1)/\hbar;\ \omega_{31} = (E_3 - E_1)/\hbar;\ \omega_{32} = (E_3 - E_2)/\hbar.$$

It is the aim of this work to investigate the behavior of the system in the presence of such a field.

The system can be described with the aid of an density matrix ρ. The latter obeys the equation

$$\frac{\partial \rho}{\partial t} = -\frac{i}{\hbar}(H\rho - \rho H) + \frac{\delta \rho}{\delta t}, \tag{1}$$

where H is the Hamiltonian of the system in an external field, $\delta\rho/\delta t$ is the change in the density matrix resulting from various kinds of relaxation processes. If the relaxation is due to collisions in a gas, it is possible to show (see, for example, Ref. 11), that

$$\delta\rho/\delta t = -\tau^{-1}(\rho - \rho_0), \tag{2}$$

where τ is the relaxation time and ρ_0 is the density matrix in the equilibrium state. Obviously, a similar equation describes the transition to the equilibrium state in paramagnetic systems (see, for example, Ref. 12). Thus, collecting (1) and (2), we get

$$\partial\rho/\partial t = -(i/\hbar)(H\rho - \rho H) - \tau^{-1}(\rho - \rho_0). \tag{3}$$

This equation can be readily generalized by considering that in radio spectroscopy, generally speaking, two relaxation times τ_1 and τ_2 are used. Here τ_1 corresponds to the relaxation of the system level population, and τ_2 is the relaxation of the average dipole moment of the system, i.e., on the average, within a time τ_1 the diagonal elements of ρ go into ρ_0 in the absence of a field, and within a time τ_2 the average dipole moment of the system becomes equal to zero (i.e., the non-diagonal elements of ρ vanish). Our generalization will then be that the quantity $\tau^{-1}(\rho - \rho_0)$ of Eq. (3) is a matrix of the form

$$[\tau^{-1}(\rho - \rho_0)]_{mn} = \begin{cases} \tau_1^{-1}(\rho - \rho_0)_{mn} & \text{for } m = n \\ \tau_2^{-1}(\rho - \rho_0)_{mn} & \text{for } m \neq n. \end{cases} \tag{4}$$

In the presence of an alternating electrical or magnetic field, the Hamiltonian of our system is

$$H = H_0 - \mu F(t), \tag{5}$$

where μ is the electric or magnetic dipole moment (and accordingly F is either an electric or a magnetic field). In a representation in which the operator H_0 is diagonal and has eigenvalues E_1, E_2 and E_3, Eq. (3) becomes

$$\frac{\partial \rho_{mn}}{\partial t} + i\omega_{mn}\rho_{mn} = \frac{i}{\hbar} F \sum_{l=1}^{3} (\mu_{ml}\rho_{ln} - \rho_{ml}\mu_{ln}) - [\tau^{-1}(\rho - \rho_0)]_{mn}, \tag{6}$$

where m, n, = 1, 2, 3; $\omega_{mn} = (E_m - E_n)/\hbar$.

We shall seek a solution of these equations for

$$F = F_{31}\cos\Omega_{31}t + F_{32}\cos\Omega_{32}t + F_{21}\cos\Omega_{21}t, \tag{7}$$

where

$$\Omega_{31} \approx \omega_{31};\ \Omega_{32} \approx \omega_{32};\ \Omega_{21} \approx \omega_{21}. \tag{8}$$

Using condition (8) and introducing

$$D_{mn} = \rho_{mm} - \rho_{nn},\quad D_{0mn} = \rho_{0mm} - \rho_{0nn}, \tag{9}$$

we obtain the approximate equations

$$\frac{\partial \rho_{mn}}{\partial t} + i\omega_{mn}\rho_{mn} + \tau_2^{-1}(\rho_{mn} - \rho_{0mn}) = \frac{i}{\hbar}\mu_{mn}FD_{nm}, \tag{10}$$

$$\frac{\partial D_{12}}{\partial t} + \tau_1^{-1}(D_{12} - D_{012}) = \frac{i}{\hbar} F\,[2(\mu_{12}\rho_{21} - \rho_{12}\mu_{21}) + (\mu_{13}\rho_{31} - \rho_{13}\mu_{31}) - (\mu_{23}\rho_{32} - \rho_{23}\mu_{32})]; \tag{11}$$

$$\frac{\partial D_{13}}{\partial t} + \tau_1^{-1}(D_{13} - D_{013}) = \frac{i}{\hbar} F\,[2(\mu_{13}\rho_{31} - \rho_{13}\mu_{31}) + (\mu_{12}\rho_{21} - \rho_{12}\mu_{21}) - (\mu_{32}\rho_{23} - \rho_{32}\mu_{23})]; \tag{12}$$

$$\frac{\partial D_{23}}{\partial t} + \tau_1^{-1}(D_{23} - D_{023}) = \frac{i}{\hbar} F\,[2(\mu_{23}\rho_{32} - \rho_{23}\mu_{32}) + (\mu_{21}\rho_{12} - \rho_{21}\mu_{12}) - (\mu_{31}\rho_{13} - \rho_{31}\mu_{13})]. \tag{13}$$

We shall seek solutions of (10) — (13) in the form*

$$\rho_{mn} = \rho_{mn}^{(+)}\exp\{i\Omega_{mn}t\} + \rho_{mn}^{(-)}\exp\{-i\Omega_{mn}t\}\ (\Omega_{mn} \equiv \Omega_{nm}),\ m \neq n, \tag{14}$$

$$D_{mn} = \text{const}. \tag{15}$$

We neglect here the higher harmonics and non-resonant terms, which is fully justified if condition (8) is taken into account.

Since the equilibrium matrix ρ_0 is diagonal, we obtain from Eq. (10)

$$\rho_{mn}^{(\pm)} = (i/2\hbar)\,F_{mn}\mu_{mn}D_{mn}/[i(\omega_{mn} \pm \Omega_{mn}) + \tau_2^{-1}]; \tag{16}$$

Here $F_{mn} = F_{nm}$. From (11) — (13) and (16), using again condition (8), we get

$$\begin{aligned} &D_{12}(1 + 2\gamma_{12}) - D_{23}\gamma_{23} + D_{13}\gamma_{13} = D_{012};\\ &-D_{12}\gamma_{12} + D_{23}(1 + 2\gamma_{23}) + D_{13}\gamma_{13} = D_{023};\\ &D_{12}\gamma_{12} + D_{23}\gamma_{23} + D_{13}(1 + 2\gamma_{13}) = D_{013}, \end{aligned} \tag{17}$$

where

$$\gamma_{mn} = F_{mn}^2 |\mu_{mn}|^2 \tau_1\tau_2^{-2}/2\hbar^4\,[(\omega_{mn} - \Omega_{mn})^2 + \tau_2^{-2}]. \tag{18}$$

From Eqs. (16), (17), and (18) we get

$$D_{12} = \frac{1}{\Delta}\,[D_{012}(1 + 2\gamma_{23} + 2\gamma_{13} + 3\gamma_{23}\gamma_{13}) - D_{013}\gamma_{13}(1 + 3\gamma_{23}) + D_{023}\gamma_{23}(1 + 3\gamma_{13})], \tag{19}$$

$$D_{23} = \frac{1}{\Delta}\,[D_{023}(1 + 2\gamma_{12} + 2\gamma_{13} + 3\gamma_{13}\gamma_{12}) - D_{013}\gamma_{13}(1 + 3\gamma_{12}) + D_{012}\gamma_{12}(1 + 3\gamma_{13})], \tag{20}$$

$$D_{13} = \frac{1}{\Delta}\,[D_{013}(1 + 2\gamma_{12} + 2\gamma_{23} + 3\gamma_{12}\gamma_{23}) - D_{023}\gamma_{23}(1 + 3\gamma_{12}) - D_{012}\gamma_{12}(1 + 3\gamma_{23})], \tag{21}$$

$$\rho_{32}^{(-)} = \frac{F_{23}\mu_{32}}{2\hbar}\,\frac{\left[D_{023} - \dfrac{D_{013}\gamma_{13}(1 + 3\gamma_{13}) + D_{012}\gamma_{12}(1 + 3\gamma_{13})}{1 + 2\gamma_{12} + 2\gamma_{13} + 3\gamma_{13}\gamma_{12}}\right]\left(\omega_{32} - \Omega_{32} + \dfrac{i}{\tau_2}\right)}{(\omega_{32} - \Omega_{32})^2 + \tau_2^{-2} + \dfrac{F_{23}^2|\mu_{32}|^2\tau_1\tau_2^{-1}}{2\hbar^2}\left(\dfrac{2 + 3\gamma_{12} + 3\gamma_{13}}{1 + 2\gamma_{12} + 2\gamma_{13} + 3\gamma_{13}\gamma_{12}}\right)}, \tag{22}$$

*The transient process will not be considered.

$$\rho_{21}^{(-)}=\frac{F_{12}\mu_{21}}{2\hbar}\frac{\left[D_{013}-\frac{D_{023}\gamma_{23}(1+3\gamma_{13})+D_{013}\gamma_{12}(1+3\gamma_{23})}{1+2\gamma_{12}+2\gamma_{23}+3\gamma_{12}\gamma_{23}}\right]\left(\omega_{21}-\Omega_{21}+\frac{i}{\tau_2}\right)}{(\omega_{21}-\Omega_{21})^2+\tau_2^{-2}+\frac{F_{13}^2|\mu_{13}|^2\tau_1\tau_2^{-1}}{2\hbar^2}\left(\frac{2+3\gamma_{12}+3\gamma_{23}}{1+2\gamma_{12}+2\gamma_{23}+3\gamma_{12}\gamma_{23}}\right)}. \tag{23}$$

$$\rho_{21}^{(-)}=\frac{F_{12}\mu_{21}}{2\hbar}\frac{\left[D_{012}-\frac{D_{013}\gamma_{13}(1+3\gamma_{23})+D_{023}\gamma_{23}(1+3\gamma_{13})}{1+2\gamma_{13}+2\gamma_{23}+3\gamma_{13}\gamma_{23}}\right]\left(\omega_{21}-\Omega_{21}+\frac{i}{\tau_2}\right)}{(\omega_{21}-\Omega_{21})^2+\tau_2^{-2}+\frac{F_{21}^2|\mu_{21}|^2\tau_1\tau_2^{-1}}{2\hbar^2}\left(\frac{2+3\gamma_{13}+3\gamma_{23}}{1+2\gamma_{13}+2\gamma_{23}+3\gamma_{13}\gamma_{23}}\right)}, \tag{24}$$

where

$$\Delta=1+2(\gamma_{12}+\gamma_{23}+\gamma_{13})+3(\gamma_{12}\gamma_{13}+\gamma_{13}\gamma_{13}+\gamma_{23}\gamma_{13}), \tag{25}$$

$$D_{mn}=-D_{nm},\ \rho_{mn}^{(+)}=(\rho_{nm}^{(-)})^*. \tag{26}$$

The last equality follows from the fact that the matrix ρ is Hermitian.

In addition to the quantities (22) – (24) and their complex conjugates, there is a whole series of quantities, such as $\rho_{13}^{(-)}$, $\rho_{12}^{(-)}$, etc., which can be neglected in this approximation.

With the solution obtained it is possible to find the average dipole moment of the system using

$$P=\mathrm{Sp}(\rho\mu)\equiv\sum_{m,\,n=1}^{3}\rho_{mn}\mu_{nm} \tag{27}$$

to calculate the dielectric constant (or magnetic permeability) at the frequencies Ω_{31}, Ω_{21}, and Ω_{32}, and to obtain the absorption coefficient at these frequencies.

Let us derive the corresponding formulas for resonance at the frequency Ω_{32}. Analogous formulas are obtained for other frequencies. The average dipole moment per unit volume* (polarization vector) at Ω_{32} has the form

$$P_{32}=\rho_{32}^{(-)}\mu_{23}\exp\{-i\Omega_{32}t\}+\rho_{23}^{(+)}\mu_{32}\exp\{i\Omega_{32}t\}=\mathrm{Re}\,(2\rho_{32}^{(-)}\mu_{23}\exp\{-i\Omega_{32}t\}) \tag{28}$$

(The remaining terms give a negligibly small contribution at the frequency Ω_{32}). On the other hand, the complex dielectric constant† is determined through the complex polarization coefficient κ:

$$\varepsilon=1+4\pi\varkappa, \tag{29}$$

where κ is determined from the relation

$$P_{32}=\mathrm{Re}\,(\varkappa F_{23}\exp\{-i\Omega_{32}t\}). \tag{30}$$

Using Eqs. (22) and (28) – (30) we get

$$\varepsilon=1+4\pi\cdot 2\rho_{32}^{(-)}\mu_{23}/F_{23}=1+4\pi\frac{|\mu_{23}|^2}{\hbar}\frac{\left[D_{023}-\frac{D_{013}\gamma_{13}(1+3\gamma_{13})-D_{012}\gamma_{12}(1+\gamma_{13})}{1+2\gamma_{12}+2\gamma_{13}+3\gamma_{13}\gamma_{12}}\right]\left(\omega_{32}-\Omega_{32}+\frac{i}{\tau_2}\right)}{(\omega_{32}-\Omega_{32})^2+\tau_2^{-2}+\frac{F_{23}^2|\mu_{32}|^2\tau_1\tau_2^{-1}}{2\hbar^2}\frac{2+3\gamma_{12}+3\gamma_{13}}{1+2\gamma_{12}+2\gamma_{13}+3\gamma_{13}\gamma_{12}}}. \tag{31}$$

The absorption coefficient α is determined from (see, for example, Ref. 11)

$$\alpha=(4\pi\Omega_{32}/c)\,\mathrm{Im}\,\varkappa=\frac{4\pi\Omega_{32}}{c}\frac{|\mu_{23}|^2}{\hbar}\frac{\left[D_{023}-\frac{D_{013}\gamma_{13}(1+3\gamma_{13})-D_{012}\gamma_{12}(1+\gamma_{13})}{1+2\gamma_{12}+2\gamma_{13}+3\gamma_{13}\gamma_{12}}\right]\tau_2^{-1}}{(\omega_{32}-\Omega_{32})^2+\tau_2^{-2}+\frac{F_{23}^2|\mu_{32}|^2\tau_1\tau_2^{-1}}{2\hbar^2}\frac{2+3\gamma_{12}+3\gamma_{13}}{1+2\gamma_{12}+2\gamma_{13}+3\gamma_{13}\gamma_{12}}}. \tag{32}$$

* We shall assume henceforth that the ρ's are normalized to unit volume.

†To be specific, we shall talk of a dielectric constant, even though all the formulas obtained are equally applicable to the magnetic permeability.

We see immediately from (32) that by proper choice of γ_{13} and γ_{12} (or one of these), i.e., by choice of the fields F_{13} and F_{12}, it is possible to obtain negative absorption at the frequency Ω_{32}. In this case this system can operate as an oscillator or amplifier. It is necessary for this purpose that the following condition be satisfied.

$$\left[D_{023}-\frac{D_{013}\gamma_{13}(1+3\gamma_{13})-D_{012}\gamma_{12}(1+\gamma_{13})}{1+2\gamma_{12}+2\gamma_{13}+3\gamma_{13}\gamma_{12}}\right]<0. \tag{33}$$

Let us consider the case when $\gamma_{12}=0$, i.e., the field $F_{12}=0$. Then Eqs. (31)—(33) become

$$\varepsilon=1+4\pi\frac{|\mu_{23}|^2}{\hbar}\frac{[D_{023}-D_{013}\gamma_{13}/(1+2\gamma_{13})](\omega_{32}-\Omega_{32}+i/\tau_2)}{(\omega_{32}-\Omega_{32})^2+\tau_2^{-2}+\frac{F_{23}^2|\mu_{32}|^2\tau_1\tau_2^{-1}}{2\hbar^2}\frac{2+3\gamma_{13}}{1+2\gamma_{13}}}, \tag{31a}$$

$$\alpha=\frac{4\pi\Omega_{32}}{c}\frac{|\mu_{23}|^2}{\hbar}\frac{[D_{023}-D_{013}\gamma_{13}/(1+2\gamma_{13})]\tau_2^{-1}}{(\omega_{32}-\Omega_{32})^2+\tau_2^{-2}+\frac{F_{23}^2|\mu_{32}|^2\tau_1\tau_2^{-1}}{2\hbar^2}\frac{2+3\gamma_{13}}{1+2\gamma_{13}}}, \tag{32a}$$

$$[D_{023}-D_{013}\gamma_{13}/(1+2\gamma_{13})]<0. \tag{33a}$$

The last inequality can be satisfied if

$$D_{023}-D_{013}/2<0. \tag{33b}$$

Let us note that (33a) changes into (33b) if

$$2\gamma_{13}\gg 1. \tag{34}$$

Taking it into account that $D_{023}=\rho_{022}-\rho_{033}$ and $D_{013}=\rho_{011}-\rho_{033}$, condition (33b) can be written

$$\rho_{022}<{}^1/_2(\rho_{011}+\rho_{033}). \tag{35}$$

It is now easy to understand the presence of negative absorption at a frequency Ω_{32}. In fact, let the equilibrium level populations ρ_{022}, ρ_{011}, and ρ_{033} satisfy the condition (35).*

A sufficiently strong field F_{13} can then saturate the populations of levels 1 and 3, i.e., in the presence of field F_{13} the populations of levels 1 and 3 become equal to $\sim(\frac{1}{2})(\rho_{011}+\rho_{033})$. But since condition (35) is satisfied, this means that at the upper level 3 the population is greater than at the lower level 2. In that case the field F_{23} induces emission at a frequency $\Omega_{32}\approx\omega_{32}$ instead of absorption. This is precisely negative absorption.

The square brackets in expressions (31), (32) and (31a), (32a) play the role of the differences in the populations of levels 2 and 3 in the presence of the field. These differences are negative under conditions (33) and (33a).

Let us note that with the aid of formula (31) it is possible to obtain directly the amplitude and frequency of the steady-state oscillations of the generator, as well as the gain of the amplifier. For this purpose it is necessary to substitute the real and imaginary parts of (31) into the corresponding formulas of the theory of the molecular generator and amplifier (see, for example, Ref. 1).

The author is indebted to Professor V. L. Ginzburg for reviewing the article in manuscript form and for comments.

[1] N. G. Basov and A. M. Prokhorov, J. Exptl. Theoret. Phys. (U.S.S.R.) 27, 431 (1954); 30, 560 (1956), Soviet Phys. JETP 3, 426 (1956).

[2] Gordon, Zeiger, and Townes, Phys. Rev. 95, 282 (1954); J. P. Gordon, Phys. Rev. 99, 1253 (1955).

[3] Shimoda, Wang, and Townes, Phys. Rev. 102, 1308 (1956).

[4] V. S. Troitskii, Радиотехника и электроника (Radio Engineering and Electronics) 2 (1956).

[5] V. M. Fain. J. Exptl. Theoret. Phys. (U.S.S.R.) 33, 945 (1957), Soviet Phys. JETP 6, 426 (1958).

[6] V. M. Fain, Usp. Fiz. Nauk (in press).

[7] N. Bloembergen, Phys. Rev. 104, 324 (1956).

[8] M. Strandberg, Proc. IRE 45, 92 (1957).

[9] Scovil, Feher, and Seidel, Phys, Rev. 105, 760 (1957).

[10] J. P. Wittke, Proc, IRE, 45, 291 (1957).

* If the inverse condition $\rho_{022}>(\frac{1}{2})(\rho_{011}+\rho_{033})$ is satisfied, negative absorption is possible at the frequency ω_{21}.

[11] R. Karplus and J. Schwinger, Phys. Rev. 73, 1020 (1948).
[12] A. Overhauser, Phys. Rev. 89, 689 (1953).

Translated by J. G. Adashko
262

SOVIET PHYSICS JETP VOLUME 6 (33), NUMBER 5 MAY, 1958

ON THE FLUCTUATIONS OF NUCLEAR MATTER

D. I. BLOKHINTSEV

Joint Institute for Nuclear Research

Submitted to JETP editor July 1, 1957

J. Exptl. Theoret. Phys. (U.S.S.R.) 33, 1295-1299 (November, 1957)

It is shown that the production of energetic nuclear fragments in collisions with fast nucleons can be interpreted in terms of collisions of the incoming nucleon with the density fluctuations of the nuclear matter.

1. INTRODUCTION

THE motion of nucleons in nuclei can result in short-lived tight nucleon clusters, in other words, in density fluctuations of nuclear matter. Since such clusters are relatively far removed from the other nucleons of the nucleus, they become atomic nuclei of lower mass in a state of fluctuating compression.

In their study of the scattering of 675-Mev protons by light nuclei, Meshcheriakov and coworkers[1,2] observed recently certain effects which confirm the existence of such fluctuations, at least for the simplest nucleon-pair fluctuations, which lead to the formation of a compressed deuteron.

We recall in this connection reports in earlier works[3,4] that high-energy nucleons can split nuclei into "supra-barrier" fragments, i.e., fragments with an energy much larger than their binding energy and the energy of the Coulomb barrier. However, there was a lack of quantitative experimental data on which to base the theoretical analysis.

Some authors related this curious process, without foundation, to hypothetical long-range nuclear forces. Others tried to connect it with nuclear many-body forces.

The experimental data on the emission of high-energy deuterons from light nuclei give support to the idea that "supra-barrier" fragments are produced also by direct collision of an incoming nucleon with a tight nucleon cluster that results from density fluctuations of the nuclear matter. We offer in the following a quantitative argument in favor of the production of fast deuterons and other "supra-barrier" fragments by such fluctuations.

Concerning the nuclear many-body forces, it should be noted that, according to existing estimates,[5] there is no reason to believe that they are considerably stronger than the two-body forces. At the instant of dense clustering both paired and collective interactions may take place. However, at present there exists no experimental information which would allow an explanation of this interaction, or in particular allow a determination of the relative contributions of the paired and the collective interactions.

2. INTERACTION OF DEUTERONS WITH FAST PROTONS

It was shown experimentally[1,2] that scattering of 675-Mev protons by deuterium produces, in addition to scattered nucleons, a small number of undestroyed deuterons of high energy (up to 660 Mev). This shows that in such collisions the nucleon imparts an appreciable fraction of its momentum to the deuteron as a whole.

According to the fluctuation representation, this collision takes place at a time when the nucleons of the deuteron are at a close distance R and are strongly interacting. Under these conditions the incoming nucleon can transfer its momentum to the tight nucleon pair as a whole. The cross section to be expected for such a special collision will be

$$\sigma = \sigma_d W_d(R), \tag{1}$$

where σ_d is the total cross section for quasi-elastic collisions and $W_d(R)$ is the probability of finding the two nucleons of the deuteron at a distance less than R. The distance R has to be of the order of the range of the strong nuclear interaction, i.e., $(2-3)\hbar/Mc$. Denoting the wave function of the deuteron by $\psi_d(R)$, we have

$$W_d(R) = 4\pi \int_0^R \psi_d^2(r)\, r^2\, dr = \frac{4\pi}{3}\psi^2(0)\, R^3. \tag{2}$$

In order to calculate $W_d(R)$ one has to know the deuteron wave function close to $r = 0$. The usual asymptotic wave function $\psi_d = \sqrt{\alpha/2\pi}e^{-\alpha r}/r$ ($1/\alpha = 4.3 \times 10^{-13}$ cm) is completely useless for this purpose, since it approaches infinity for $r = 0$. The deuteron wave function has no singularities. Therefore we can approximate $u = r\psi_d$ by $\sqrt{\alpha/\pi}\, e^{-\alpha r}$ for large r and by $u = \psi(0)[r - \beta r^2 + \ldots]$ for small r and match the functions and derivatives at $r = b = 1/2\beta$. The quantity 2β is the logarithmic derivative $(\psi'/\psi)_0$. This yields $\psi(0) \sim \beta\sqrt{\alpha/2\pi}$.

Using Hulten's function

$$r\psi_d = \sqrt{\alpha/2\pi}\,(e^{-\alpha r} - e^{-\beta r})$$

We obtain the same result. According to known data β is a few times larger than α. Restricting ourselves to an order-of-magnitude estimate, we have

$$\psi_d(0) = \beta\sqrt{\alpha/2\pi}, \tag{3}$$

where the quantity β is to be considered as determining the logarithmic derivative of the deuteron wave function at $r = 0$.

From (2) and (3) we find

$$W_d(R) = \frac{2}{3}\alpha\beta^2 R^3. \tag{4}$$

Expressing R in units of $\hbar/Mc = 2 \times 10^{-14}$ cm this becomes

$$W_d(R) = 7 \cdot 10^{-5} R^3 (\beta/\alpha)^2. \tag{4'}$$

The experimental value for this quantity is 7×10^{-3}. Thus $R^3(\beta/\alpha)^2 \sim 10^2$, a fully reasonable value.

We note that neither the pick-up theory nor the impulse approximation are applicable in the present case. In both these theories it is assumed that the incoming nucleon interacts either with one nucleon or with two nucleons, but in an independent fashion. In the present case the momentum transfer is so large that the process is due to very high harmonics of the deuteron wave function, i.e., to such states in which both nucleons are very close together. One therefore cannot consider their collision with a third nucleon as an independent event.

For other light nuclei, an estimate of the function W(R) is still more difficult. For tritium, for example, we find that $W_T(R)$ is approximately on the order of $W_d^2(R)$, with a correction for the fact that the quantity α_T will be larger than α by a factor $\sqrt{m_T\epsilon_T/m_d\epsilon_d}$ (here ϵ_T and ϵ_d are the binding energies of tritium and deuterium respectively; m_T and m_d are reduced masses of tritium and deuterium, respectively, relative to one nucleon removed from the nucleus). This reduction of α_T reflects the fact that the tritium represents a tighter nucleon cluster than the deuteron.

For He, similarly, α_{He} will be larger than α by a factor $\sqrt{m_{He}\epsilon_{He}/m_d\epsilon_d}$.

Taking the above value for $W_d(R)$, we find $W_T \sim 2 \times 10^{-4}$ and $W_{He} \sim 2 \times 10^{-5}$.

These numerical values can be checked experimentally.

3. ESTIMATE OF THE FLUCTUATIONS IN NUCLEI

Let the wave function of a nucleus $A = Z + N$ be

$$\Psi_A = \Psi_A(x_1, x_2, \ldots, x_Z;\ y_1, y_2, \ldots, y_N), \tag{5}$$

where $x_1, x_2, \ldots$ are the coordinates of the protons, and $y_1, y_2, \ldots$ the coordinates of the neutrons. As is well known, the density operator, say of the protons, is given by

$$\rho(x) = \sum_{k=1}^{Z} \delta(x - x_k). \tag{6}$$

Similarly, one can introduce a second-order density operator

$$\rho(x, x') = \sum_{k \neq s}^{Z} \delta(x - x_k)\,\delta(x - x_s). \tag{6'}$$

In general the density operator of order a, involving z protons and n neutrons (a = n + z), will be

$$\rho(x, x', \ldots x^{(z)};\ y, y', \ldots y^{(n)}) = \sum_{k \neq s \neq \ldots} \delta(x - x_k)\,\delta(x' - x_s)\ldots,\ \delta(y^{(n)} - y_n). \tag{7}$$

The mean value of this density is

$$\overline{\rho(x, x', \ldots y^{(n)})} = \int \Psi_A^* \rho(x, x', \ldots y^{(n)})\,\Psi_A\, dx_1\, dx_2 \ldots dy_N. \tag{8}$$

In order to obtain the exact value of this integral, one needs to know the wave function Ψ_A. However, one can find an estimate of (8) by observing that the integral should be equal to

$$\overline{\rho(x, x', \ldots y^{(n)})} = MD(x, x' \ldots x^{(z)}, y, y', \ldots y^{(n)}), \tag{9}$$

where D is the probability density for the protons (z) and neutrons (n) to be at the positions (x, x', ... $y^{(n)}$), and M is equal to the number of permutations of the protons and the neutrons that would realize this configuration.

We are interested in the case where the relative coordinates of these nucleons, $\xi_1, \xi_2, \ldots \xi_{a-1}$, are within a small volume $\Omega < R^3$. Introducing further the center-of-mass coordinate of the cluster, X, and integrating with respect to $\xi_1, \xi_2 \ldots \xi_{a-1}$ over the volume Ω and with respect to X over the nuclear volume, we find

$$\overline{\rho_a(\Omega)} = MW_a(R), \tag{10}$$

where

$$W_a(R) = \int_{\Omega} D(\xi_1, \xi_2, \ldots \xi_{a-1}\ X)\, d\xi_1 \ldots d\xi_{a-1} dX \tag{11}$$

is the probability for such a cluster, compressed into the small volume Ω, to appear.

Since only small values of R are of interest, this probability is close to the probability of a similar density fluctuation of a free nucleus of atomic number a = n + z. This allows the determination of this probability from studies of collisions of a nucleon with a free nucleus (A).*

For light nuclei, M is the number of states by which one can construct the cluster of interest, i.e., it is roughly proportional to Z^z.

On the other hand, in nuclei where the density of nuclear matter is distributed like in a liquid drop, the number M will be proportional to the number of fragments with a = z + n contained in the nucleus; it thus is proportional to Z. In heavy nuclei one further has to account for the probability, P, that an energetic fragment will leave the nucleus from a certain depth.

Assuming that the energetic fragments appear uniformly with the volume of the nucleus, move in the direction of the momentum of the incoming fast nucleon, and have a mean free path

$$l = 1/n_0 \sigma_a, \tag{12}$$

(where n_0 is density of nucleons in the nucleus, and $\sigma_a \sim \pi r_0^2 a^{2/3}$ is the cross section of a fragment of

*Leksin and Kumekin[6] have made an attempt to determine this probability for carbon from (p, C) collisions. Within the accuracy of this experiment, they did not observe energetic protons scattered backwards from the carbon as a whole. From the estimates made above for T and He, one can conclude that the probability for an appropriate fluctuation in carbon is completely negligible.

atomic weight a) it is easy to show that the probability that the fragment will emerge from the nucleus is

$$P = \frac{3}{\eta}\left[\frac{1}{2} - \frac{1}{\eta^2} + \left(\frac{1}{\eta} + \frac{1}{\eta^2}\right)e^{-\eta}\right], \tag{13}$$

where $\eta = D/\ell$, and $D = 2r_0A^{1/3}$ is the diameter of the nucleus. In particular, if $P_A \ll 1$ then

$$P = (\pi r_0^2/\sigma_a)A^{-1/3} = \sigma_A/A\sigma_a, \quad \sigma_A = \pi r_0^2 A^{2/3}.$$

Combining all factors, we obtain for the production of a fast fragment of atomic number a from a nucleus of atomic number A the following cross section

$$\Sigma_a = PM\sigma_a W_a(R) \cong (\sigma_A/A)MW_a(R), \tag{14}$$

while the yield of fragments a per collision is given by

$$q_a = PM(\sigma_a/\sigma_A)W_d(R) = (M/A)W_a(R), \tag{15}$$

where σ_A is the total cross section of the target nucleus.

We now consider the special case of the deuteron (a = 2). For light nuclei the number M will be given by the number of ways in which a deuteron can be obtained from the nucleons of the nucleus. In the deuteron, the spins of the neutron and proton are parallel. Therefore $M_d = 2(ZN/4) = \frac{1}{2}ZN$. We thus have for deuterons produced from light nuclei

$$\Sigma_d' = \frac{1}{2}(ZN/A)\sigma_A W_d(R). \tag{16}$$

For heavy nuclei, owing to saturation of nuclear forces, we have $M_d = Zn$, where n is the number of neutron neighbors of a proton with antiparallel spin. This number is ~ 6. We therefore have for heavy nuclei

$$\Sigma_d'' = (Zn/A)\sigma_A W_d(R). \tag{16'}$$

The yield for this case is almost constant:

$$q_d'' = (Zn/A)W_d(R). \tag{15'}$$

Considering that $\sigma_d = 70 \times 10^{-27}$ cm^2 and $W_d(R) \sim 7 \times 10^{-3}$, we have from (16) the following values for Σ_d in millibarns:

Element	Li	Be	C	O
Σ_d	1.4	2.1	3.6	5.8.

As for heavy elements, we expect, according to (15), a deuteron yield $q_d'' \sim 2\%$.

The obtained results agree essentially with the experimental values.* A more conclusive check could be obtained from a study of deuteron yields from heavier nuclei.

We further note that the given estimate of density fluctuations of tritium, $W_T(R) \sim 2 \times 10^{-4}$, leads to an expected tritium yield of 2—3% of the deuteron yield. This is not in disagreement with Ref. 1.

Quantitative calculations for fragments heavier than deuterons lack a sufficient theoretical foundation. It would therefore be of great interest to determine experimentally the probability of large momentum transfers for such nuclei. It would then be possible to calculate the yield of such fragments from heavy nuclei.

In conclusion the author expresses his thanks to M. G. Meshcheriakov and G. A. Leksin for many valuable discussions.

[1] Azhgirei, Vzorov, Zrelov, Meshcheriakov, Neganov, and Shabudin, J. Exptl. Theoret. Phys. (U.S.S.R.) 33, 1185 (1957), Soviet Phys. JETP 6, (1958) (this issue).

[2] G..A. Leksin, J. Exptl. Theoret. Phys. (U.S.S.R) 32, 440 (1957), Soviet Phys. JETP 5, 371 (1957).

[3] D. H. Perkins, Proc. Roy. Soc. A203, 399 (1950).

*Comparing the present results with the data of Table 3, Ref. 1, one has to keep in mind that there the cross section is given for all deuterons while we give only the cross section for fast deuterons. According to estimates of Refs. 1, 2 these numbers should differ by a factor of 3. Therefore our table agrees satisfactorily with the data of Ref. 1.

[4] S. O. C. Sörensen, Phil. Mag. 42, 188 (1952).
[5] B. B. Kadomtsev, Thesis, Moscow State University (1952).
[6] G. A. Leksin and Iu. P. Kumekin, J. Exptl. Theoret. Phys. (U.S.S.R) 33, 1147 (1957), Soviet Phys. JETP 6, (1958) (this issue).

Translated by M. Danos
263

LETTERS TO THE EDITOR

MEASUREMENT OF POLARIZATION QUANTITIES

A. G. ZIMIN

Submitted to JETP editor June 27, 1957

J. Exptl. Theoret. Phys. (U.S.S.R.) **33**, 1300 (November, 1957)

To determine in practice the polarization $\langle \sigma_1 \rangle$ and the polarization correlation $\langle \sigma_{ik} \rangle$ in nucleon-nucleon scattering, one measures the integral intensities of the nucleons subjected to secondary scattering by analyzer nuclei. Let us consider how the polarization formulas vary for "point" intensities (see Refs. 1 and 2) when integrating over a solid angle.

The total scattering cross section of nucleons by analyzers with spin zero is

$$\sigma(\theta_1, \theta_2, \theta) = J_1(\theta_1) J_2(\theta_2) \{1 + \langle \sigma_{1i} \rangle n_{1i} P_1(\theta_1) + \langle \sigma_{2i} \rangle n_{2i} P_2(\theta_2) + \langle \sigma_{ik} \rangle n_{1i} n_{2k} P_1(\theta_1) P_2(\theta_2)\}, \quad (1)$$

where $\theta_1(\theta_1, \varphi_1)$ and $\theta_2(\theta_2, \varphi_2)$ are the angles of scattering by analyzers 1 and 2, $J_{1,2}$ and $P_{1,2}$ are the cross sections and the polarizations, respectively, while n_1 and n_2 are the vectors normal to the planes of these scatterings, along whose directions the integration is carried out.

Integration with respect to φ_1 and φ_2 in a cone 2φ gives, for example, for the normal correlation (relative to the nucleon-nucleon scattering plane)

$$\langle \sigma_{nn} \rangle = \frac{J_{++} + J_{--} - (J_{+-} + J_{-+})}{J_{++} + J_{--} + J_{+-} + J_{-+}} \frac{1}{P_1 P_2} \frac{\varphi^2}{\sin^2 \varphi}, \quad (2)$$

where, for example, $J_{++} \equiv \sigma(\varphi_1 = 0, \varphi_2 = 0)$ and $J_{+-} \equiv \sigma(\varphi_1 = 0, \varphi_2 = \pi)$ etc. Integration over the polar angles does not change the structure of formula (2), but the quantities J and P become integral (with respect to θ_1 and θ_2).

Compared with $\langle \sigma_{nn} \rangle$ for point intensities, formula (2) contains a factor $\alpha(\varphi) = \varphi^2/\sin^2\varphi$, which varies from 1 (at $\varphi = 0$, corresponding to "point" intensities) to ∞ (for $\varphi = \pi$, corresponding to integration over the total sphere). It is seen from formula (2) that increasing the count intensity (increasing the aperture of the 2φ counters) leads to a reduction in the asymmetry of the scattering

$$\varepsilon = \frac{J_{++} + J_{--} - (J_{+-} + J_{-+})}{J_{++} + J_{--} + J_{+-} + J_{-+}},$$

and consequently, to an increased error in $\langle \sigma_{nn} \rangle$. The optimum 2φ aperture can be determined from the minimum error. An estimate yields $\pi/2 \lesssim 2\varphi \leq 2$. The quantity $\alpha(\varphi)$ can be called the coefficient of "smearing" of the asymmetry of scattering. When measuring the polarization, this coefficient turns out to be $[\alpha(\varphi)]^{1/2}$. Corresponding formulas, analogous with (2), are obtained if only one analyzer is considered in (1), as proposed Ia. A. Smorodinskii.

[1] Ia. A. Smorodinskii and V. V. Vladimirskii, Dokl. Akad. Nauk SSSR **103**, 713 (1955).

[2] Ia. G. Zimin, J. Exptl. Theoret. Phys. (U.S.S.R.) **32**, 1239 (1957).

Translated by J. G. Adashko
264

RADIATION CORRECTIONS IN THE DISPERSION RELATIONS FOR $\pi^{\pm} + p \to \pi^{\pm} + p$

V. K. FEDIANIN

Moscow State University

Submitted to JETP editor July 3, 1957

J. Exptl. Theoret. Phys. (U.S.S.R.) 33, 1301-1303 (November, 1957)

PUPPI and Stanghellini[1] again investigated the problem of determining the value of f^2 from the dispersion relations. Analyzing separately $\pi^+ + p$ and $\pi^- + p$ charge states, they reach the conclusion that for energies below resonance* $f^2_{(+)} = 0.08$ and $f^2_{(-)} = 0.04$, and that for energies above resonance $f^2_{(+)} = f^2_{(-)} = 0.08$. Thus, they actually found that f^2 depends on the energy. Yet in earlier works[2] it was found that $f^2_{(+)} = f^2_{(-)} = 0.08$ for the entire energy range. Puppi and Stanghellini attribute this to the fact that the authors of Ref. 2 determine the values of f^2 by using the phases for $T = 3/2$, where $\pi^+ + p \to \pi^+ + p$ predominates.

One can assume that the difference is due to electromagnetic interaction. In a recent work[3] Agodi and Cini attempted to explain the difference in the presence of the $\pi^{\pm}$ and π^0 masses in the interaction Hamiltonian. This gave a difference on the order of 1% between $f^2_{(+)}$ and $f^2_{(-)}$.

This work is an attempt to determine the difference between $f^2_{(+)}$ and $f^2_{(-)}$ by successively including in the total system of functions also the intermediate states in which both the nucleon and the photon exist.

Using the notation of Ref. 4 for the antihermitian portion of the scattering amplitude, we have

$$A_{\alpha\omega}\left(\frac{q+q'}{2}\right) = \frac{1}{2i}\int \exp\left(i\,\frac{q+q'}{2}\,x\right)\left(F^{(-)}_{\alpha\omega}(x) - \hat{P}_{\rho\rho'}F^{(-)}_{\alpha\omega}(-x)\right)dx, \tag{1}$$

where $F^{(-)}_{\alpha\omega}(x)$ is determined by the following relation:

$$\langle p', s'|\,\hat{j}_{\rho'}(x)\,\hat{j}_{\rho}(y)\,|p,s\rangle = -i\,\exp\left\{i\,\frac{p-p'}{2}\,(x+y)\right\}F^{(-)}_{\alpha\omega}(x-y), \tag{2}$$

and $\hat{j}_{\rho}(x)$ is the meson-current operator. Inserting (2) into (1) and using the expansion theorem, we get

$$A_{\alpha\omega}(E) = A^{-}_{\alpha\omega}(E) + A^{+}_{\alpha\omega}(E), \tag{3}$$

with $A^{-}_{\alpha\omega}(E) = -\hat{P}_{\rho\rho'}A^{+}_{\alpha\omega}(-E)$, and

$$A^{+}_{\alpha\omega}(E) = -\frac{(2\pi)^4}{2}\sum_{s'',\,\nu}\int d\mathbf{k}\,\langle p', s'|\,j_{\rho}(0)\,|\mathbf{p}'', s'', \mathbf{k}, l_{\nu}\rangle\langle \mathbf{p}'', s'', \mathbf{k}, l_{\nu}|\,j_{\rho'}(0)\,|p,s\rangle\delta(E+k_0+p''_0-E_{\mathbf{p}}). \tag{4}$$

All the calculations are carried out in the system $\mathbf{p} + \mathbf{p}' = 0$, $E_{\mathbf{p}} = \sqrt{M^2 + \mathbf{p}^2}$, $k_0 = |\mathbf{k}|$, $p''_0 = \sqrt{M^2 + (-\lambda e - \mathbf{k})^2}$, $\mathbf{p}'' = -\lambda e - \mathbf{k}$, $\lambda e = (\mathbf{q} + \mathbf{q}')/2$, E is the meson energy, and l_{ν} and $\mathbf{k}$ are the polarization and momentum of the photon in the intermediate state. Using Ref. 4, we reduce $\langle \mathbf{p}'', l_{\nu}, s'', \mathbf{k}|\,j_{\rho'}(0)\,|\mathbf{p}, s\rangle$ from (4) to the fourth variational derivative of the S matrix.

Estimating the fourth variational derivative by perturbation theory in the lower order relative to e and relative to g with the usual Lagrangian meson-nucleon-photon interaction, we obtain

$$\langle p'', s'', \mathbf{k}, l_{\nu}|\,j_{\rho'}(0)\,|p, s\rangle$$

$$= -\frac{eg}{(2\pi)^{3/2}\sqrt{2k_0}}\,\bar{u}^{s''}(p'')\left\{\hat{l}_{\nu}\frac{1+\tau_3}{2}\,S^c(p+q)\,\gamma^5\tau_{\rho'} + \tau_{\rho'}\gamma^5 S^c(p-k)\,\hat{l}_{\nu} + (ql_{\nu})\,\gamma^5\Delta^c(k-q)\,[\tau_{\rho'}\tau_3]\right\}u^s(p), \tag{5}$$

$\hat{a} = a_0\gamma_0 - a\gamma$, $\gamma_0^+ = \gamma_0$, $\gamma^+ = -\gamma$, and $S^c(k)$, $\Delta^c(k)$ are the Fourier images of the electron and photon propagation functions (see Ref. 4).

For forward scattering, inserting (5) into (4), we obtain for the (+) and (-) processes:

$$A^{+}_{\alpha\omega}(E) = \frac{e^2}{4\pi}\frac{g^2}{4\pi}\frac{\tau_{\rho}\tau_{\rho'}}{2M}\,F_{+}(E), \tag{6}$$

$$F_{+}(E) = \frac{2M-5E-5Eq}{\varkappa}\tan^{-1}\frac{\varkappa}{E-M} + \frac{4Eq}{\varkappa}\tan^{-1}\frac{\varkappa}{E} + \frac{2E}{E+Eq}\left(1+\frac{Eq}{\varkappa}\tan^{-1}\frac{\varkappa}{E}\right), \quad \varkappa = \sqrt{\mu^2 - E^2}; \quad Eq = -\mu^2/2M.$$

From the δ-function (4) we deduce that

$$F_+(E) = \begin{cases} = 0 & \mu^2/2M \leqslant E \leqslant \mu \\ \neq 0 & -\mu \leqslant E \leqslant \mu^2/2M. \end{cases} \tag{7}$$

An analysis of the isotopic structure of the scattering amplitude[4] yields for $\pi^{\pm} + p \to \pi^{\pm} + p$ the following expression:

$$A_{\pm}(E) = \frac{e^2}{4\pi}\frac{g^2}{4\pi}\frac{2}{M}F_{\pm}(E), \quad F_+(E) = -F_-(-E), \tag{8}$$

$A_{\pm}(E)$ is the antihermitian portion of the scattering amplitude for $\pi^{\pm} + p \to \pi^{+} + p$. Taking this into account, the inhomogeneous term in the dispersion relations[4] is rewritten

$$\Delta_{\pm} = \Delta_{\pm}^0 + \Delta_{\pm}^1 = \pm\frac{2f^2q^2}{\mu^2(E \mp \mu^2/2M)} + \frac{2f^2q^2}{\mu^2}\frac{4M}{\pi}\alpha\int_{-\mu^2/2M}^{\mu}\frac{F_-(E')\,dE'}{(E' \pm E)(E'^2 - \mu^2)}, \tag{9}$$

$\alpha = 1/137$ and q is the meson momentum.

In the calculation of the integral with respect to E we obtain the following singularities: at $E = -\mu^2/2M$ the divergence is of the infrared type; it is eliminated by infinite renormalization of f^2. The divergence at $E = \pm\mu$ is eliminated by extrapolation of $A_{\pm}(E)$ to the value given by (8) for $E \to \mu$. The terms in $\Delta_{\pm}^1$, which diminish as the fundamental term of $\Delta_{\pm}^0$, give a finite charge renormalization; it is the same for (+) and (-). Those terms in $\Delta_{\pm}^1$, which diminish more rapidly than $\Delta_{\pm}^0$ as $E \to \infty$, i.e., which give a contribution at small values of E, comprise the sought correction. Finally,

$$\Delta_{\pm}(E) = \pm\frac{2f^2q^2}{\mu^2(E \mp \mu^2/2M)}\left(1 \pm \frac{\alpha}{\pi}I_{\pm}\right), \tag{10}$$

where $I_{\pm}$ is a complicated expression of the form

$$I_{\pm} \approx \frac{a}{E \pm \mu} + b\frac{\ln(E \mp c)}{E \pm \mu} + \cdots$$

a, b, c are small constants.

The above estimate gave for the energies $(1.5-2)\mu$ of interest to us a difference on the order of 3% between $f_{(+)}^2$ and $f_{(-)}^2$.

I express my deep gratitude to D. V. Shirokov, under whose leadership this work was performed.

Note added in proof (October 16, 1957). It is reported in Ref. 5 that the difference between $f_{(+)}^2$ and $f_{(-)}^2$ has been calculated from the dispersion relations by a method that gives a difference between $f_{(+)}^2$ and $f_{(-)}^2$ on the order of 5% at energies 150 – 200 Mev.

*The (-) sign will be used below to denote the process $\pi^- + p \to \pi^- + p$, while the (+) sign will be used for $\pi^+ + p \to \pi^+ + p$.

[1] G. Puppi and A. Stanghellini, Nuovo cimento 5, No. 5 (1957).

[2] U. Haber-Schaim, Phys. Rev. 104, 1113 (1956); W. C. Davidon and M. L. Goldberger, Phys. Rev. 104, 1119 (1956).

[3] A. Agodi and M. Cini, Nuovo cimento 5, No. 5 (1957).

[4] N. N. Bogoliubov and D. V. Shirkov, Введение в теорию квантованных полей (Introduction into the Theory of Quantized Fields), Gostekhizdat, Moscow 1957.

[5] A. Agodi and M. Cini, Nuovo cimento 6, 3 (1957).

Translated by J. G. Adashko
265

REMARKS ON THE ARTICLE BY COOPER AND GROSSART, "TIME DELAYS IN INTERNAL ELECTRIC BREAKDOWN OF SOLID DIELECTRICS"[1]

K. K. SONCHIK

Tomsk Polytechnic Institute

Submitted to JETP editor August 1, 1957

J. Exptl. Theoret. Phys. (U.S.S.R.) 33, 1303 (November, 1957)

In the breakdown of the ionic crystals NaCl, KCl, and KBr under 1/5000 microsecond pulses, Cooper and Grossart[1] obtained anomalously large delay times for the discharge, of the order of 10^{-6} to 10^{-5} seconds. In our opinion, this result followed from deficiencies in the method of investigation. In the first place, a test made by the full-wave method (repeating the voltage pulses with increasing amplitudes) may lead to an incomplete breakdown if the field is not sufficiently uniform.[2] In this case, there would be a distortion of the field within the dielectric. In addition, when a 1/5000 microsecond pulse is used, and especially when several such pulses are repeated, the voltage is applied to the dielectric for a considerable time, which may lead to the introduction of various secondary factors, such as heating effects, etc.,[3] which complicate the interpretation of the results.

In determining the delay time for discharges in ionic crystals it is sounder to make the test by means of individual rectangular voltage pulses with amplitudes exceeding the breakdown voltage by, say, 10, 20, 30%, and so on. Experiments which we have carried out in this way on NaCl samples 0.12 mm thick, in a uniform field at 20% over-voltage, gave time delays of the order of 4 to 5×10^{-8} seconds. Experiments with repeated rectangular voltage pulses (rise time of the order of 3×10^{-8} sec), of uniform amplitude somewhat below the breakdown value, showed that the effect of each successive pulse was to lower the electric strength, and that the breakdown took place, not at the first pulse, but at the n-th, where n has been found to range from 2 to 81.

In the article cited, the authors do not give the values of electric strength for the dielectrics they studied, nor do they show how they measured the time delays from the oscillograms and the pulse repetition rate, which limits the value of their paper.

[1] R. Cooper and D. T. Grossart, Proc. Phys. Soc. 69, 1351 (1956).
[2] A. Walter and L. Inge, J. Tech Phys. (U.S.S.R.) 1, 389 (1931).
[3] F. Lehmhaus, Arch. Elektr. 32, 281 (1938).

Translated by D. C. West
266

THE n-ELECTRON GREEN'S FUNCTION IN THE BLOCH-NORDSIECK APPROXIMATION

R. V. TEVIKIAN

Physics Institute, Academy of Sciences, Armenian S.S.R.

Submitted to JETP editor July 5, 1957

J. Exptl. Theoret. Phys. (U.S.S.R.) 33, 1304 (November, 1957)

On the basis of the results of Schwinger[1] one can write for the n-electron Green's function G_n in the Bloch-Nordsieck[2] approximation, i.e., after replacing the matrices γ^μ by c-numbers, the following equation:

$$\left\{iu^\mu \partial/\partial x_1^\mu - m + \sqrt{4\pi}eu^\mu A_\mu(x_1) + i\sqrt{4\pi}eu^\mu \int D_{\mu\nu}(x_1, \xi) \frac{\delta}{\delta A_\nu(\xi)} d\xi\right\} G_n(x_1, \ldots, x_n; y_1, \ldots, y_n | A)$$
$$= -\sum_l (-1)^l \delta(x_1 - y_l)\, G_{n-1}(x_2, \ldots, x_n; y_{l+1}, \ldots, y_n, y_1, \ldots, y_{l-1} | A), \qquad (1)$$

where the summation is taken over all possible cyclic permutations of the arguments $y_1, \ldots, y_n$, and l is the number of interchanges necessary to go from $y_j \ldots y_n y_1 \ldots y_{j-1}$ to $y_1 \ldots y_n$.

We seek the solution of Eq. (1) in the form

$$G_n(x_1, \ldots, x_n;\ y_1, \ldots, y_n \mid A) = -\sum_p (-1)^l [G_1(x_1, y_j \mid A)\, G_{n-1}(x_2, \ldots, x_n;\ y_{j+1}, \ldots, y_n, y_1, \ldots, y_{j-1} \mid A)$$

$$+ G_{1n}(x_1, \ldots, x_n;\ y_j, \ldots, y_n, y_1, \ldots, y_{j-1} \mid A)]. \qquad (2)$$

The equation for G_{1n} in the momentum representation can be solved exactly by a method used previously.[3] We get as the result

$$G_{1n}(p_1, \ldots, p_{2n-1} \mid A) = -\sqrt{4\pi}\frac{eu^{\mu_1}}{(2\pi)^3}\int_0^\infty d\nu e^{-\varepsilon\nu} \exp\left\{-i\left[m - \sum_{l=1}^{2n-1}(up_l)\right]\nu + f(\nu)\right\} \exp\left\{-\sqrt{4\pi}\frac{eu^\mu}{(2\pi)^3}\int \frac{e^{-i(up)\nu} - 1}{(up)} A_\mu(p)\, dp\right\}$$

$$\times \int D_{\mu,\nu_1}(k) \left\{G_1(p_2 \mid A)\left[\frac{\delta G_{n-1}(p_3, \ldots, p_{2n-1} \mid A)}{\delta A_{\nu_1}(k)}\right]_{A \to T_2 A}\right\}_{A \to A^{T_\nu}} \exp\left\{i\left(k + p_2 - \sum_{l=1}^{2n-1} p_l\right)x\right\} dx\, dk. \qquad (3)$$

It follows that the probability for the emission of n low-energy photons is given by the Poisson formula

$$w_n = e^{-W}\frac{W^n}{n!}, \quad W = \frac{2e^2}{\pi}\ln\frac{E_2}{E_1}, \qquad (4)$$

where the energy of the photons lies between E_1 and E_2.

[1] J. Schwinger, Proc. Nat. Acad. Sci. **37**, 452 (1951).

[2] F. Bloch and A. Nordsieck, Phys. Rev. **52**, 54 (1937).

[3] R. V. Tevikian, J. Exptl. Theoret. Phys. (U.S.S.R.) **32**, 1573 (1957), Soviet Phys. JETP **5**, 1282 (1957).

Translated by W. H. Furry
267

ON THE SPEED OF PROPAGATION OF ELECTROMAGNETIC WAVES AT AUDIO FREQUENCIES

Ia. L. AL'PERT and S. V. BORODINA

Institute of Terrestrial Magnetism, the Ionosphere, and Radio-Wave Propagation

Submitted to JETP editor August 3, 1957

J. Exptl. Theoret. Phys. (U.S.S.R.) **33**, 1305-1307 (November, 1957)

THE speed of electromagnetic waves has been investigated experimentally in various researches, over a frequency range approximately from 10^{15} cps (optical waves) to 10^6 or 10^5 cps (so-called medium radio waves). Recently we have determined the speed of electromagnetic waves under natural conditions at lower, audio frequencies, namely from about 3×10^4 to 10^3 cps; in addition, the investigations are about to be extended down to frequencies of some tens of cycles per second.

The method used in our work was that of complete harmonic analysis of photo-oscillograms of individual atmospheric events $E(t, r)$, taken at various distances from their sources (thunderstorm discharges).[1,2] The distances r from the sources were determined by means of three direction-finders. The method consists in the following.

The spectral density of the signal $E(t, r)$ can be written in the form

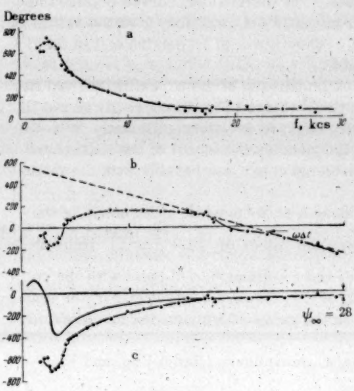

FIG. 1

$$Q(\omega, r) = A(\omega, r)\, e^{i\varphi(\omega, r)} = \int_0^\infty E(t, r)\, e^{-i\omega t}\, dt, \qquad (1)$$

where $A(\omega, r)$ and $\varphi(\omega, r)$ are determined by harmonic analysis of $E(t, r)$. If the radiated signal $E(t, r)$ is assigned the "standardized" spectral density $A(\omega, 0) \times e^{i\varphi(\omega, 0)}$, then from (1) one immediately obtains the propagation function

$$E(\omega, r)\, e^{-i\Phi(\omega, r)} = \frac{A(\omega, r)}{A(\omega, 0)}\, e^{i[\varphi(\omega, r) - \varphi(\omega, 0)]}, \qquad (2)$$

which describes the variation of the amplitude and phase of the received spectrum of the wave. The complete phase is

$$\Phi(\omega, r) = \omega \int_0^r \frac{dr}{v(\omega, r)} = \frac{\omega r}{\bar{v}(\omega, r)} = \frac{\omega r}{c} + \psi(\omega, r), \qquad (3)$$

where v and $\bar{v}$ are respectively the differential and the mean phase velocity of the wave, and where $\psi(\omega, r)$ is the so-called supplementary phase, describing the deviation of the phase of the wave and of its speed from their values in free space, where $v = c$. Since

$$E(t, r) = \frac{1}{2\pi} \int_{-\infty}^{\infty} A(\omega, r)\, e^{i[\omega t + \varphi(\omega, r)]}\, d\omega = \frac{1}{2\pi} \int_{-\infty}^{\infty} E(\omega, r)\, A(\omega, 0)\, e^{i[\omega(t - r/c) - \psi(\omega, r) + \varphi(\omega, 0)]} d\omega \qquad (4)$$

does not depend on the linear term $\omega r/c$ in the phase (it leads only to a uniform displacement of $E(t, r)$ along the time axis), the Fourier analysis determines the value of the phase only to within a term $\omega r/c$, i.e.,

$$\varphi(\omega, r) = -\psi(\omega, r) + \varphi(\omega, 0). \qquad (5)$$

Consequently, the mean phase velocity is equal to

$$\bar{v}(\omega, r) = c \Big/ \left[1 - \frac{\varphi(\omega, r) - \varphi(\omega, 0)}{\omega} \frac{c}{r}\right]. \qquad (6)$$

In this connection it is important to take the following into consideration. Usually the recorded signal $E(t, r)$ is cut off at the beginning, because of the threshold of sensitivity of the apparatus. This means that in the analysis the quantity determined is $\{\varphi(\omega, r) - \omega\Delta t\}$, i.e., the phase characteristic with an additional linear term $\omega\Delta t$, where Δt is the cutoff time of the signal. However, the value of Δt can be determined from the experimental phase curve. For in the high-frequency part of the range being considered, $d\psi/d\omega \sim 0$; therefore if the experimental curve has a linear behavior in this region, this is caused by the term $\omega\Delta t$. Atmospheric events were studied by the method described in various seasons, at various times of day from 9 AM to 5 PM local time, and at $r \sim 800$ to 3100 km. One example of the treatment of an individual atmospheric event is shown in Fig. 1. In it, a is the phase curve obtained by the harmonic analysis of $E(t, r)$. Subtracting from curve a of the phase characteristics of the receiver and of the standardized source we obtain curve b, while curve c corresponds to the desired function $\psi_i(\omega, r_i)$, obtained after subtracting the straight line $\omega\Delta t$ from b. From the figure it is evident that the theoretical values of $\psi(\omega, r)$ (the continuous curve in Fig. 1c) begin to deviate from the experimental at $f \sim 7$ to 8 kcs.

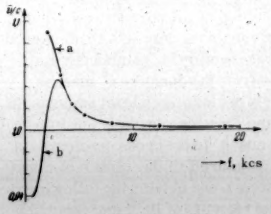

FIG. 2

All the individual signals were treated in similar fashion, and the results were used to plot curves showing the distribution of the quantity $\left(1 + \frac{\psi_i}{\omega} \frac{c}{r_i}\right)$, which determines $\bar{v}/c$, for seven frequency inter-

Most probable values of $\bar{v}/c$

f, kc	1.5—2.5	3—3.5	4—4.5	5—6	7—9	10—14	16—20
v/c, exptl.	1.09	1.05	1.024	1.014	1.006	1.004	1.002
f, kc	2	3		5	7	10	20
$\bar{v}/c$, theoret.	1.014	1.0456		1.017	1.0085	1.0041	1.0015

vals. The distribution curves obtained had pronounced maxima; they give the values of $\bar{v}/c$ shown in Fig. 2 (points) and in the table.

Comparison of the experimental and theoretical[3] values (Fig. 2, curve b) shows that they begin to deviate significantly at $f < 3$ kcs. This deviation is perhaps due to the fact that at such low frequencies the model of the ionosphere chosen in the calculations becomes inappropriate, since the wavelengths are comparable with the thickness of the ionospheric layers.

It should be pointed out that since, at the distances r considered, only the zero-order mode of the spectrum of the received wave plays an important part, therefore the values of $\left(1 + \frac{\psi}{\omega}\frac{c}{r}\right)$ immediately determine the imaginary values S_{01} of the wave numbers; and a comparison of them with the corresponding theoretical values of S_{01} may permit determination of the effective conductivity of the ionosphere with respect to transmission of electromagnetic waves in the range of frequencies investigated.

[1]Ia. L. Al'pert, Usp. Fiz. Nauk **60**, 369 (1956); Радиотехника и электроника (Radio Eng. and Electronics) **1**, 293 (1956).

[2]S. V. Borodina, Trudy, Inst. for Terr. Magn., Ionosphere, and Radio-Wave Propagation **13**, 3 (1957).

[3]Ia. L. Al'pert, Распространение электромагнитных волн низкой частоты над земной поверхностью (Propagation of Low-Frequency Electromagnetic Waves above the Surface of the Earth, Acad. Sci. Press, 1955).

Translated by W. F. Brown, Jr.
268

SCATTERING OF 333 MEV NEGATIVE π MESONS BY HYDROGEN

V. G. ZINOV and C. M. KORENCHENKO

Joint Institute for Nuclear Research

Submitted to JETP editor August 5, 1957

J. Exptl. Theoret. Phys. (U.S.S.R.) **33**, 1307-1308 (November, 1957)

THE elastic and exchange scattering of π^- mesons by hydrogen has been studied by us. The beam of π^- mesons was obtained with the use of the synchrocyclotron of the Joint Institute for Nuclear Research. The energy of the beam was found to be 333 ± 9 Mev. Measurements were made with the use of scintillation counters. Liquid hydrogen was used as the target and was contained in a foamed plystyrene container.

Table I presents the measured differential elastic scattering cross-section for π^- mesons after the inclusion of all corrections. Table II presents the corrected differential cross-section for gamma ray emission from the decay of π^0 mesons.

TABLE I

ϑ^*_{cms}	$\frac{d\sigma}{d\omega}$, 10^{-27} cm²/sterad
41.9	1.28±0.14
61.3	0.90±0.10
79.2	0.69±0.09
100.8	0.51±0.03
119.7	0.52±0.07
140.6	0.96±0.10
159.2	0.93±0.13

TABLE II

ϑ^*_{cms}	$\frac{d\sigma}{d\omega}$, 10^{-27} cm²/sterad
20.8	6.52±1.37
41.0	6.31±1.30
60.0	3.72±0.77
77.7	2.36±0.50
99.0	1.55±0.34
128.8	0.95±0.23
146.9	1.29±0.31
159.7	1.10±0.24

By performing a least squares fit of the function $d\sigma/d\omega = a + b\cos\vartheta + c\cos^2\vartheta$ to the cross-section data (ϑ measured in the center of mass system), one obtains the following results (in units of 10^{-27} cm²/sterad):

a) Elastic scattering of π^-

mesons: $a_- = 0.54 \pm 0.024$, $b_- = 0.34 \pm 0.058$, $c_- = 0.90 \pm 0.098$.

b) Gamma emission from π^0 meson decay; $a_\gamma = 1.87 \pm 0.24$, $b_\gamma = 2.89 \pm 0.44$, $c_\gamma = 2.32 \pm 0.59$.

The angular distribution of the π^0 mesons can be easily obtained from a_γ, b_γ, and c_γ. One obtains $a_0 = 0.68 \pm 0.20$, $b_0 = 1.80 \pm 0.27$, $c_0 = 1.90 \pm 0.50$.

The total elastic cross-section as determined by the above angular representation is $(10.7 \pm 0.6) \times 10^{-27}$ cm^2; the total exchange cross-section is $(16.6 \pm 1.4) \times 10^{-27}$ cm^2. The total cross-section for π^- meson interaction with hydrogen is $(28.8 \pm 1.8) \times 10^{-27}$ cm^2 where we have included the production of mesons by mesons[1] to the elastic and exchange contributions. For comparison one may cite the meson attenuation measurements in hydrogen[2] which gave a total cross-section of $(25.7 \pm 1.0) \times 10^{-27}$ cm^2.

[1] V. G. Zinov and C. M. Korenchenko, J. Exptl. Theoret. Phys. (U.S.S.R.) **34**, 301 (1958), Soviet Phys. JETP 7 (in press).

[2] Ignatenko, Mukhin, Ozerov, and Pontecorvo, Dokl. Akad. Nauk SSSR **103**, 45 (1955).

Translated by A. Skumanich
269

SCATTERING OF 307 MEV NEGATIVE π MESONS BY HYDROGEN WITH CHARGE EXCHANGE

V. G. ZINOV and C. M. KORENCHENKO

Joint Institute for Nuclear Research

Submitted to JETP editor August 5, 1957

J. Exptl. Theoret. Phys. (U.S.S.R.) **33**, 1308-1309 (November, 1957)

WE have measured the angular distribution of γ rays emitted in the decay of π^0 mesons which were formed by exchange scattering of π^- mesons by hydrogen ($\pi^- + p \rightarrow \pi^0 + n$). The π^- meson beam was obtained by the use of the synchrocyclotron of the Joint Institute for Nuclear Research. The energy of the π^- mesons was measured at 307 ± 9 Mev as obtained from range measurements in copper. Scintillation counters were used to obtain the data. Liquid hydrogen which was contained in a foamed polystyrene container was used as the target.

ϑ^*_{cms}	$\frac{d\sigma}{d\omega}$, 10^{-27} cm^2/sterad
20.5	9.80 ± 2.02
40.5	8.46 ± 1.74
59.2	4.05 ± 0.83
76.8	2.24 ± 0.46
98.0	1.50 ± 0.31
128.1	1.40 ± 0.31
146.4	1.32 ± 0.30
159.4	1.32 ± 0.29

The measured differential cross-section for gamma ray emission in the center of mass system is presented in the table. These cross-sections include all necessary corrections.

A least squares fit of the function $d\sigma/d\omega = a + b\cos\vartheta + c\cos^2\vartheta$ (ϑ measured in center of mass system) to the data results in the following values for the coefficients (in units of 10^{-27} cm^2/sterad): $a_\gamma = 1.87 \pm 0.24$, $b_\gamma = 3.30 \pm 0.53$, $c_\gamma = 3.14 \pm 0.71$. From these coefficients one can easily obtain the angular distribution of π^0 mesons and one finds $a_0 = 0.57 \pm 0.23$, $b_0 = 2.10 \pm 0.34$, $c_0 = 2.67 \pm 0.60$.

The total cross-section for charge exchange scattering as determined by the above angular distribution is $(18.4 \pm 1.6) \times 10^{-27}$ cm^2. Adding this cross-section to the elastic scattering cross-section[1] and including meson production by mesons[2] one obtains a total interaction cross-section for π^- meson in hydrogen of $(30.2 \pm 1.8) \times 10^{-27}$ cm^2. Meson attentuation measurements in hydrogen[3] yield a total interaction cross-section of $(3.16 \pm 1.6) \times 10^{-27}$ cm^2 (interpolated to 307 Mev).

In the accompanying figure the four dashed curves represent calculations based on four sets of phase shifts. These were obtained[1] from a preliminary phase analysis of elastic scattering of π^- mesons by hydrogen where one assumed that only the S and P states participate in the scattering. The measurements of the present work are indicated in the figure.

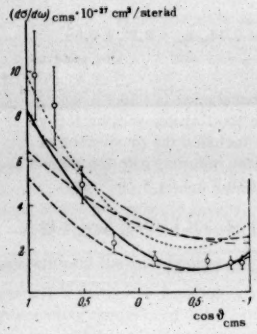

The solid curve represents $d\sigma/d\omega = 1.87 + 3.30\cos\vartheta + 3.14\cos^2\vartheta$. It is apparent that none of the computed γ distribution curves agree with the measured distribution, as was pointed out earlier.[1]

[1] V. G. Zinov and C. M. Korenchenko, J. Exptl. Theoret. Phys. (U.S.S.R.) **33**, 335 (1957), Soviet Phys. JETP **6**, 260 (1958).
[2] V. G. Zinov and C. M. Korenchenko, J. Exptl. Theoret. Phys. (U.S.S.R.) **34**, 301 (1958), Soviet Phys. JETP **7** (in press).
[3] Ignatenko, Mukhin, Ozerov, and Pontecorvo, Dokl. Akad. Nauk SSSR **103**, 45 (1955).

Translated by A. Skumanich
270

EFFECT OF QUANTUM FLUCTUATIONS IN THE ELECTRON RADIATION OF THE SYNCHROTRON OSCILLATIONS

E. M. MOROZ

P. N. Lebedev Physics Institute, Academy of Sciences, U.S.S.R.

Submitted to JETP editor August 10, 1957

J. Exptl. Theoret. Phys. (U.S.S.R.) **33**, 1309-1310 (November, 1957)

THE problem of quantum fluctuations in the radiation of electrons in the synchrotron has been considered in a series of articles (see, for example, Refs. 1 – 4).

In this note we generalize the well known results of Sands,[3] namely, we take into account the damping of synchrotron oscillations caused by the increase in electron energy, and give several practical results.

Putting the damping coefficient

$$\rho = \frac{\dot{E}}{E} + \frac{3-4n}{1-n}\frac{2ce^2}{3R^2}\frac{\gamma^3}{1+\lambda}, \qquad (1)$$

where $\gamma = E/mc^2$, $\lambda = N\ell/2\pi R$, ℓ is the length of the straight section of the race track, N is the number of sections, into the phase equation of the synchrotron it is possible to obtain a formula for the stationary value of the mean square amplitude for synchrotron oscillations

$$\langle A_\varphi^2 \rangle = \frac{55\sqrt{3}}{32}\frac{\hbar c q\cot\varphi}{e^2(1+\lambda)^2(3-4n)\gamma}F_1F_2. \qquad (2)$$

This expression differs from the result of Sands[3] by the presence of the factor F_1F_2, where

$$F_1 = \left(1+\alpha\frac{1-n}{3-4n}\frac{\dot{E}}{P}\right)^{-1}; \quad F_2 = \left(1+\frac{\dot{E}}{P}\right)^{-1}; \quad P = \frac{2ce^2}{3R^2}\frac{\gamma^4}{1+\lambda},$$

and α is a coefficient of order unity. At energies of several hundred Mev the factor F_1F_2 is important and, essentially, determines the energy dependence of $\langle A_\varphi^2 \rangle$. Analysis of Eq. (2) shows that there is no danger of particle loss connected with a maximum of $\langle A_\varphi^2 \rangle$ which, under the assumption $\cot\varphi = \text{const}$, occurs for $P = 7\dot{E}\alpha(1-n)/(3-4n) \approx 1$. The condition $\cot\varphi = \text{const}$ is, in fact, superfluous. Employing another law of increase for the accelerating voltage, it is easy to avoid this maximum.

At high energies where $F_1F_2 \to 1$, using results obtained by Sands,[3] one can find the excess of the amplitude of the accelerating voltage over the value of the amplitude, necessary to accelerate the elec-

trons and to compensate their energy loss by radiation

$$\frac{1}{\cos\varphi} > \frac{4}{\pi} + \frac{55\sqrt{3}}{64\pi^2}\,\frac{\hbar c}{e^2(1+\lambda)^2(3-4n)}\,\ln\frac{\lambda_1^2}{\frac{2}{\lambda_1 J_1(\lambda_1)}}\,\frac{q}{\gamma}. \qquad (3)$$

Here λ_1 is the first root of the Bessel function $J_0(x)$, q is the number of harmonics of the radio frequency employed in the synchrotron.

Satisfaction of the condition Eq. (3) is very difficult in accelerators with a large number of harmonics of the radio frequency and with weak focusing. Failure to satisfy this condition can lead to loss of a substantial fraction of the particles in the accelerator.

In conclusion, the author would like to thank M. S. Rabinovich for advice and suggestions. The author is grateful to V. I. Veksler for the interest he has shown in the present work.

[1] A. A. Kolomenskii and A. N. Lebedev, Proc. Geneva Conf. on Accelerators 1, 447 (1956).
[2] A. A. Sokolov and I. M. Ternov, Dokl. Akad. Nauk SSSR 97, 823 (1954).
[3] M. Sands, Phys. Rev. 97, 470 (1956).
[4] I. G. Henry, Phys. Rev. 106, 1057 (1957).

Translated by G. E. Brown
271

ON THE USE OF THE DISPERSION IN ENERGY AS A CRITERION FOR THE ACCURACY OF THE VARIATIONAL METHOD

D. P. LEPER and D. S. CHERNAVSKII

P. N. Lebedev Physics Institute, Academy of Sciences, U.S.S.R.

Submitted to JETP editor August 10, 1957

J. Exptl. Theoret. Phys. (U.S.S.R.) 33, 1311-1312 (November, 1957)

UP to now the accuracy of a solution of the Schrödinger equation by the variational method has been estimated by comparing the calculated energy value with its experimental value. However, this method is totally inapplicable when the experimental value of the level is unknown. Apart from this the error in the energy obtained in this way can reflect not only the inaccuracy of the trial function, but also the inaccuracy of the Hamiltonian. It is therefore of interest in a number of cases to estimate separately the magnitude of the error due to the inaccuracy of the trial function. We shall show below that this can be done by using the dispersion in the energy of the trial functions.

We consider a typical case, namely, the determination of the ground state of the system. This level is non-degenerate and its wave function is real. The deviation of the trial function Ψ from the eigenfunction Ψ_0 is thus equal to $\delta^2 = \|\Psi - \Psi_0\|$ (Ψ and Ψ_0 are normalized). We shall assume in the following that $\delta^2 \ll 1$. We expand the trial function for the complete system in terms of the normalized eigenfunctions of the Hamiltonian H,

$$\Psi = \sum_{k=0}^{\infty} C_k \Psi_k;\ \|\Psi\| = \sum_{k=0} |C_k|^2 = 1. \qquad (1)$$

For the error δ^2 we obtain the expression

$$\delta^2 = 2(1 - C_0) \approx 1 - C_0^2. \qquad (2)$$

The dispersion in energy in the state Ψ is equal to $D = (\Psi, H^2\Psi) - (\Psi, H\Psi)^2$. Using the expansion (1) we can obtain for D the expression

$$D=\sum_{k=1}\sum_{\substack{i=0\\k>i}}(E_k-E_i)^2\,|C_k|^2\,|C_i|^2\equiv\sum_{k=1}(E_k-E_0)^2\,|C_k|^2C_0^2+\sum_{k=2}|C_k|^2\sum_{i=1}(E_k-E_i)^2\,|C_i|^2. \tag{3}$$

In this expression for the dispersion we discard small terms. Let us therefore estimate the second term. In it we replace $(E_k - E_i)$ by the larger quantity $(E_k - E_0)$ and using equations (1) and (2) we get $\sum_{i=0}(E_k - E_i)^2\,|C_i|^2 < (E_k - E_0)^2\delta^2$. We have thus up to terms of the order δ^2.

$$D=\sum_{k=1}^{\infty}(E_k-E_0)^2\,|C_k|^2=\Sigma_2, \tag{4}$$

where Σ_2 denotes the quadratic error in energy in the state described by the trial function Ψ.

We estimate now the error in the function, that is δ^2. We replace thereto in Eq. (4) $(E_k - E_0)$ by the smaller quantity $(E_1 - E_0)$ and, using Eqs. (1) and (2) we get, up to terms of the order δ^4,

$$\delta^2<D/(E_1-E_0)^2. \tag{5}$$

Similarly we estimate the error in energy $\Sigma_1 = (\Psi, H\Psi) - E_0$ (E_0 is the true energy level value) and the relative error in energy $\sigma = \Sigma_1/(\Psi, H\Psi)$. To do that we note that

$$D=(\Psi,\,[H-(\Psi,\,H\Psi)]^2\,\Psi)=\Sigma_2-\Sigma_1^2.$$

After neglecting the second term in Eq. (3) we have $D > C_0^2\Sigma_2$, and we can easily show that $\Sigma_1^2 = \Sigma_2 - D < \delta^2\Sigma_2$. We have thus up to terms of the order δ^4

$$\sigma^2<\delta^2\frac{D}{(\Psi,\,H\Psi)^2}<\frac{D^2}{(\Psi,\,H\Psi)^2(E_1-E_0)^2}. \tag{6}$$

We must note that if the right hand sides of inequalities (5) and (6) are not small, it does not necessarily mean that the error is large since in principle it is not possible to conclude the other way round that the dispersion should be small if δ^2 and σ are small [the inequalities (5) and (6) can be very strong]. The possibility of a very large overestimate of the upper limits is thus the essential drawback of the estimates we have obtained. Apart from this, they also contain the unknown difference between the eigenvalues $(E_1 - E_0)$. In the estimate for σ we can avoid this by multiplying the right hand side by the quantity $(E_1 - E_0)/\sqrt{D}$ which according to (5) is of the order of $1/\delta^2 \gg 1$. We get thus the following, strongly exaggerated estimate: $\sigma < \sqrt{D}/(\Psi, H\Psi)$.

As an example we can consider Hylleraas' first approximation[1] for the ground state of the helium atom,

$$\Psi=\frac{\lambda^3}{\pi a_0^3}\exp[-\lambda(r_1+r_2)/a_0], \tag{7}$$

where λ is the variational parameter, which after minimization has the value $\lambda_0 = 27/16$, and where a_0 is the Bohr radius.

In this case $(E_1 - E_0) \sim (\Psi, H\Psi)$. We can thus conclude that $\sigma < D/(\Psi, H\Psi)^2$. Evaluating this we get $\sigma < 11\%$.

The corresponding calculation for Platt's approximation[1] for the ground state of the lithium atom leads to an unreasonably large result which is apparently connected with the above mentioned possibility of a large overestimate of the upper limit.

[1] P. Gombas, The Many-Body Problem in Quantum Mechanics, (Russ. Transl.), 2nd Edition, Moscow-Leningrad, IIL, 1953.

Translated by D. ter Haar
274

CONTENTS—continued

		Page	Russian Reference
Investigation of the Equilibrium Form of Atomic Nuclei	B. L. Birbrair	951	33, 1235
Diffraction Scattering and Nucleon Structure	S. Z. Belen'kii	960	33, 1248
Inverse Dispersion Relations	V. Z. Blank and D. V. Shirkov	962	33, 1251
Electron Losses Due to Phase Oscillations Induced by Radiation Fluctuations in Synchrotrons	A. N. Matveev	965	33, 1254
Nonlinear Effects in Metals at Low Temperatures	M. I. Koganov and V. G. Peschanskii	970	33, 1261
Invariant Representation of the Scattering Matrix	V. I. Ritus	972	33, 1264
Application of Dispersion Relations for the Determination of Bound States	V. I. Serdobol'skii	975	33, 1268
The Quantum States of Particles Coupled with Arbitrary Strength to a Harmonically Oscillating Continuum. II. The Case of Translational Symmetry	V. M. Buimistrov and S. I. Pekar	977	33, 1271
On the Problem of the Excited States of Nucleons	N. F. Nelipa	981	33, 1277
On the Theory of the Anomalous Skin Effect in Metals	V. P. Silin	985	33, 1282
Aging Equation for Gamma Quanta	B. V. Novozhilov	989	33, 1287
Saturation Effect in a System with Three Energy Levels	M. V. Fain	991	33, 1290
On the Fluctuations of Nuclear Matter	D. I. Blokhintsev	995	33, 1295

LETTERS TO THE EDITOR

		Page	Russian Reference
Measurement of Polarization Quantities	A. G. Zimin	1000	33, 1300
Radiation Corrections in the Dispersion Relations for $\pi^{\pm} + p \rightarrow \pi^{\pm} + p$	V. K. Fedianin	1001	33, 1301
Remarks on the Article by Cooper and Grossart, "Time Delay in Internal Electric Breakdown of Solid Dielectrics"	K. K. Sonchik	1003	33, 1303
n-Electron Green's Function in the Bloch-Nordsieck Approximation	R. V. Tevikian	1003	33, 1304
On the Speed of Propagation of Electromagnetic Waves at Audio Frequencies	Ia. L. Al'pert and S. V. Borodina	1004	33, 1305
Scattering of 333-Mev Negative π Mesons by Hydrogen	V. G. Zinov and S. M. Korenchenko	1006	33, 1307
Scattering of 307-Mev Negative π Mesons by Hydrogen with Charge Exchange	V. G. Zinov and S. M. Korenchenko	1007	33, 1308
Effect of Quantum Fluctuations in the Electron Radiation of the Synchrotron Oscillations	E. M. Moroz	1008	33, 1309
On the Use of Dispersion in Energy as a Criterion for the Accuracy of the Variational Method	D. P. Leper and D. S. Chernavskii	1009	33, 1311

SOVIET PHYSICS JETP VOLUME 6 (33), NUMBER 5 MAY, 1958

CONTENTS

	Page	Russian Reference
The Development of Physics in the U.S.S.R. in 40 Years of Soviet Power	835	33, 1081
Investigation of the Thermal Properties of Superconductors. I. Tin (Down to 0.15° K) N. V. Zavaritskii	837	33, 1085
The Interaction Between Light Atomic Nuclei and Particles with Energies of 10^{12} to 10^{13} ev N. L. Grigorov, V. Ia. Shestoperov, V. A. Sobiniakov, and A. V. Podgurskaia	848	33, 1099
Angular Distribution of Axes of Extensive Air Showers at Sea Level A. T. Abrosimov, V. I. Goman'kov, I. A. Ivanovskaia, and L. I. Sarycheva	856	33, 1110
Determination of Nuclear Moments of Gd^{155} and Gd^{157} from the Hyperfine Structure of Paramagnetic Resonance A. A. Manenkov and A. M. Prokhorov	860	33, 1116
An Anomalous Magnetic Transition in Anhydrous Copper Sulfate A. S. Borovik-Romanov and I. M. Kreines	862	33, 1119
Yield and Angular Distribution of Fast Photoneutrons from Deuterium and Carbon P. S. Baranov, V. I. Gol'danskii, and V. S. Roganov	865	33, 1123
Alpha Particles Emitted by Heavy Emulsion Nuclei in Emulsions Bombarded by High-Energy Protons P. A. Vaganov and V. I. Ostroumov	871	33, 1131
The $Bi^{212} - Po^{212}$ Decay Scheme A. G. Sergeev, E. M. Krisiuk, G. D. Latyshev, Iu. N. Trofimov, and A. S. Remennyi	878	33, 1140
The Decay Scheme of Tl^{208} E. M. Krisiuk, A. G. Sergeev, G. D. Latyshev, K. I. Il'in, and V. I. Fadeev	880	33, 1144
On the Elastic Backward Scattering of 660-Mev Protons Against Carbon Nuclei G. A. Leksin and Iu. P. Kumekin	883	33, 1147
On the Form of the Beta-Decay Interaction G. R. Khutsishvili and S. G. Matinian	885	33, 1150
Concerning a Model for a Non-Ideal Fermi Gas A. A. Abrikosov and I. M. Khalatnikov	888	33, 1154
Nuclear Reactions in Li^7 and C^{12} Induced by N^{14} Ions D. G. Alkhazov, Iu. P. Gangrskii, and I. Kh. Lemberg	892	33, 1160
A Study of Slow μ Mesons in the Stratosphere by the Method of Delayed Coincidences V. F. Tulinov	894	33, 1163
Electron Spectrum at 3200 m Above Sea Level M. I. Daion	897	33, 1166
Experimental Data on Cascade Multiplication of Electrons in Lead M. I. Daion	903	33, 1175
Observation of Particles of Charge $Z > 2$ in Disintegrations Produced in Photographic Emulsions by High-Energy Neutrons. V. M. Sidorov and E. L. Grigor'ev	906	33, 1179
Knockout of Deuterons from Li, Be, C, and O Nuclei by Protons of Energy 675 Mev L. S. Azhgirei, I. K. Vzorov, V. P. Zrelov, M. G. Meshcheriakov, B. S. Neganov, and A. F. Shabudin	911	33, 1185
A Group-Theoretical Consideration on the Basis of Relativistic Quantum Mechanics. II. Classification of the Irreducible Representations of the Inhomogeneous Lorentz Group Iu. M. Shirokov	919	33, 1196
A Group-Theoretical Consideration on the Basis of Relativistic Quantum Mechanics. III. Irreducible Representations of the Classes P_0 and O_0, and the Non-Completely-Reducible Representations of the Inhomogeneous Lorentz Group Iu. M. Shirokov	929	33, 1208
Equations for the Green's Functions of a System of Fundamental Particles V. G. Solov'ev	935	33, 1215
Interactions of Slow π Mesons with Nuclei A. M. Baldin and A. I. Lebedev	940	33, 1221
Oscillations of a Fermi-Liquid in a Magnetic Field V. P. Silin	945	33, 1227

(Contents continued on inside back cover)